SPATIAL AND TEMPORAL PATTERNS OF EASTERN OYSTER (*CRASSOTREA VIRGINICA*) POPULATIONS AND THEIR RELATIONSHIPS TO DERMO (*PERKINSUS MARINUS*) INFECTION AND FRESHWATER INFLOWS IN WEST MATAGORDA BAY, TEXAS

A Dissertation

by

JAN CHERYL CULBERTSON

Submitted to the Office of Graduate Studies of
Texas A&M University
in partial fulfillment of the requirements for the degree of

DOCTOR OF PHILOSOPHY

December 2008

Major Subject: Wildlife and Fisheries Sciences

SPATIAL AND TEMPORAL PATTERNS OF EASTERN OYSTER (*CRASSOTREA VIRGINICA*) POPULATIONS AND THEIR RELATIONSHIPS TO DERMO (*PERKINSUS MARINUS*) INFECTION AND FRESHWATER INFLOWS IN WEST MATAGORDA BAY, TEXAS

A Dissertation

by

JAN CHERYL CULBERTSON

Submitted to the Office of Graduate Studies of
Texas A&M University
in partial fulfillment of the requirements for the degree of

DOCTOR OF PHILOSOPHY

Approved by:

Chair of Committee,	Frances Gelwick
Committee Members,	Sammy Ray
	John Schwarz
	William Wardle
Head of Department,	Tom Lacher

December 2008

Major Subject: Wildlife and Fisheries Sciences

ABSTRACT

Spatial and Temporal Patterns of Eastern Oyster
(*Crassostrea virginica*) Populations and Their Relationships to
Dermo (*Perkinsus marinus*) Infection and Freshwater Inflows
in West Matagorda Bay, Texas.
(December 2008)
Jan Cheryl Culbertson, B.A., University of Delaware;
M.S., University of Georgia
Chair of Advisory Committee: Dr. Frances Gelwick

The present study explored the spatial and temporal demographic trends in oyster population dynamics and their relationships to freshwater inflows and the pathogen Dermo (*Perkinsus marinus*) on three reefs (Shell, Mad Island, and Sammy's) in West Matagorda Bay, Texas. The objectives were to design and link three population models that simulate oyster population dynamics and integrate the environmental factors that influence growth, reproduction and settlement of larvae among these three reefs. The following variables were evaluated: relative abundance of oyster spat, submarket- and market-size oysters, average weighted incidence of Dermo and percent Dermo infection (prevalence) in submarket- and market-size oysters and their relationships to environmental variables of salinity, temperature, flow and distance from freshwater sources. Using a 30-month continuous dataset, environmental variables accounted for

36% of the variation in Dermo-related variables among the three reefs, and were also positively correlated with distance from freshwater sources. The relative abundance of spat and dead oysters was related to peaks in freshwater inflows occurring 30 days prior to larval settlement.

Using these spatial and temporal relationships among biological and environmental variables, and data from five years of monitoring three reefs in Matagorda Bay, an integrated Stella model was developed that simulated oyster population responses to stochastic environmental changes over a 50-year period. Although the geological and structural complexity of each reef appeared to be similar, the model showed the relationship of growth, spawning and spat set were related to hydrologic variation between different reefs and time periods. The model revealed that up-estuary reefs relied on the distribution of larvae from down-estuary reefs following mortality related to freshwater inflow. The model also indicated that loss of freshwater inflows to down-estuary reefs resulted in higher sustained Dermo infections, thus loss of spawning potential and subsequent distribution of larvae to up-estuary reefs. The three oyster populations in West Matagorda Bay provide spawning connectivity and function as an integrated resource for sustaining all oyster reef populations in this bay system.

The model presented in this research provides a basis for understanding the population dynamics of WMB as well as a better understanding of the interaction among the reefs that sustain these populations. The model developed in this investigation provides a basis for developing oyster population models for other bay systems and for future research regarding hydrologic influences on oyster population dynamics.

DEDICATION

This dissertation is dedicated to my loving and supportive parents George and Norma Culbertson; my brothers Kirk, Steven, and Alexander Culbertson; my sister Dr. Bonnie Culbertson; my loving husband Gary James Templeton; and to my valued and esteemed mentors Drs. Sammy Ray and Frances Gelwick. This dissertation also honors two significant women that made an early impression on my life - Mrs. Stella Ciemny Culbertson and Dr. Esther Boyer Kirkpatrick Bauer.

ACKNOWLEDGEMENTS

I would like to thank my committee chair, Dr. Frances Gelwick, for her gentle, patient but firm guidance and support throughout the course of this research. I would also like to acknowledge Dr. Sammy Ray for his dedication to teaching students of all ages about oysters and their physiological responses to Dermo. I would also like to thank Drs. John Schwarz and William Wardle for their patience and support throughout the course of this research. I would also like to acknowledge Dr. William Neill for his valuable insights and contributions to the Stella integrative oyster population model developed during this research effort.

I appreciate the following Texas Parks and Wildlife staff that provided technical assistance on this research: Brenda Bowling, Josh Harper, Rodney Girndt, Wen Lee, Lynne Hamlin, Cindy Bohannon, Fernando Martinez-Alvarez, Dave Buzan, Cindy Loeffler, Jamie Schubert, Bill Balboa, Norman Boyd, Page Campbell, Mark Fisher, Lance Robinson, Rebecca Hensley, and Lynn Benefield; and other staff that collected Dermo samples. I appreciate the special consideration Golden Pass Seafood Company in Palacios provided for this research project, by allowing evaluation of the oysters they collected from Matagorda Bay.

I appreciate the special assistance with datasonde information and Colorado Delta intertidal reefs provided by Bryan Cook at Lower Colorado River Authority. I also recognize and appreciate Drs. Ruben Solis, Carla Guthrie, and Junji Matsumoto for their assistance on datasonde information and TXBLEND comparison information on West

Matagorda Bay. I appreciate Dr. George Ward's permission for use of the digital version of Moore's 1904 historical map of Matagorda Bay in this document.

I also want to thank my friends, colleagues, faculty and staff for making my time at Texas A&M University a great experience. I also appreciate the TAMU COALS Tom Slick Fellowship and Texas Parks and Wildlife Foundation Fellowship, which provided funds to support my tuition, travel, and presentation of this research at the National Shellfish Association meetings in Rhode Island.

I appreciate the patience, encouragement and support provided by my father and mother, and my loving husband Gary Templeton.

NOMENCLATURE

TPWD	Texas Parks and Wildlife Department
TPWC	Texas Parks and Wildlife Commission
TWDB	Texas Water Development Board
TDSHS	Texas Department of State Health Services
USACE	United States Army Corps of Engineers
USFWS	United States Fish and Wildlife Services
USGS	United States Geological Services
LCRA	Lower Colorado River Authority
WMB	West Matagorda Bay
EMB	East Matagorda Bay
RDA	Redundancy Analysis
DCA	Detrended Correspondence Analysis
CCA	Canonical Correspondence Analysis

TABLE OF CONTENTS

Page

ABSTRACT iii

DEDICATION v

ACKNOWLEDGEMENTS vi

NOMENCLATURE viii

TABLE OF CONTENTS ix

LIST OF FIGURES viii

LIST OF TABLES ix

CHAPTER

I INTRODUCTION: LITERATURE REVIEW OF SPATIAL AND TEMPORAL PATTERNS OF TEXAS OYSTER POPULATIONS .. 1

Introduction 1
Historical and current conditions among Texas reefs 3
Structure differences among reefs 6
Distance from freshwater sources 8
Distances among reefs 15
Biotic interactions among reefs and environmental variables.. 17
Interactions among oyster populations and Dermo 18
Biotic and abiotic interactions in oyster models 21
Dissertation objectives 23

II SPATIAL AND TEMPORAL PATTERNS OF OYSTER POPULATION DEMOGRAPHICS IN WEST MATAGORDA BAY 26

Introduction 26
Historical and current oyster population distributions 30
Spawning interactions 34
Larvae and spat settlement interactions 35
Individual growth and trophic interactions 38

CHAPTER Page

Harvest patterns and DSHS closures 42
Methods 45
Study area 45
Data source: LCRA environmental data 45
Environmental factors: daily and monthly differences 46
Data sources for daily discharge, tide and precipitation 55
Direction of flow and tidal amplitude 55
Distance from discharge to LCRA datasonde 57
Data source: TPWD Resource Monitoring Program data 58
Length frequency distributions 60
Oyster weights and density estimates 60
Growth estimates 62
Temporal trends in relative abundance in each size class 65
Gradient analyses 65
Results 67
Trends of shell length-weight distributions for Mad Island Reef 67
Temporal trends in relative abundances of each size class among reefs 72
Exploratory analyses of temporal variation in each size class among reefs 81
Spatial differences in temporal trends of relative abundance of each size class among reefs 85
Direct gradient analyses 85
Discussion 91
Spatial and temporal oyster reef population dynamics 91
Conclusions 93

III SPATIAL AND TEMPORAL PATTERNS OF DERMO INFECTION IN OYSTERS ON MATAGORDA BAY REEFS 94

Introduction 94
Environmental interactions with Dermo infection 95
Spatial interactions with Dermo infection 96
Methods 97
Oyster collection methods for Dermo samples 97
Dermo infection evaluation methods 98
Exploratory analysis of Dermo in submarket and market size classes and environmental factors among reefs 101
Analytical methods 101

CHAPTER Page

Direct gradient analysis of environmental variables and index values among reefs using RDA 102
Results 103
Relationships of Dermo in submarket and market size classes and environmental factors among reefs 103
Direct gradient analysis 106
Discussion 108
Spatial and temporal Dermo dynamics 108
Conclusions 109

IV INTEGRATIVE MODEL FOR OYSTER POPULATION DYNAMICS AMONG MATAGORDA BAY REEFS 110

Introduction 110
Methods 112
Environmental submodels 112
Salinity submodels 114
Temperature submodels 115
Colorado River inflow submodel 116
Matagorda Bay tide submodel 117
Oyster population submodels 118
Shell Island Reef population submodel 121
Mad Island Reef population submodel 123
Sammy's Reef population submodel 125
Larval distribution submodels 127
Size class submodels 129
Results 130
Comparison of environmental variables among reefs for 2001-2005 130
Comparison of oyster reef populations among reefs for 2001-2005 132
Comparison of environmental variables among reefs for 50 years (1.0 SD) 136
Comparison of oyster reef populations among reefs for 50 years (1.0 SD) 138
Comparison of environmental variables among reefs for 50 years (0.5 SD) 141
Comparison of oyster reef populations among reefs for 50 years (0.5 SD) 143
Comparison of environmental variables among reefs for 50 years (2.0 SD) 147

CHAPTER Page

Comparison of oyster reef populations among reefs for 50 years (2.0 SD) 149
Spatial and temporal trends of Dermo infection among three reef populations 153
Discussion 158
Conclusions 160

V SUMMARY AND CONCLUSIONS 162

Summary 162
Conclusions 165

LITERATURE CITED 167

APPENDIX A 183

VITA 192

LIST OF FIGURES

FIGURE		Page
1	Matagorda Bay ecosystem and Colorado and Lavaca River watersheds...	27
2	Matagorda and Lavaca Bays, minor bays and tributaries	28
3	Matagorda Bay Reefs in 1904-1905 from Moore (1907), reprinted with permission from Figure 4-8 page 91 in Ward et al. 1980.	31
4	Mad Island, Shell Island and Dog Island Reefs, and Tiger Island Channel in Matagorda Bay in 1904-1905 from Moore (1907), reprinted with permission from Figure 4-8 page 91 in Ward et al.1980	32
5	Matagorda and Lavaca Bay oyster reef sites sampled by TPWD; Shell Island (0.59 km^2 or 145 acres), Mad Island (0.38 km^2 or 93 acres), and Sammy's Reef (0.038 km^2 or 9.6 acres).....	34
6	Commercial Landings reported to TPWD for Matagorda Bay (not including Lavaca Bay)	45
7	TPWD Sample grids on Matagorda Reefs (red circles): Shell Island, Mad Island and Sammy's Reef.	46
8	Average monthly salinity at Shell Island LCRA water quality station for 2001-2005.....	47
9	Average daily salinity at LCRA Shell Island water quality station for 2001-2005.....	47
10	Average daily salinity measured at LCRA Shell Island datasonde water quality station measurements (dotted line) compared with TPWD average monthly salinity measurements at Shell Island Reef (Shell Saln), Mad Island Reef (Mad Saln), and Sammy's Reef (Sam Saln) from January 2003 through September 2005.	48
11	TPWD Shell Island Reef salinity values as a function of LCRA average daily datasonde salinity data 2001-2005	49
12	TPWD Mad Island Reef salinity values as a function of LCRA average daily datasonde salinity data 2001-2005.....	50

FIGURE Page

13 TPWD Sammy's Reef salinity values as a function of LCRA average daily datasonde salinity data for 2001-2005 50

14 Average monthly temperature at LCRA Shell Island water quality station for 2001-2005 51

15 Average daily temperature at LCRA Shell Island water quality station 2001-2005 52

16 TPWD Shell Island Reef monthly temperature as a function of LCRA average daily temperature data 2001-2005 53

17 TPWD Mad Island Reef monthly temperature as a function of LCRA Shell Island Reef average daily temperature data 2001-2005 53

18 TPWD Sammy's Reef monthly temperature as a function of LCRA Shell Island Reef average daily temperature data 2001-2005 54

19 Average daily discharge from USGS 08162500 Colorado River at Bay City, TX from 2000-2007 56

20 Average daily discharge from USGS 08162500 Colorado River at Bay City, TX, average daily tidal amplitude from NOAA: Station 8773701 at Port O'Connor, and extreme precipitation events recorded by National Weather Service from 2001-2005 57

21 Average daily discharge from USGS 08162500 Colorado River at Bay City, TX, and average daily salinity data at LCRA's Shell Island datasonde for 2001-2005 58

22 Monthly growth rate applied for Matagorda Bay oysters following methods by Hofstetter (1977) 64

23 Incremental daily growth rates applied for Matagorda Bay following methods by Kraueter et al. (2007) where Incremental growth rate = $Growth(K)*10^{(-0.0079*Length)}$. 64

24 Mad Island Reef length-frequency by size class of 160 oysters in a commercially harvested sack sampled on March 12, 2008 68

25 Relationship of Mad Island Reef total shell length to total weight for 160 oysters in a commercially harvested sack sampled on March 12, 2008..... 70

FIGURE Page

26 Relationship of Mad Island Reef total meat weight to total weight for 160 oysters in a commercially harvested sack sampled on March 12, 2008..... 71

27 Relationship of Mad Island Reef total meat weight to total length for 160 oysters in a commercially harvested sack sampled on March 12, 2008..... 72

28 Annual relative abundance of market oysters for three Matagorda Bay Reefs, Shell Island (Shell), Mad Island (Mad) and Sammy's Reef (Sam) 1998-2007..... 73

29 Annual relative abundance of submarket oysters for three Matagorda Bay Reefs, Shell Island (Shell), Mad Island (Mad) and Sammy's Reef (Sam) 1998-2007..... 74

30 Annual relative abundance trends of spat for three Matagorda Bay Reefs, Shell Island (Shell), Mad Island (Mad) and Sammy's (Sam) Reefs 1998-2007 75

31 Temporal trends of oysters for Shell Island Reef by size classes 1998-2007. 76

32 Temporal trends of oysters for Mad Island Reef by size classes 1998-2007. 76

33 Temporal trends of oysters for Sammy's Reef by size classes 1998-2007. 77

34 Relative abundance of submarket and market size classes of oysters at Shell Island Reef 1998-2007. 78

35 Relative abundance of submarket and market size classes of oysters at Mad Island Reef 1998-2007. 78

36 Relative abundance of submarket and market size classes of oysters at Sammy's Reef 1998-2007. 79

37 LOESS Curves for Shell Island Reef populations of a continuous 30-month dataset (March 2003 to August 2005) for (A) spat, (B) submarket, and (C) market oysters.. 82

38 LOESS Curves for Mad Island Reef populations of a continuous 30-month dataset (March 2003 to August 2005) for (A) spat, (B) submarket and (C) market oysters.. 83

FIGURE Page

39 LOESS Curves for Sammy's Reef populations of a continuous 30-month dataset (March 2003 to August 2005) for (A) spat, (B) submarket, and (C) market oysters.. 84

40 Spatial and temporal patterns of market oysters on Matagorda Bay Reefs, 1998-2006. (A) Shell Island Reef (Shl_Nmark), (B) Mad Island Reef (Mad_Nmark), (C) Sammy's Reef (Sam_Nmark). 86

41 Spatial and temporal patterns of submarket oysters on Matagorda Bay Reefs, 1998-2006. (A) Shell Island Reef (Shl_Nsub), (B) Mad Island Reef (Mad_Nsub), (C) Sammy's Reef (Sam_Nsub)..... 87

42 Spatial and temporal patterns of spat on Matagorda Bay Reefs, 1998-2006. (A) Shell Island Reef (Shl_Nspat), (B) Mad Island Reef (Mad_Nspat), (C) Sammy's Reef (Sam_Nspat) 88

43 Bi-plot of CCA showing relationships among centroids (centers of distribution as open triangles) for live and dead oysters in market (NMrk, MrkDd) and submarket (NSub, SubDd) size classes, and for spat (NSpat) in samples on three Matagorda Bay Reefs.. 90

44 Market oyster mantle tissue, 10X magnification, Disease code = 0.00; No infection or Dermo cells detected..... 100

45 Market oyster mantle tissue, 10X magnification, Disease code = 4.33; Moderately heavy + infection, mostly well enlarged and thin walled cells 101

46 Shell Island Reef submarket and market WI levels with temperature and salinity measurements on sample collection date. 104

47 Mad Island Reef submarket and market WI levels with temperature and salinity measurements on sample collection date. 104

48 Sammy's Reef submarket and market WI levels with temperature and salinity measurements on sample collection date. 105

49 Bi-plot of RDA showing relationships among response variables and explanatory variables..... 107

FIGURE Page

50 Environmental submodels to simulate 50 years of data for three runs corresponding to each of 0.5, 1.0, 2.0 SD based on five years of 2001-2005 historical data for temperature, salinity, flow, and tide 114

51 Salinity submodel to simulate 50 years of data for three runs corresponding to each of 0.5, 1.0, 2.0 SD based on five years of 2001-2005 historical data from Shell Island station..... 115

52 Temperature submodel to simulate 50 years of data for three runs corresponding to each of 0.5, 1.0, 2.0 SD based on five years 2001-2005 historical data from Shell Island station..... 115

53 Colorado River flow submodel to simulate 50 years of data for three runs corresponding to each of 0.5, 1.0, 2.0 SD based on five years of 2001-2005 historical data recorded at Bay City, TX 116

54 Tidal amplitude submodel to simulate 50 years of data for three runs corresponding to each of 0.5, 1.0, 2.0 SD based on five years of 2001-2005 historical data recorded at Port O'Connor, TX..... 117

55 Shell Island Reef oyster population submodel overview of interactions among environmental variables and Dermo disease 122

56 Mad Island Reef oyster population submodel overview of interactions among environmental variables and Dermo disease 124

57 Sammy's Reef oyster population submodel overview of interactions among environmental variables and Dermo disease 126

58 Shell Island Reef larvae population submodel..... 127

59 Mad Island Reef larvae population submodel..... 128

60 Sammy's Reef larvae population submodel..... 128

61 Colorado River Delta intertidal larvae population submodel..... 129

62 Comparison of average daily salinity among reefs for 2001-2005 131

63 Comparison of average daily temperature among reefs for 2001-2005 were similar; shown are data for Sammy's Reef..... 131

FIGURE Page

64 Comparison of Colorado River flow and Matagorda Bay tides among reefs for 2001-2005 132

65 Comparison of larvae among reefs for 2001-2005..... 133

66 Comparison of spat set among reefs for 2001-2005 133

67 Comparison of submarket oysters among reefs for 2001-2005 134

68 Comparison of market oysters among reefs for 2001-2005..... 135

69 Comparison of market-plus oysters among reefs for 2001-2005..... 135

70 Comparison of average daily salinity among reefs for 50 years (1.0 SD) 136

71 Comparison of average daily temperature among reefs for 50 years (1.0 SD) 137

72 Comparison of Colorado River flow and Matagorda Bay tide among reefs for 50 years (1.0) 138

73 Comparison of larvae among reefs for 50 years (1.0 SD)..... 139

74 Comparison of spat set among reefs for 50 years (1.0 SD)..... 139

75 Comparison of submarket oysters among reefs for 50 years (1.0 SD) 140

76 Comparison of market oysters among reefs for 50 years (1.0 SD)..... 140

77 Comparison of market-plus oysters among reefs for 50 years (1.0 SD).... 141

78 Comparison of average daily salinity among reefs for 50 years (0.5 SD) . 142

79 Comparison of average daily temperatures among reefs for 50 years (0.5 SD) 142

80 Comparison of Colorado River flow and Matagorda Bay tide among reefs for 50 years (0.5 SD) 143

81 Comparison of larvae among reefs for 50 years (0.5 SD)..... 144

FIGURE Page

82 Comparison of spat set among reefs for 50 years (0.5 SD)..... 144

83 Comparison of submarket oysters among reefs for 50 years (0.5 SD) 145

84 Comparison of market oysters among reefs for 50 years (0.5 SD)..... 146

85 Comparison of market-plus oysters among reefs for 50 years (0.5 SD).... 146

86 Comparison of average daily salinity among reefs for 50 years (2.0 SD) . 148

87 Comparison of average daily temperatures among reefs for 50 years (2.0 SD) 148

88 Comparison of Colorado River flow and Matagorda Bay tide among reefs for 50 years (2.0 SD) 149

89 Comparison of larvae among reefs for 50 year simulation (2.0 SD) 150

90 Comparison of spat set among reefs for 50 year simulation (2.0 SD) 150

91 Comparison of submarket oysters among reefs for 50 year simulation (2.0 SD) 151

92 Comparison of market oysters among reefs for 50 year simulation (2.0 SD) 152

93 Comparison of market-plus oysters among reefs for 50 years (2.0 SD).... 154

94 Comparison of Dermo infection in submarket, market, and market-plus size classes of Shell Island Reef oyster populations for 50 year simulation (1.0 SD) 155

95 Comparison of Dermo infection in submarket, market, and market-plus size classes of Mad Island Reef oyster populations for 50 year simulation (1.0 SD) 156

96 Comparison of Dermo infection in submarket, market, and market-plus size classes of Sammy’s Reef oyster populations for 50 year simulation (1.0 SD) 156

FIGURE Page

97 Comparison of Dermo infection in submarket, market, and market-plus size classes of Shell Island Reef oyster populations for 50 year simulation (2.0 SD) 157

98 Comparison of Dermo infection in submarket, market, and market-plus size classes of Mad Island Reef oyster populations for 50 year simulation (2.0 SD) 157

99 Comparison of Dermo infection in submarket, market, and market-plus size classes of Sammy's Reef oyster populations for 50 year simulation (2.0 SD) 158

LIST OF TABLES

TABLE		Page
1	Historical and current growth rates applied to Matagorda Bay oysters	63
2	Descriptive statistics for Mad Island Reef shell length weight analysis for oysters collected on March 12, 2008	68
3	Model summary for stepwise multiple regression of Mad Island Reef oyster for weight.....	69
4	Historical and current density estimates of oyster populations for three reefs in Matagorda Bay among size market and submarket classes.....	80
5	Eigenvalues for four axes and total variance for three reefs in Matagorda Bay	89
6	Descriptions of Dermo incidence levels in oyster tissue (Craig et al. 1989).	99

CHAPTER I

INTRODUCTION: LITERATURE REVIEW OF SPATIAL AND TEMPORAL PATTERNS OF TEXAS OYSTER POPULATIONS

Introduction

The Eastern oyster, *Crassostrea virginica* (Gmelin) is the dominant species on Texas oyster reef habitats (Hedgpeth 1953). Oysters are dynamic engineers that secrete calcareous shells, and in so doing, create three dimensional structural habitats with interstitial heterogeneity appropriate for the population and a diverse community of commensal, predatory and parasitic organisms that live, feed, or seek refuge on these reefs (Dame 1979; 1996; Bartol et al. 1999; Minello 1999).

Oysters are considered to be the best indicators of changes in estuaries because reefs form where conditions are optimum for oyster population's survival and reproduction (Chatry et al. 1983; Gutierrez et al. 2003; Dame 1996; Bergquist et al. 2006). Chatry et al. (1983) found an inverse relationship between spat set and oyster production in Louisiana bays. Their study showed that years with heavy spat set were followed by years of poor oyster production, whereas lighter sets often resulted in better oyster production. Galveston Bay oyster populations have demonstrated a similar relationship with higher spat sets in years with higher freshwater inflows, initially followed one year later with lower abundances of market size oysters (≥76 mm), then followed two years later with higher abundances of market oysters (Buzan et al. 2008).

This dissertation follows the style of *Journal of Shellfish Research*.

One study of oyster populations along a salinity gradient in a Florida estuary (Bergquist et al. 2006) found that the percent cover of living oysters and densities of various oyster size classes were inversely correlated with salinity measured 12 months and 24 months earlier. The abundance, mortality, and production of those oysters varied substantially with salinity and river flow conditions in Florida's Suwannee River estuary (Bergquist et al. 2006). In comparison, oysters located in Florida's Apalachicola Bay estuary, further from freshwater sources with highly variable salinity regimes, had higher mortalities than those closer to freshwater sources (Livingston et al. 2000). Although *C. virginica* has a wide range of physiological tolerance to salinity compared to other oyster species (Butler 1949, 1954), higher salinity indirectly results in higher mortality rates due to increased pressure from marine predators and parasites (Shumway 1996).

Oyster reefs are considered in this review as composed of live oysters and dead shells in consolidated formations or as clusters of live oysters on firm bottoms that provide direct and indirect ecosystem services for estuaries. These ecosystem services include water filtration, transfer of biomass production between bottom sediments and the water column through benthic-pelagic coupling, nutrient dynamics, sediment stabilization, creation of refugia for mobile and sessile organisms, and feeding habitat for resident and transient fish and invertebrates (Cake 1983; Stanley and Sellers 1986; Coen et al. 1999; Minello 1999; Plunket 2003; Street et al. 2005). Until recently, these valuable ecosystem services have been underestimated as essential fish habitat (Coen et al. 1999; Shervette and Gelwick 2008).

Oysters play a significant role as filter feeders that improve water quality in coastal ecosystems (Langdon and Newell 1996). The volume of water a single oyster can

filter per hour at 25º C (77º F) is approximately 8 l/hr (2.1 gal/hr) or about 1500 times the volume of the oyster's body size (Loosanoff and Nomejko 1946). Higgins (1980) showed that oyster filtration rate was independent of available food supply, tidal stage, and time of day. Oyster valves were observed to be generally closed when food was absent (Higgins 1980). Before the end of the 19th century, Chesapeake Bay oyster populations were reported to filter the entire volume of the bay in a little more than three days, but under conditions of severely reduced Chesapeake Bay oyster populations in 1988, the estimated time increased to 325 days (Newell 1988). Twenty years later, after near total loss of this valuable habitat, the estimated filtering time would be far greater than Newell's 1988 estimates. Other researchers concurred that the loss of oyster populations from estuaries removes an important water quality function for potential control of phytoplankton blooms, nutrient enrichment and overall coastal eutrophication (Officer et al. 1982; Dame et al. 1984; Lenihan and Peterson 1998; Coen et al. 1999; Jackson et al. 2001).

Oyster shells provide a valuable function of carbon storage in the form of calcium carbonate (Hargis and Haven 1999; Powell and Klinck 2007). The sequestered carbon in these shells is taken out of atmospheric circulation, and provides a valuable ecosystem service by partially offsetting the observed trend of increasing concentrations in the atmosphere of CO_2, an important greenhouse gas associated with global warming (Street et al. 2005).

Historical and current conditions among Texas reefs

Between 1904 and 1985, oyster surveys along the Texas coast were done by traditional methods such as poling, dredging, or coring (Moore 1907; Moore and

Danglade 1915; Galtsoff 1931; Price and Gunter 1942; Collier and Hedgpeth 1950; Ladd 1951; Norris 1953; Scott 1968; Byrne 1975; Benefield and Hofstetter 1976; King 1989). Oyster surveys of Matagorda Bay (Moore 1907) and of Lavaca Bay (Moore and Danglade 1915) were performed to determine oyster population sizes and densities, and to map the spatial patterns and extent of reef area within these estuaries. With similar objectives, Galtsoff (1931) surveyed oyster reefs from Galveston Bay to Corpus Christi Bay, as well as portions of the intercoastal waterway and the Laguna Madre. His surveys included salinity and temperature measurements. He summarized his findings with a map of each bay system that showed the location each reef and its spatial distribution relative to freshwater and tidal influences, including projected isohaline lines between reef sampling stations. Butler (1954) later classified Texas oyster reefs according to their spatial and temporal relationships to freshwater sources within these estuaries. Hedgpeth (1953; 1954) also provided an historical overview of oyster reefs and their associated bottom communities among the seven major coastal bay systems of Texas.

In 1940, Ladd (1951) investigated “oyster-reef facies” in Texas, which he associated with distinct molluscan faunal assemblages found in Corpus Christi and Aransas Bays. Oyster reef formation in Texas estuaries was associated with the Pleistocene Ingleside Barrier Complex (Leblanc and Hodgson 1959; Bernard and Leblanc 1965). These studies categorized oyster reefs into two specific depositional environments: lagoons formed behind barrier islands, and bays associated with drowned river basins. Scott (1968) later described four distinct Texas reef formations that he associated with these two geological depositional systems while surveying both buried and live reefs in Copano and San Antonio Bays. Surveys of buried and live reefs in other

Texas bays revealed similar associations with these types of depositional systems: Lavaca Bay (Byrne 1975), Aransas Bay (Norris 1953), San Antonio Bay (Hayes and Scott 1964; Scott 1968; Benefield and Hofstetter 1976), and Galveston Bay (Benefield and Hofstetter 1976).

Although dredging for dead oyster shells for roads and fill material, referred to as "mudshell dredging," was informally conducted in Texas bay systems prior to 1907 (Moore 1907; Galtsoff 1931), the Texas Parks and Wildlife Commission (TPWC) formally authorized mudshell dredging within 91 meters of natural oyster reefs in 1963, provided that resuspension of sediments did not damage live reefs. However, after several mudshell dredging violations occurred in 1963, Galveston and San Antonio Bay reefs were surveyed for post-sedimentation effects by Benefield (1976). He reported that reefs with low vertical relief suffered greater mortalities from sedimentation than ridge types of reefs that had greater vertical relief and higher flows along their periphery. He concluded that the distance between live reefs and dredging operations was not as critical to oyster survival as reef configuration and current flow when excessive sedimentation occurred.

Galveston and Lavaca Bays have been recently surveyed using either side scan or chirp sonar with sub-bottom profiling between 1990 and 2003 (Smyth and Anderson 1988; Powell et al. 1995; Bronikowski 2004; Sager et al. 2004; Patch 2005). Galveston Bay surveys (Powell et al. 1995) compared the extent of spatial changes among oyster reefs, previously surveyed by Benefield and Hofstetter (1976); and also documented the location of both consolidated live oyster reefs as well as clusters of live and dead shell on firm mud bottom habitats. Lavaca Bay surveys (Bronikowski 2004; Sager et al. 2004;

Patch 2005) also determined the extent of spatial changes among oyster reefs, previously surveyed by Moore and Danglade (1915) and Byrne (1975). At present, the Lavaca Ship Channel is being considered for widening and deepening in the next few years; and these surveys were used to assess the potential environmental impacts to existing oyster habitats in this bay system.

Currently oyster reefs in every Texas bay system are surveyed by oil and gas development companies by even more sophisticated and modern technologies as part of the "avoidance-minimization-compensation" procedures required prior to obtaining a 404 United States Army Corps of Engineers (USACE) permit for dredging, and installing pipelines or drilling platforms in Texas bay systems. TPWD and TAMUG are using similar technologies to map oyster reef habitats in Copano Bay, Sabine Lake and Galveston Bay estuaries (TPWD unpublished data).

Structural differences among reefs

Oyster reef communities provide unique three-dimensional hard bottom substrate in various geometric configurations that are situated relative to the sediment stability and currents in that area. Five reef configurations were historically identified for Texas bays. Three of these principal reef formations were first reported in two surveys of oyster reefs on the north central Texas Coast in Matagorda and Lavaca Bays (Moore 1907; Moore and Danglade 1915).

The first reef formation Moore (1907) described as "transverse ridge reefs" that formed perpendicular to the land and prevailing currents. This formation also grew vertically upwards into three dimensional ridge crests where the current was deflected (Moore 1907). Transverse ridge reefs were also observed to grow most rapidly towards

the strongest currents and less rapidly along the sides where the currents were slack (Moore 1907). Transverse ridge reefs were noted to be the main type of reef formed along the north shore of Matagorda Bay where the Colorado River currents flowed from east to west towards Pass Cavillo and the Gulf of Mexico (Moore 1907). Transverse ridge reefs were also reported to be the dominant reef type forming across Galveston, Trinity, East and West Bays on the upper Texas Coast; and across Aransas, San Antonio, Lavaca and Matagorda Bays on the middle coast (Moore 1907; Moore and Danglade 1915; Galtsoff 1931; Price 1954).

The second type of reef Moore (1907) described as clusters of shells formed in short rounded mounds or lumps in deeper waters away from shore, with even distribution of currents flowing around and over the formation. These types of reefs were later described as “tow-heads” by Price (1954) or as “patch reefs” by Hofstetter (1977). These types of reefs are typically found in the slower moving currents of East Matagorda Bay (Moore 1907) and in East Bay adjacent to Galveston Bay (Hofstetter 1977).

The third type of reef found in Lavaca Bay by Moore and Danglade (1915) and later by Galtsoff (1931) was described as a thin layer of scattered live shell in flat beds and patches that were deposited over firm sediments, at nearly the same elevation as the surrounding bottom. These types of reefs were also observed in San Antonio Bay and were classified as “pancake” reefs by Scott (1968). This same type of reef formation was similar to the “salt and pepper flats” of scattered live oysters lying on a stiff mud or clay bottom as described for South Redfish Reef by Hofstetter (1977). He reported that these reefs seldom exceeded one meter in thickness, had little vertical relief, and were the most vulnerable to sedimentation from mud-dredging operations.

Price (1954) described a fourth type of “longitudinal reef” which commonly formed in pairs along tidal channels, and elongated parallel to the dominant currents of the channel. He indicated these reefs were primarily associated with slightly elevated natural levees along rivers, which flooded during the last Pleistocene’s low sea level stage. Winslow (1889) first observed this type of oyster reef formation where denser numbers of oysters formed along tidal channels. Stenzel (1971) later defined these dense formations along channels as “fringing reefs”. Galtsoff (1931) also described similar “parallel linear reefs” in pairs along the many inner water bodies of central San Antonio Bay, and also along the initial Houston Ship Channel cut through North Redfish Reef in Galveston Bay. Hofstetter (1977) also documented that this fringing, longitudinal type reef became the most common reef formation after the Houston Ship Channel was dredged, due to the greater transfer of currents and tidal waters between the former transverse ridge formations of North Redfish Reef.

A fifth type of reef was described by Hofstetter (1977) as “concave shaped” where the central portion of the reef is several centimeters lower than the surrounding mud bottom. He found this type of reef during surveys of Galveston and San Antonio Bays (Benefield and Hofstetter 1976). The oysters on this type of reef are partially buried with only the upper margins of their bills exposed, which results in growth of long narrow shells. Galtsoff (1931) referred to these as “coon oysters” or “snapper oysters” when he found them in Aransas and Copano Bays.

Distance from freshwater sources

Structural formations of oyster populations have been noted in several studies as being related to several spatial and temporal features: distance from freshwater sources,

current velocities, duration of flows, and the timing of inflows relevant to their life cycle (Winslow 1889; Grave 1901; Galtsoff 1931; 1964; Hedgpeth 1954; Butler 1954; Price 1954; Hofstetter 1977; Ray 1987; McCormick-Ray 1998; Powell et al. 2003; Bergquist et al. 2006). These features have been referred to as "seascape" patterns in subtidal areas of bays, and "landscape" patterns in intertidal areas along shorelines and channels (Winslow 1882; McCormick-Ray 1998). Hofstetter (1977) recognized that low salinity following high-inflow events often corresponded to enhanced survival of oyster populations in central Galveston Bay depending on the spatial orientation of reefs. Historically, North and South Redfish Reefs in central Galveston Bay have produced the greatest amount of oyster biomass and maintained consistently stable oyster populations despite floods or droughts (Hofstetter 1977). Powell et al. (2003) also described how distance from freshwater sources, volume of freshwater inflow, size of navigation channels, and the ability of oysters to modify their habitat, could potentially determine future abundances of oysters in Galveston Bay.

Butler (1954) provided a description of four categories of oyster populations that form reefs dependent on their distance from freshwater sources and their salinity regimes. His first type was located near the head of the estuary with salinity regimes of 0 to 15 ppt, with average annual means of 10 ppt, with sparse populations, living in marginal environments. These populations will be referred to as "up-estuary" populations in this discussion. Butler (1954) described these populations as being composed of mostly small, rounded oysters with smooth, white shells due the absence of fouling organisms. He indicated that these populations typically received low rates of spat setting on the reef. He indicated there would be relatively good growth of younger

or submarket-size oysters during their first season, but slower growth of older market-size oysters. He characterized these oyster populations as having a higher-than-average annual mortality, and periodically decimated in flood years by excessive fresh water. However, periodic flooding reduced predators and parasites, thus increasing chances for survivors after flooding occurred. He also commented that these subtidal up-estuary populations had many characteristics in common with intertidal populations, which grow at or above mean low water regardless of salinity level. Typical transverse ridge reefs such as Fishers Reef in Galveston Bay and Shell Island Reef in West Matagorda Bay (WMB) are examples of Butler's up-estuary populations, which are located only a few kilometers from freshwater sources.

Butler (1954) described a second oyster population type located further "down-estuary," where salinity levels fluctuate between 10 and 20 ppt, and annual mean salinity is near 15 ppt. He indicated that population density or numbers of oysters on the down-estuary reefs often reached a maximum carrying capacity for spat set due to the population's collective spawning potential, increased availability of shell substrate, and relatively low density of predators within these salinity ranges. However, such high oyster population densities often lead to intense competition for food, and contribute to reduced growth and survival of newly settled spat (Zajac et al. 1989). Butler stated the individual oysters in these populations exhibit moderately well to uniform shell growth, and form definite year classes. He described a typical oyster in this type of population as having relatively smooth and dense or thick shell valves, with evidence of moderate fouling organisms and infections from boring sponge and clam. He indicated these types of populations often form interlocking clusters of long narrow shaped shells, depending

on the stability of the bottom sediment type. He also reported that although the meat of these populations might have high nutritional value based on its quality and size, these oysters would taste less salty and therefore be less appetizing to eat. Whereas this type of oyster population may be productive in most years, Butler indicated that during drought years, these populations were more likely to experience increased mortality from predation by the oyster drill *Stramonita haemastoma.* Butler also pointed out that in flood years individual growth of oysters in these populations could be delayed for several months, and their shells may show signs that indicate negative (or loss of previous year's) growth, hence the term "retrogressed shells" (Ray 1987). Typical "down-estuary" oyster populations are located several kilometers from the Trinity and San Jacinto Rivers in Galveston Bay. These down-estuary populations include the pancake reef formations on South Redfish Reef and the bisected transverse-ridge formations remaining on North Redfish Reef since construction of the Houston ship channel. Typical down-estuary oyster populations in Matagorda Bay are best exemplified by the transverse-ridge formation of Mad Island Reef. This reef receives intermittent overland flow especially following locally intense precipitation events in addition to direct inflows from the Colorado River. Typical down-estuary oyster populations are also found on the transverse reef formation known as Gallinipper Reef in Lavaca Bay.

Lavaca Bay oyster populations also tend to form longitudinal parallel reefs from up-estuary to down-estuary positions along the Lavaca Ship Channel, which are similar in form to Galveston Bay's longitudinal reefs along the Houston Ship Channel. These transitional types of reef populations benefit from both strong tidal currents and

freshwater inflows due to their proximity to deepwater channels in shallow bay systems (Galtsoff 1931; Scott 1968).

A third category of oyster populations described by Butler (1954), which will be referred to in this study as “gateway” populations, are found closer to the mouth of estuaries and passes to the Gulf of Mexico. Butler characterized this type of oyster population as having a mean annual salinity level of 25 ppt with seasonal fluctuations ranging from 10 to 12 ppt during the wet season, to 30 ppt during the dry season. This type of oyster population is characterized by unusually high individual growth rates, although actual growth patterns may be difficult to discern due to the amount of shell erosion and damage from predators associated with this salinity regime. Butler (1954) indicated that these gateway oyster populations are located in higher salinity regimes and their reefs have the greatest diversity of both marine and estuarine organisms. He also indicated that the reduced density of individuals in gateway populations living in higher mean salinity regimes have a much lower spawning potential and growth rates than are generally found in the down-estuary populations, which thrive in lower mean salinity regimes. He emphasized that the numerous parasites and predators residing under these conditions of higher salinity prevalent in gateway populations provide a counter-balance between other limiting factors influencing population density of oysters and spat survival. He pointed out that young oysters and spat of gateway populations have initially-higher mortality rates, which prevents oyster clusters from becoming too densely set, or “wrapped up in spat”. Thus less dense sets provide new individuals an opportunity to rapidly accumulate shell growth and increase tissue weight; and to achieve higher survival rates after their first growing season. Butler described the shells

of gateway oyster populations as being thick and well rounded, with ample substrate for burrowing activities of predators and commensals. He noted that these population's shells would also show heavy concentric ridges, indicating periods of fast growth. Butler also reported the meat from these oysters had excellent texture and taste. Butler concluded that these populations were more likely to benefit from being scraped or worked by dredges during the harvest season, which removes accumulations of "undesirable predators and commensals." Typical gateway populations are best exemplified by Hanna's Reef in East Bay, Dollar Reef in Lower Galveston Bay, Sammy's Reef in WMB, Indian Point Reef in Lavaca Bay, and First Chain Island Reef in San Antonio Bay.

Butler (1954) described a fourth type of oyster population that is located at the junction of the estuary near passes to the Gulf of Mexico, where salinity levels are consistently high and where there is little or no influence from freshwater sources. He referred to these as "pass" oyster populations. Although these types of populations form reefs in these higher salinity locations, the environmental conditions are marginal for their survival compared to down-estuary or gateway oyster populations. Butler characterized pass oyster populations as having low population density, slow growth rates, and high mortality rates. Butler observed that the scarcity of suitable substrate or "cultch" in addition to higher concentrations of predators were most likely to be the "driving factors" for lower spat survival rates in these populations. He indicated that these populations were of negligible commercial importance and had very low reproductive capacity. However, Butler speculated that pass oyster populations could provide supplemental distribution of larvae to up-estuary oyster populations following

disastrous floods; and potentially could repopulate flooded areas where recently dead oyster shells provided optimum setting substrates. According to historical records, Half Moon Reef at the junction of WMB and the main portion of Matagorda Bay displayed characteristics of Butler's pass oyster populations where population numbers on Half Moon Reef increased substantially following flood years, and declined following drought years (Moore 1907; Galtsoff 1931). This pass type of reef has been documented to be close enough to the Gulf of Mexico to be primarily influenced by marine predators and commensals, with higher mortality rates than other reefs in WMB (Butler 1954; King 1989). The oyster population on Half Moon Reef has been substantially reduced over the last century, and additional forces from hurricanes have continued to reduce its vertical relief to that of surrounding bottom elevations.

Pass reef oyster populations are also found near Blue Buck Point Reef at the junction of Sabine Pass with the Gulf of Mexico along the Texas and Louisiana border (Hedgepeth 1953). These oyster populations endure strong freshwater inflows from the Neches River and strong tidal influences from the Gulf of Mexico (Diener 1975). These populations have high reproductive and growth success in years following floods or lowered abundance of market oysters and poor growth following drought years. These pass oyster populations do not have the potential larval sources from up-estuary populations to replenish their depleted populations following drought years. Sabine Lake contains primarily soft substrates overlying clay bottoms, and there are no oyster reef formations in up-estuary areas where larvae spawned from the Blue Buck Point Reef would be able to survive if they set on these sediments.

Another type of oyster population forming marginal reefs in South Bay, in the southern part of the Laguna Madre, near the Texas-Mexico border was reported to survive 35-60 ppt salinity regimes (Hedgepeth 1953; Diener 1975). These oyster populations initially appeared to be adapted to nearly oceanic salinity regimes where they have no direct source of freshwater inflow from rivers or bayous (Hedgpeth 1953). However, King et al. (1994) found that these oysters were genetically distinct populations that differed from oyster populations in other bays along the Texas Coast. They attributed these genetic variations to adaptations to physiologically different ecotypes. They based their conclusions on a study by Stauber (1950), which provided evidence that differential spawning behaviors in response to thermal stimuli created opportunities for genetic variations. They also referenced Breuer's study (1962) which claimed that variation in growth rates is due to adaptation to hypersaline conditions. These populations are not typical of "pass communities" because they are adapted to hypersaline conditions.

Distances among reefs

The locations of oyster communities in a bay system are not random. They develop across estuaries from organized density patterns that correlate to sediment stability, tides, distances from sources of freshwater inflow (previously discussed), current velocities and durations, and other hydrological features of bay systems (Winslow 1882; Grave 1901; Galtsoff 1931; 1964; Hedgpeth 1954; Butler 1954; Price 1954; Hofstetter 1977; Ray 1987; McCormick-Ray 1998; Powell et al. 2003; Bergquist et al. 2006). These studies show that oyster populations form reefs in response to their surrounding environment. Oysters can grow as single individuals or as clusters of

multiple individuals across mud and sand, or in dense beds of their own accumulated shells (Winslow 1882; Galtsoff 1964; Baher and Lanier 1981; Dame 1996). The location of oyster populations in estuaries is related to current speed and bottom roughness (Wildish and Kristmanson 1979), and to hydrology (Hedgpeth 1953; Powell et al. 2003). Greatest abundances of oysters were reported for tidal streams where current velocities diverge from the main flow (Keck et al. 1971) or in estuaries where reefs intersect the flow of major currents (Hedgpeth 1953; Scott 1968). Reefs have the potential to divide bays and change circulation patterns (Diener 1975), thus altering local environments and associated flora and fauna (Britton and Morton 1989).

In describing the development of transverse reefs across bays, Scott (1968) provided a rational explanation as to why oyster communities accrete vertically more than horizontally, to the point at which the reef crest is within a few centimeters of the mean level for high tide. These vertical ridge reefs having intertidal crests can act as barriers or strongly affect circulation patterns in Texas bay systems. Where currents flow over and through the interstitial spaces of the accreting reef, velocities become greater along segments with smaller diameters. Currents within a bay system will generally be stronger where the water crosses a shoal or reef crest than over bottom areas with lower relief. These currents over reef crests also provide more favorable conditions for vertical oyster reef development and growth of larger populations. However, transverse-ridged oyster reefs have a biological problem of “self-siltation” that limits formation of adjacent reefs (Scott 1968). As the flow passes over the reef’s crest, oysters repeatedly shut their valves to eject pseudofeces, which are composed of particles rejected by their filtering system bound in mucous strings. These ejected “sticky” pseudofeces collect on adjacent

bottom sediments and prevent any larvae from setting in these areas that might otherwise accrete along the periphery of the reef. Scott (1968) indicates that the spacing between transverse reefs depends on several variables including current velocity, population densities on the reef producing pseudofeces, the amount of suspended sediments in the water column, and water depth of inter-reef areas.

Biotic interactions among reefs and environmental variables

Lengthy periods of drought and/or low freshwater inflow allow salinities to rise and oyster mortality from predation and parasitism to increase (Ray 1987). Alternatively, floods can suppress salinities long enough to cause massive oyster deaths (Hofstetter 1977; Wilber 1992). However, abundant spat set in Galveston Bay was synchronous with above-average freshwater inflows (Hofstetter 1977). In such years, oyster mortality from flooding was more than compensated by increased spat set on dead shells. Recent analysis of unbiased fisheries-independent data for Galveston Bay shows that oyster population abundance increases one- to two-years after increased freshwater inflows and associated decreases in salinity (Buzan et al. 2008).

Oyster commercial landing records for Matagorda Bay were reported to be correlated with salinity regimes, before and after freshwater inflows from the Colorado River were diverted to the Gulf of Mexico (Wilber and Bass 1998). Oyster landings from reefs nearer to freshwater sources were negatively associated with the duration of low flows that had occurred two years earlier, as well as with the maximum annual river flows in the current year. Therefore, expected benefits to the oyster harvest from increases in freshwater inflows during low flow periods would be realized two years later.

Along the eastern United States coast, tidal height has been demonstrated to be an important variable in the responses of both intertidal and subtidal oysters to salinity changes (Street et al. 2005). Along the Gulf of Mexico, average daily change in tidal height rarely exceeds 0.5 m, whereas wind forces, along with flood water height and duration, have a much greater influence on immersion-emersion regimes for intertidal reef communities (Hedgpeth 1954). However there are semi-annual tides that lead to extreme high tides in the spring and fall and extreme low tides in the summer and winter (Smith 1978) that may have important influences on all Texas oyster populations. Oysters living in intertidal zones grow slower and support less-diverse communities of associated species, as compared to oysters in subtidal zones, where greater mortality is related to increased exposure to predators and parasites (Roegner and Mann 1995; Bartol et al. 1999; O'Beirn et al. 2000).

Interactions among oyster populations and Dermo

The first major oyster pathogen in Texas is the protozoan *Perkinsus marinus* (Levine 1978), synonymous with *Dermocystidium marinum* (Mackin et al. 1950), and later as *Labyrinthomyxa marina* (Quick and Mackin 1971). Mackin used histological methods to describe features of this parasite, which is commonly referred to as Dermo disease. Histological sections of this parasite in oyster tissues showed a direct relationship of pathogen intensity to oyster deaths (Mackin 1951). Dermo is a major cause of oyster mortality and strongly influences oyster population dynamics (Ray 1954; Quick and Mackin 1971). Ray (1966) developed a partial culture technique for Dermo that facilitates early disease diagnosis and provides an opportunity to understand its interactions with its host. Dermo has a direct life cycle where waterborne infective

stages pass from oyster to oyster (Craig et al. 1989). The division rate of Dermo cells within oysters has been related to both temperature and salinity of the surrounding water (Hofmann et al. 1995). When salinities are greater than 10 ppt, Dermo cell division is primarily affected by and increases in temperature; however when salinities are less than 10 ppt, Dermo cell growth decreases sharply with salinity and is also affected by temperature (Hofmann et al. 1995). Although these terms for cell division rate are generally applicable to most oyster populations, there are other complex interactions within populations and surrounding populations that suppress or enhance cell division rate (i.e. density of oyster populations, recent spawning and depletion of tissue weight, etc.).

The focus of previous efforts to control Dermo infection have primarily been through management of the oyster harvest (Hofstetter 1977), rather than managing the oyster's response to infection (Soniat et al. 1998). Soniat (1996) provided a review of the chronology of selected epizootiological and related studies on Dermo from the Gulf of Mexico. Dermo suppresses the oyster's immune response by reducing the effectiveness of oyster phagocytes, which makes the oyster more susceptible to many other opportunistic organisms. The Eastern Oyster Biological Review Team (2007) reported that Dermo typically infects oysters in their first year of life, proliferates, causes up to 50% mortality of infected oysters in their second summer season, and results in 80-90% mortality by their third year of life. They concluded that oysters infected with Dermo rarely survived past their fourth season of life.

The chronic nature of Dermo disease allows infected oysters to spawn during the first summer, and some even spawn a second or third time before succumbing to the

infection. Although Quick and Mackin (1971) did not identify the specific relationship between levels of infection in pre- and post-spawning oysters, they noted degeneration of oyster gonads if Dermo was present during the early stages of gonadal development. Wilson et al. (1988) and Choi et al. (1989) found that spawning success selectively reduced oyster biomass more than Dermo biomass, thus raising the relative density of Dermo cells per gram of oyster tissue weight to lethal levels as the spawning oyster depleted the energy reserves that it would otherwise have to fight the infection. Therefore, they concluded that successful spawning significantly increased Dermo infection levels and disease progression in oyster populations, resulting in additional Dermo-related mortality and is likely to have an indirect influence on subsequent oyster fecundity.

Powell et al. (1992) suggested that recruitment failure could be a principal mechanism for increasing infection levels in oyster populations and initiating an epizootic event. A contrasting scenario is that an epizootic event in an oyster population could be terminated by a massive spawning event wherein new and uninfected biomass replaces old infected oysters that die from the disease (Powell et al. 1996; Soniat et al. 1998). In the latter scenario, Dermo infection in immature submarket (< 76 mm shell length) oysters is reduced and, given enough food sources, these oysters could grow fast enough to dilute the *P. marinus* density in the population and recoup the fecundity of an uninfected oyster population (Powell et al. 1996; Soniat et al. 1998).

Several studies have shown that the size class of the oyster also should be considered in understanding Dermo infections (Ray 1996; Kennedy et al. 1996). Ray (1996) showed that submarket sized oysters generally have lower percent infections or

weighted incidence (WI) until they reach market size (≥ 76 mm shell length). He also showed that Dermo-related mortalities (10-50 %) occurred primarily in mature oysters, whether they were market-size or submarket-size, rather than in submarket oysters that had not spawned during their first season of life (Ray, 1996). Dermo levels in spat (< 26 mm shell length) have only recently been investigated for West Bay and indicate that spat on intertidal reefs are less infected than those on subtidal reefs. This may be related to different submersion and exposure cycles and the proximity of infected market or submarket individuals (Ray 2008). Because higher Dermo levels occur primarily in mature oysters, the potential for Dermo-related mortality is higher for market-size oysters, and could negatively affect production of harvestable oysters.

Biotic and abiotic interactions in oyster models

Environmental variables that influence oyster population dynamics in complex spatial (geographical and structural) and temporal (seasonal) patterns have been studied by several researchers (Song 1993; Wilbur and Bass 1998; Powell et al. 1998; Powell et al., 2003; Turner 2006, Buzan et al. 2008*)*. These studies established that fluctuating salinity regimes provide the optimum conditions for growth, reproduction, control of predators, and distribution of larvae. Several of these studies have defined specific time lags of 18 to 24 months for oyster populations to respond to high or low inflow events that occurred earlier in time (Wilber and Bass 1998; Buzan et al. 2008). These time lags can be directly correlated with the amount of time it takes spat to grow to market size (Hofstetter 1977; Kraueter et al. 2007; Buzan et al.2008). However, the complex interactions of salinity with other abiotic factors such as temperature and biotic factors such as nutrients (phytoplankton populations) may not be as easily correlated with 18 to

24 month time lags for reefs that are spatially separated or structurally different in population size and density.

The majority of oyster models that have been developed to date have attempted to incorporate complex ecological and spatial relationships for salinity and temperature to entire bay systems with the assumption that oyster populations are nearly homogeneous, density independent, and that their reefs are all flat “pancake-like” structures such as South Redfish Reef (Hofmann et al. 1992; Powell et al. 1994; Hofmann et al. 1995; Powell et al. 1996; Dekshenieks et al. 2000; Powell et al. 2003). These models consider individual oyster responses to environmental variables in terms of food assimilation and respiration, under the assumption that their valves were constantly open and that their responses were instantaneous or dependent on average temperature or salinity conditions over monthly or seasonal periods of time. Oyster populations as previously discussed in this study form at specific distances from other reefs and freshwater sources; and also have distinct salinity and temperature regimes that are characteristic of that specific type of reef formation. Oyster population dynamics of these individual reefs may depend on their interaction with other species within their own community, on the relative proportion of different size classes in each population, or on how each reef population interacts with other reef populations. Comparisons of oyster densities at pancake reef formations with those of transverse or longitudinal ridge type reefs have shown that large expanses of oysters without extensive vertical reef relief react differently to sediment deposits due to the available space between oysters and the current speed over the reef. Whereas the former structure has advantages for growth and

reproduction under normal flow conditions, the later has advantages that enable it to survive during extreme current speeds and sedimentation conditions.

Oyster population response times to lower salinities following flood conditions are primarily dependent on water temperatures. However, oysters may close their valves for almost 30 days when temperatures are less than 20 °C, whereas their valves may not remain closed for longer than 10 days when temperatures are greater than 25 °C (Higgins 1980). Overlooking simple timing factors such as how long an individual oyster may keep its valves closed during extreme freshwater inflow events may not initially appear important to understanding the complexity of the collective oyster population's response. However the abiotic factor of warmer temperatures in combination with the biotic factor of time that an oyster's valves are closed becomes synergistic or elicits a response threshold not generated by one factor alone. Complex population responses to harsh environmental conditions may occur over discrete time periods. The timing or duration of a flood or a drought may also result in long term responses of increased mortality; increased spat settlement; shorter or longer growth rates; delayed or increased reproduction; or spat recruitment to another up-estuary reef. Averaging monthly or yearly environmental variables often diminishes the response pattern being investigated.

Dissertation objectives

Previous oyster population dynamic models have attempted to tie in all of the biotic and abiotic factors that influence oyster physiology, respiration, assimilation of nutrients, growth, and mortality from harvest as well as disease interactions. However, these models have been applied to one bay system, and were not focused on one regional

area or one reef in determining the spatial and temporal patterns that have formed that reef into either a longitudinal, transverse, pancake or tow-head reef configuration. These "individual-based" oyster models have accounted for interaction of the environmental and biotic factors without attempting to distinguish conditions for up-estuary or down-estuary reefs that are spatially separate although they may have similar rationales for their formation.

In this study, the historical and current spatial and temporal trends in oyster population dynamics and the interaction of Dermo infection and freshwater inflows on three reefs along a salinity gradient in WMB were examined. Chapter I reviews the historic and current spatial and temporal trends of oyster reefs and their potential interactions with regard to temperature, salinity, flow and distance from freshwater inflows. Chapter II examines spatial and temporal patterns in demographics of three oyster reef populations along a salinity gradient in WMB. Population variance of these three communities appears to be influenced by distance and flow from freshwater sources; and spat set is observed to be influenced by the duration and volume of flow at least one month prior to major spawning events (Ray 2003-2007 unpublished data). Although these three reef populations are spatially disconnected, they are temporally connected through environmental factors influencing their reproductive strategies for survival. Chapter III emphasizes the importance of spatial and temporal patterns of Dermo infection in oysters on these three oyster reef types along a salinity gradient in WMB. Variation in levels of Dermo infection (prevalence) and number of hypnospores of Dermo per gram of wet tissue weight derived from weighted incidence (WI) are shown to be influenced by distance from freshwater sources. An evaluation of distance

shows both spatial and temporal influences on environmental factors such as temperature and salinity, and thus distance indirectly affects spawning interactions of these three populations and their response to Dermo. Those populations that have recently spawned appear to have higher levels of Dermo infection and thus greater mortalities than those preparing to spawn or not in reproductive modes. Chapter IV discusses the development of an interactive Stella oyster community based model to quantify and integrate the spatial and temporal patterns influencing reproduction, larval distribution, larval settlement, individual growth of each size class (larvae, spat, submarket, market, market that are older than two years of age) and population growth on these three oyster reefs. The three reef population submodels in Chapter IV incorporate spatial and temporal trends revealed in Chapters II and III. Simulations over a 50-yr period using historical five-year environmental records show that reef populations located farthest from Colorado River will decrease in abundance with loss of freshwater over time. Simulations also show that reef populations located closest to Colorado River will be impacted by lower larval recruitment following declining spawning potentials from increased salinity and increased disease levels at reefs located further from the Colorado River. The three reef population submodels also include a proportion of larvae recruited from the Colorado Delta based on recently mapped areas by the Lower Colorado River Authority (LCRA) and average densities of intertidal oyster populations along the Texas Coast.

CHAPTER II

SPATIAL AND TEMPORAL PATTERNS OF OYSTER POPULATION DEMOGRAPHICS IN WEST MATAGORDA BAY

Introduction

The West Matagorda Bay Ecosystem Complex is the second largest estuarine system in Texas with a surface area of approximately 1070 km^2 (Fig. 1) (Ward et al. 1980). The discharge of the Colorado River, with mean annual flows of approximately 76.5 m^3/s, is relatively small compared to the size of Matagorda Bay (Ward et al. 1980). Mean annual low flows were estimated to be 14 m^3/s (500 cfs), which result in no net movement (over tidal influences) of freshwater from the Colorado River into the eastern arm of West Matagorda Bay (WMB) during low-flow conditions (Ward et al. 1980).

The WMB watershed comprises two major river basins and a number of smaller tributaries (Fig. 2). The Colorado River Basin drains approximately 101,171.41 km^2 (25 million acres) and stretches from New Mexico across Texas to WMB. Lavaca Bay, a secondary bay of WMB, receives its freshwater input from the Lavaca-Navidad River Basin. The Lavaca-Navidad River Basin drains approximately 5,665.6 km^2 (1.4 million acres) of south central Texas. About another 6,070.28 km^2 (1.5 million acres) are drained by smaller tributaries such as the Tres Palacios River, Turtle Creek, Carancahua Creek, and Keller Creek. Altogether, WMB receives water from over 25% of Texas counties.

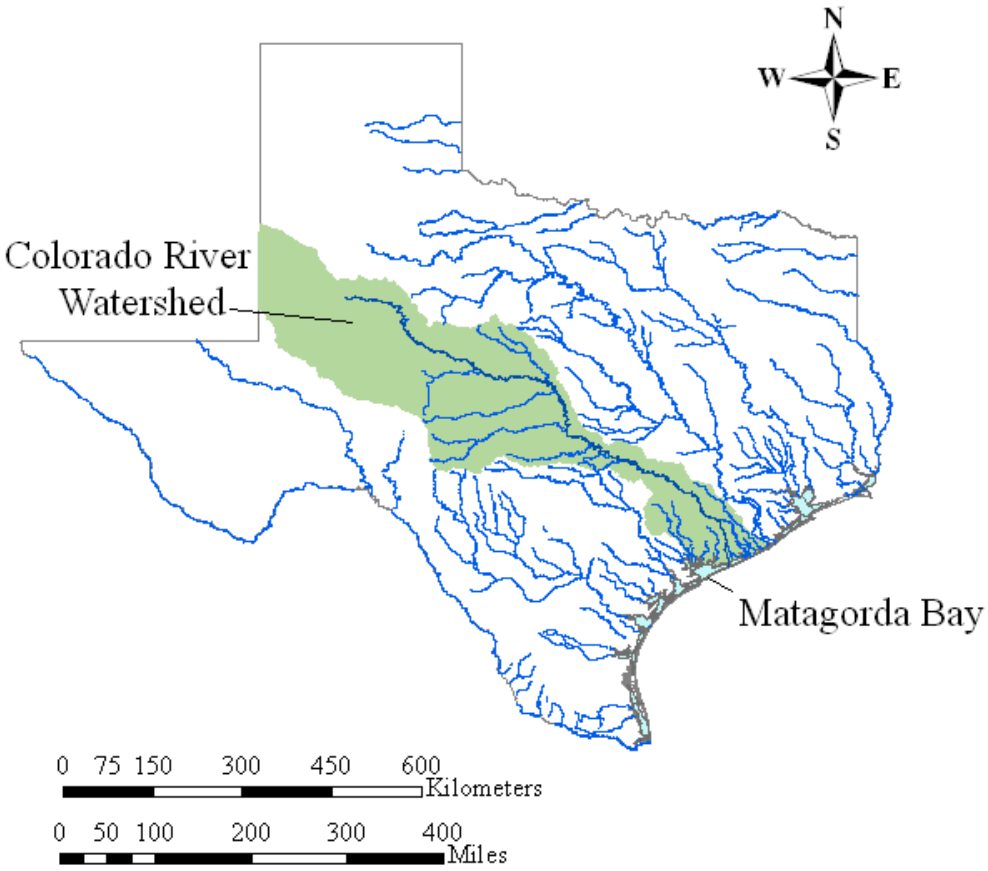

Figure 1. Matagorda Bay ecosystem and Colorado and Lavaca River watersheds.

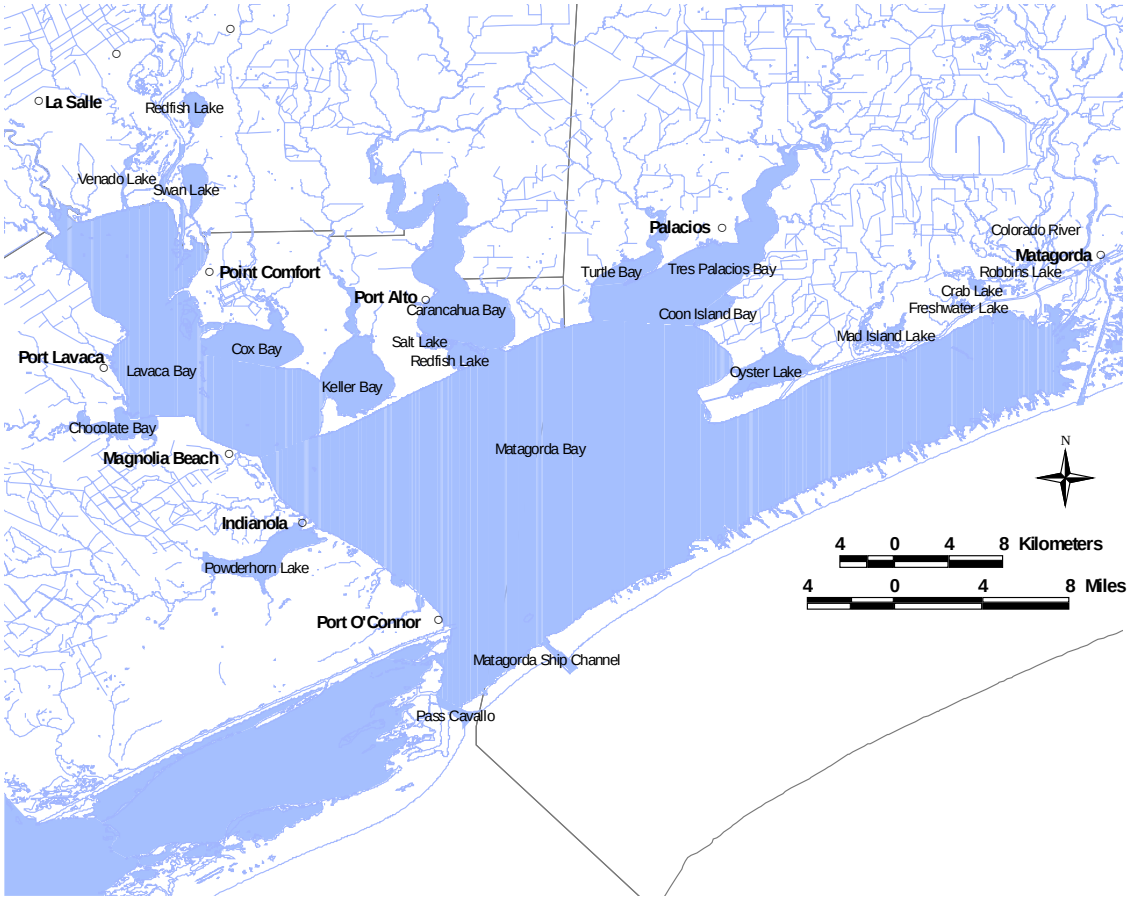

Figure 2. Matagorda and Lavaca Bays, minor bays and tributaries.

Historically Matagorda Bay was a single bay, which became two bays by the Colorado River Delta formation between 1929 and 1941, which resulted from removal of a log jam from the Colorado River, and released sediments across Matagorda Bay (Ward and Armstrong 1980). In 1934, a dredging operation cut through Matagorda Peninsula, allowing the Colorado River to flow directly into the Gulf of Mexico, expediting the delta formation that separated East and West Matagorda Bays. In 1991, the USACE completed the Matagorda Diversion Channel to increase freshwater inflows into the eastern arm of WMB and to restore estuarine salinity regimes to those present

before the 1934 Colorado River diversion project. Currently the Colorado River flows primarily into WMB, and small portions escape to EMB and the Gulf of Mexico.

Currently, three major oyster reefs lie between the Colorado River Delta and the land cut for the Gulf Intercoastal Waterway (GIWW) at the edge of the eastern arm of WMB. Two are historic reefs known as Shell Island and Mad Island, which are included in this study. Texas Parks and Wildlife Department (TPWD) monitored these reefs for oyster population growth, mortality rates, reproduction, and disease rates from 1959 to 1977 (Hofstetter and Heffernan 1959; Moffett and Murray 1963; Heffernan 1963; King 1964; Hofstetter et al. 1965; Hofstetter 1965; Hofstetter 1966; Hofstetter 1967). Additional population and disease studies on these reefs were conducted by U.S. Fish and Wildlife Service (USFWS) prior to the 1991 Colorado River Diversion Project re-establishing the flow back into the eastern arm of WMB (King 1989). Thereafter, the USACE monitored these reefs (Wilber and Bass 1998) as part of their post-diversion efforts. The USACE also restored portions of Shell Island and Mad Island Reefs, and constructed a third reef, known as Sammy's Reef in 1995. Although multiple patch types of reefs in East Matagorda Bay (EMB) were similarly impacted by loss of freshwater inflows prior to 1991, they were not included in the USACE restoration plan. TPWD has conducted routine resource monitoring of the three WMB reefs since the coastal resource monitoring program began in 1986 (Martinez-Andrade et al. 2003).

The objectives of this study were to determine the spatial and temporal patterns in demographics of these three oyster reef populations along a salinity gradient in WMB. Although these three reef populations are spatially separated by distance from each other and freshwater sources, they appear to be spatially and temporally connected through

environmental factors that influence oyster population reproduction and survival strategies in WMB.

Historical and current oyster population distributions

Prior to the Colorado Delta formation, Moore (1907) reported 12.57 km^2 (3,108 acres) of viable subtidal oyster reef habitat in WMB (Fig. 3). Although he was unable to survey two tidally connected embayments north of Mad Island Reef (Oyster and Mad Lakes), he noted they contained densely populated intertidal oyster reefs. Extensive intertidal oyster reefs were associated with the crests of Dog Island Reef (3.8 km^3 or 932 acres (Fig. 4), one of the most productive reefs in Matagorda Bay according to Moore (1907) and Galtsoff (1931).

After the log jam was removed from the Colorado River in 1929, the once-confined sediments that had been stored over many years were suddenly released and completely buried Dog Island Reef. The sediments from the Colorado River Delta are currently forming intertidal reef populations along this new waterway, which are located within and close to the footprint of the former Dog Island Reef (MBHE 2006).

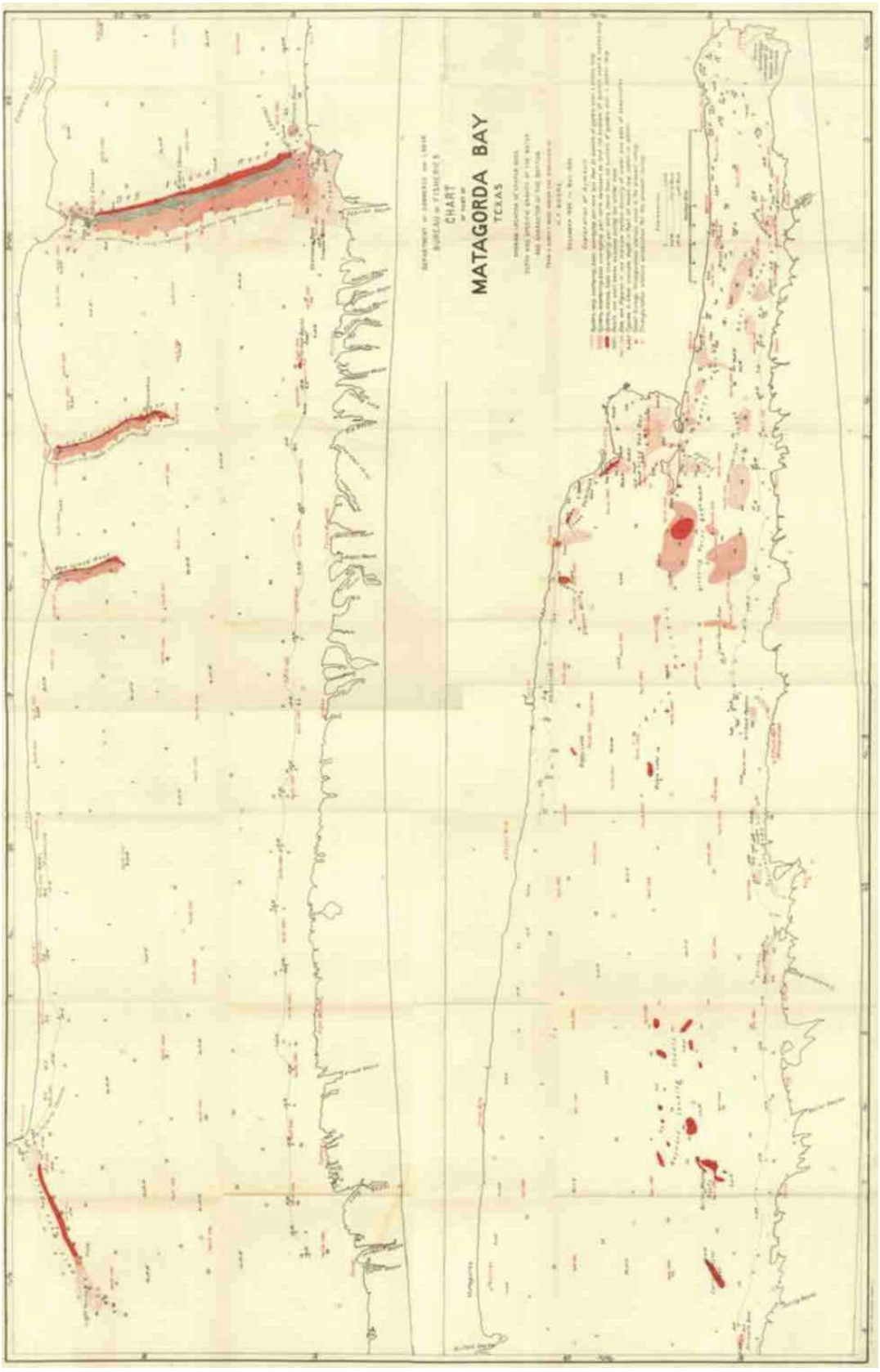

Figure 3. Matagorda Bay Reefs in 1904-1905 from Moore (1907), reprinted with permission from Figure 4-8 page 91 in Ward et al. 1980.

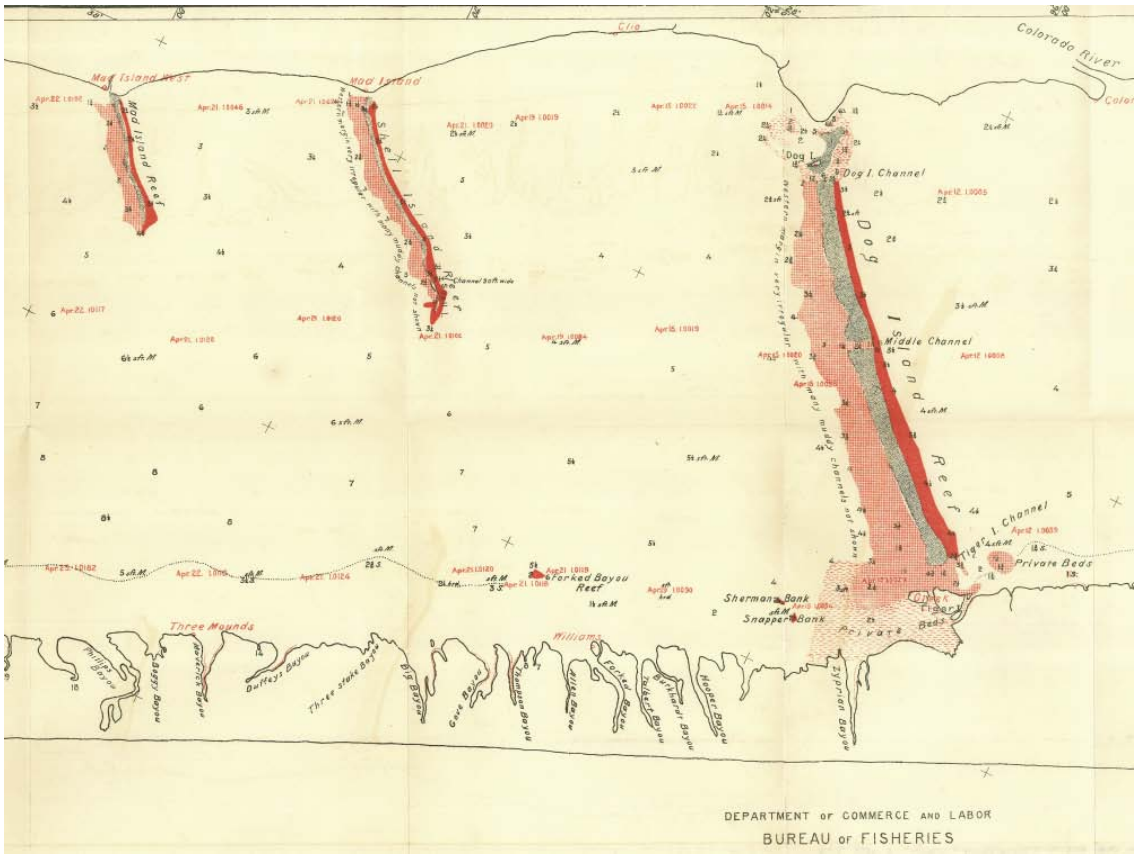

Figure 4. Mad Island, Shell Island and Dog Island Reefs, and Tiger Island Channel in Matagorda Bay in 1904-1905 from Moore (1907), reprinted with permission from Figure 4-8 page 91 in Ward et al. 1980.

After the Colorado River Diversion Channel to the Gulf of Mexico was completed in 1934, salinity gradually increased in WMB; and resulted in reduced fluctuations of freshwater inflows at gateway types of reefs like Half Moon Reef, furthest from the entrance to the Colorado River. Species diversity on this and other down-estuary reefs changed from *Crassostrea virginica* dominance to more marine-oriented species dominated by *Ostrea equistris*, *Busycon spiratum*, *Mercenaria mercenaria*, and *Astrangia astreiformis* according to King (1989). He linked the loss of freshwater inflows into WMB to increased predation by gastropods such as *Stramonita*

haemastoma as well as competition from other marine invertebrates on Half Moon Reef (1.99 km^3or 494 acres), at the junction of eastern arm of WMB.

In contrast, Shell Island Reef and Mad Island Reef had somewhat marginal estuarine conditions due to their proximity (within 1.6 km) to intermittent flows from the Colorado River through the GIWW and from coastal prairie run-off through Culver's Cut and Mad Island Slough (Fig. 5). These reefs continued to grow and reproduce on the up-estuary sides of their transverse ridge-type formation, but subsided on their down-estuary sides (King 1989).

Since the Matagorda Diversion Channel was opened in 1991, Shell Island and Mad Island Reefs have benefitted from their close proximity (6 to 9 km) to freshwater inflows from the Colorado River. These reefs also receive precipitation and run-off from coastal prairies along the north shore of WMB.

Although Mad Island and Shell Island Reefs are historically significant, they, along with Sammy's Reef, are currently being evaluated by multiple resource agencies (MBHE 2007) in regard to their potential to function as indicators of the environmental health of the eastern arm of WMB. The Lower Colorado River Authority (LCRA) is in the process of developing suitable criteria for freshwater inflows to ensure that any future freshwater diversions will continue to provide inflows adequate to maintain the ecological health and productivity of the Matagorda Bay ecosystem.

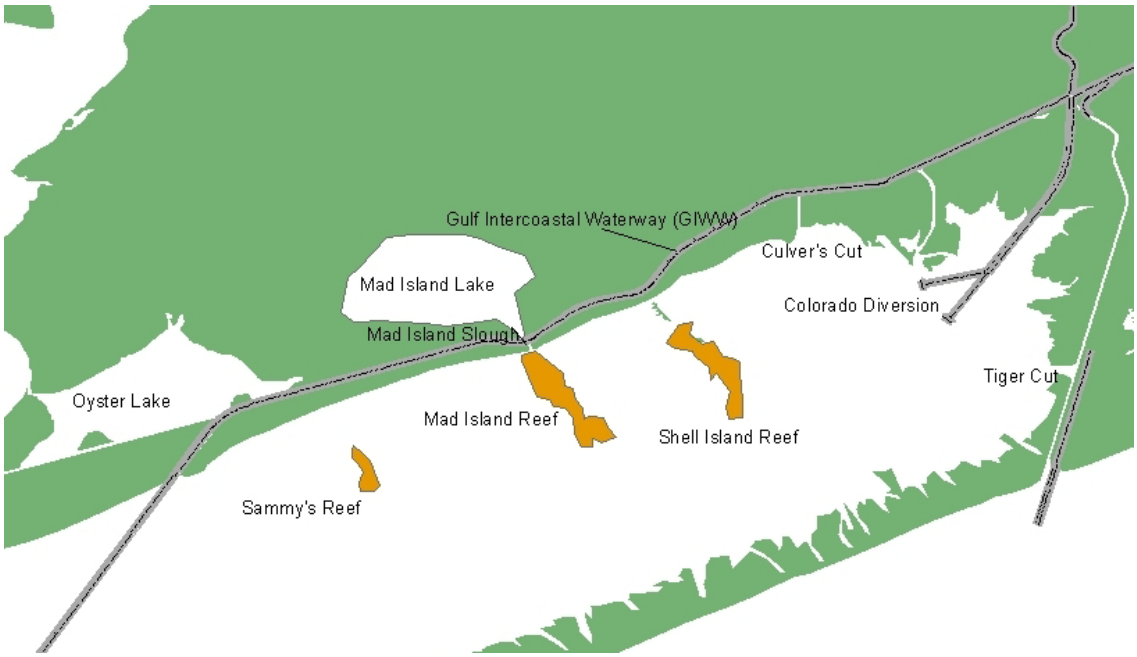

Figure 5. Matagorda and Lavaca Bay oyster reef sites sampled by TPWD; Shell Island (0.59 km^3 or 145 acres), Mad Island (0.38 km^3 or 93 acres), and Sammy's Reef (0.038 km^2 or 9.6 acres).

Spawning interactions

There is a wealth of information on eggs, larvae, spat, growth phases, fecundity, spawning potential, and natural mortality rates related to spawning stress for *C. virginica* (Hopkins 1954; Davis and Chanley 1955; Galtsoff 1964; Hofstetter 1977; Quast et al. 1988; and Kennedy et al. 1996). In Texas, spawning occurs primarily from April through November (Hofstetter 1977) although it also has been recorded in every month of the year in shallow-water bay systems where water temperatures remain optimum for spawning, as observed for Matagorda Bay (Hofstetter and Heffernan 1959; Hofstetter et al. 1965). Spawning by individual oysters can be induced by water temperatures that are consistently above 20º C, and temperatures above 25º C induce mass spawning (Hopkins 1931), but when water temperatures exceed 35º C, spawning is limited (Stanley and Sellers 1986). Under favorable conditions of temperature and food supply, oysters may

produce gonadal tissue and be ready to spawn within 10 days of receiving appropriate temperature stimulus (Loosanoff and Davis 1953). On Texas reefs, oysters may spawn several times a year (Hofmann 1992).

Spawning in oysters has been linked to ectocrines secreted from phytoplankton species (Gosling, 2002). Synchronicity and intensity of spawning is initiated by the males that release sperm accompanied by a pheromone into the water column (Andrews 1979). The females spawn either when sperm enter their water transport systems, or when the pheromone stimulates release of eggs in a mass spawning event (Bahr and Lanier 1981). Each female oyster produces from 23 to 86 million eggs per spawning event, in proportion to the size of the individual, and may spawn several times per season (Davis and Chanley 1955). Sexual maturity may be reached as early as six weeks post-settlement. Oysters are protandrous hermaphrodites, maturing initially as males and changing to females about one year later or whenever conditions are right for spawning. The sex ratio (number of females to males) of a population can be influenced by food limitations, shell damage, or sex of adjacent oysters (Kennedy et al. 1996).

Larvae and spat settlement interactions

Spat set (also referred to as spat fall) is reported to occur from 14 to 20 days post-spawning as larvae settle and undergo transformation (Stanley and Sellers 1986; Dekshenieks et al. 1993). The tissues of recently-dead, decomposing oysters release a pheromone that attracts larval oysters and increases spat set on the inside of these shells, which increases spat survival (Keck et al. 1971). In the laboratory Haskin (1964) showed that larvae increased their swimming activity in response to increasing salinities from 7 to 14 ppt, but swimming behavior was inhibited by declining salinities. Larvae

also responded to dim yellow-green light (575 nm) indicating phototaxis response (Hidu and Haskins 1978). Upward swimming rate under normal salinity and temperature conditions can be nearly 1 cm/s (Andrews 1979). Although oyster larvae are considered to be weak swimmers (1.0 mm/s) in the horizontal plane, they can become rapid swimmers (3.13 mm/s) when moving downward or responding to chemical cues on the bottom (Turner et al.1994; Kennedy et al. 1996; Newell et al.2005;). Swimming velocities of larvae increased threefold (to 3 cm/min) in either an upward or downward direction when salinity was increased by 0.5 ppt/hr (Hidu and Haskin 1971). This combination of behavioral traits appears to result in selective tidal transport towards the head of the estuary, even against a net downstream flow (Seliger et al. 1982).

Tidal currents can carry larvae considerable distances; for example, oyster larvae have been found to travel 10 km up-estuary in Louisiana (Gunter 1951). This directional transport increases their access to available estuarine substrate for settlement and prevents them from being flushed downstream towards the less favorable marine environment of the Gulf of Mexico. Estuaries subjected to strong tidal exchanges tend to have low, but consistent, pulses of larval oyster recruitment, whereas those with weak freshwater inflows and sluggish circulation cause larvae to undergo extended residence time and higher, albeit less regular, recruitment (Kennedy et al. 1996). Larval retention is generally explained by either “passive” transport induced by physical factors, or “active” transport in which larvae swim up-estuary, or a combination of both as observed in Galveston Bay (Dekshenieks et al. 1996).

Distribution of oyster larvae in Matagorda Bay had not been determined during previous studies conducted by TPWD. However, one could expect that the burial or

disruption of Dog Island Reef, formerly the largest transverse reef in WMB, would have adversely affected larval recruitment for WMB. Higher salinities recorded by TPWD between 1959 and 1990 resulted in poor recruitment of spat and low population estimates (King 1989; Wilber and Bass 1998). Previous studies have indicated that oyster larval distribution is correlated with an up-estuary transport pattern, and larvae have been shown to swim towards lower salinities and are less inclined to increase swimming speed against currents when salinities are greater than 20 ppt in a flood tide (Hidu and Haskins 1971; Kennedy et al. 1996).

Salinity regimes have changed in WMB since the Colorado River Diversion was opened in 1991. Oysters populations have accreted along the Colorado Delta (MBHE 2006) and were recently estimated to have increased in aerial extent by 0.591 km^2 (146 acres). Shell Island and Mad Island Reefs have accreted along their leading edges as shown by recent side scan surveys conducted by oil and gas developers in WMB (TPWD unpublished records for Palace Exploration). Although larval transport models are not currently available for this bay system, the present study will explore the potential interaction among reefs to determine the probability of larvae moving from down-estuary reefs to accreted oyster shell substrate in up-estuary reefs.

Individual growth and trophic interactions

Oysters have characteristically discrete growth patterns—larvae, spat, and submarket oysters grow relatively fast, then enter a no-growth period when energy is diverted to gonadal tissue production and spawning, after which growth resumes until oysters reach market size or greater (Kraueter et al. 2007). After oysters reach maturity, whether at market or submarket size, growth proceeds more slowly. These discrete patterns in growth can lead to oscillations or "limit cycles" in oyster populations (Kraueter et al. 2007). Environmental stresses (temperature, salinity, and disease) can also cause diversion of energy that would otherwise support growth or spawning. In cases of extended environmental stress when an oyster becomes too weak to filter enough food to sustain itself, retrogression in growth of shell and somatic tissues occurs in order to maintain basic metabolism for survival. Evidence of these patterns is most easily observed in the shell (Kraueter et al. 2007). Kraueter et al. (2007) reviewed previous studies on oyster growth rates over the past 75 years. These authors found a difference between growth patterns that result from studies using trays suspended above the bottom compared to studies of oysters placed on the bottom with or without the use of trays. They found that higher growth rates were reported for tray off the bottom where currents provide more food, and where filtration for food and respiration was maximized. They also found that bottom placement provided growth rates more typical of those found on the reefs where density of oysters played a major role in influencing filtration rates, and thus nutrition and respiration.

Oysters have been reported to grow optimally in salinities of 10 to 25 ppt (Cake 1983). Those exposed to fluctuating salinities within normal ranges grew faster than

those than those held at a relatively constant salinity (Pierce and Conover 1954). Oysters grow optimally at water temperature of approximately 25°C, whereas temperatures over 30°C can cause filter feeding to stop (Kennedy et al. 1996). When winter water temperatures ranged from 10 to 15°C, oysters ceased to grow somatic tissue mass.

Oysters grow faster where phytoplankton densities are high (Manzi et al. 1977), or when specific, nutrient-rich phytoplankton are available (Örnólfsdóttir 2002; Paerl et al. 2003). As suspension feeders, oysters filter water in the 3-4 µm particle-size range of phytoplankton as their primary food (Stanley and Sellers 1986). However, oysters are selective grazers and are able to ingest large volumes of seston in excess of that which they need for nutrients (Kiorboe and Mohlenberg 1981; Newell and Jordan 1983; Shumway et al 1985; Pastoureaud et al. 1995; Cognie et al. 2001). Seston with high detrital carbon content is a poor food source for oysters (Crosby et al. 1989). Food quality of the phytoplankton body composition (lipid and carbohydrate and protein amounts) in one study was found to be significantly correlated with the ratio of the oyster gonad thickness to adductor muscle diameter, also called the gonadal index (Soniat and Ray 1985). They concluded that food quality and quantity in the form of specific phytoplankton species in the spring and summer was most important for gametogenesis and spawning in Galveston Bay.

Recent surveys of phytoplankton functional groups (PFG) in Galveston Bay have identified the preferred phytoplankton groups for oyster nutrition as: diatoms, cyanobacteria, chrysophytes, and cryptophytes (Sheridan et al. 1995; Örnólfsdóttir 2002). Historical studies in Matagorda Bay also show that similar PFGs were dominant in this bay system in 1904 (Moore 1907).

Although dinoflagellates (some species cause red and brown tides), chlorophytes (green algae) and euglenoids only bloom periodically in Galveston Bay, these PFGs may only represent a small proportion of the total phytoplankton community (Örnólfsdóttir 2002). However, the nutritional value of phytoplankton varies among both major taxonomic groups and among individual species (Brown et al. 1997). Diatoms, prymnesiophytes and cryptophytes are rich in polyunsaturated fatty acids (5-35%), prasinophytes have low to moderate levels (4-10%), and chlorophytes are deficient (0-3%) (Brown et al. 1997; Paerl et al. 2003). Phytoplankton derived fatty acids, polyunsaturated fatty acids and amino acids beneficially affect the egg production and hatching success of most zooplankton and are directly linked to oyster nutrition (Kleppel and Burkart 1995).

Although oysters ingest entire cells of phytoplankton, it appears that the species (not its chemical composition, size or shape) is an important feature used in sorting particles for ingestion (Shumway 1996; Brown et al. 1997). However grazing by oysters can affect the structure and diversity of the phytoplankton community dynamics (Örnólfsdóttir 2002; Paerl et al. 2003). Nanoflagellates (cryptophytes) were abundant in Galveston Bay during the winter of 2000 following specific seasonal salinity and temperature conditions of a dry summer followed by fall flooding (Örnólfsdóttir 2002; Paerl et al. 2003). This group of phytoplankton was also found in gut contents of oysters and appears to be the responsible agent for causing red coloration to the meat tissue within a few hours to days post-harvest, making them unmarketable despite the absence of any toxins related to this microalga (Paerl et al. 2003). The pink coloration in oysters has been attributed to the cryptophyte's red accessory pigments (water-soluble

phycoerythrins), which were present in high abundance in the water of Galveston Bay during December 2000, and to small amounts of alloxanthin (the indicator carotenoid pigment for cryptophytes) that were detected by HPLC methods in oyster guts (Paerl et al. 2003). Galtsoff (1931) previously reported nearly blood red oysters from Galveston Bay in 1926 but was unable to correlate it with this alga. Paerl et al. (2003) showed that understanding community-level food value of phytoplankton is a critical component controlling somatic and gonadal growth mechanisms in oysters, and that evaluating chlorophyll *a* levels only would not provide an understanding of these biotic mechanisms.

Previous studies have reported that larval oysters prefer small, naked flagellates of the Phylum Chrysophyta, such as *Isochrysis albana* and *Monochrysis lutheri*, (Guillard 1957). Oyster larvae avoid or selectively remove specific chrysophytes like *Prymnesium parvum*, which produce toxins (Guillard 1957). However, when preferred foods (chrysophytes) become less available at temperatures exceeding 27ºC, or when other naked algae are scarce, the abundance of Chlorophyta can increase both in the environment and in the diet of larval oysters (Davis and Calabrese 1964). Juvenile oysters (size range 25-50 mm) begin to include diatoms like *Skeletonema* and cryptomonads in their diet as they grow towards mature market size oysters (Guillard 1957). However, when primary food sources are unavailable and temperatures are high, oysters may consume any species of diatoms and dinoflagellates in Texas estuaries (David and Calabrese 1964).

Oysters' retention efficiency and selective absorption of food particles may also depend on particle shape, mobility, density, and on chemical cues such as ectocrines

secreted by the plankton (Shumway 1985; Hawkins and Bayne, 1992; Gosling, 2002). Water flow regimes, including current speed and direction across the reef have also been shown to facilitate as well as inhibit capture of food particles by oysters (Newell and Langdon 1996). They found that excessive water flow causes food particles to move through the area before oysters can extract them.

An oyster population model of Galveston Bay simulated various amounts of chlorophyll *a* as an indicator of available nutrients to oyster populations (Dekshenieks et al. 2000). The conclusions of this study suggested that 14% reduction in phytoplankton biomass would cause a 43% decrease in the number of oysters and a 40% reduction in the number of recruits. These results do not take into account changes in phytoplankton species composition or selective grazing pressure by oysters. Powell et al. (1996) showed that slight reduction in food supply (<15%) may restrict oyster population growth in Galveston Bay as a whole, and increase the likelihood of epizootics and subsequent mass mortalities from Dermo disease. Although Matagorda Bay has been recently studied to quantify chlorophyll *a*, species composition has not been attempted (MBHE 2006).

Harvest patterns and DSHS closures

Commercial oyster landings recorded by TPWD for West Matagorda Bay, (excluding Lavaca Bay landings) reached its lowest levels in May 1991 immediately following the re-diversion of the Colorado River into WMB, with only 5,479 lbs of meat weight and ex-vessel value of $12,903 reported by seafood dealers (Culbertson et al. 2004). Oyster landings were consistently low for West Matagorda Bay reefs during the following four years, which was partially attributed to sedimentation and burial of

portions of Shell Island Reef, which is closest to the redirected Colorado River mouth (Wilbur and Bass 1998). WMB is currently located in a "conditionally approved area" for harvesting shellfish. This refers to whether or not an area is closed to oyster harvesting due to high bacteria levels following heavy rainfall or during harmful algal blooms (e.g., red tide caused by *Karenia brevis* (*Gymnodinium breve*). A map of "conditionally closed areas" regulated by Texas Department of State Health Services (TDSHS) for Matagorda Bay is available at: http://www.dshs.state.tx.us/seafood/classification.shtm#maps.

High inflows from the Colorado River since the 1991 diversion project was completed have affected harvesting primarily on Shell Island Reef. Shellfish markers placed by TDSHS on the edge of this reef delimit a restricted area west of Shell Island Reef, where no harvest is allowed at any time regardless of bacterial counts. Harvest of market sized oysters is only allowed from the conditionally approved area to the west of these shellfish markers in WMB during the public season; and only when bacteria counts are not exceeded by TDSHS standards. According to TDSHS harvest closure records all conditional areas of WMB were closed under Shellfish Marine Restriction order (MR-794) on November 2000 until December 2000 due to potential red tide conditions for all of Matagorda Bay. TDSHS records indicate that "conditionally approved" areas of Shell Island Reef have been closed during the majority of public harvest seasons between 1992 and 2007 due to high bacteria levels following heavy rainfall (TDSHS closure records; Kirk Wiles, personal communication). With Shell Island Reef closed to harvest, the majority of the Matagorda Bay (not including Lavaca Bay) landings reported by seafood dealers to TPWD are from Mad Island Reef, Sammy's Reef, and also from Tres

Palacios Reef whenever bacterial counts are within normal limits in these conditionally approved areas. Intertidal reefs located in enclosed embayments are restricted from harvesting. There are three tow-head reefs on the south side of WMB near the Matagorda Peninsula near Forked Bayou that also lie within restricted areas for harvesting.

Independent harvest records collected by TPWD show that landings have greatly increased on Mad Island Reef and Sammy's Reef in post-restoration and construction years when 293,516 lbs of meat weight valued at $651,811 were reported in 1997, and 259,968 lbs of meat weight valued at $692,443 were reported in 2006 (Fig. 6). Floods and excessive rainfall from Hurricane Claudette (July 2003) reduced the populations of market-size and submarket-size oyster on these reefs between the 2003 and 2004 harvest seasons. However, TPWD's unpublished commercial landings (TPWD 2007a unpublished data) show that populations on these reefs rebounded in subsequent years (Fig. 6).

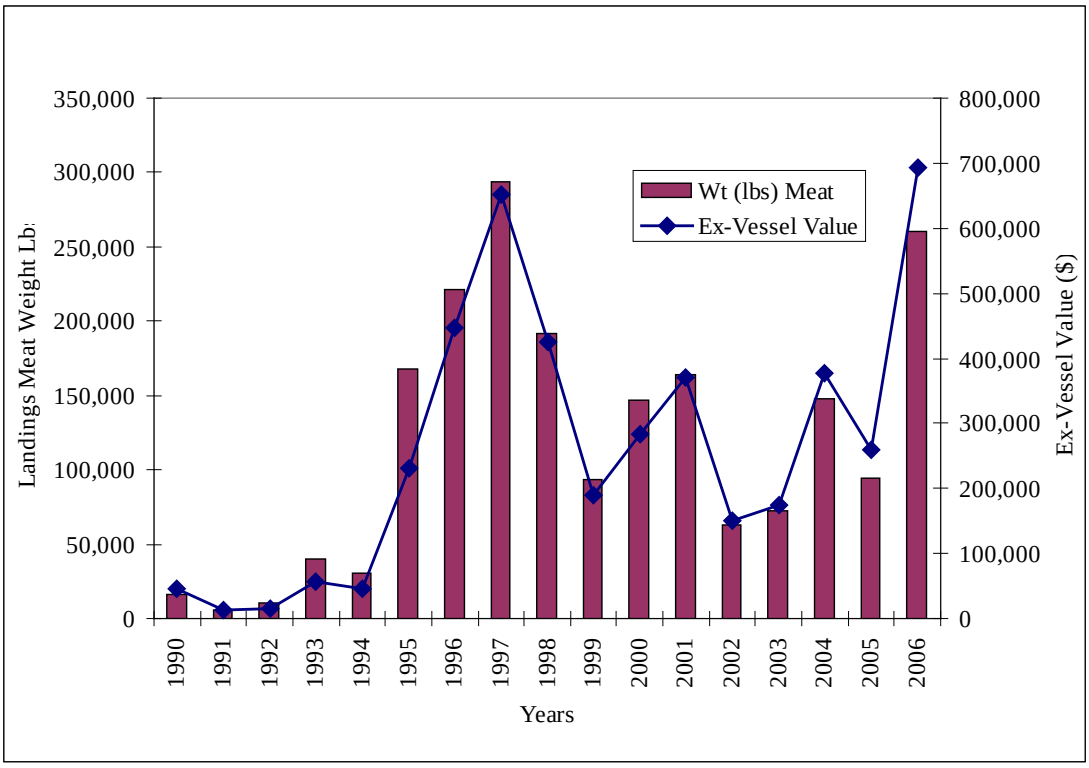

Figure 6. Commercial Landings reported to TPWD for Matagorda Bay (not including Lavaca Bay).

Methods

Study area

The study area is in WMB on three transverse-ridge reefs. Two were described by Moore (1907) as Shell Island and Mad Island Reefs, which were restored in 1995; and the third, Sammy's Reef, was created by the United States Army Corps of Engineers (USACE) (Fig. 7).

Data source: LCRA environmental data

Lower Colorado River Authority provided daily temperature and salinity data collected at three continuous-record datasonde stations (Fig. 7): Shell Island Reef, West Matagorda Bay Tripod, and West Bay Channel Marker #4. These data were collected from January 1, 2001 through December 31, 2005.

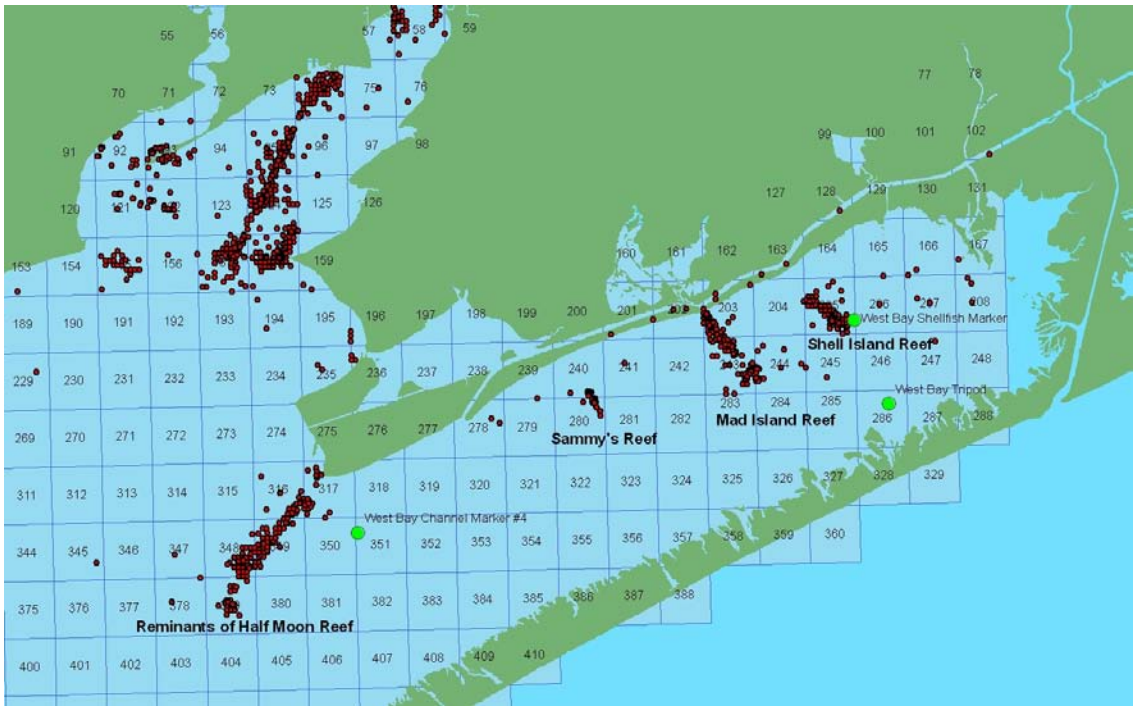

Figure 7. TPWD Sample grids on Matagorda Reefs (red circles): Shell Island, Mad Island and Sammy's Reef. Three green circles designate the LCRA datasonde water quality monitoring.

Environmental factors: daily and monthly differences

Distinct environmental patterns that influence oyster population dynamics may be observed when comparing monthly and daily temperature and salinity measurements over a five year period of record for one LCRA datasonde sampling location (Shell Island) in WMB. Average monthly salinities were less than 5 ppt in March 2005, July 2002, July 2004, and November 2002 (Fig. 8). These average monthly measurements strongly contrast with average daily salinity measurements at the same station (Fig. 9), and show that salinity was less than 5 ppt during a 5-day period in September 2001, 20 days in July 2002, 10 days in November 2002, 5- and 20-day periods in March 2003, more than 30 days in July 2004, and 25 days in December 2004.

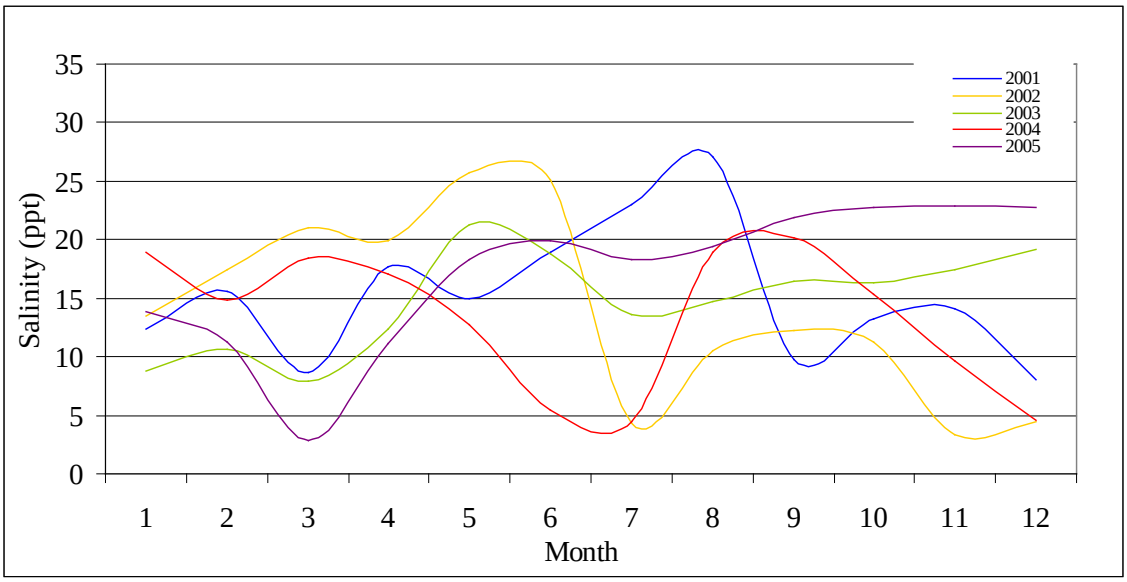

Figure 8. Average monthly salinity at Shell Island LCRA water quality station for 2001-2005.

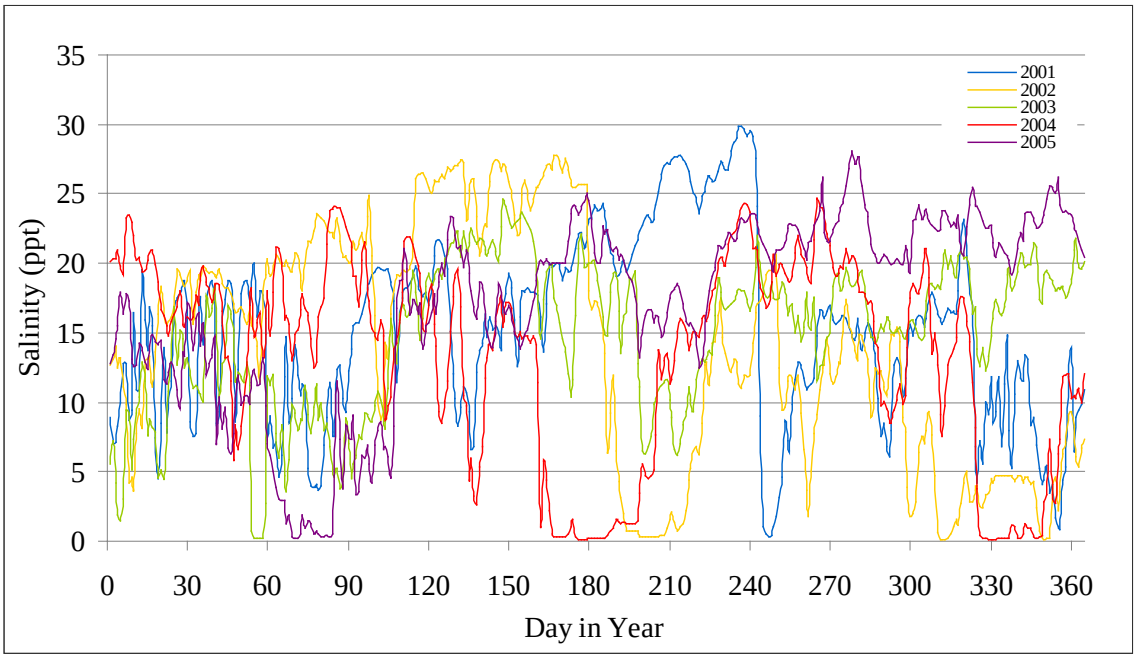

Figure 9. Average daily salinity at LCRA Shell Island water quality station for 2001-2005.

Although there were several periods of one or two days in various months that salinities were less than 5 ppt, the difference between average monthly and average daily

salinity illustrates that oysters can survive one to ten days without feeding, with their valves closed in order to survive a sudden freshwater inflow event. However, when the water temperatures are higher in summer, or when freshwater influxes are of longer durations, which sometimes causes low salinity conditions that last for 20-30 consecutive days—then most oysters will use up all energy reserves, expire, and their tissues will decompose in the closed valves. These dead, closed shells are referred to as "boxes" because the dead organism has left an intact hinged valve on the reef or buried in the mud. Alternatively, the valves will open and the decomposing meat will protrude, and these are referred to as "gapers".

TPWD salinity records from Shell Island, Mad Island and Sammy's Reefs plotted for the same date and the same time of day as salinity recorded by the LCRA datasonde are shown in Fig. 10. Although the general trends are similar for highs and lows, there appears to be a time lag between reefs, possibly related to distance and flow.

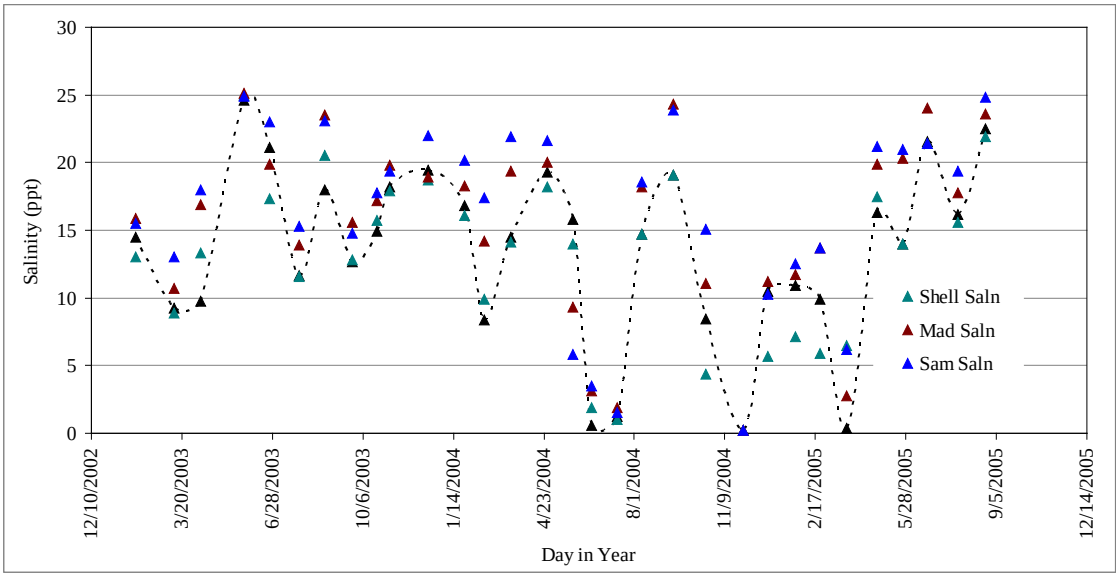

Figure 10. Average daily salinity measured at LCRA Shell Island datasonde water quality station measurements (dotted line) compared with TPWD average monthly salinity measurements at Shell Island Reef (Shell Saln), Mad Island Reef (Mad Saln), and Sammy's Reef (Sam Saln) from January 2003 through September 2005.

Linear regression was applied to estimate daily average salinity for Mad Island and Sammy's Reef using continuous daily records from the up-estuary Shell Island LCRA datasonde and the 30 month continuous record from TPWD's resource monitoring data. This information was used to generate daily spatial and temporal patterns for each of the three reefs. The LCRA average daily salinity estimated the TPWD salinity data (taken one day each month) for Shell Island Reef (R^2 =0.88; Fig. 11), Mad Island Reef (R^2 =0.85; Fig. 12) and Sammy's Reef (R^2 =0.77; Fig. 13) in a down-estuary pattern of declining goodness of fit. Compared to Shell Island, the intercept for each reef increased 1 to 2 ppt down-estuary at each reef, but the slope increased by only 0.012 or less.

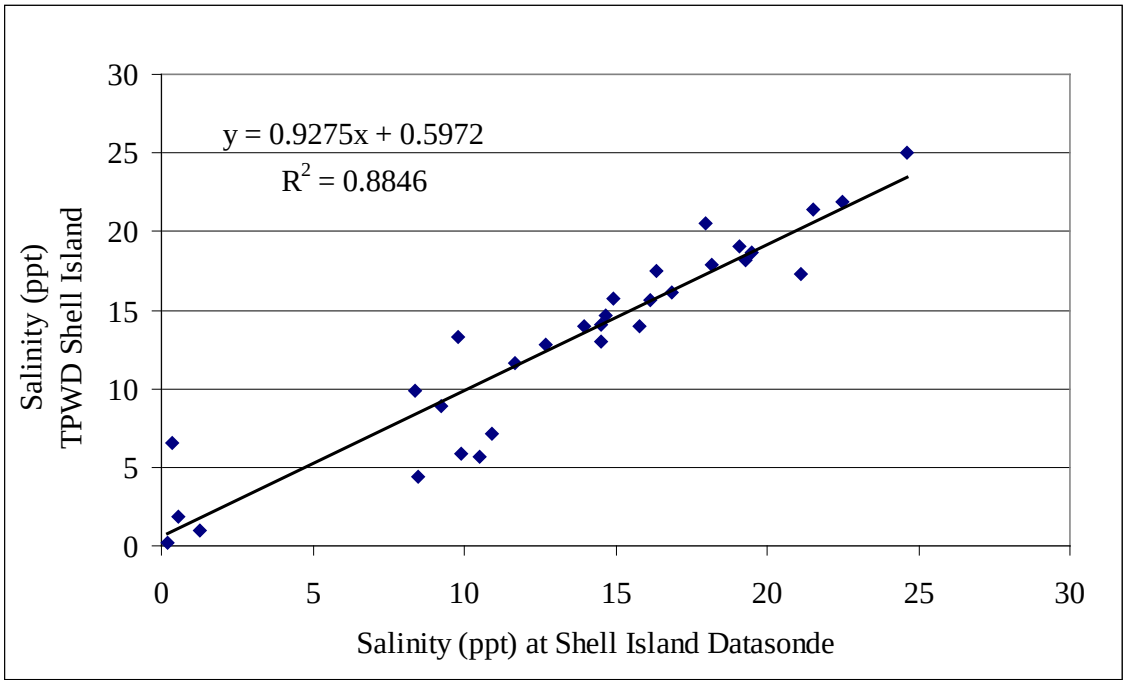

Figure 11. TPWD Shell Island Reef salinity values as a function of LCRA average daily datasonde salinity data for 2001-2005.

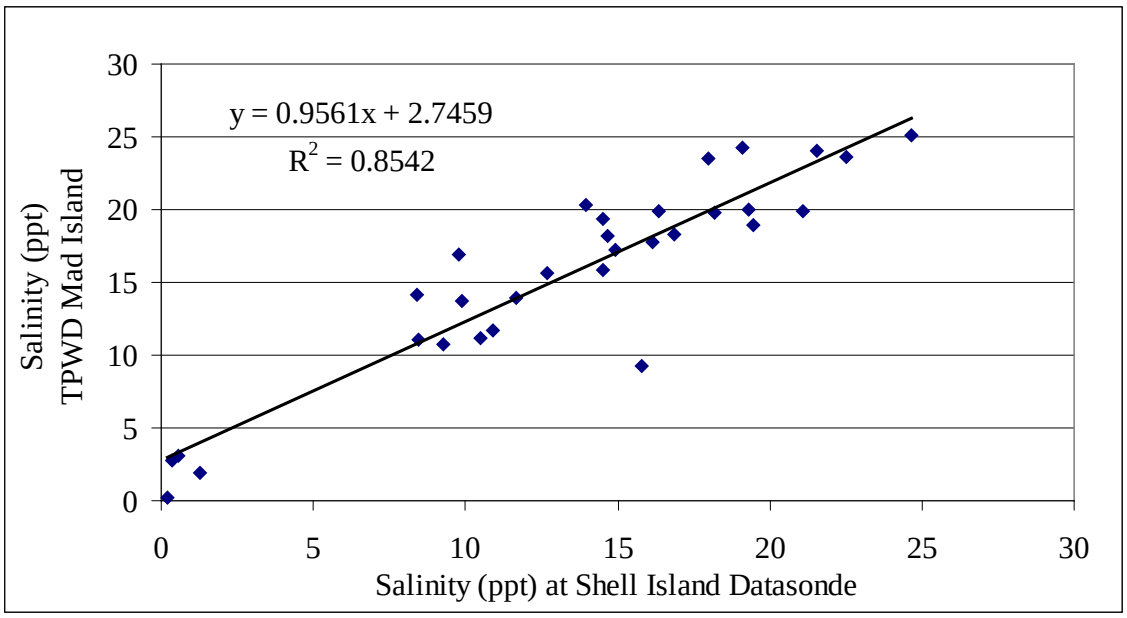

Figure 12. TPWD Mad Island Reef salinity values as a function of LCRA average daily datasonde salinity data for 2001-2005.

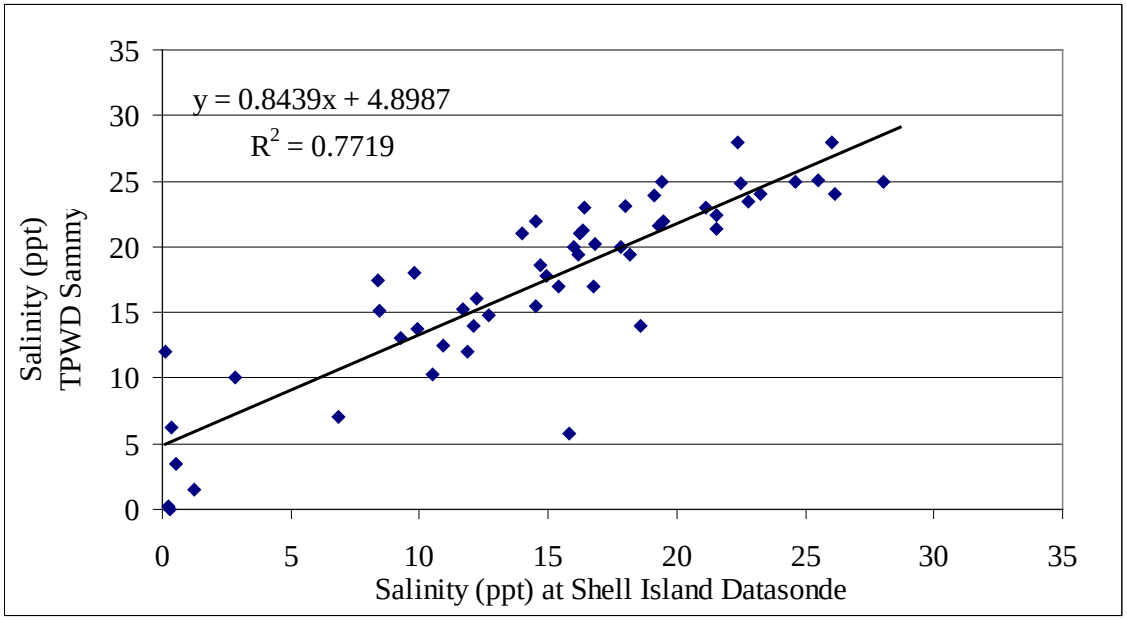

Figure 13. TPWD Sammy's Reef salinity values as a function of LCRA average daily datasonde salinity data for 2001-2005.

The same temporal patterns observed for monthly and daily salinity records emerged for average monthly temperatures (Fig. 14) and average daily temperature (Fig.

15) for the LCRA datasonde sampling location (Shell Island) in WMB between 2001 and 2005. There appeared to be uniform patterns for average monthly temperatures, but the actual duration of average daily temperatures reveals that longer durations of higher or lower extremes in daily temperatures during some months of each year were not observed in the monthly data for that specific year. The extremes in average daily temperatures are of shorter duration than the extremes for average daily salinity measurements. However, the continuous record of both variables simultaneously provides a better understanding of what environmental conditions submerged oysters were forced to tolerate or not survive between 2001 and 2005.

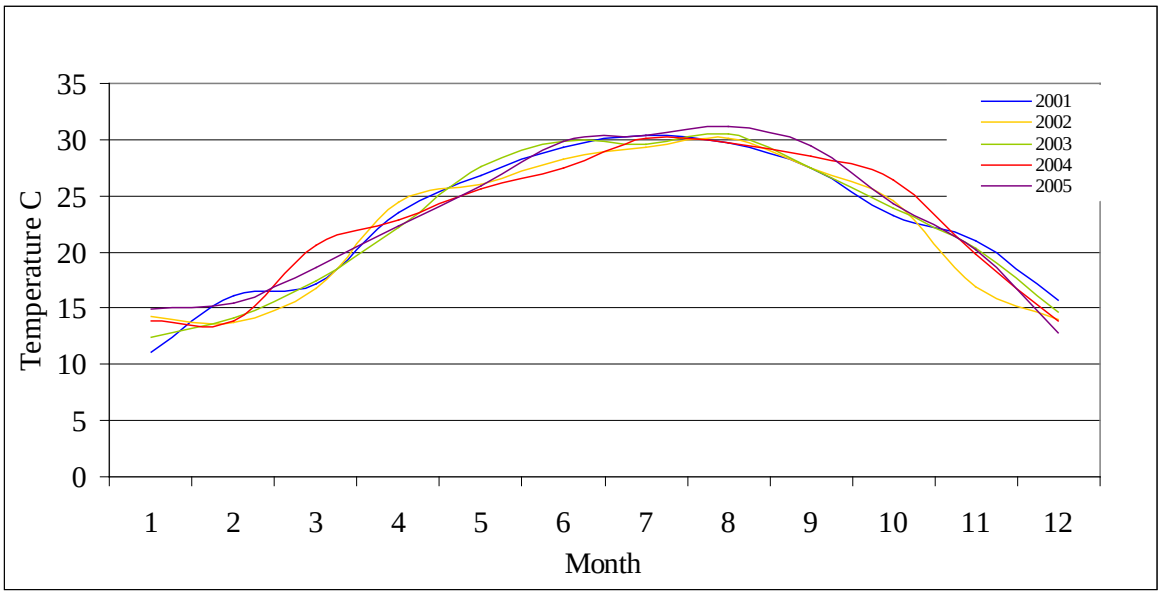

Figure 14. Average monthly temperature at LCRA Shell Island water quality station for 2001-2005.

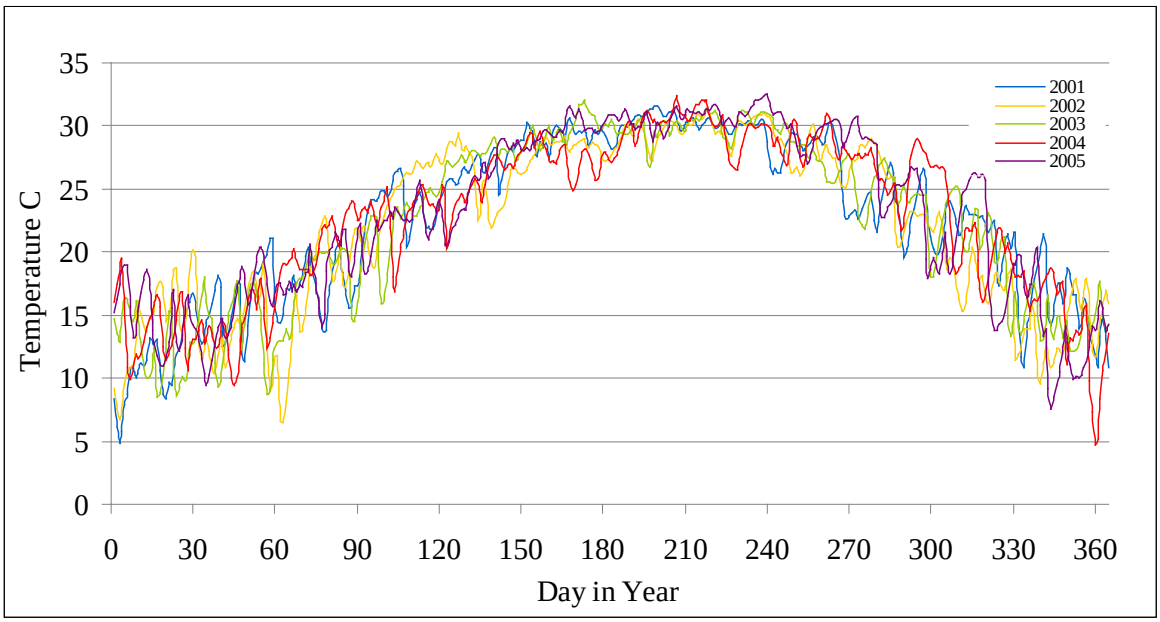

Figure 15. Average daily temperature at LCRA Shell Island water quality station for 2001-2005.

Linear regression was used to estimate daily average temperatures for Mad Island and Sammy's Reef using data from the up-estuary Shell Island LCRA datasonde, and to generate daily spatial and temporal patterns for each of the three reefs. The LCRA average daily temperature estimated the TPWD salinity data (taken one day each month) for Shell Island Reef (R^2 =0.94; Fig. 16), Mad Island Reef (R^2 =0.94; Fig. 17), and Sammy's Reef (R^2 =0.83; Fig. 18), and (as for salinity) showed the pattern of down-estuary declining goodness of fit, albeit a better fit than for salinity. Compared to Shell Island, the intercept for temperature at the other two reefs increased 0.8 and 1.7^{o}C in the down-estuary direction, but the spatial pattern for slope of temperature appeared to be stronger than the pattern for salinity, increasing by 0.017 and 0.8 ^{o}C at each down-estuary reef.

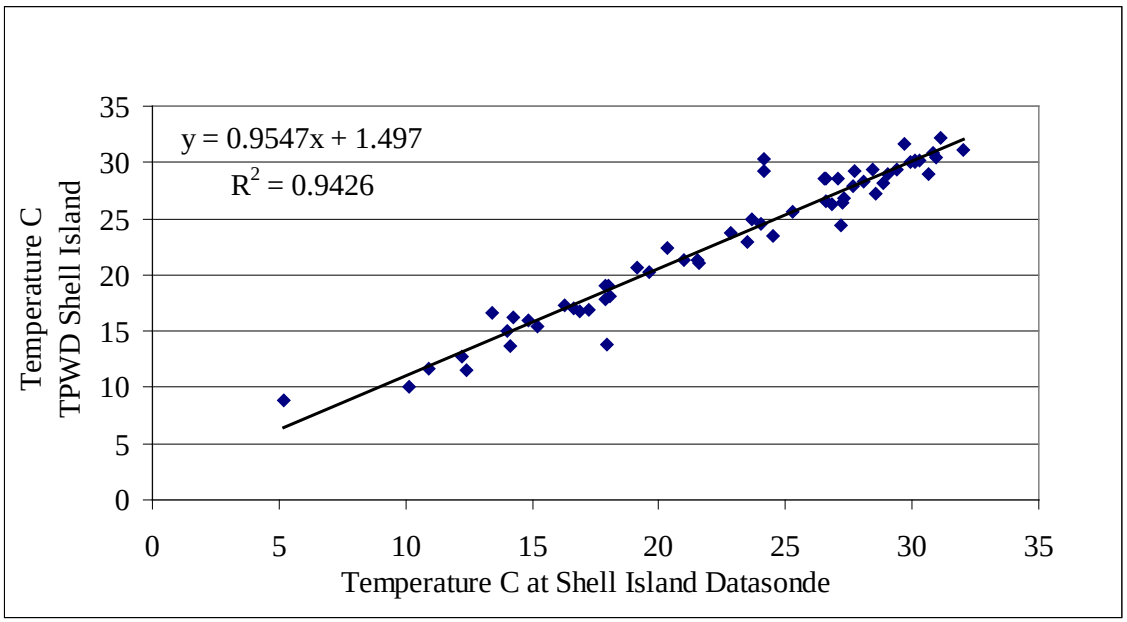

Figure 16. TPWD Shell Island Reef monthly temperature as a function of LCRA average daily temperature data for 2001-2005.

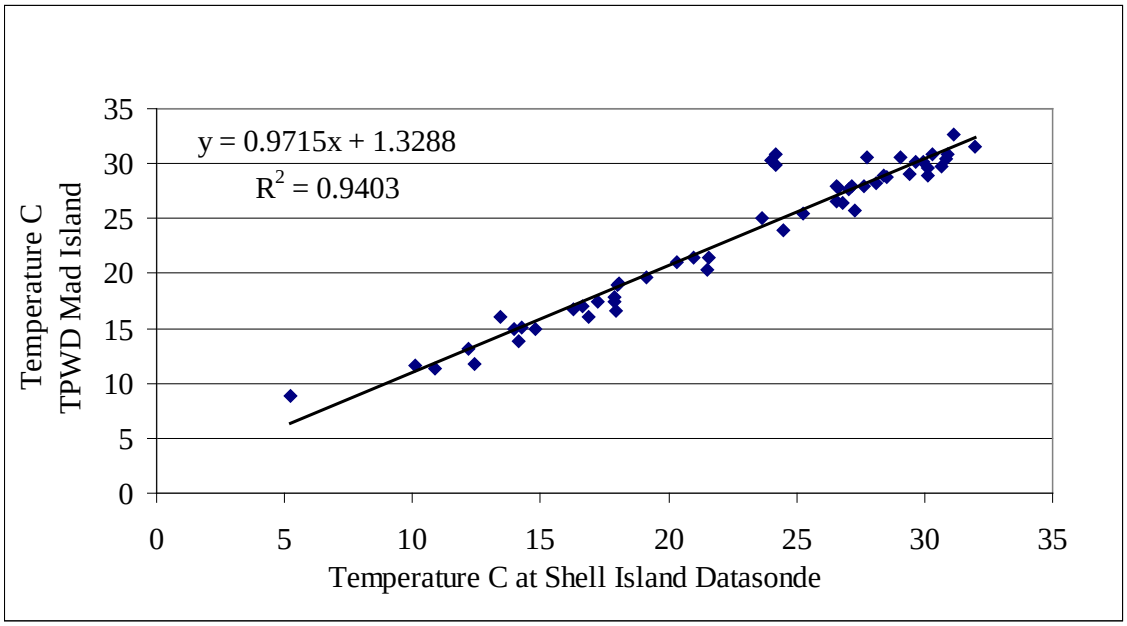

Figure 17. TPWD Mad Island Reef monthly temperature as a function of LCRA Shell Island Reef average daily temperature data for 2001-2005.

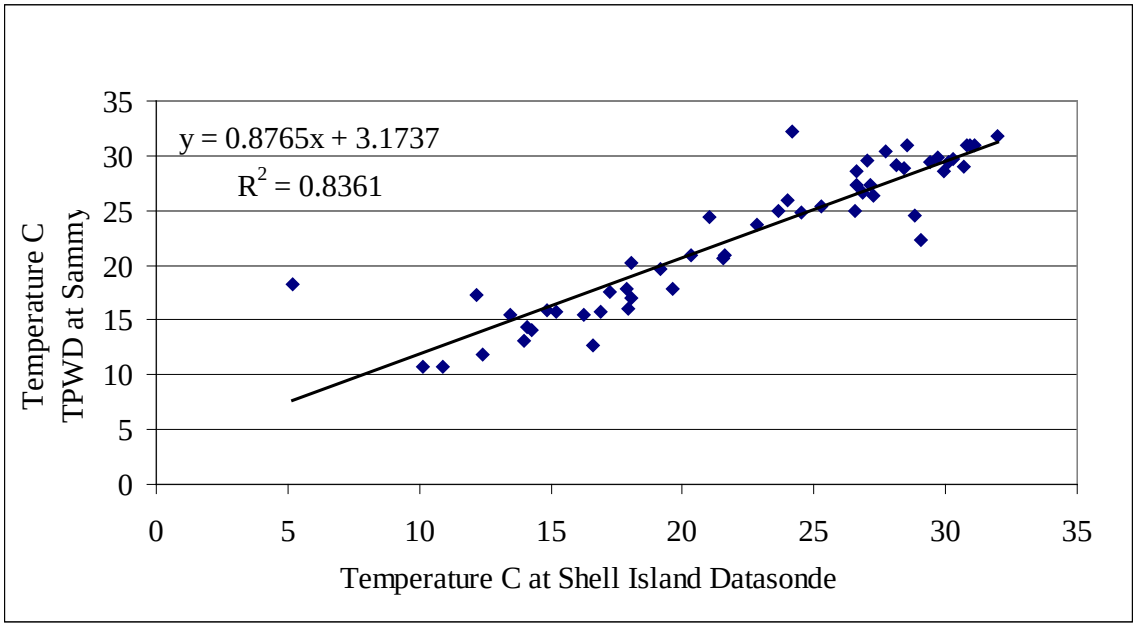

Figure 18. TPWD Sammy's Reef monthly temperature as a function of LCRA Shell Island Reef average daily temperature data for 2001-2005.

The temporal patterns observed for average monthly and daily salinity and temperature, demonstrate not only the differences in variation, but also the differences in duration of average daily conditions. Longer durations of higher and lower extreme conditions during some months were revealed for some years, that were not reflected in monthly averages for those specific years. Although extremes in average daily temperatures were of shorter duration than extremes for average daily salinity, one can see the importance of having a continuous record of both variables between 2001 and 2005, which provides a much better understanding of environmental conditions at biologically meaningful (daily) time steps related to whether submerged oysters would be expected to either thrive, only tolerate, or die.

Data sources for daily discharge, tide and precipitation

Average daily discharge in cfs recorded from 2001 through 2005 was downloaded for USGS 08162500 Colorado River near Bay City, TX from website: http://waterdata.usgs.gov/nwis/?automated_retrieval_info.

Average hourly tide data in feet for 2001-2005 were downloaded for NOAA: Station ID: 8773701 at Port O'Connor, TX from the following website; and then the 24 hour record was averaged to calculate the daily tidal amplitude: http://tidesandcurrents.noaa.gov/data_menu.shtml?bdate=20010101&edate=20051231&unit=1&shift=g&mins=60&datum=6&stn=8773701+Port+Oconnor%2C+TX&type=Tide+Predictions&format=View+Data.

Daily historical precipitation data for 2001 through 2005 were requested from National Weather Service Center web site for archived data for Matagorda, TX at: http://www7.ncdc.noaa.gov/IPS/CDPubs and the files were downloaded from: http://www1.ncdc.noaa.gov/pub/orders/659461480522dat.txt.

Direction of flow and tidal amplitude

Average daily discharge over the period of record 2000-2007 is shown in Fig. 19. The average daily tidal amplitude with average daily discharge for period of record 2001-2005 is shown in Fig. 20. Extreme precipitation events recorded by the National Weather Service for Matagorda Bay, TX were included in Fig. 20 to illustrate when rainfall events may not have been captured in records for gauging stations upstream of the study area. Tides occurred twice a day on normal cycles. However, daily tidal amplitudes provided an indication of directional changes in those tides. Daily tidal amplitude in Fig. 20 shows a predominantly seasonal bimodal trend that is consistently

observed across all five years of data. Bimodal tidal amplitudes begin rising between January and May (days 0 to 150) then decrease around July (days 210 to 230), then begin rising again between August and October (days 240 to 300) and then decline in strength towards December. Tidal amplitudes appear to be greater in the second half of the year. These bimodal patterns are consistent with meteorologically wind driven forces described for Gulf of Mexico estuaries (Solis 1999).

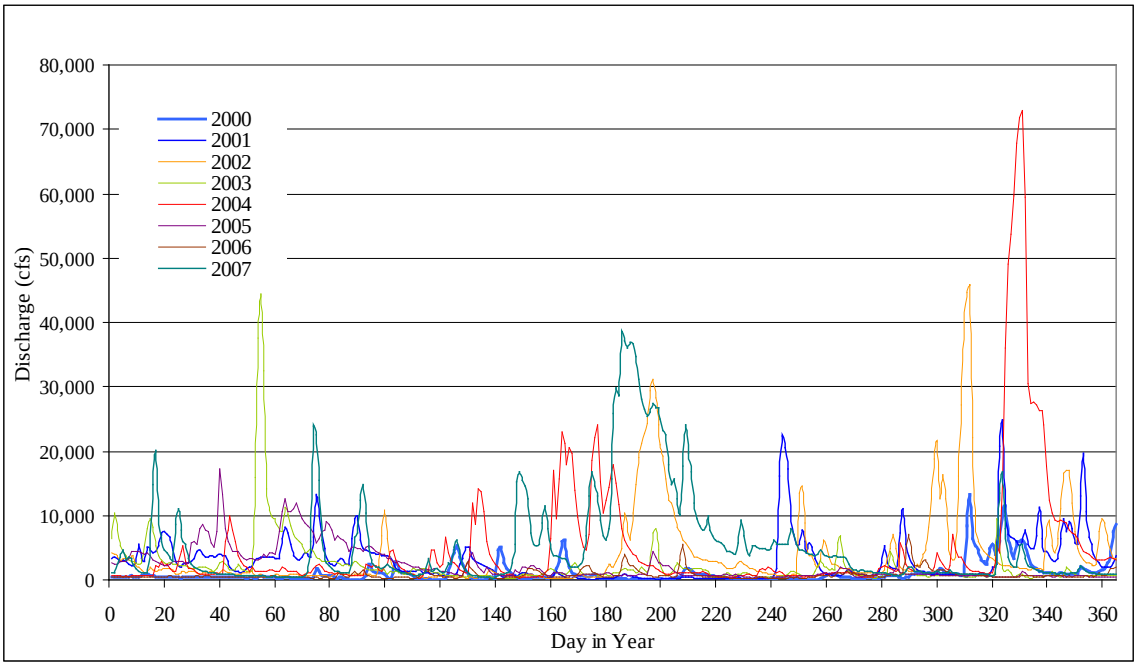

Figure 19. Average daily discharge from USGS 08162500 Colorado River at Bay City, TX for 2000-2007.

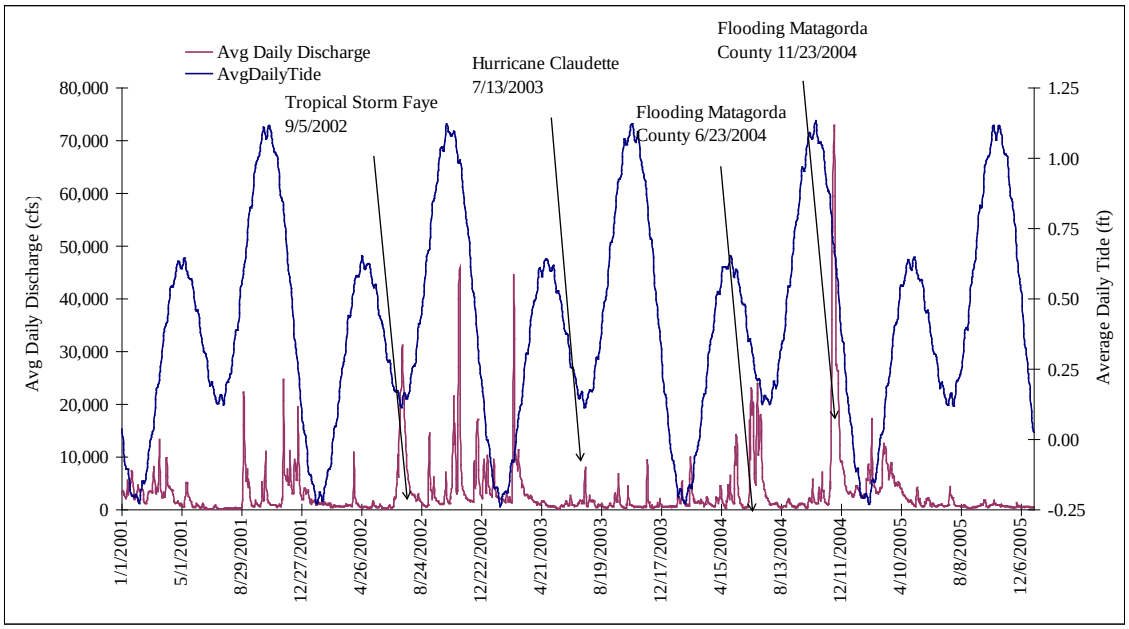

Figure 20. Average daily discharge from USGS 08162500 Colorado River at Bay City, TX, average daily tidal amplitude from NOAA: Station 8773701 at Port O'Connor, and extreme precipitation events recorded by National Weather Service from 2001-2005.

Distance from discharge to LCRA datasonde

The Colorado River discharge from Bay City, TX travels over 10 miles before reaching Matagorda Bay through the Colorado River Diversion cut created by the USACE in 1991. In addition to potentially long time lags during low flow conditions, precipitation over the regional area of the bay has an ungauged influence on salinity readings measured at the LCRA Shell Island datasonde station. However, high inflow events appear to be responsive to cumulative effects of both coastal prairie run-offs from the local water shed and the daily discharge measured at the Bay City gauge. Salinity and temperature data used in this analysis are actual continuous monitoring records measured by a datasonde at LCRA Shell Island Reef for 2001-2005 (Fig. 21).

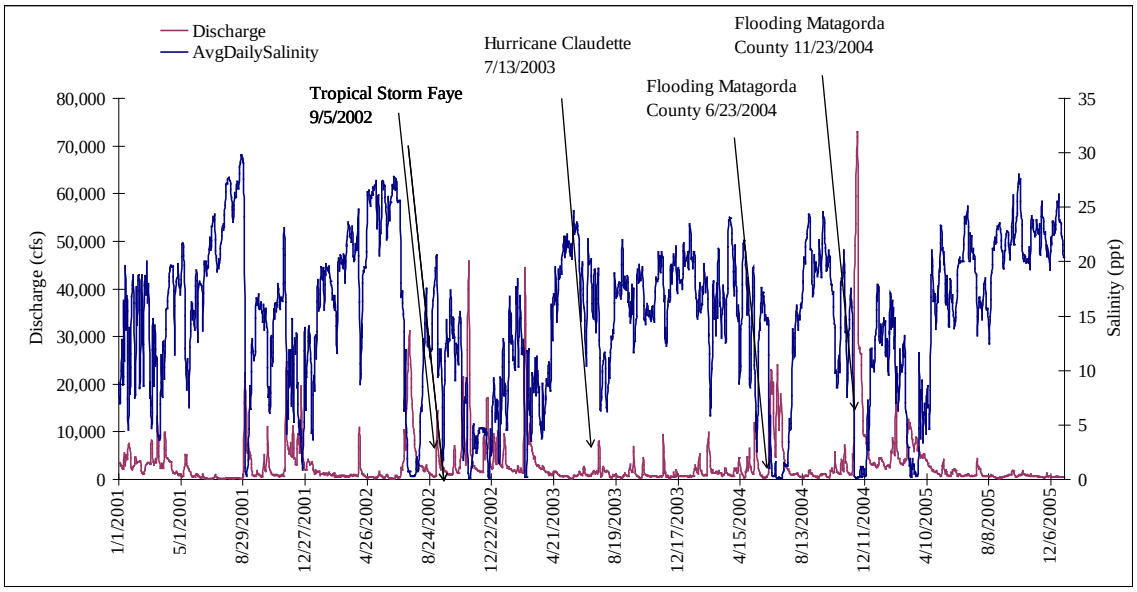

Figure 21. Average daily discharge from USGS 08162500 Colorado River at Bay City, TX, and average daily salinity data at LCRA's Shell Island datasonde from 2001-2005.

Data source: TPWD Resource Monitoring Program data

Texas Parks and Wildlife Department uses established protocols for monitoring Texas oyster reefs (TPWD 2002). In each major oyster producing bay (Galveston Bay, Matagorda Bay, San Antonio Bay and Aransas Bay) oyster reef areas were mapped as "defined reefs" (Matlock and Osburn 1982). TPWD's criteria for "defined reefs" were "Eastern oyster reefs that were > 0.2-m higher than adjacent bottom for a continuous distance of > 91.4 m long and 0.4 m wide". Oyster dredge sampling sites were randomly selected from among bay grids containing defined reefs. Each grid was divided into 144 5-second "gridlets". Each gridlet that contained defined oyster reefs were potential available sample sites to be randomly chosen each month. One half of the oyster samples were collected during each of two halves of the month (days 1-15 and 16-31). Dredges (Louisiana style 9-tooth, 46 cm wide and 25 cm tall with a 36 cm deep bag) were pulled

linearly for 30 seconds at a speed of 3 knots. The distance these dredges were pulled was not measured. The same sample sites were not duplicated within a month.

Salinity was measured with a refractometer or digital conductivity/salinity meter 0.3 m above the bottom substrate at the dredge starting point. Temperature was measured with a digital temperature meter 0.3 m above the bottom substrate at the dredge starting point. All live Eastern oysters in each dredge sample were counted, and 19 live individuals were chosen at random and measured for total length. Eastern oysters were categorized by size as spat (5-25 mm), small oysters (26-75 mm) referred to as sub-market oysters in this study, and market oysters (> 76 mm). Total length (TL) of oysters in each dredge pull were processed as follows: 19 individuals randomly selected from among all oysters measured and all others in the sample were recorded as dead or alive; five live oysters and five dead oysters were randomly selected and total spat set on these shells was counted and recorded.

Methods for calculating catch per unit of effort used by TPWD were not used as the measure of relative abundance for this study. Instead, relative abundances of submarket and market oysters were calculated by multiplying the proportion of live oysters that were < 76 mm (submarket) and ≥ 76 mm TL (market) in a 30-s drag sample, by the total number of live oysters in that sample to convert dredge results to relative numbers of oysters in each size class. A monthly value for relative number in each size class (market, submarket and spat) in a 30-s dredge sample was recorded as a measure of relative abundance. This value was calculated as an average for a reef if more than one grid on that reef happened to be sampled twice in a month.

The population data generated and analyzed in this study were from sample collections taken through the TPWD Coastal Fisheries Resource Monitoring Program (TPWD 2007b unpublished data). These data included only grids for Shell Island Reef (grid 205), Mad Island Reef (grids 203, 243) and Sammy's Reef (grids 240, 280) sampled between 1998 and 2007 (Fig. 7).

Length frequency distributions

Three size classes of oysters collected by TPWD were evaluated as described above. Box plots of each reef and all reefs combined were constructed to evaluate spatial and temporal length frequency patterns.

Oyster weights and density estimates

Density estimates for only Mad Island Reef were made by analyzing data from a shell weight relationship for commercially harvested oysters. During this study, harmful algal blooms from *Dinophysis* occurred on the lower Texas Coast, which prevented commercial fishermen from harvesting oysters from San Antonio and Aransas Bay. Consequently, nearby commercial oyster-shucking houses were unable to spare (for use in this study) any sacks of oysters harvested from WMB that had already been designated for sale. However, one shucking house did allow use of their product before shucking each oyster of its meat for market sale. Each whole oyster was labeled, total shell and meat were weighed (0.1 g), and shell length and width measured (mm) using calipers. Each oyster was shucked of their meat by the facility's staff, and the meat was weighed (g) before returning the two valves (labeled) for re-weighing without meat. Each pair of valves without meat was subtracted from each oyster's total weight to estimate meat and fluid weight removed. Actual meat weights were compared to

calculated meat weights and were found to have less than a one percent measurement error (probably from fluid lost during shucking). Two of the shells measured consisted of four submarket oysters that had grown together in pairs and likely had been mistaken by the harvesters for two market sized oysters. These four shells were included in the shell weight length-frequency analysis.

The oyster sack used in the shell weight analysis contained 160 oysters that had been collected the previous day on March 12, 2008 by commercial dredges on Mad Island Reef. The shells were large, and generally free of any additional benthic materials. Prior to weighing and measuring each oyster, these shells were placed in a 0.33 m x 0.33 m (one square foot) box to simulate the positions of these oysters that would probably have grown up on the reef within a similar size patch, which is slightly higher than TPWD's standard of 0.2 m vertical relief used to designate reef habitat. Between 40 and 42 oysters were placed in each of four boxes from one commercial oyster sack. (one sack of oysters equals one-third of a barrel, the standard weight of live oysters with shell and meat weight). Thus, four of these boxes placed on the seafloor would represent the number (and weight) of oysters in a square area measuring 0.66 m on each side, which would be 0.43 m^2 total area. Density was estimated to be 372 market sized oysters per m^2 for Mad Island Reef. Although this estimate is only based on one commercial oyster sack without reference to geographic location on the reef, it correlates well with Moore's estimate of 378 market oysters per m^2 (42 per yd^2) on Mad Island Reef (Moore 1907).

Descriptive statistics for total shell length, shell width, total meat weight, meat weight alone and shell weight alone were evaluated for the 160 oysters from the one

commercial oyster sack harvested from Mad Island Reef. These oysters were grouped into size classes previously used for Galveston Bay oysters (Powell et al. 1994) and the total shell length-frequency analysis was evaluated.

Linear stepwise multiple regression using software SPSS 12.01 (SPSS 2003) was used to estimate total shell length by evaluating all other variables (total weight, total width, meat weight, and shell weight alone) and diagnostic tools for partial plots were used to determine the best predictor of total shell length in this study.

Linear step wise multiple regression using software SPSS 12.01 (SPSS 2003) was used to estimate meat weight by evaluating all other variables (total length, total width, total shell weight, and shell weight alone) and diagnostic tools for partial plots were used to determine the best predictors of meat weight, which was used in this study as a proxy for a health condition index. Curve estimation procedures in SPSS 12.0 were also applied as an alternative method to find the best predictor for meat weight from all other variables (total length, total width, total shell weight, shell weight alone).

Growth estimates

Growth was estimated using two methods. The first method used Hofstetter's 1977 monthly estimates for growth of larvae to spat, spat to submarket, and submarket to market sized oysters in Galveston and Matagorda Bays. His estimates were based on 20 years of tray studies in Galveston and for a shorter period of time in Matagorda Bay (Table 1). Kraueter et al. (2007) reviewed previous growth studies in every United States bay system in order to compare results and also to derive an equation for incremental growth that might apply to Gulf of Mexico oyster populations. The present study used both methods and applied them to an average oyster population on each of the three reefs

using TPWD length data (1998-2006), and the shell-length data from the analysis of commercial oysters harvested from Mad Island Reef (March 12, 2008). Using Hofstetter's monthly rates for growth once spat were set, and applying that rate to a daily increment of growth for oysters in Matagorda Bay (Table 1), each oyster in these populations required 4.6-yrs to grow from a newly settled spat to a market size oyster.

Table 1. Historical and current growth rates applied to Matagorda Bay oysters.

Hofstetter (1977) method			Kraueter et al. (2007) method		
Monthly converted to daily growth rate			Growth Rate = Growth(K)*$10^{(-0.0079*Length)}$		
Total Days	Size Class	Monthly growth rate mm/m	Total Days	Size Class	Daily growth rate mm/d
30	Larvae to Spat	3.0	20	Larvae to Spat	0.015
270	Spat to Submarket	2.68	37	Spat to Submarket	0.9
600	Submarket to Market	2.58	146	Submarket to Market	0.9
750	Market to Market Plus*	2.18	527	Market to Market Plus*	0.9
1620	Total Time = 4.6 yrs		730	Total Time = 2 yrs	

*Note: Market Plus Oysters are Market Oysters (≥ 76 mm) that are greater than 2-yrs old

Applying the method from Kraueter et al. (2007), each oyster in this population required 2-yrs to grow from newly settled spat to market size oyster, which is comparable to growth estimates by White et al. (1988) for Galveston Bay. Growth relationships following Hofstetter (1977) are shown in Fig. 22; and growth relationships following Kraueter et al. (2007) are shown in Fig. 23.

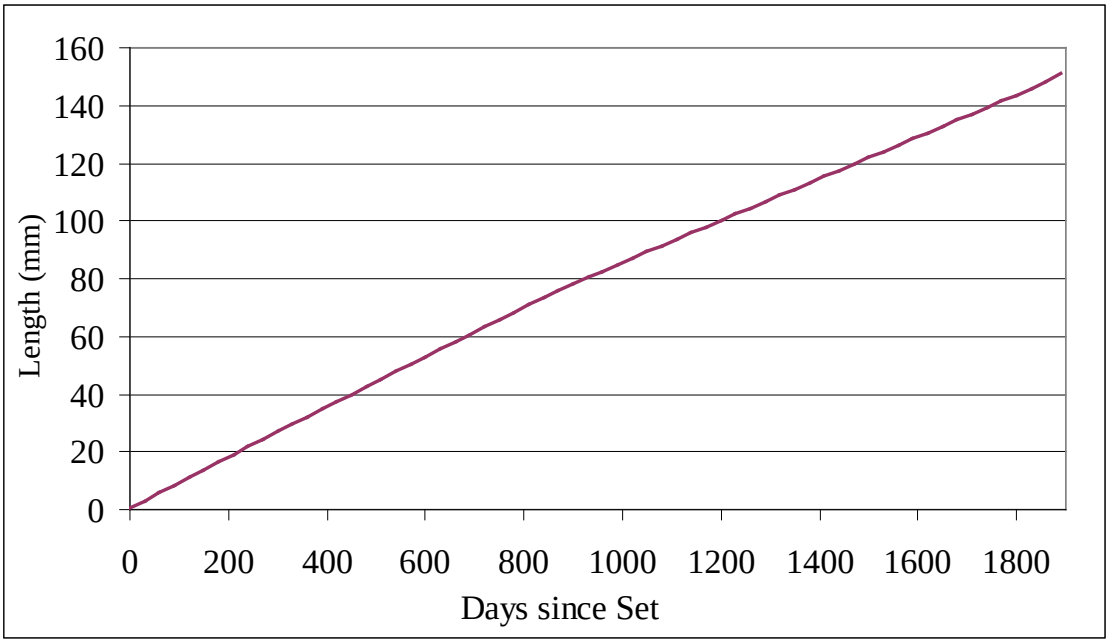

Figure 22. Monthly growth rate applied for Matagorda Bay oysters following methods by Hofstetter (1977).

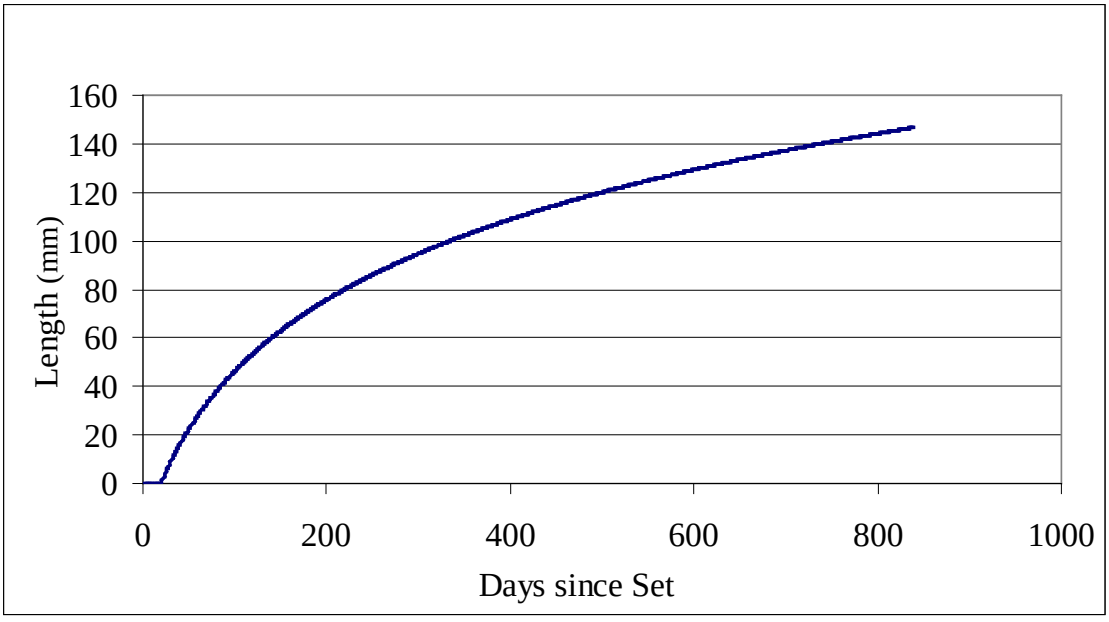

Figure 23. Incremental daily growth rates applied for Matagorda Bay following methods by Kraueter et al. (2007) where Incremental growth rate = Growth(K)*$10^{(-0.0079*\text{Length})}$.

Temporal trends of relative abundance in each size class

A LOESS smoothing curve was applied to the relative abundance data for Matagorda Bay oysters using the software Brodgar version 2.6.0, 2005 (Zuur et al. 2007). The data set used in this analysis consisted of a continuous monthly record (30 months from March 2003 to August 2005) of environmental and biological variables for each of the three reefs. A span of 0.4, representing 40 percent of the dataset (values spanning six months on either side of each data point) produced trends for oyster populations for each reef. In addition, temperature, salinity and relative abundances of spat, submarket and market size oysters were compared across a longer dataset between 1998 and 2006 using time series plots. These curves were examined to determine residual temporal and spatial trends among reefs and oyster size classes after removing the seasonal component from the data.

Gradient analyses

Exploratory indirect gradient analyses—Principal Components Analysis (PCA) and Detrended Correspondence Analysis (DCA) were run using the software CANOCO version 4.5 (ter Braak and Smilauer 2002) to evaluate the length of the ecological gradient as measured in standard deviations (SD) in the dataset (Jongman et al. 1995) for the three biological variables (market, submarket and spat size classes) and environmental variables (salinity, temperature, distance and flow, and Julian date) from the dataset for 1998 to 2006.

Variables were transformed as needed (distance was log transformed) to linearize and normalize their distributions. This is an indirect gradient analysis (Jongman et al. 1995) because it does not include explanatory variables. Rather, explanations for the

gradients are inferred from ecological relationships revealed by their order. The biological dataset contained a short (< 2.4 Standard Deviations; SD) ecological gradient (a change of four SD indicates a complete change in the composition of response variables ordered across all samples). Long gradients and those with many zeroes, are more suited to analysis using non-linear relationships (such as weighted averaging and correspondence analysis) among variables (Jongman et al. 1995). Because the dataset included many zeros, the non-linear direct gradient method of Canonical Correspondence Analysis (CCA) was used to build a multivariate model to test the relationships between the biological responses and potential explanatory environmental variables. The CCA produces new canonical variables (axes) that are linear combinations of the explanatory variables that constrain the relationships among the biological (dependent) variables to also be a function (multivariate regression) of the canonical axes. Starting with the full model (all explanatory variables included), sequentially variables were eliminated if the variance inflation factor (VIF) was greater than 5, in order to minimize redundancy (colinearity among explanatory variables) that could inflate significance tests of the multivariate relationships among response variables and the canonical axes.

A CCA was used to identify the gradients that were combinations of environmental variables (salinity, temperature, distance and flow, and Julian date) correlated with relative abundances of the three size classes for live oysters (spat, submarket, and market) and two size classes for dead oysters (submarket and market) in each reef population using the software CANOCO (ter Braak and Smilauer 2002) for the March 2003 - December 2007 continuous data sets. Forward selection and Monte Carlo

permutations to test the significance ($p < 0.05$) of each selected variable were used to determine in the final CCA model. In addition to the values for data with zero-lag in time (i.e., dependent and independent variables measured on the same day, month and year), explanatory variables measured at one month before those for response variables (i.e., a time lag of -1), were also included. These were included based on significance tests for maximum cross-correlations among response and explanatory variables for a range of time lags (from 0 to -3 months), which were screened using the software Brodgar version 2.6.0, 2005 (Zuur et al. 2007). These procedures allowed tests of the importance of lagged responses among oyster size classes to environmental conditions that had occurred one to three months earlier. To visualize and interpret the results of CCA with and without the time lags, both results are each plotted in a bi-plot (both biological and explanatory variables plotted on the same ordination axes).

Results

Trends of shell length-weight distributions for Mad Island Reef

Average total shell length was 106 mm (ranged 70 to 135 mm) among the 160 oysters in a commercially harvested sack (117 lbs, 53 kg) from Mad Island Reef on March 12, 2008. Average meat weight in this analysis was 38 g (range 13 to 64 g). The smaller meat weights were those recorded for the submarket oysters that were included in this sample. Descriptive statistics for the oysters used in this analysis are summarized in Table 2.

Table 2. Descriptive statistics for Mad Island Reef shell length weight analysis for oysters collected on March 12, 2008.

	Mean	Std. Deviation	N
Total Length (mm)	105.6	13.8	160
Total Width (mm)	78.2	9.9	160
Total Wt (g)	306.8	98.3	160
Shell Wt (g)	268.4	88.7	160
Meat Wt (g)	38.4	10.2	160

The total shell length-frequency analysis by size classes resulted in a unimodal curve where $y = -3.7381x^2 + 31.048x - 26.571$ (Fig. 24, $R^2 = 0.8506$). Greatest frequency occurred in the 100 to 109 mm size class, which is one length size class larger than reported for Galveston Bay oysters (Powell et al. 1994).

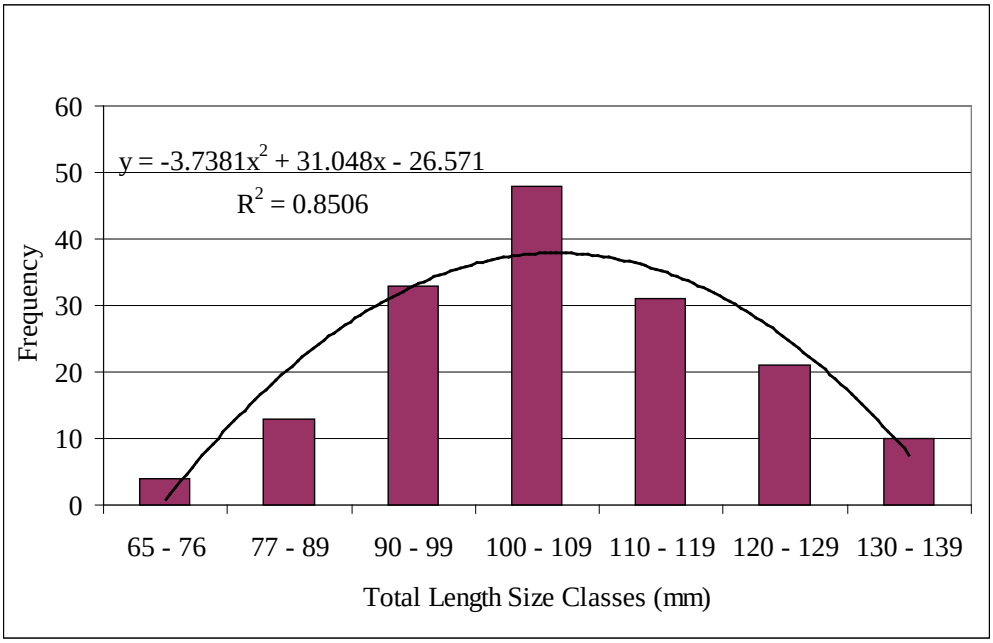

Figure 24. Mad Island Reef length-frequency by size class of 160 oysters in a commercially harvested sack sampled on March 12, 2008.

The results of the stepwise multiple regression analysis for predicting total shell length across all other variables (total width, total weight, meat weight alone, and shell weight alone) indicated total weight was the most important predictor for total shell length (Table 3). Other variables tested were excluded when only one model was found to be significant (ANOVA, $F = 376.116$, $P < 0.000$). This model produced a linear relationship where total shell length (y) was predicted as a function of total weight (x) by the following equation: $y = 5.9652x - 323.06$ (Fig. 25, $R^2 = 0.7042$). Shell width, meat weight alone, or shell weight alone were not strongly related to total shell length, most likely due to the very large, round, thick shells of the oysters in the Mad Island Reef harvest sample.

Table 3. Model summary for stepwise multiple regression of Mad Island Reef oyster weight.

Model	R	R^2	Adj. R^2	Std. Error	Durbin-Watson
1	0.8392	0.7042	0.7023	7.5421	1.8862
a	Predictors: (Constant), Total Wt				
b	Dependent Variable: Total Length				

The results of the stepwise multiple regression analysis for meat weight across all other variables (total length, total width, shell weight, and shell weight alone) indicated that total weight was the best predictor for meat weight using equation $y = 0.0979x + 8.3916$ ($R^2 = 0.8893$). Although the results of this analysis indicated meat weight has a linear relationship with total weight (ANOVA, $F = 1269.47$, $P < 0.000$).), a stronger relationship for these two variables was found using curve estimation procedures (ANOVA, $F = 1899.68$, $P < 0.000$). This analysis produced a power function relationship where meat weight (y) was predicted as a function of total weight (x) by the

following equation: $y = 0.4087x^{0.7945}$ (Fig. 26, $R^2 = 0.9239$). This power function relationship is similar to the oyster meat weight relationship found by White et al. (1988) that was also used by Powell et al. (1994) to model oyster populations of Galveston Bay. Shell weight alone was not strongly related to meat weight, possibly because the oysters from Mad Island Reef had large thick shells; and much of their tissue mass consisted of gonadal tissue weight and not somatic tissue weight in March, prior to spawning. However, regardless of differences in shell thickness and weight, Matagorda Bay oyster's average size meat weights were comparable to average size meat weights from Galveston Bay oysters (White et al. 1988).

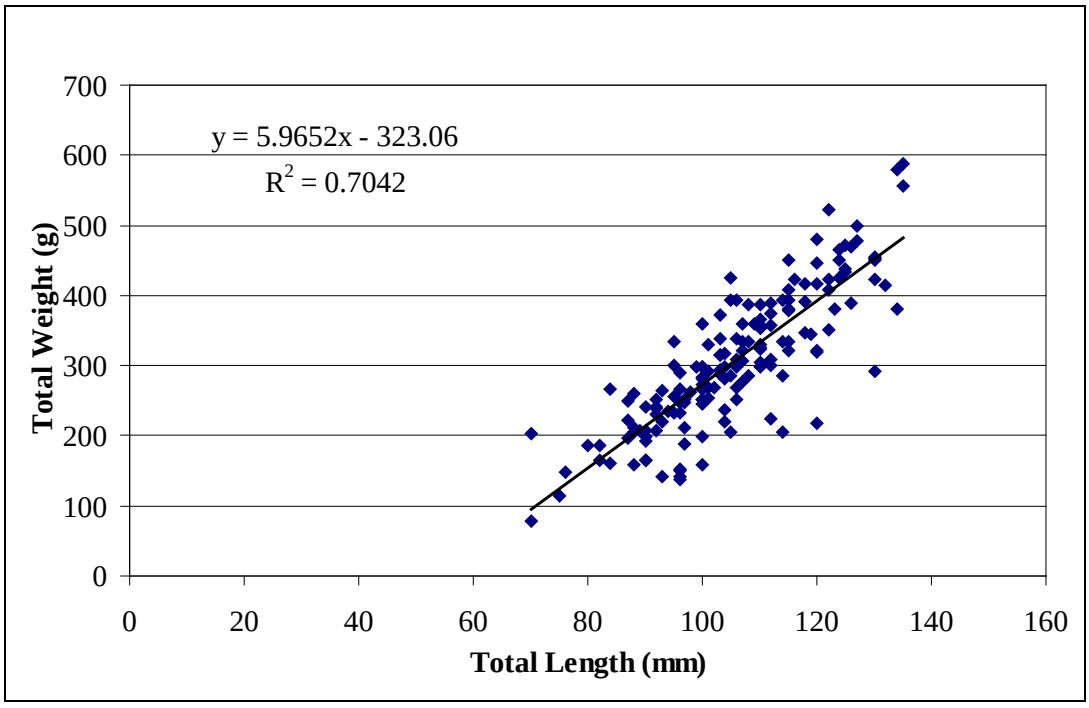

Figure 25. Relationship of Mad Island Reef total shell length to total weight for 160 oysters in a commercially harvested sack sampled on March 12, 2008.

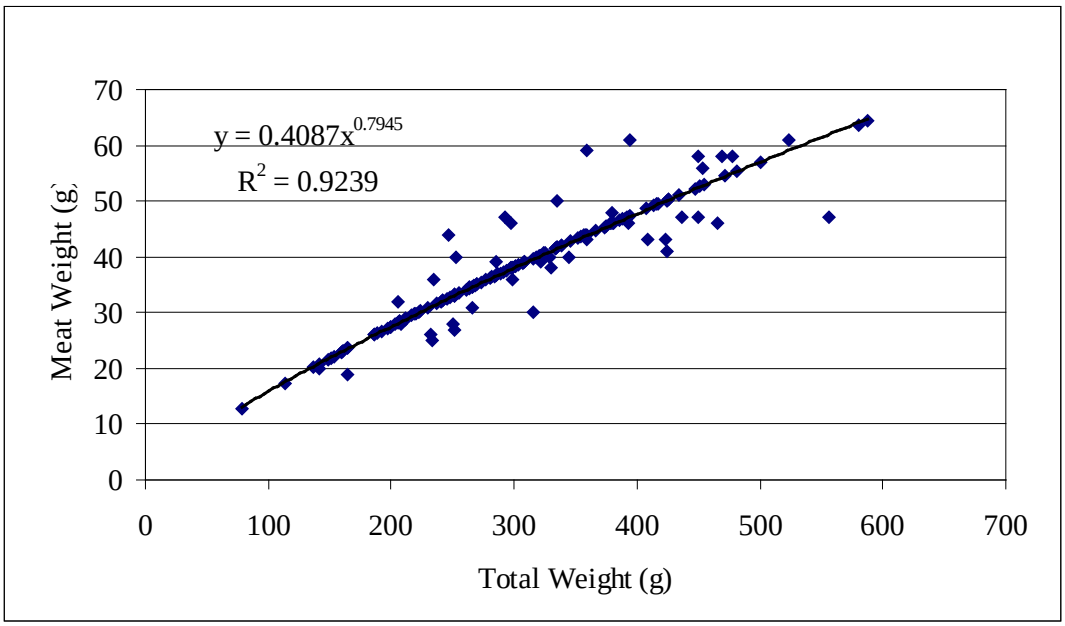

Figure 26. Relationship of Mad Island Reef total meat weight to total weight for 160 oysters in a commercially harvested sack sampled on March 12, 2008.

Although the previous results for predicting total shell length indicated a linear relationship with total weight (Fig. 25), curve estimation procedures were used to examine the potential non-linear relationship between total shell length and meat weight. This analysis produced a power function relationship where meat weight (y) was predicted as a function of total length (x) by the following equation: $y = 0.0144x^{1.6885}$ (Fig. 27, $R^2 = 0.6301$). These results did not indicate a strong relationship as shown for meat weight and total weight for one commercial sack of oysters sampled in this bay system.

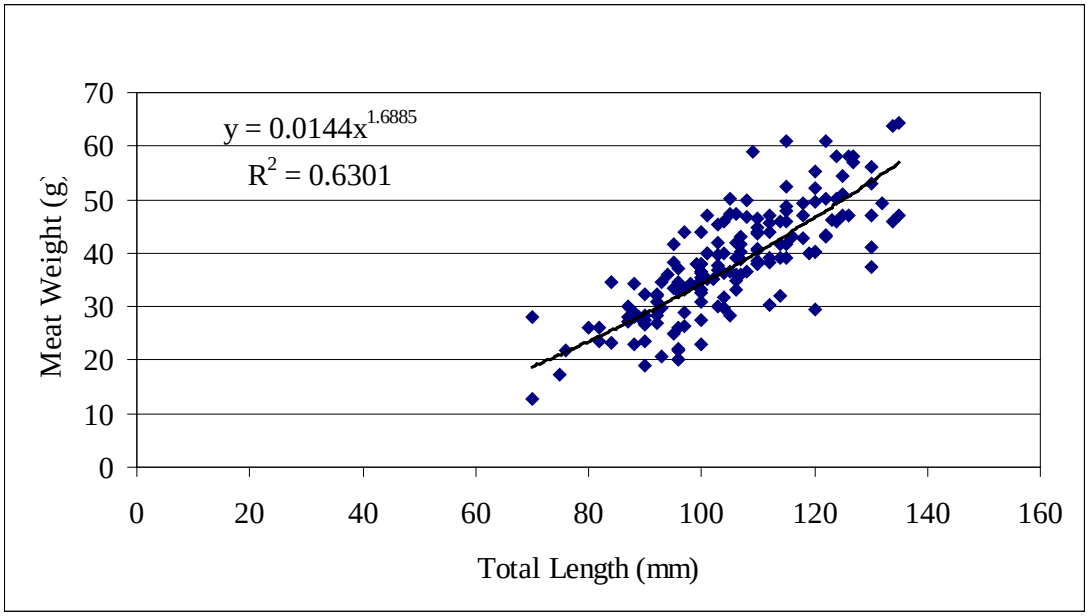

Figure 27. Relationship of Mad Island Reef total meat weight to total length for 160 oysters in a commercially harvested sack sampled on March 12, 2008.

Temporal trends in relative abundance of each size class among reefs

Box plots of annual relative abundances of each size class (Figs. 28, 29, 30) from TPWD data 1998-2007 indicate different relative abundances of each size class on the three reefs across years. For example high relative abundances of market size oysters such as 2006 were observed for all reefs, but these did not result in similarly high relative abundances of spat or submarket oysters in the following year 2007 across all reefs. Also, Mad Island and Sammy's Reefs exhibit greater annual variations in relative abundances of spat whereas Shell Island Reef exhibits greater annual variations in relative abundance of submarket oysters.

Review of monthly relative abundances of each size class using TPWD data 1998-2007 for these three reefs indicates there are similar temporal patterns for Mad Island and Sammy's Reefs that are not found at Shell Island Reef (Figs. 31, 32, 33). Shell Island Reef is characterized by higher numbers of submarket oysters in monthly

samples whereas Mad Island and Sammy's Reef are characterized by higher numbers of spat and moderate numbers of market size oysters.

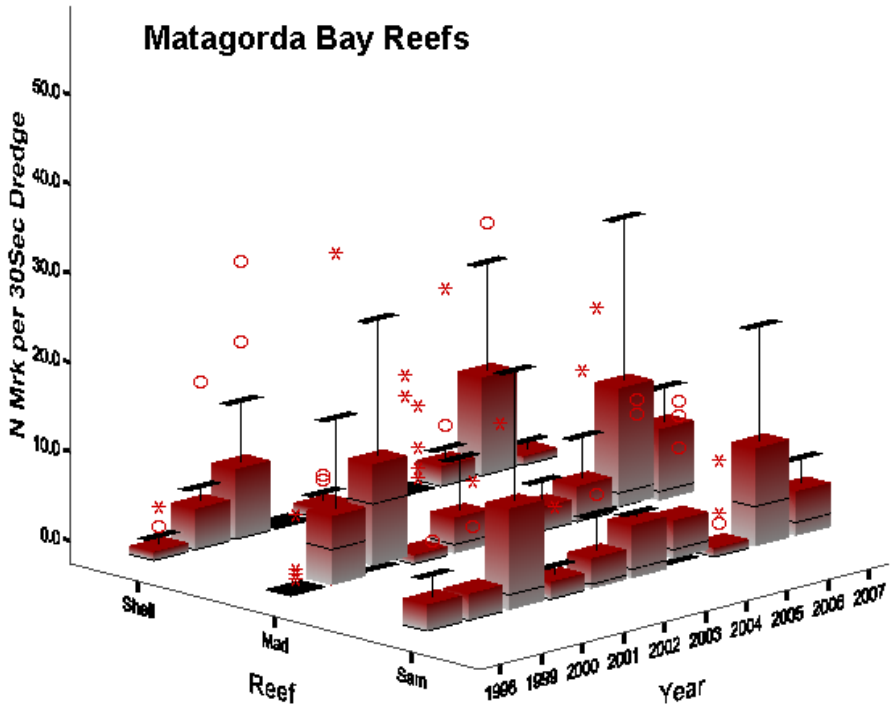

Figure 28. Annual relative abundance of market oysters for three Matagorda Bay Reefs, Shell Island (Shell), Mad Island (Mad) and Sammy's Reef (Sam) 1998-2007. Note outliers are designated by the symbol *.

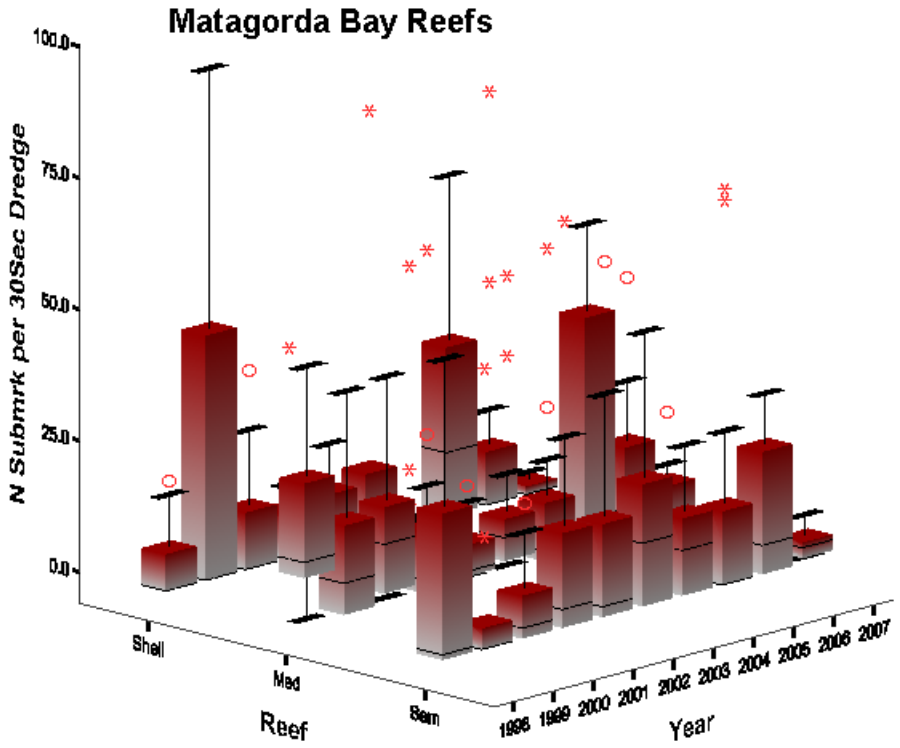

Figure 29. Annual relative abundance of submarket oysters for three Matagorda Bay Reefs, Shell Island (Shell), Mad Island (Mad) and Sammy's Reef (Sam) 1998-2007. Note outliers are designated by the symbol *.

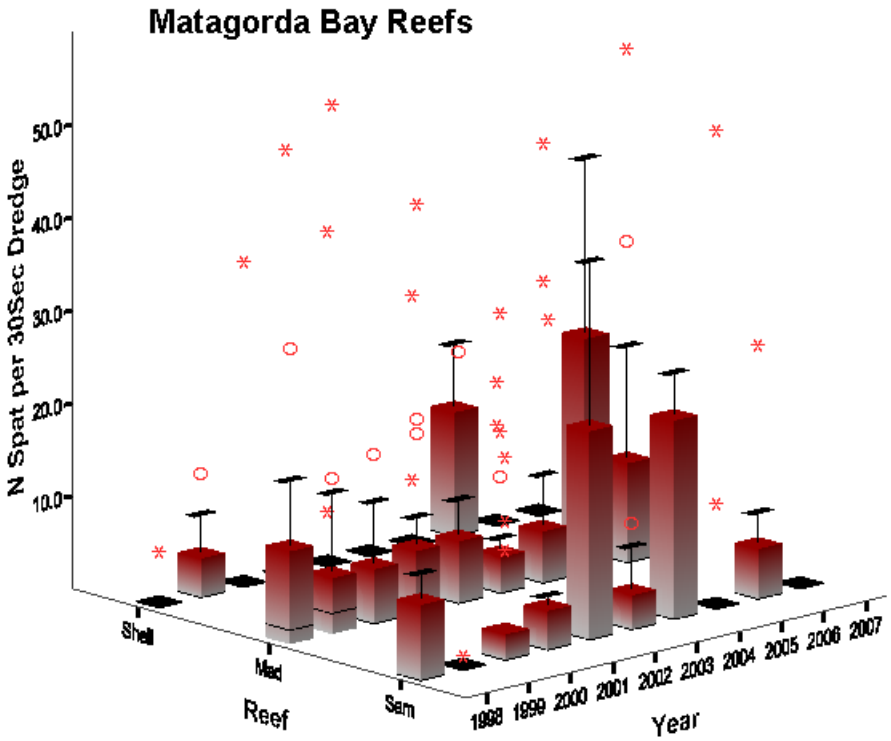

Figure 30. Annual relative abundance trends of spat for three Matagorda Bay Reefs, Shell Island (Shell), Mad Island (Mad) and Sammy's (Sam) Reefs 1998-2007. Note outliers are designated by the symbol *.

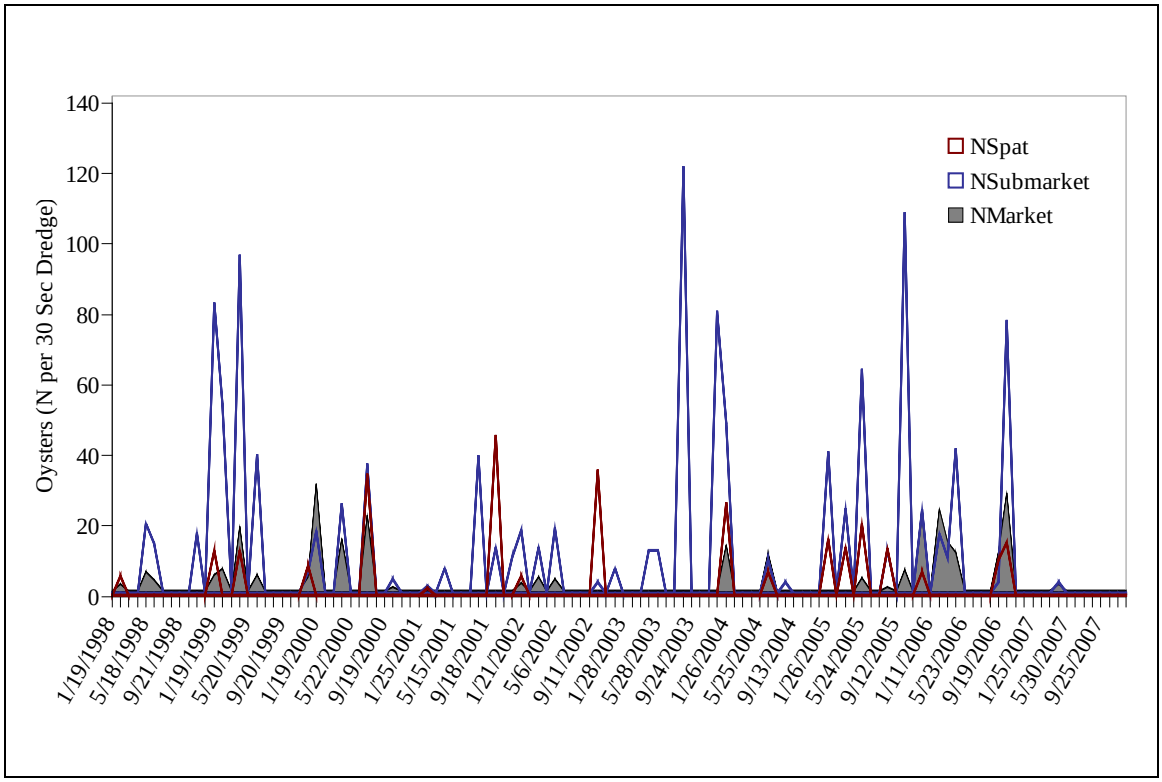

Figure 31. Temporal trends of oysters for Shell Island Reef by size classes 1998-2007.

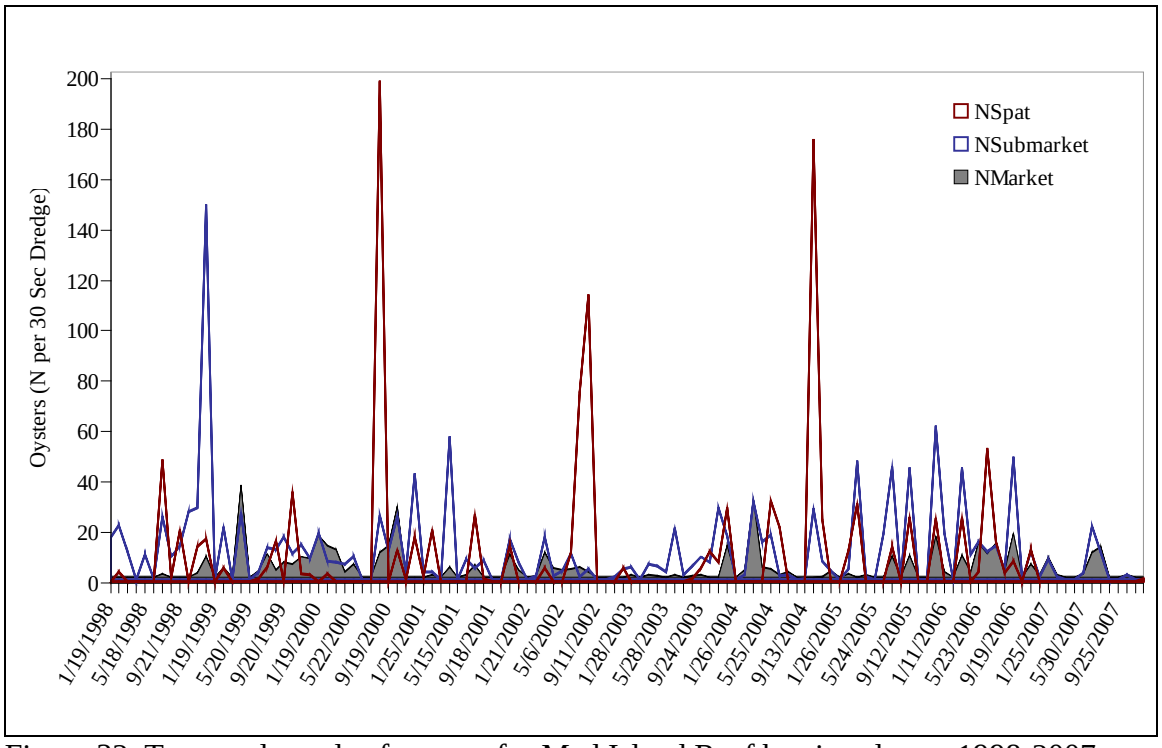

Figure 32. Temporal trends of oysters for Mad Island Reef by size classes 1998-2007.

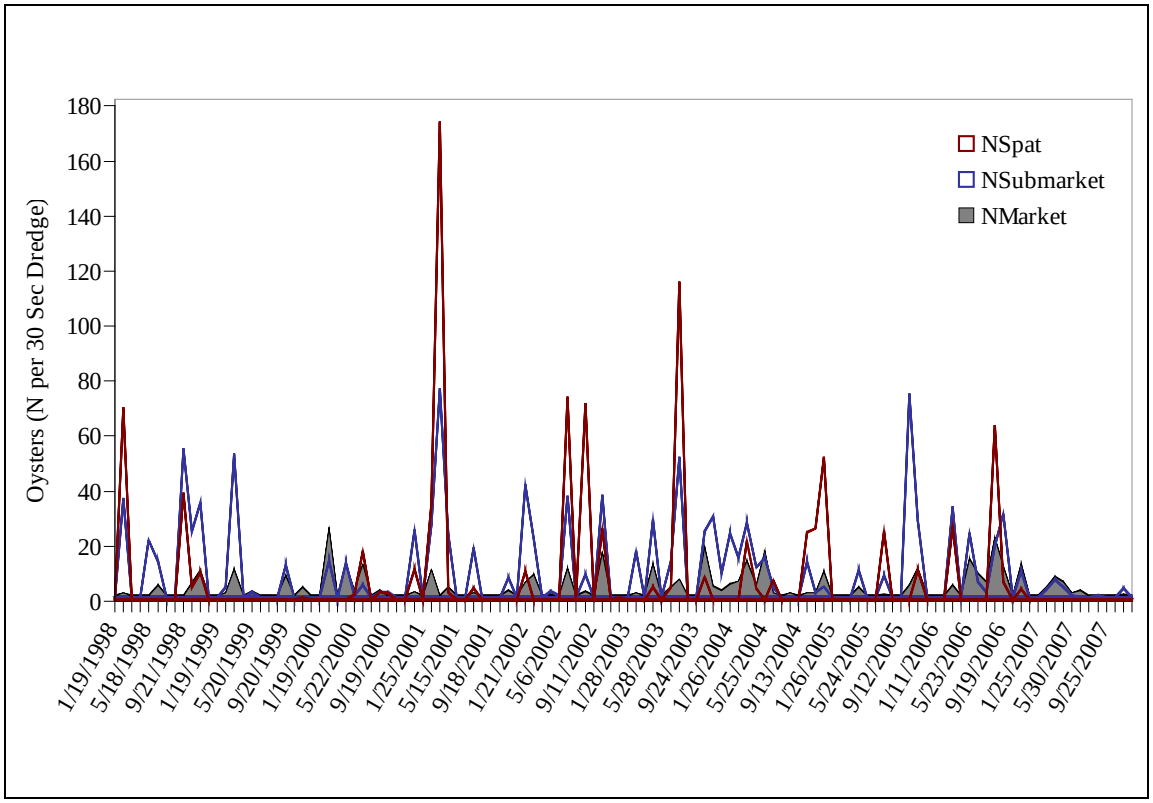

Figure 33. Temporal trends of oysters for Sammy's Reef by size classes 1998-2007.

A comparison of monthly relative abundance of submarket and market size classes for the three reefs between 1998 and 2007 is shown in Figs. 34, 35, 36. As previously observed, Shell Island Reef was dominated by submarket class oysters in every month that samples were collected with the exception of winter months during 2000 and 2001, in addition to the summer - fall months of 2006 (Fig. 34). Mad Island Reef had moderate relative abundances of market and submarket oysters, with a two year lag between higher relative abundance of submarket size classes, as observed in 2001 followed by 2003 monthly samples (Fig. 35). Sammy's Reef had higher relative abundances of market sized oysters in every month, with the exception of samples collected in 2005 (Fig. 36), which were not observed in Mad Island Reef market sized populations.

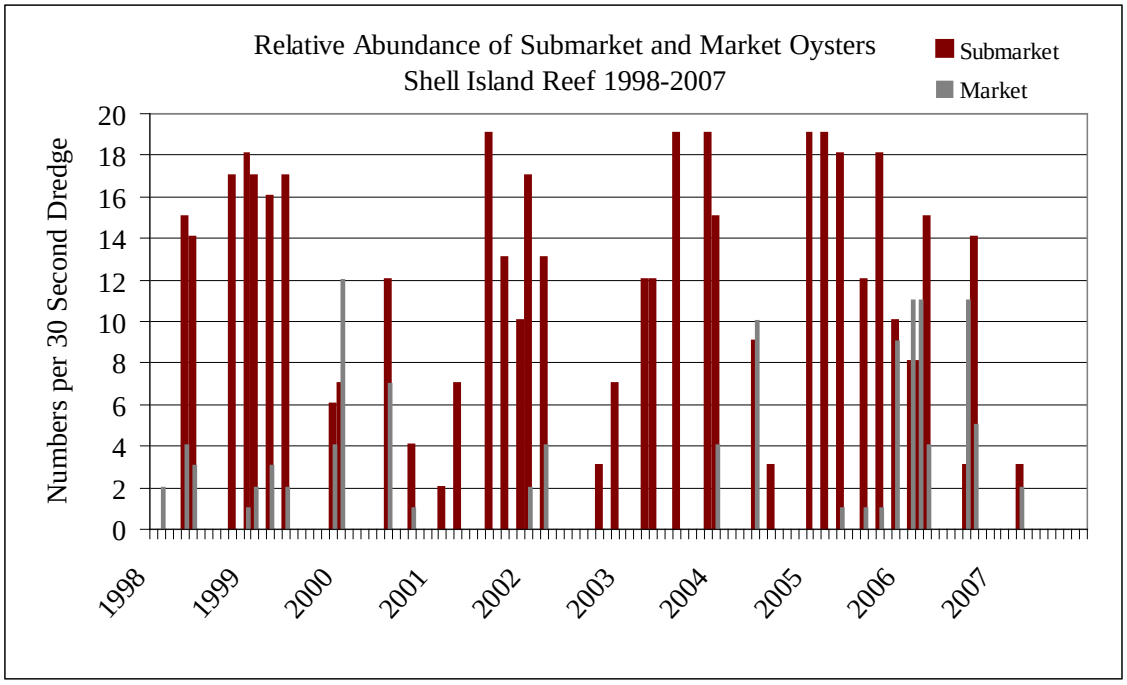

Figure 34. Relative abundance of submarket and market size classes of oysters at Shell Island Reef 1998-2007.

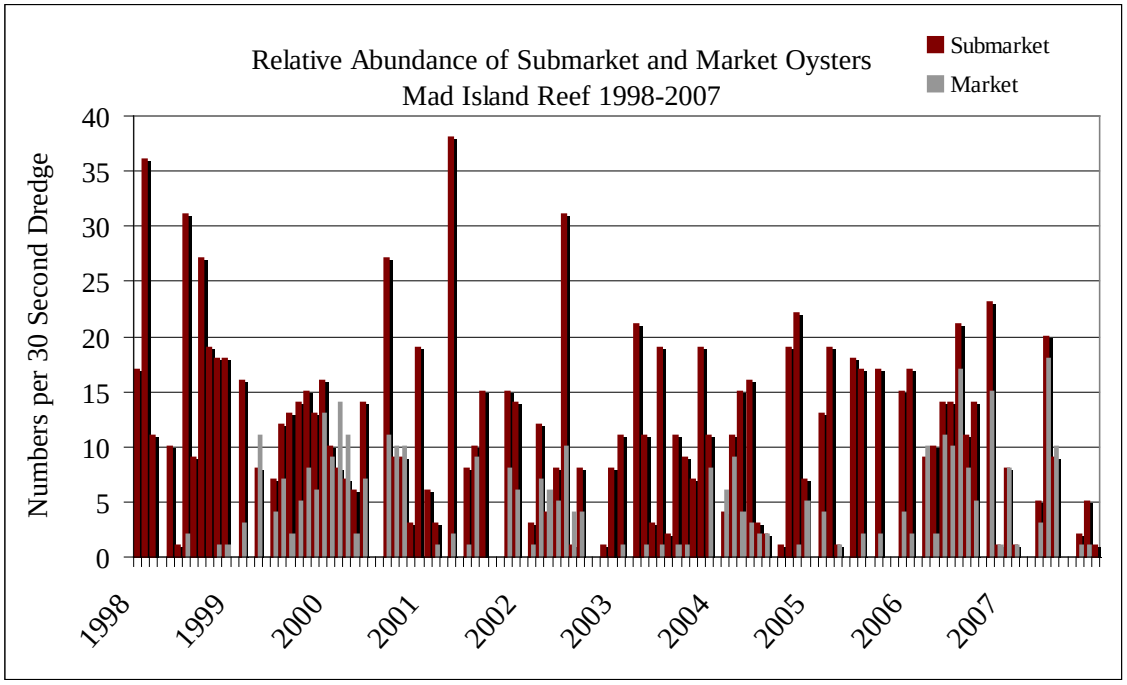

Figure 35. Relative abundance of submarket and market oysters at Mad Island Reef 1998-2007.

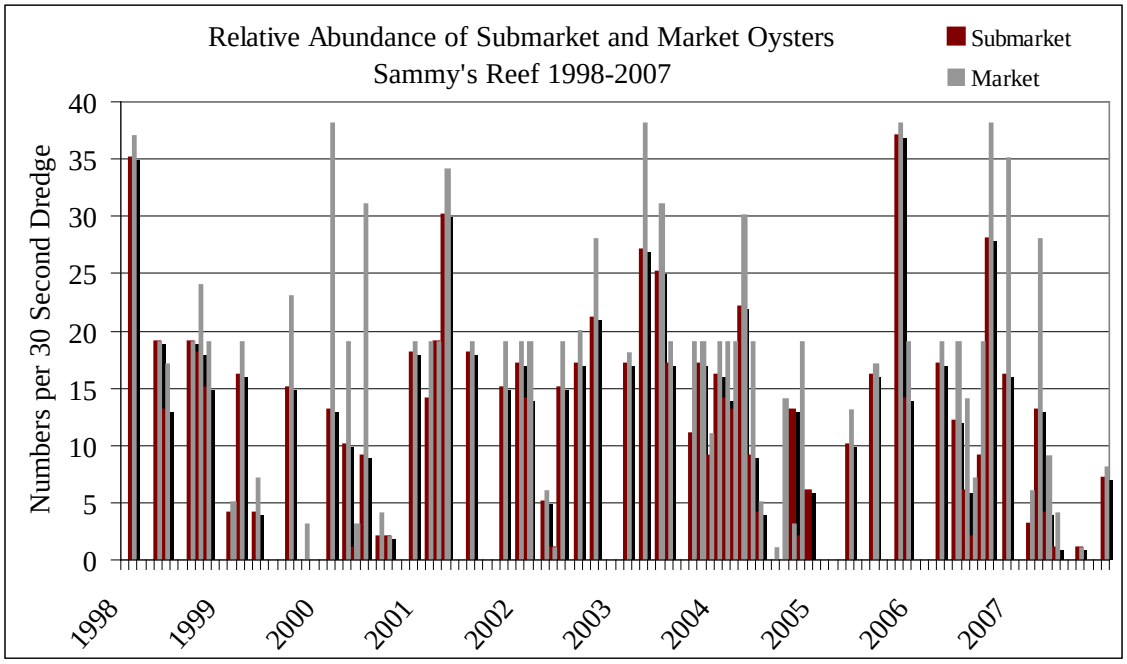

Figure 36. Relative abundance of submarket and market oysters at Sammy's Reef 1998-2007.

Historical information collected by Moore (1907) distinguished different densities of oysters in both market and submarket oysters dependent on whether the sample was located on the up-estuary or down-estuary slopes of Shell Island and Mad Island Reefs. He observed that the water flow and the structure of these reefs were important in determining how many oysters could feed in the current or the potential for spat settlement on the up-estuary sides of these two transverse ridged reefs. Using Moore's estimates of density and known spatial coverage of these reefs in 2008, the present study predicted the potential density and population size for each of these two reefs (Table 4). Although Sammy's Reef was created in 1995 by the USACE, its spatial orientation and restoration design imitate that of Shell Island and Mad Island Reefs, so similar estimates were made for this third reef.

Table 4. Historical and current density estimates of oyster populations for three reefs in Matagorda Bay among market and submarket size classes.

Matagorda Bay Reefs	Acres	Yd^2	Km^2	N Mrk/ yd^3	N SubMrk/ yd^3	N Mrk	N SubMrk	Total N Oysters
Shell Island Leading Edge/Crest Up-Estuary	25	121,000	0.101	106	70	128,260	84,700	212,960
Shell Island Trailng Edge Down-Estuary	120	580,800	0.485	16.75	67	48,642	194,568	243,210
Shell Island Total Reef in 1904	145	701,800	0.586					456,170
Shell Island Enhancement 1993	9.3	45,012	0.038	42	28	18,905	12,603	31,508
Shell Island Total Reef in 2008	154	746,812	0.624			195,807	291,871	487,678
Mad Island Leading Edge Up Estuary	23	111,320	0.093	42	28	46,754	31,170	77,924
Mad Island Trailing Edge Down Estuary	70	338,800	0.283	16	36	27,104	60,984	88,088
Mad Island Total Reef in 1904	93	450,120	0.376					166,012
Mad Island Enhancement 1993	18.6	90,024	0.075	42	28	37,810	25,207	63,017
Mad Island Total Reef in 2008	112	540,144	0.451			111,668	117,360	229,029
Sammy's Reef Creation in 1993 -2008	9.3	45,012	0.037	42	28	18,905	12,603	31,508

The total number of submarket and market sized oysters for Shell and Mad Island Reefs in 2008 was nearly the same or slightly greater for these reefs in 1904. The creation of Sammy's Reef provided an additional down-estuary population of oysters that survived floods and had the potential to supplement larval distribution up-estuary to both Mad Island and Shell Island Reefs, whenever populations of market size oysters were periodically decimated by floods.

Exploratory analyses of temporal variation in each size class among reefs

LOESS curves spanning from 0.1 to 0.9 (10 to 90%) of the continuous 30-month dataset for each of the three oyster size classes indicated that a 12-month span (span distance 0.4) best represented their relationships on each of the three reefs (Shell Island Reef Fig. 37, Mad Island Reef Fig 38, and Sammy's Reef Fig. 39). Span distance 0.4 (left box in center row of each figure) represents points smoothed across a 6-month span on either side of each point. Temporal patterns were strongest for Mad Island Reef, and primarily showed increased abundances of submarket and market oysters in the 12th month following increased spat abundances (Fig. 38). Shell Island Reef data contained lesser numbers of live oysters in all size classes resulting in discontinuous curves (Fig 37).

A. Spat

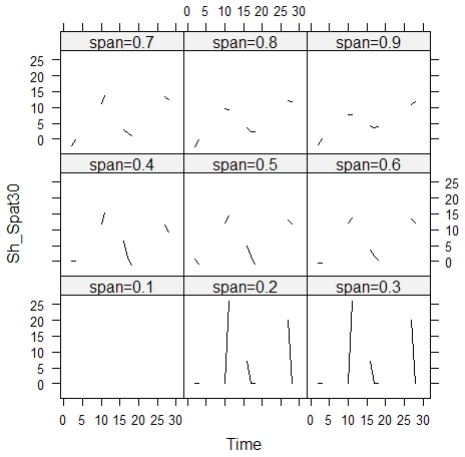

B. Submarket

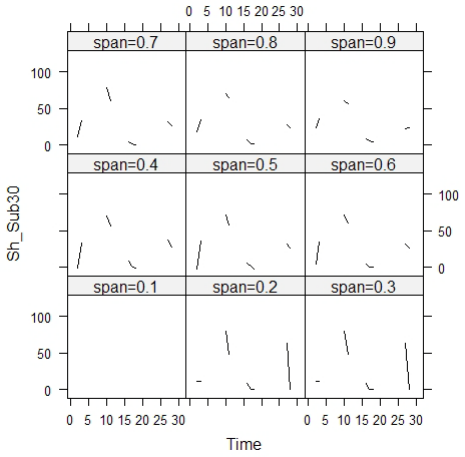

C. Market

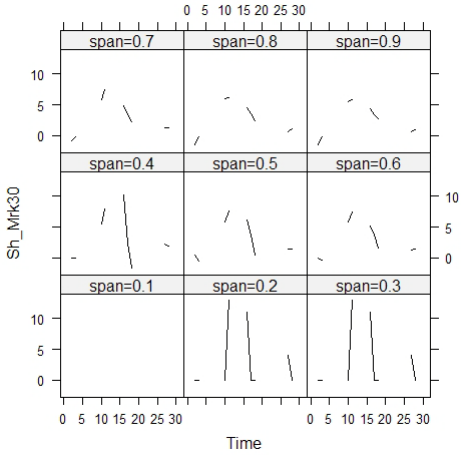

Figure 37. LOESS Curves for Shell Island Reef populations of a continuous 30-month dataset (March 2003 to August 2005) for (A) spat, (B) submarket, and (C) market oysters. Span distance 0.4 (left box in center row of each figure) represents points smoothed across 6-month span either side of each point.

A. Spat

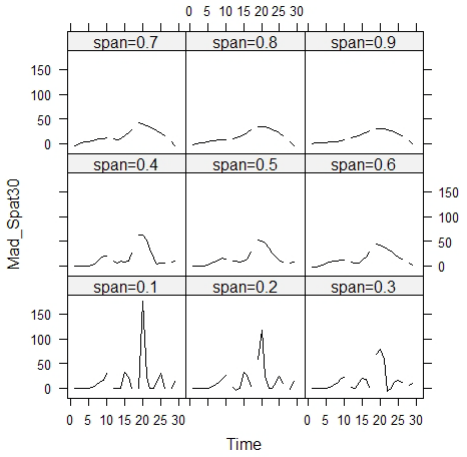

B. Submarket

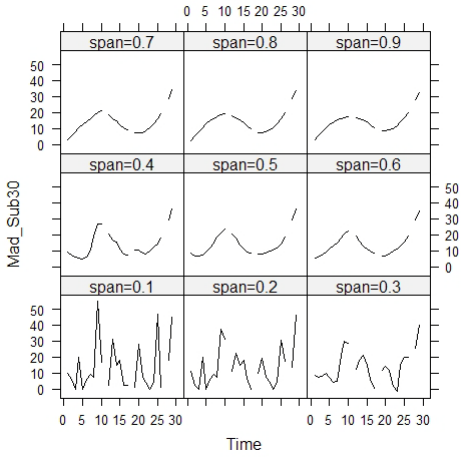

C. Market

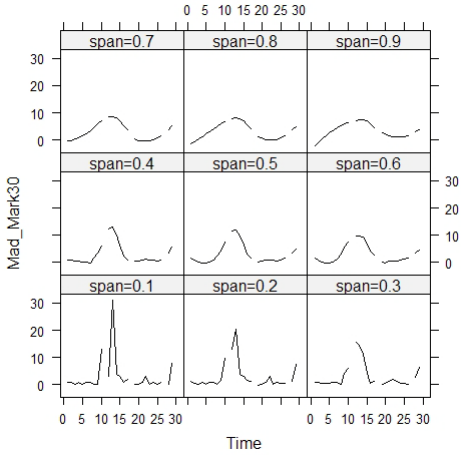

Figure 38. LOESS Curves for Mad Island Reef populations of a continuous 30-month dataset (March 2003 to August 2005) for (A) spat, (B) submarket, and (C) market size classes. Span distance 0.4 (left box in center row of each figure) represents points smoothed across 6-month span either side of each point.

A. Spat

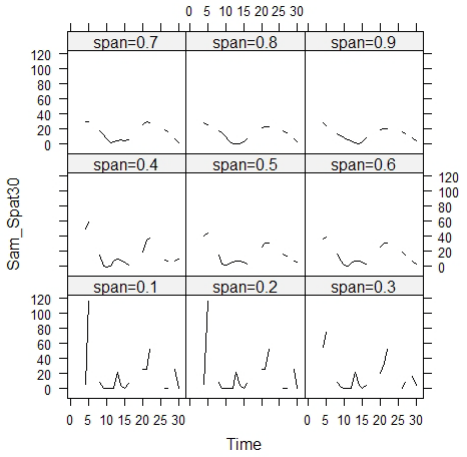

B. Submarket

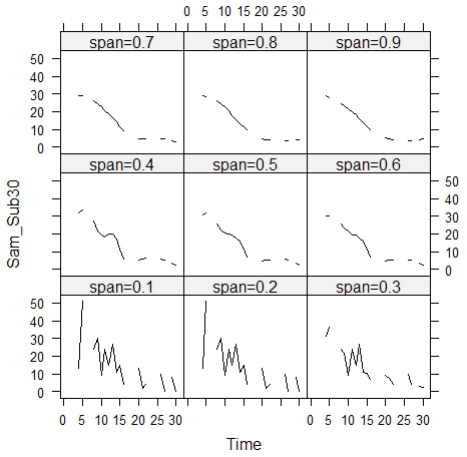

C. Market

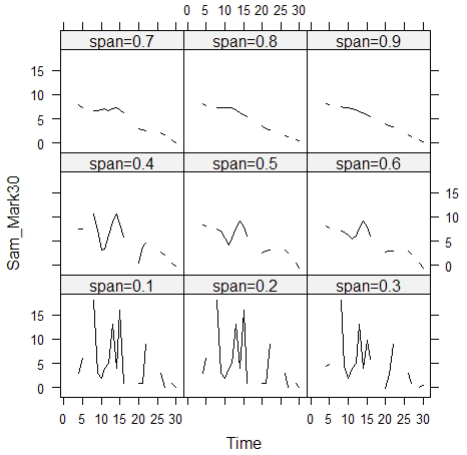

Figure 39. LOESS Curves for Sammy's Reef populations of a continuous 30-month dataset (March 2003 to August 2005) for (A) spat, (B) submarket, and (C) market size classes. Span distance 0.4 (left box in center row of each figure) represents points smoothed across 6-month span either side of each point.

Spatial differences in temporal trends of relative abundance of each size class among reefs

Seasonal and longer-term patterns were characteristically different among the three reefs and among oyster size classes (market Fig. 40, submarket Fig. 41, and spat Fig. 42). In general, seasonal trends were more variable for Shell Island Reef than for Mad Island and Sammy's Reefs. The Colorado River's irregular flow patterns (Fig. 20) appear to have greater affect on seasonal trends for the oyster population at Shell Island Reef compared to the other two reef populations. After removing seasonal trends for market (Fig. 40) and submarket (Fig. 41) oysters, the longer-term trends showed similar patterns (four peaks) for Shell (A) and Mad Island Reef (B) data, but showed a somewhat later occurrence of this same pattern at Sammy's Reef (C) data. However the longer term trend for spat at Shell Island Reef (Fig. 42A) showed a strong additional peak in the earlier months of the data set, which contrasts with the trend for Sammy's Reef (Fig. 42C), which showed a declining trend in the earlier months for spat.

Direct gradient analyses

The CCA for three size classes of live oysters (spat, submarket and market) and two size classes of dead oyster (submarket and market) resulted in total model inertia (total variance) of 1.27. Eigenvalues for the first four multivariate axes are summarized in Table 5. Cumulative percent variance of species-environmental relationship for all four CCA axes was 100%. The results of the CCA showed the combination of all nine explanatory variables accounted for a significant ($F = 2.932$, $P = 0.002$) 24% of the total variation among abundances of spat and oyster size classes.

A. Shell Island Reef

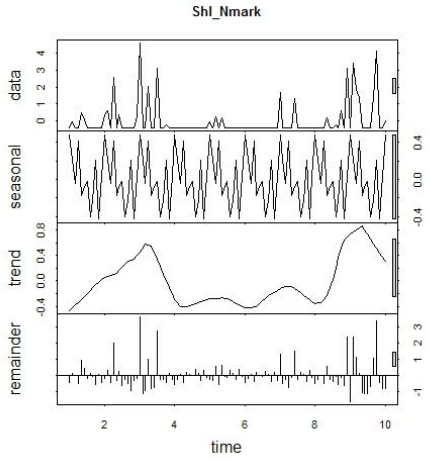

B. Mad Island Reef

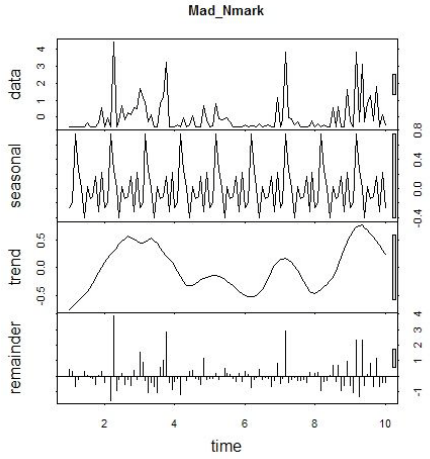

C. Sammy's Reef

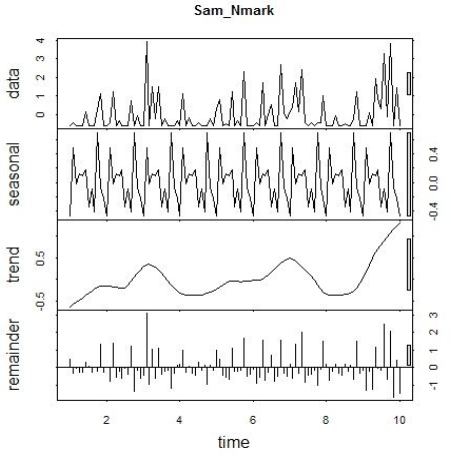

Figure 40. Spatial and temporal patterns of market oysters on Matagorda Bay Reefs, 1998-2006. (A) Shell Island Reef (Shl_Nmark), (B) Mad Island Reef (Mad_Nmark), (C) Sammy's Reef (Sam_Nmark).

A. Shell Island Reef

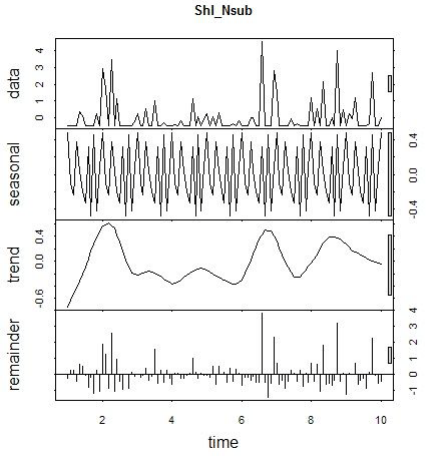

B. Mad Island Reef

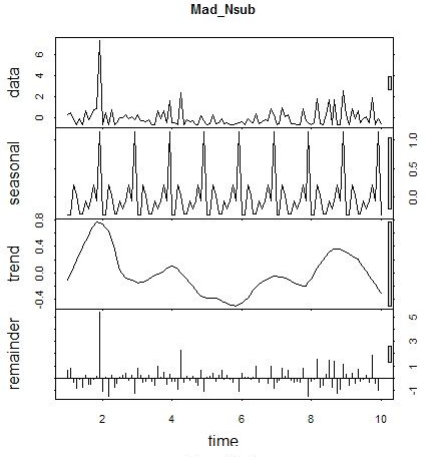

C. Sammy's Reef

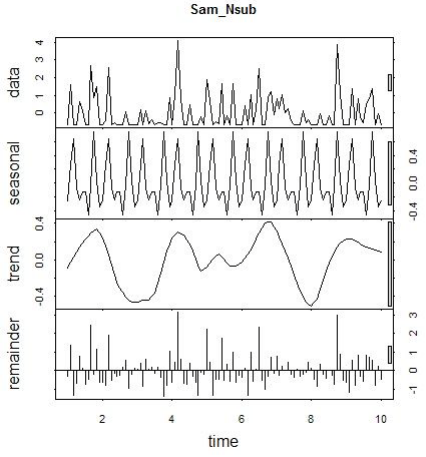

Figure 41. Spatial and temporal patterns of submarket oysters on Matagorda Bay Reefs, 1998-2006. (A) Shell Island Reef (Shl_Nsub), (B) Mad Island Reef (Mad_Nsub), (C) Sammy's Reef (Sam_Nsub).

A. Shell Island Reef

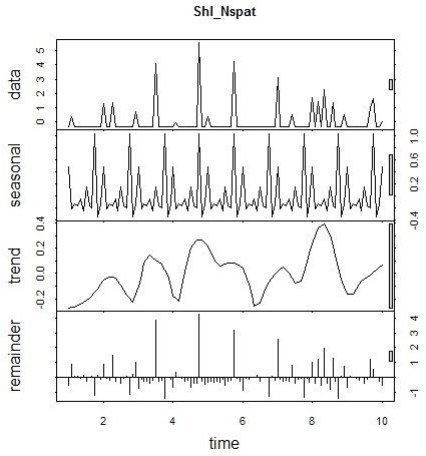

B. Mad Island Reef

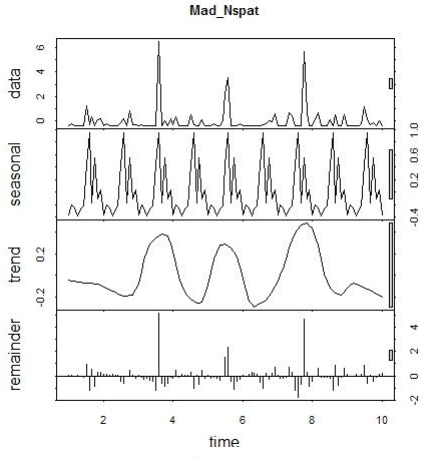

C. Sammy's Reef

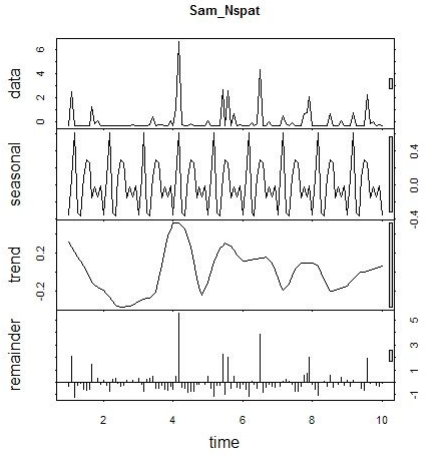

Figure 42. Spatial and temporal patterns of spat on Matagorda Bay Reefs, 1998-2006. (A) Shell Island Reef (Shl_Nspat), (B) Mad Island Reef (Mad_Nspat), (C) Sammy's Reef (Sam_Nspat).

Table 5. Eigenvalues for four axes and total variance for three reefs in Matagorda Bay.

Axis	1	2	3	4	Total inertia
Eigenvalues	0.169	0.078	0.06	0.001	1.277
Species-environment correlations	0.647	0.429	0.412	0.106	
Cumulative percentage variance					
species data	13.2	19.3	24	24.1	
species-environment relationship	54.9	80.1	99.7	100	
Sum of all eigenvalues					1.277
Sum of all canonical eigenvalues					0.308

The first canonical axis accounted for a significant (F = 12.661, P = 0.004) 13% of the variation (Fig. 43). The first axis contrasts primarily differences along a gradient among samples that had more spat in early months of the year, moderate temperatures, especially one month before the sample date (right side in Fig. 43) versus samples with lower to moderate salinity on the sample date and higher densities of live oysters (left side in Fig. 43). The second canonical axis contrasts reef population samples closer to the Colorado River, that had dead oysters and higher flow rates in the month before the sample date (top in Fig. 43) versus samples down-estuary that had more live oysters and higher salinity in the month before the sample date (Sammy's Reef; bottom in Fig. 43). Dead oysters in both submarket and market size classes are important substrates for spat settlement and their location on the right side of the axis one in the plot indicated they are also positively correlated to spat abundance.

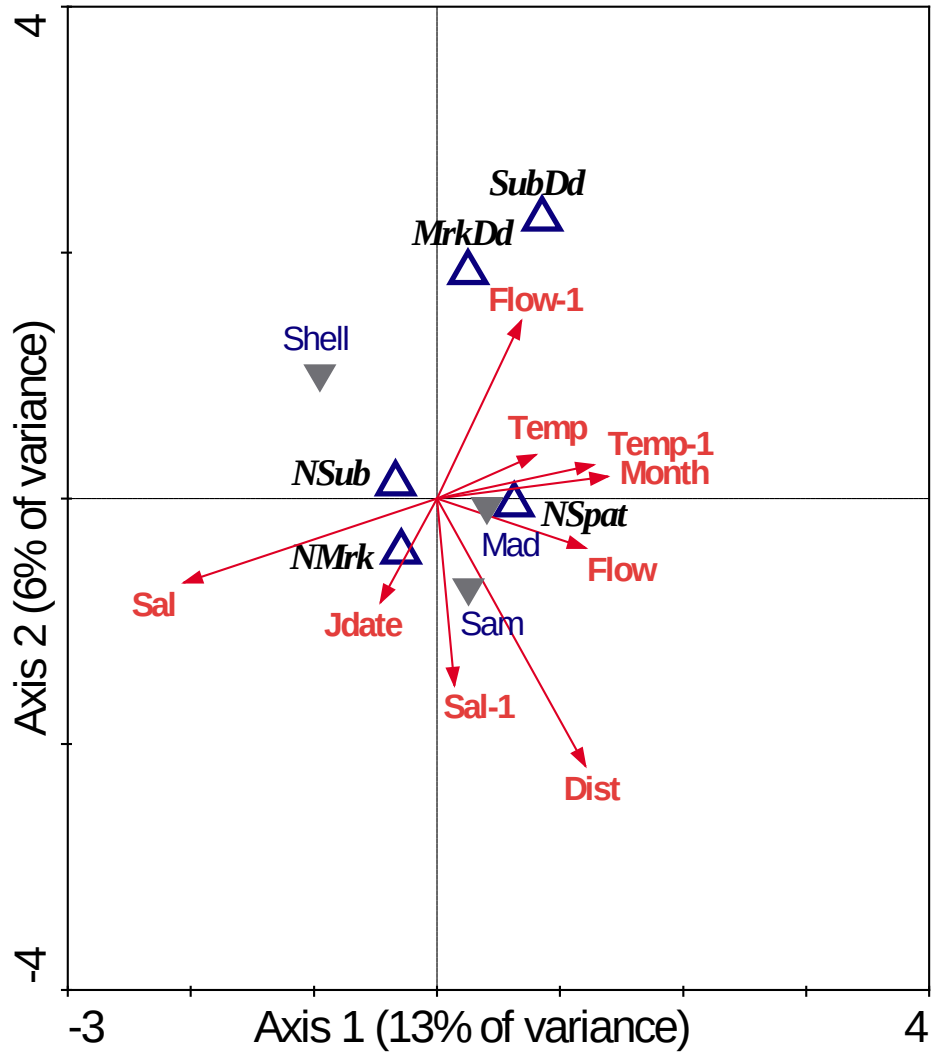

Figure 43. Bi-plot of CCA showing relationships among centroids (centers of distribution as open triangles) for live and dead oysters in market (NMrk, MrkDd) and submarket (Nsub, SubDd) size classes, and for spat (Nspat) in samples on three Matagorda Bay Reefs (Shell, Mad, and Sam are centroids for supplemental variables as indicated by closed triangles). Explanatory variables are shown as vectors for continuous variables indicating their direction and range of variation (length) correlated with each of the first two major canonical axes; Julian date, number for month, and distance (Jdate, Month, Dist), and both zero-lag and one-month lag for flow, temperature and salinity (Flow, Temp, Sal). Smaller angles between axes and vectors indicate stronger contributions of the variable to the canonical axis. Percentage of the variance among response variables that is explained by the combinations of variables on each axis is noted in parentheses.

Discussion

Spatial and temporal oyster reef population dynamics

Although the three reef populations in WMB are differently distanced (1-5 km) from each other and from their main source of freshwater-Colorado River, they appear to be spatially and temporally connected through environmental factors that influence oyster reproduction and survival strategies for populations in WMB. The classic transverse ridge reef type of formation provided them similar benefits, such as increased water circulation and currents from freshwater and tidal influences. The timing and duration of both freshwater flows and meteorological (wind driven) tidal forces influence oyster population dynamics of these three reefs. The gradient analysis of the biological and environmental variables indicated that the higher abundance of dead oysters at Shell Island Reef following high freshwater inflow events, during the month prior to samples being taken, provided this oyster reef population valuable substrate for larvae (spawned from down-estuary populations like Mad Island or Sammy's Reef) to set. Larvae also appeared to be distributed up-estuary from Sammy's Reef to Shell Island and Mad Island Reefs through tidal amplitude and meteorological forced winds between May and June and again in September through October of each year. Larvae also appeared to be distributed down-estuary to Sammy's Reef, from oysters that spawned either in the Colorado Delta's intertidal populations or Shell and Mad Island Reefs when spawning occurred up-estuary prior to high inflow events and during *minima* tidal cycles.

The gradient analysis of biological and environmental variables revealed that oyster populations at Shell Island Reef, located closer to the Colorado River, had higher

relative abundance of dead oysters and experienced higher flow rates in the month before the samples were taken in contrast to down-estuary reef populations, such as Sammy's Reef, that had higher relative abundance of live oysters in all size classes, and experienced higher salinity in the month before the sample date. Relative population abundance data shows that Mad Island and Sammy's Reef have higher numbers of live oysters than Shell Island Reef, which corresponded with distance from the Colorado River. However, these three reefs appeared to have spatial and temporal differences that provided opportunities to replenish up-estuary or down-estuary oyster populations that had been depleted by floods or droughts. The timing of these hydrodynamic forces appeared to be an important factor to the population dynamics of each reef and their connectivity with each other. The time required for larvae to travel up-estuary or down-estuary for successful spat settlement (20-30 days) also appeared to be an important factor in determining recruitment success for these three oyster populations. Although each reef population was identified to have similar seasonal patterns for spawning and growth, the data indicated the relative abundances of spat, submarket, and market populations were dependent on a 12 – 24 month lag time. Growth and reproduction in each oyster population appeared to interact with the environmental variables (salinity, temperature, flow and tide) at least one month prior to the sample date. Spawning success (using spat settlement as an indicator of recent spawning effort) in each population also appeared to depend on the relative abundance of submarket and market oysters in the resident population. Spatial limitations for available nutrients resulted in poor reproductive success when high densities of submarket and market oysters occurred on these reefs, in contrast to when less-dense populations occurred on these reefs.

Conclusions

The three oyster population in this study appeared to be connected with one another through distribution of their larvae and their relative abundance of dead shells for spat settlement. These two biological variables interacted with the environmental variables of salinity and temperature to determine survival and mortality of oyster populations in WMB. The timing and duration of freshwater and tidal influences appeared to be critical factors for reproductive success and growth of these three populations. Analysis results for Shell Island and Mad Island Reef populations were consistent with survival of up-estuary populations, which depend on the number of days they are required to endure lowered salinity conditions during warmer temperature months. Analysis results for Sammy's Reef population were comparable with down-estuary populations, which benefit from longer distance away from freshwater sources, and the length of time they are required to endure lowered salinity conditions. Daily temperature and salinity records of subtidal oyster populations were identified in this study as being important information in assessing the health of these oyster populations.

CHAPTER III

SPATIAL AND TEMPORAL PATTERNS OF DERMO INFECTION IN OYSTERS ON MATAGORDA BAY REEFS

Introduction

Relatively few studies of the effects of *Perkinsus marinum* on oyster production were conducted in WMB from 1959, when this parasite was first discovered in this bay system, until 1996 (Hofstetter and Heffernan 1959; Heffernan 1963; Hofstetter 1965; 1966; King 1964; 1989; King et al. 1994; Craig et al. 1989; Ray 1966; 1987; Ray 1996;). Since then, Dermo infection has been monitored on the three populations of Shell Island, Mad Island and Sammy's Reef after the Colorado River connection to WMB was re-established through a cooperative effort by TPWD and TAMUG from 2003 and continues until the present study. Results are available to the public on the www.oystersentinel.org web site.

Although the three oyster reef populations in WMB are spatially separated along a salinity gradient from the Colorado River to Matagorda Bay, they are linked through environmental factors that influence up-estuary larvae distribution (see Chapter II). These larvae provide an additional biological factor for increasing transmission of Dermo disease to oyster populations on Shell Island Reef, which may otherwise only contain residual levels of Dermo infection due to the predominance of lower salinity conditions (Craig et al 1989; Powell et al. 1996; Soniat et al. 1998).

Environmental interactions with Dermo infection

Dermo disease can withstand a wide range of temperatures and salinities. Under lower salinity conditions (< 15 ppt), increased Dermo disease can reduce oyster populations, and at higher salinity (>15 ppt) and temperature (> 25 °C) combinations, Dermo infection appears to increase and spread within an oyster population (Ray 1987, Song 1993, Soniat 1996; Kennedy et al. 1996). Therefore, Dermo-related mortality generally peaks during the summer, when conditions are optimal for parasite growth. Elevated infection levels are associated with higher salinities and higher temperatures related to drought, independent of seasonal conditions (Burreson and Andrews 1988). Colder temperatures generally reduce the effect of Dermo infections. However, large-scale climatic conditions, such as those associated with El Niño southern oscillation (ENSO) cycles, may facilitate the initiation and progression of Dermo disease along the coast of the Gulf of Mexico (Powell et al. 1992; 1996; Kim and Powell 1998; Soniat et al. 2005).

ENSO cycles result from disruption of the oceanic atmospheric system in the tropical Pacific, which relaxes the trade winds and allows warm water to accumulate along the equator which in turn, reduces upwelling of cold water in the eastern Pacific Ocean (Ropelewski and Halpert 1986, Philander 1989). El Niño periods are marked by changes in the amount and pattern of rainfall across the Gulf of Mexico coastline causing the cooler and wetter conditions that tend to lower Dermo infection levels (Soniat et al. 2005). These conditions alternate with La Niña periods that occur when stronger trade winds and increased upwelling in the eastern tropical Pacific bring

warmer and drier conditions to the Gulf of Mexico coast (Ropelewski and Halpert 1986, Philander 1989, Soniat et al. 2005).

Epizootic Dermo infections are correlated with reduced food supply and lower recruitment (to harvestable-size oysters), which generally occur prior to, or coincidental with, salinity and temperature conditions that increase biological stress on oysters (Soniat and Ray 1985; Powell et al. 1996; Dittman et al. 2001). Ray (1987) showed that increased growth rates, and therefore increased recruitment of oysters, could effectively "dilute" the infection enough to terminate an epizootic event. These relationships suggested that disease management strategies should include harvesting infected market-sized oysters in order to reduce the number of diseased oysters and reduce the percent infection of Dermo in host populations (Powell et al. 1996).

Spatial interactions with Dermo infection

The most likely method of long-distance transfer of Dermo infection among reefs, within and between bay systems, may be linked through transplantation of previously infected oysters (Powell et al. 1997). Once introduced, Dermo rapidly spreads through oyster populations (Ray 1954, Ray 1966, Craig et al. 1989; Powell et al. 1997; Soniat et al. 1998). Private oyster leases are currently available only in Galveston Bay. However, in the early 1950's after this pathogen and its effect on oyster populations was first discovered (Mackin et al 1951), there were private leases for transplanting oysters were available in every Texas coastal bay. Although oysters were sampled and evaluated for Dermo along the Texas Coast between 1954 and 1960, Dermo was not considered to be widespread in Galveston, Matagorda, and Aransas Bays until 1959 (Hofstetter and Heffernan 1959). In 1962 mortality studies among tray-held oysters were conducted to

determine the influence of Dermo in Galveston, Matagorda and Aransas Bay systems (Hofstetter et al. 1965). The results of those and subsequent studies found that every Texas bay system (salinity ranged from 6 to 36 ppt) was infected with Dermo (Hofstetter et al. 1965; Quick and Mackin 1971; Hofstetter 1977).

The present study describes the spatial and temporal patterns of Dermo disease on three oyster reef populations (Shell Island, Mad Island and Sammy's Reefs) in WMB along a salinity gradient between the Colorado River Delta and the land cut through the Gulf Intercoastal Waterway (GIWW) into Matagorda Bay.

Methods

Oyster collection methods for Dermo samples

Oysters were monitored between 1986 and 2007 by the TPWD Coastal Fisheries Resource Monitoring Program, which followed specific protocols (TPWD 2002) that were discussed in Chapter II. However, TPWD used a modified procedure for collecting oysters for Dermo disease evaluation in this study. Routine monitoring samples are generally collected monthly in the same calendar year from two potential sampling grids on the three oyster reefs within WMB. Because sampling sites are randomly chosen from among gridded sections on a map, more than one grid per reef is sometimes sampled each month, or sometimes no grids are selected for sampling within those reefs each month. In such cases when more than one sample was collected on a reef, the oysters were saved and pooled from each 30-s dredge sample; and oysters were randomly chosen for Dermo disease evaluation. In cases when no grids were selected on a reef, samples were collected by conducting a standard 30-s dredge on the reef in

known grids that are routinely sampled by TPWD. Market-size (≥ 76 mm) and submarket-size (< 76 mm) oysters were randomly chosen and removed from these dredge samples; and placed in plastic coolers with frozen bottles of water to prevent freshwater contamination of these samples. These samples containing at least 15 oysters of each size class from each reef were transported within 48-hrs to TAMUG laboratory for Dermo disease evaluation.

Dermo infection evaluation methods

Dermo infection was assessed using several parameters in this study. The amount of Dermo infection present in the sample from each reef will be referred to as percent infection or "prevalence", which is the percentage of oysters in each size class evaluated that have Dermo present in their mantle tissue. Percent infection values range from 0 (no infection detected) to 100 percent (all oysters infected). To detect the presence of Dermo infection in an oyster, a tissue sample from the mantle of each oyster was processed and cultured using procedures originally developed and modified by Ray (1952; 1966). Slides of these cultured tissues were stained, viewed through a microscope (10X magnification), and then were interpreted by Dr. Ray. (Note: Because one person used the same procedures and interpretation method, consistently comparable results over time were available for this study.) The slide from each oyster was assigned a "disease code" by counting the relative number of parasites (hypnospores) per tissue sample, also referred to as Dermo intensity for an individual oyster, as described by Ray (1966) and modified by Craig (1989).

The average of these disease codes (across all oysters in the sample) was calculated to quantify the weighted incidence (WI) of Dermo disease in each sample of

10-15 oysters, which conveys information about the disease status among individual oysters in the population. Ray interpreted 16 potential levels of infection which were assigned a disease code value (Craig et al. 1989) between 0 and 5 (Table 6). The lowest level of Dermo incidence is scored as 0, indicating a healthy oyster (Fig. 44). Although the highest level of Dermo incidence is scored as 5, the next highest level of Dermo incidence, 4.33 (Fig. 45) indicates a heavily infected oyster.

Table 6. Descriptions of Dermo incidence levels in oyster tissue (Craig et al. 1989).

Description	Incidence	*Perkinsus marinus* cell density
Negative	0.00	no cells present
Very Light -	0.33	1-10
Very Light	0.67	11-74
Light -	1.00	75-125
Light	1.33	> 125 cells but < 25% of tissues is cells
Light +	1.67	< 25% of tissues
Light/moderate -	2.00	25% of tissues
Light/moderate	2.33	> 25% but much < 50% of tissues
Light/moderate +	2.67	> 25% but < 50% of tissues
Moderate -	3.00	50% of tissue
Moderate	3.33	>50% but much < 75% of tissues
Moderate +	3.67	>50% but < 75% of tissues
Moderately Heavy -	4.00	75% of tissues
Moderately Heavy	4.33	> 75% but < 100% of tissues
Moderately Heavy +	4.67	>75% but some oyster tissue visible
Heavy	5.00	~100% with no oyster tissue visible

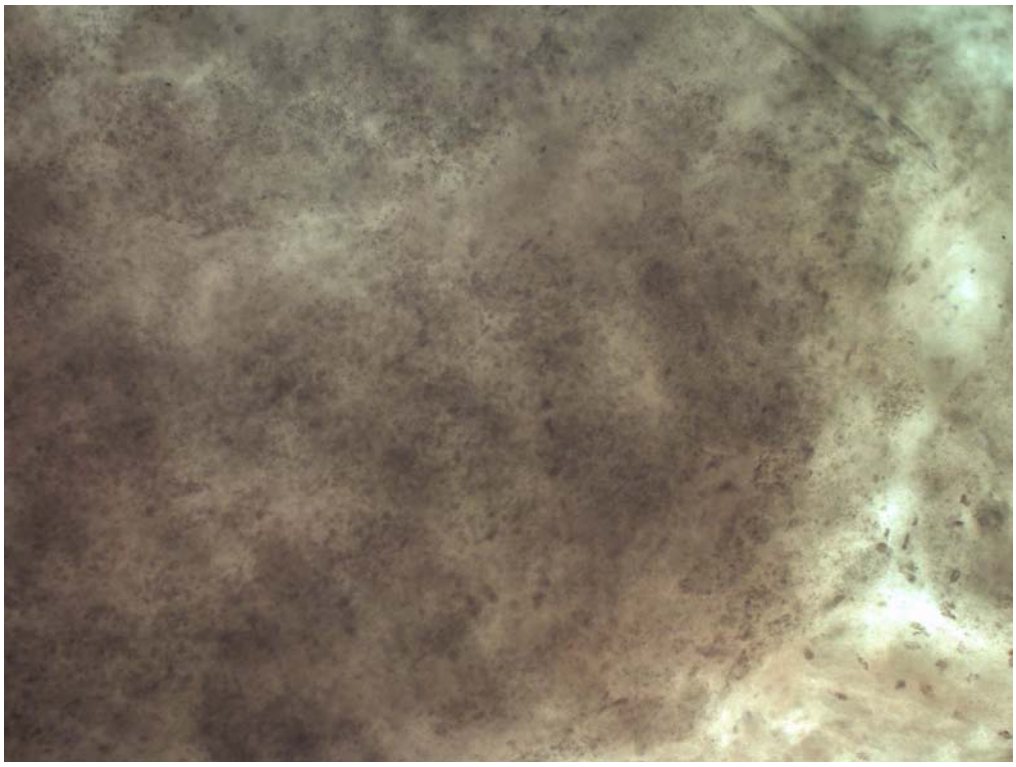

Figure 44. Market oyster mantle tissue, 10X magnification, Disease code = 0.00; No infection or Dermo cells detected. Photograph by J. Culbertson.

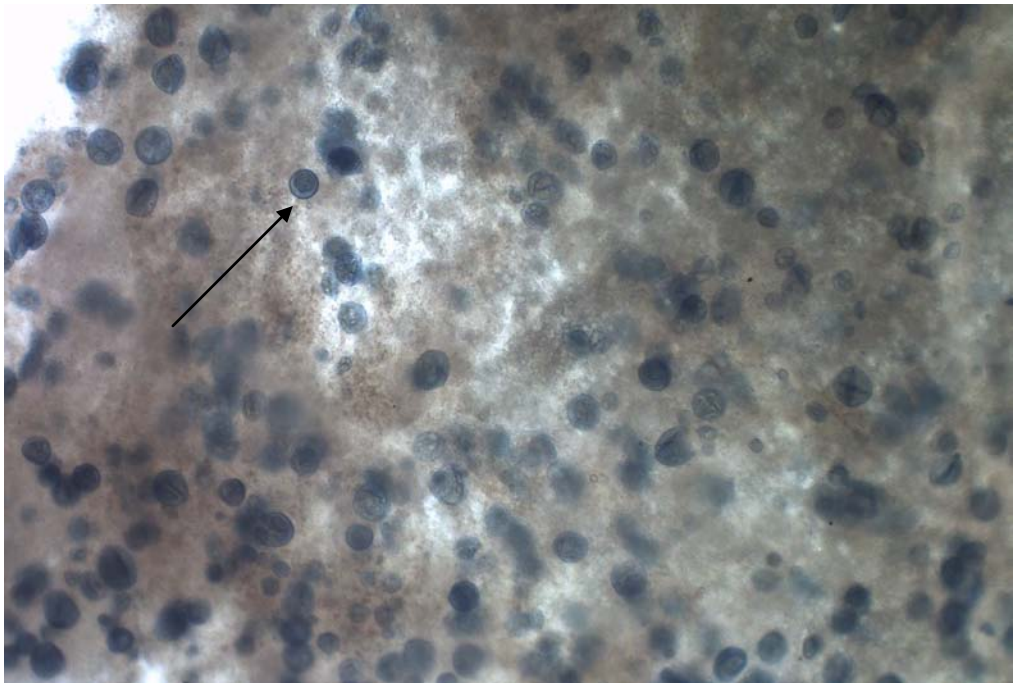

Figure 45. Market oyster mantle tissue, 10X magnification, Disease code = 4.33 Moderately heavy + infection, mostly well enlarged and thin walled cells. Photograph by J. Culbertson.

Exploratory analysis of Dermo in submarket and market size classes and environmental factors among reefs

Monthly WI data for submarket and market size oysters were evaluated from 2003 through 2007 in the present study, with the exception of six months during the later part of 2005 when Dermo samples were not collected. Temperature and salinity measurements were collected by TPWD regardless of whether live oysters were or were not collected in their routine monitoring dredge samples. Zero values in this study did not indicate live oysters were not present on the reef, only that live oysters were not collected in the sample on the reef at that specific location, according to TPWD's protocols (TPWD 2002).

Analytical methods

Indirect gradient analyses—Principal Components Analysis (PCA) and Detrended Correspondence Analysis (DCA) were run using the software CANOCO (ter Braak and Smilauer 2002) to evaluate the length of the ecological gradient (Jongman et al 1995) contained in the datasets for the six biological variables (number of spat, market and submarket oysters, hypnospore densities and percent Dermo infection in market and submarket oysters, and a categorical variable indicating when only dead oysters were collected in a size class for a sample) and Julian date, month, distance from the Colorado River, and values for zero lag and one month lag of environmental variables (salinity, temperature, and flow) from the 1998-2006 data sets.

Before analysis, variables were transformed to linearize and normalize the distribution of some variables; percentages of Dermo infection were converted to proportions and arcsine square-root transformed; density of hypnospores (in market and submarket oysters) and distance were log transformed. A preliminary analysis showed

that the biological dataset contained short ecological gradients (a change of less than three standard deviations in the response variables across all samples) and therefore was suitable for analysis of linear relationships among variables (Jongman et al. 1997).

Direct gradient analysis of environmental variables and index values among reefs using RDA

A linear direct gradient analysis, Redundancy Analysis (RDA), was used to build a multivariate linear model to test the relationships between biological and explanatory environmental variables. This analysis produces new canonical variables (axes) that are linear combinations of the explanatory variables. These canonical axes are then used in a constrained ordination in which the relationships among the biological (dependent) variables are modeled as a function (multivariate regression) of the canonical axes. Starting with the full model (all explanatory variables included), sequentially variables were eliminated if the variance inflation factor (VIF) was greater than 5, in order to minimize redundancy (colinearity among explanatory variables) that could inflate significance tests of the multivariate relationships for the canonical axes. To interpret and visualize the results, they were plotted in a bi-plot (singular plot of both biological and explanatory variables). RDA was also used to test the relationships between 30-day lagged responses of the biological variables to the explanatory environmental variables.

Results

Relationships of Dermo in submarket and market size classes and environmental factors among reefs

Weighted incidence (WI) for each oyster size class (submarket and market) was evaluated for relationships to temperature and salinity recorded on the day oyster samples were collected for Dermo evaluation (Figs. 46, 47, 48). Shell Island Reef populations of oysters typically have very low levels (WI < 1.0) of Dermo infection (Fig. 46) and lower salinity levels than Mad Island or Sammy's Reefs. In July 2006, there were slightly higher infection levels (WI = 1.5) associated with relatively higher abundances of both submarket and market sized oysters (previously shown in Fig. 34), and also higher salinity and temperature conditions at Shell Island Reef (Fig. 44). Lower levels of WI were also observed during several consecutive months in 2007. Low salinity levels at Shell Island Reef that were continuously recorded for several months after a June 2007 flood, resulted in dredge samples that were devoid of live submarket or market oysters, which precluded evaluation of these samples for Dermo infection.

Mad Island Reef oyster populations typically have moderate to low levels of Dermo infection between 0.33 and 1.5 (Fig. 47). WI was recorded as higher than normal on the same date in July 2006 as previously observed in Shell Island Reef oyster populations (Fig. 46). Both salinity and temperature were higher than previous months and relative abundance of submarket and market oysters at Mad Island Reef were also recorded as having moderately high relative abundance (Fig 35) during this period.

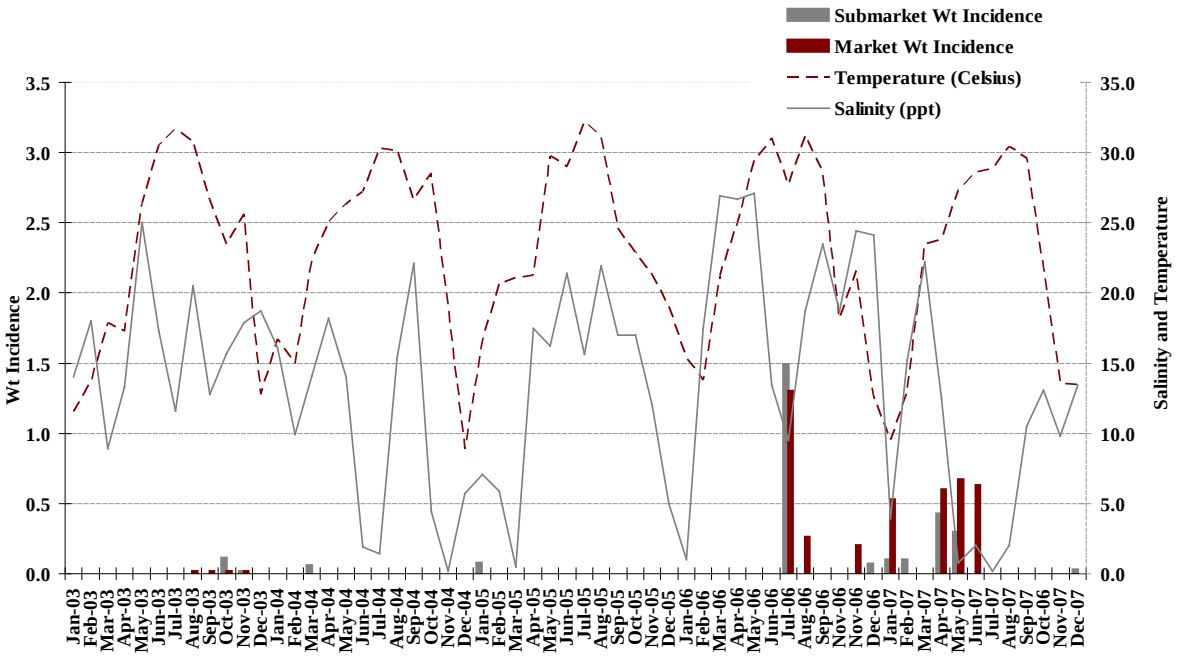

Figure 46. Shell Island Reef submarket and market WI levels with temperature and salinity measurements on sample collection date. Dermo samples were not collected from September 2005 through February 2006.

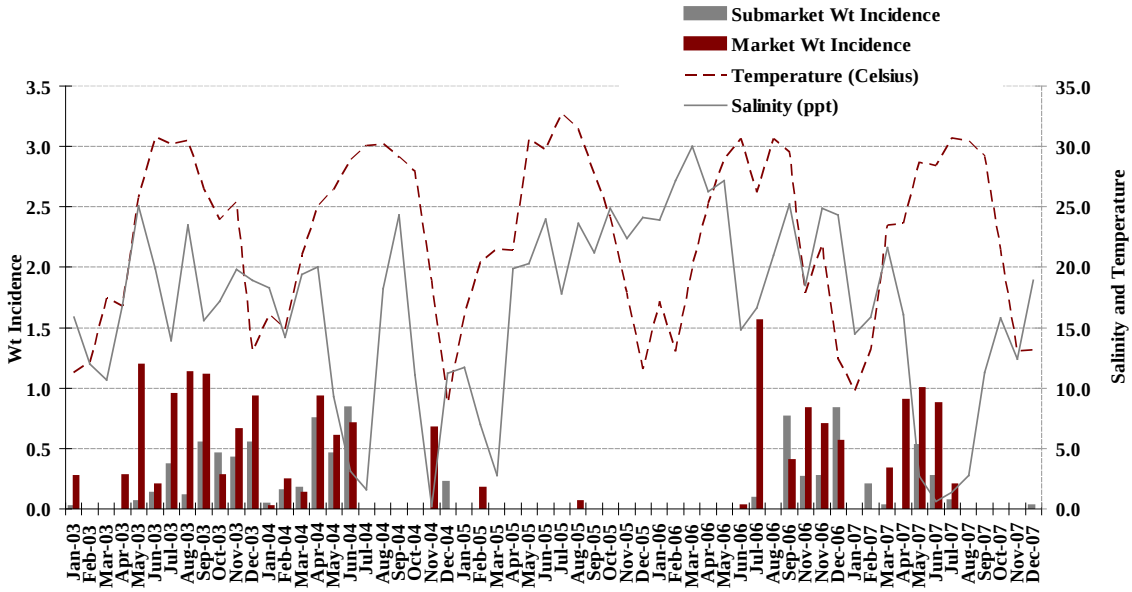

Figure 47. Mad Island Reef submarket and market WI levels with temperature and salinity measurements on sample collection date. Dermo samples were not collected from September 2005 through February 2006.

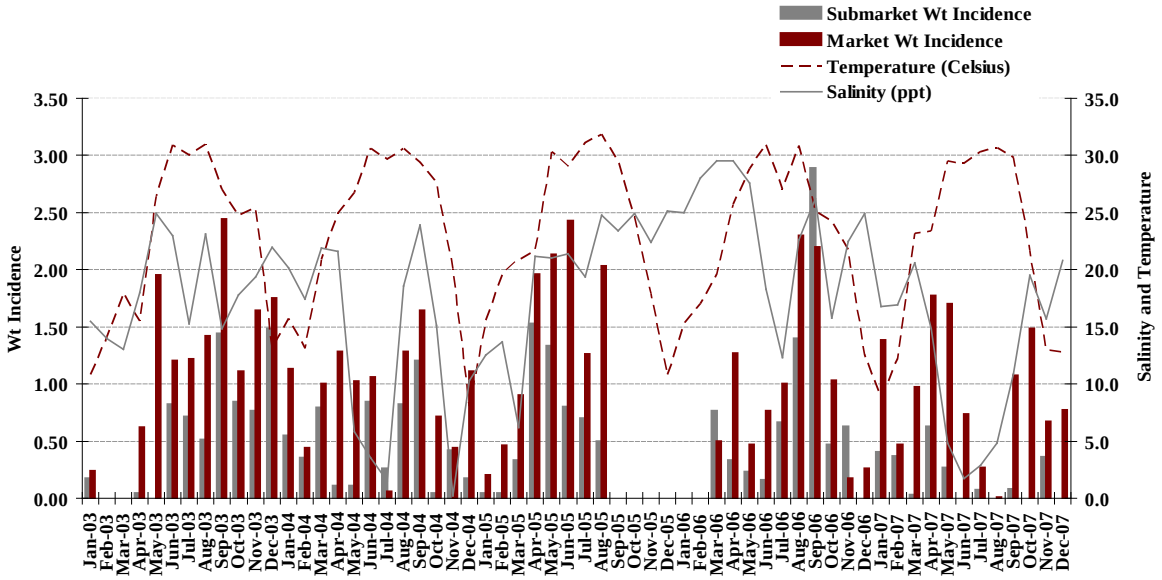

Figure 48. Sammy's Reef submarket and market WI levels with temperature and salinity measurements on monthly sample collection date. Dermo samples were not collected from September 2005 through February 2006. Zero WI between February 2003 and March 2003 are actual samples evaluated with zero Dermo infection.

Sammy's Reef oyster populations typically have moderate to high levels of Dermo infection between 0.5 and 2.8 (Fig. 48). WI was recorded as higher than normal at Sammy's Reef in July as well as August 2006, on the same date as recorded for both Shell Island (Fig. 46) and Mad Island (Fig. 47) Reefs' oyster populations. Both salinity and temperature exhibited seasonal trends that were previously described as meteorological forcing by winds and not astronomical tidally influenced (Solis 1999) and were discernible in this evaluation of WI and environmental conditions at Sammy's Reef. Salinity and temperature extremes that were shown in Figs. 46 and 47 for Shell Island and Mad Island Reefs were not unusual for Sammy's Reef (Fig. 48). However, WI remained at higher levels at Sammy's Reef for additional months after both Shell and Mad Island Reefs' WI levels decreased. Although relative abundance of submarket

and market oyster populations at Sammy's Reef are typically higher than Mad or Shell Island Reefs, these size classes at Sammy's Reef were higher than previous months on July 2006 (Fig 36). Although higher salinity and temperature conditions promote the growth of hypnospores, higher densities of these three reef populations could also promote the transmission of the disease to more individuals in each population as well as transmission of the hypnospores through larval distribution to other reefs.

Direct gradient analysis

The results of the RDA showed the combination of explanatory variables accounted for a significant ($F = 5.584$, $P = 0.002$) 36% of the total variation among Dermo-related variables. The first canonical axis accounted for a significant ($F = 34.25$, $P = 0.002$) 32% of the variation (Fig. 49). It contrasts primarily differences between samples farther from the Colorado River, that had higher salinity on both the sample date and one month before the sample date and higher infection rates and densities of hypnospores (Sammy's Reef; upper left in Fig. 49) versus samples up-estuary that had more dead oysters and higher inflows one month before the sample date (Shell and Mad; lower right in Fig. 49). The second canonical axis was primarily related to the temporal gradient in lower abundances of live oysters in both size classes, higher infection rates in populations, and more dead oysters, in later years and months (top of Fig. 49) versus earlier years and months (bottom of Fig. 49).

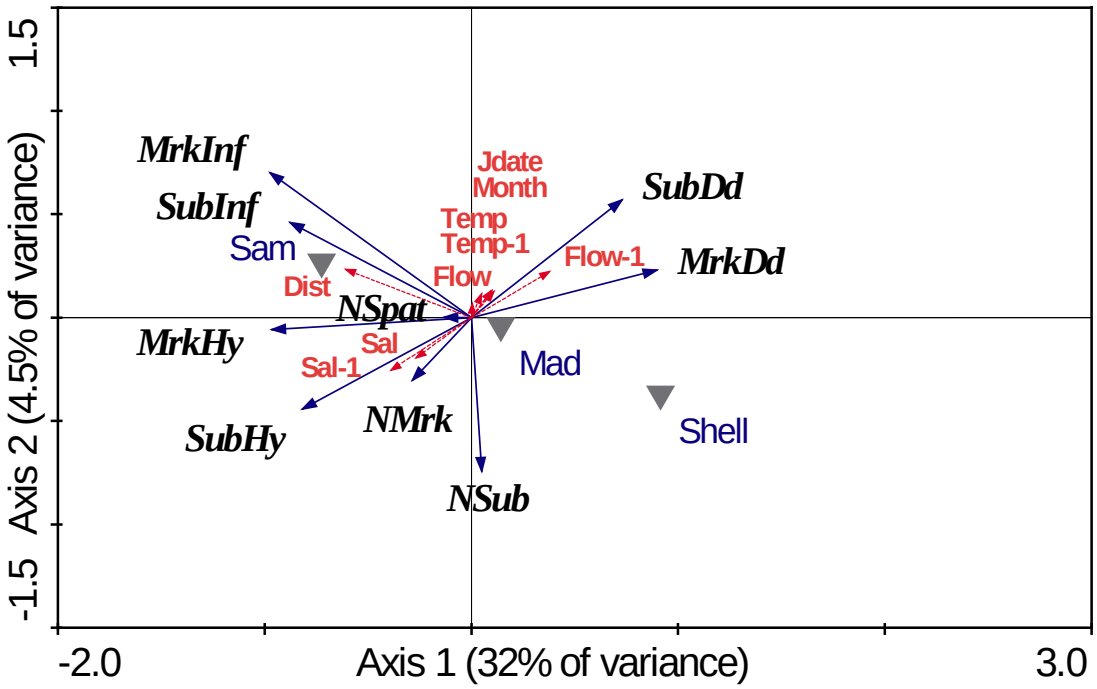

Figure 49. Bi-plot of RDA showing relationships among response variables and explanatory variables. Response variables are shown as blue vectors for live spat (NSpat), live and dead market and submarket oysters (NMrk, NSub), Dermo hypnospore densities per individual and population infection rates for each size class (MktHy, SubHy, MktInf, SubInf), in samples on three Matagorda Bay Reefs (Shell, Mad, and Sam). Three reefs are shown as centroids for supplemental variables, as indicated by filled, down turned triangles). Explanatory variables are shown as vectors (red lines) for continuous variables indicating their direction, range of variation (length), and correlation with each of the first two canonical axes for Julian date, month, and distance from the Colorado River (Jdate, Month, Dist), and both zero lag and -1 month lag for flow, temperature and salinity (Flow, Temp, Sal). Note: vectors also extend in the opposite direction (indicating negative correlations), but for simplicity are not shown. Smaller angles between axes and vectors indicate stronger contributions (correlations) of the explanatory variable to the canonical axis. Percentage of the explained variance for response variables is noted in parentheses on each axis.

Discussion

Spatial and temporal Dermo dynamics

The results of this study revealed a complex spatial and temporal relationship among the biological variables of Dermo infection in each size class, and the environmental variables of temperature, salinity, timing and duration (residence time) of floods, and distance from the Colorado River's freshwater sources. Oyster populations at Sammy's Reef showed typical down-estuary spatial patterns, due to its distance farther from the Colorado River, with typically higher salinity conditions regulated more by wind driven tidal factors rather than by freshwater inflows regardless of lag times or duration of flows. Thus, consistently higher salinity levels resulted in higher Dermo infection rates and densities of hypnospores. This study also showed that Dermo infection dynamics at Sammy's Reef were different from those at Shell Island and Mad Island Reefs; and Dermo infection levels were not completely reduced by lower salinity conditions and may act as a "reservoir" for Dermo infection in oyster populations in WMB, when Dermo levels are no longer detected on up-estuary reefs after major floods or harvest mortality removes infected individuals.

However, Shell Island and Mad Island Reefs were shown to have similar spatial and temporal patterns, characteristic of up-estuary oyster populations located closer to freshwater sources, and with less Dermo infection levels that were related to higher freshwater inflows that occurred during and one month before the sample date. Shell Island Reef oyster populations were also shown to have higher numbers of dead oysters related to freshwater inflows, while Mad Island Reef oyster populations had moderate numbers of dead oysters related to freshwater inflows. These two oyster populations

showed similar temporal trends with lower abundances of live oysters in each size class, higher Dermo infection rates during higher temperature and salinity conditions, and more dead oysters, in later years and months versus earlier years and months. These temporal patterns may also be related to increased Dermo infection and mortalities following spawning activities that occurred in earlier months. Ray recorded gonadal development in these three oyster populations (Ray unpublished data) that indicate Dermo infection levels increase one month following release of gonadal material. This lag time in Dermo related mortality and the subsequent shell substrate provided by dead oysters also contribute to the temporal patterns interacting within each reef population as well as among adjacent reef populations as discussed in Dittman et al. (2001).

Conclusions

WMB oyster populations have spatial and temporal patterns that are linked to Dermo infection and larvae distribution and spawning dynamics. These three oyster populations in this study were shown to not be separate reef systems; and up-estuary oyster populations that were devoid of Dermo infection became infected when environmental conditions changed and promoted the growth and transmission of Dermo disease from adjacent or down-estuary oyster populations. Although distance and timing of freshwater inflows were shown to influence Dermo infection dynamics on each reef, higher Dermo infection levels on down-estuary reefs (Mad and Sammy's Reef) appeared to have greater influence on mortality rates following spawning cycles for these reefs. Thus, the integrated response of these three populations appeared to be linked to the timing of spawning and larval distributions within and among populations in WMB.

CHAPTER IV

INTEGRATIVE MODEL FOR OYSTER POPULATION DYNAMICS AMONG MATAGORDA BAY REEFS

Introduction

The majority of oyster population models that have been developed to date (Hofmann et al. 1992; Hofmann et al. 1995; Powell et al. 1998, Dekshenieks et al. 2000; Powell et al. 2003) have attempted to incorporate the complex ecological and spatial relationships that exist in bay systems by including freshwater inflow information available from separate studies of food availability, spawning and growth estimates, natural and fishing mortality, and temperature and salinity tolerances of the organism as an individual unit. These models were unable to incorporate all of this data into the model and still be able to define a specific reef or a specific geographic region in order to determine responses to spatial and temporal features of each oyster population or their collective responses for each bay system.

Previous oyster models have simulated environmental conditions, food availability, predators, growth, reproduction, and energy requirements for individual oysters for Galveston Bay Reefs (Hofmann et al. 1992; Hofmann et al. 1995; Powell et al. 1994, Dekshenieks et al. 2000; Powell et al. 2003). However, there are physical characteristic of Galveston Bay that are not found in other Texas bay systems, including Matagorda Bay. Galveston Bay has a long hydraulic residence time of inflows into the estuary (40 to 88 days) (Santschi 1995) from Trinity and San Jacinto Rivers. The Houston Ship Channel also bisects the main land constrictions between Eagle Point and

Smith Point where major reefs (North and South Redfish Reefs, Todd's Dump) are formed between these two land masses. The complex factors, which influenced the formation of these reefs, need to be considered when developing models that simulate oyster population dynamics for Galveston Bay. These models must also consider the structural diversity of reef types (longitudinal and transverse ridge, pancake, tow-head, and inverted) present along a salinity gradient. Considering these complex interactions, Galveston Bay's oyster reefs should be viewed differently from those of Matagorda Bay's oyster reefs; and therefore separate oyster population models of each bay system should be developed to incorporate these differences.

Surprisingly, to date, oyster population models have not been developed for Matagorda Bay, specifically targeting WMB's reefs. When compared to Galveston Bay, WMB has a much shorter hydraulic residence time (20-21 days), and only one main freshwater source, which is from the Colorado River, in addition to ungauged flows from undeveloped coastal prairie along Mad Island Marsh and the tidal lakes (including Oyster Lake) on the north side of the GIWW (Ward 1980). The oyster populations in Galveston Bay are separated by longer distances, along environmental gradients from shallow to deeper water, and a temporally longer salinity gradient. WMB reefs have similar structural complexity despite being either naturally formed over centuries or recently constructed. They are all transverse ridge type reefs with similar current flow characteristics, in contrast to the wide diversity of reef structures and current flow patterns for Galveston Bay.

The three WMB reefs are relatively small compared to the reefs in Galveston Bay. The WMB Reefs are perpendicular to the current and land mass, and are not

located between land masses or deep water ship channels where currents and flow produce additional complexity for simulation models. However WMB's three oyster population reefs provide a valuable comparison of the response of nearly identical transverse reefs to environmental and biotic factors along a constrained salinity gradient.

The objective of this study was to develop of an interactive population based model for WMB. It uses Stella software (Stella 9.02. 2007) to quantify and integrate among the three reefs, the spatial and temporal patterns influencing reproduction, larval distribution, spat settlement, individual growth rates for each size class (larvae, spat, submarket, market, market plus - older than two years old) and oyster population growth. The three reef oyster population submodels developed in this study, incorporated spatial and temporal trends revealed in Chapters II and III. The three oyster population submodels were integrated to distribute larvae among reefs and also included a portion of larvae recruited from the Colorado Delta based on areas recently mapped by the LCRA, and average densities of intertidal populations along the Texas Coast. Model simulations were run for a 50 year period based on five years of actual continuously recorded environmental data collected by LCRA in order to determine the response of oyster subpopulations on each reef to changes in salinity and temperature over time.

Methods

Environmental submodels

Five years of environmental data, that were continuously recorded on a daily basis for 2001 through 2005 by multiple agencies (previously discussed in Chapter II), were used to generate data in four environmental submodels (salinity, temperature,

Colorado River flow, and Matagorda Bay tide). These environmental submodels were used to simulate environmental conditions that were comparable with the actual historical record for each oyster population submodel (Shell Island, Mad Island and Sammy's Reefs). Representation of these four environmental submodels is shown in Fig. 50. The original five years of environmental data were loaded into separate "converters" (denoted by circles) that associated these values with a discrete time step of one day. The "run specification" for this model was in daily increments of time. The equations used to simulate data by the environmental submodels using normal deviation of actual data (salinity, temperature, flow, and tide) are included in Appendix A.

Each environmental submodel calculated new data within one standard deviation (1.0 SD) around each original data point during a 50 year (18250 days) simulation "run-time". Each environmental submodel was set up to use the original five years of environmental data for each specific oyster population submodel during the first 1825 days; and then the environmental submodels generated 1.0 SD around this data for the remaining run-time (16425 days). These submodels were run multiple times in this manner to determine the response within and among oyster populations in WMB to environmental changes that could potentially occur over the next 50 years. A sensitivity analysis of this model was also run using half the variation (0.5 SD) of the original salinity and temperature data sets; and also running it using twice the variation (2.0 SD) of the original salinity and temperature data.

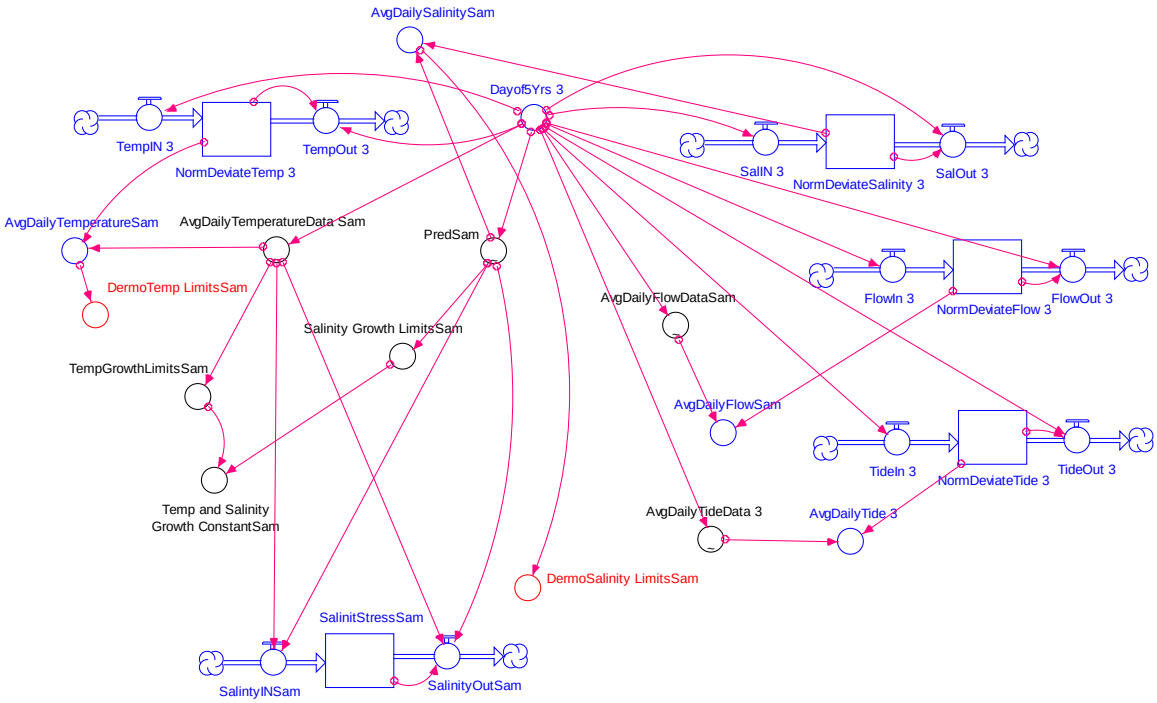

Figure 50. Environmental submodels to simulate 50 years of data for three runs corresponding to each of 0.5, 1.0, and 2.0 SD based on five years of 2001-2005 of historical data for temperature, salinity, flow, and tide.

Salinity submodels

The salinity submodels (Fig. 51) are represented by an inflow arrow pointed into a reservoir (open rectangle) of data, generated within the reservoir until specific conditions trigger its release through an outflow arrow. The salinity submodel for the Shell Island Reef population submodel used the continuous daily salinity data from the five year (2001-2005) historical monitoring records, which were collected by LCRA at Shell Island datasonde station. This data was used to calculate daily salinity (see Chapter II) for the salinity submodels used for Mad Island and Sammy's Reefs' population submodels. These three salinity submodels were used in the 50 year simulation runs for generating continuous daily records within one standard deviation of the actual data values for each population submodel (Shell Island, Mad Island and Sammy's Reef).

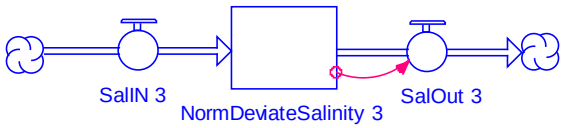

Figure 51. Salinity submodel to simulate 50 years of data for three runs corresponding to each of 0.5, 1.0, and 2.0 SD based on five years of 2001-2005 of historical data from Shell Island station.

Temperature submodels

The temperature submodels (Fig. 52) are represented by an inflow arrow pointed into a reservoir (open rectangle) of data, generated in the reservoir until specific conditions trigger the release of data through an outflow arrow. The temperature submodel for Shell Island Reef population submodel used continuous daily temperature data from the five year (2001-2005) historical monitoring records, which were collected by LCRA at Shell Island datasonde station. This data was used to calculate daily temperature (see Chapter II) for the temperature submodels used for Mad Island and Sammy's Reefs' population submodels. These three temperature submodels were used in the 50 year simulation runs for generating continuous daily records within one standard deviation of the actual data values for each population submodel (Shell Island, Mad Island and Sammy's Reef).

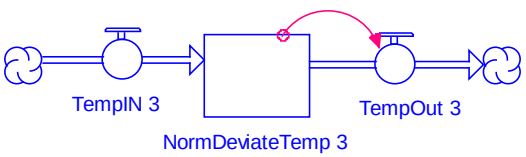

Figure 52. Temperature submodel to simulate 50 years of data for three runs corresponding to each of 0.5, 1.0, and 2.0 SD based on five years of 2001-2005 of historical data from Shell Island station.

Colorado River inflow submodel

The Colorado River inflow submodel (Fig. 53) is represented by an arrow pointed into a reservoir of data that accumulates, until specific conditions trigger release of data through an outflow arrow. This flow submodel used continuous daily flow data from the historical five year (2001-2005) monitoring records collected by USGS station at Bay City, Texas, (see Chapter II). This submodel generated continuous daily records, within one standard deviation of the actual data values in the five year historical record, for the 50 year simulation runs. The data simulated by this Colorado River inflow submodel were used for all three population submodels (Shell Island, Mad Island and Sammy's Reefs).

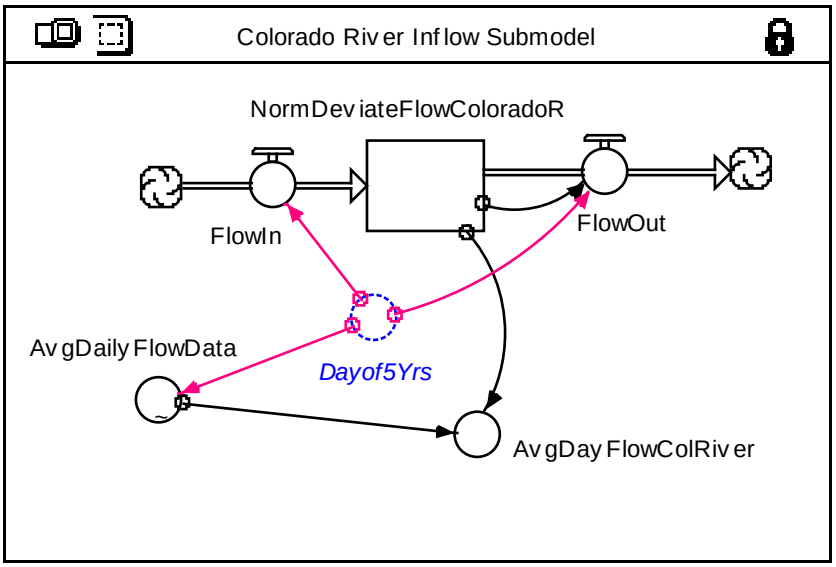

Figure 53. Colorado River flow submodel to simulate 50 years of data for three runs corresponding to each of 0.5, 1.0, and 2.0 SD based on five years of 2001-2005 historical data from Bay City, TX.

Matagorda Bay tide submodel

The Matagorda Bay tide submodel (Fig. 54) is represented by an arrow pointed into a reservoir of data that accumulates, until specific conditions trigger release of data through an outflow arrow. This submodel used continuous daily flow data from the five year (2001-2005) historical monitoring records collected at NOAA's Port O'Connor tide station, (see Chapter II). This tide submodel generated continuous daily records, within one standard deviation of the actual data values in the five year historical record, for the 50 year simulation runs. This data generated by this tidal submodel was used for all three population submodels: Shell Island, Mad Island and Sammy's Reefs.

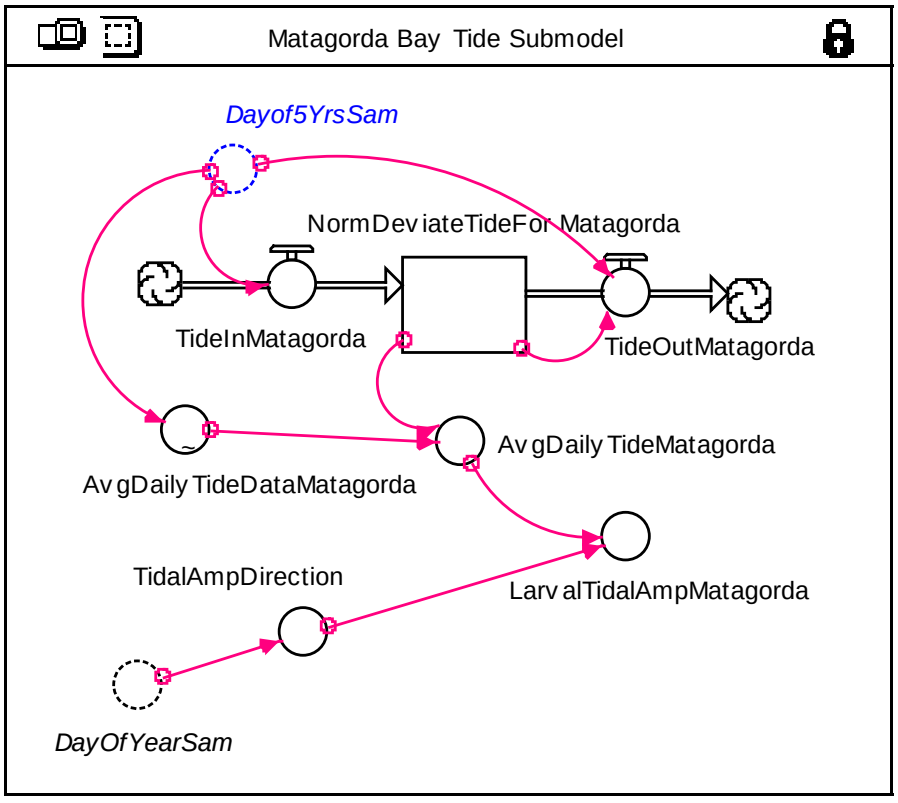

Figure 54. Tidal amplitude submodel to simulate 50 years of data for three runs corresponding to each of 0.5, 1.0, and 2.0 SD based on five years of 2001-2005 historical data recorded at Port O'Connor, TX.

Oyster population submodels

Three oyster population submodels were developed for each reef in WMB (Shell Island, Mad Island, and Sammy's Reef) based on the population density estimates for each size class and reef size in Table 4 (see Chapter II). These population submodels incorporated patterns for fast growth (Kraueter et al. 2007) and slow growth (Hofstetter 1977) in each size class (spat, submarket, market and plus market) of these oyster populations (see Table 1, in Chapter II). The criteria for growth in each size class was based on whether these populations were exposed to optimum water temperature ranges (> 10 ºC and < 30 ºC) combined with optimum salinity ranges (>10 ppt and < 26 ppt), which resulted in fast growth; in contrast to populations exposed to temperature and salinity ranges outside of optimum environmental conditions, which resulted in slow growth of individuals in each size class. These temperature and salinity restrictions on growth were based on previous estimates for Texas oysters (Loosanoff and Davis 1953; Cake 1983; Hofmann et al. 1992).

Spawning submodels were developed for oysters that reached maturity in each size class (submarket, market and market-plus), so they could spawn several times each year as environmental conditions allowed, and were not limited to one or more spawning cycles, or specific time periods. Spawning criteria for each size class were determined in these submodels by limiting the release of larvae to optimum environmental conditions, according to temporal patterns previously identified (Chapter II). These submodels also constrained spawning to not occur at least 60 days following a spawning event in order to allow the spawning population time to regenerate gonadal tissues. This 60 day time delay was based on the population submodel responding to optimum temperature

(>25 ºC and < 31 ºC) and salinity (> 16 ppt and < 26 ppt) ranges for gonadal tissue regeneration (Loosanoff and Davis 1953; Soniat and Ray 1985; Hofmann et al. 1992). Although food availability (phytoplankton) has an important role in gonadal tissue regeneration (Soniat and Ray 1985), that information was not available for inclusion in this submodel.

Each size class containing potential spawners (submarket, market, and market-plus) was monitored as to its relative abundance so that when high population densities (>3 million oysters) occurred on the reef, spawners were restricted from producing large numbers of larvae (2.6 million larvae per spawner); and when low population densities (<2.7 million oysters) occurred, spawners were able to produce large numbers of larvae (86 million larvae per spawner). The values for density dependence and numbers of larvae produced per spawner used in these submodels were based on previous fecundity studies of Texas oysters (Hopkins 1931; Davis and Chanley 1955).

Low-salinity stress submodels were also developed using counters to monitor the number of days each oyster population tolerated low salinity levels (< 1 ppt) and high temperatures (>25 º C). These salinity stress submodels accumulated the number of days when low salinity and high temperature conditions occurred, until 10 consecutive days had passed, and provided feedback to each population submodel by increasing the natural mortality rate. These salinity stress submodels also accumulated days when low salinity levels (< 1 ppt) and low temperature conditions (< 26 º C) occurred, until 30 consecutive days had passed, and provided feedback to each population submodel by increasing the natural mortality rate. These salinity stress counters were reset to zero if salinity levels increased before the limit of days had accumulated in the counter, thus

sparing the population from additional stress if the duration of low-salinity conditions was shorter time than needed (10 or 30 days according to high or low temperatures) to increase mortality rates.

Dermo infection submodels were developed in this study for three size classes (submarket, market, and market plus) of each oyster population submodel in order to separate the mortality rates that differ for less mature versus mature oyster populations. Submarket oysters have previously been shown to have lower levels of Dermo infection than market or mature oysters (see Chapter III). The Dermo submodels functioned as counters of "infection-days", which were accumulated based on salinity and temperature restrictions for proliferation of Dermo disease (Ray 1987; Hofmann et al. 1995). After this submodel accumulated 120 days of Dermo infection, mortality was increased in the size class of infected oysters in the population submodel. If environmental conditions improved and were no longer optimum for promoting growth of Dermo disease, then mortality was not increased during that time step. However, the numbers of "infection-days" were retained in the counter until conditions for promoting growth of Dermo disease returned; at which time additional infection days were again accumulated by the submodel until 120 days were attained, resulting in increased mortality of that size class in the population submodel. Thus each size class of the population infected with Dermo retained their own separate infection levels for longer periods of time than 120 days, or until natural mortality from other variables occurred. Spawning conditions were also incorporated into the Dermo submodel, and used to increase mortality due to Dermo disease if the spawning population was infected. These temporal patterns of Dermo influence on increased population mortality according to their maturity level were

incorporated into each reef's population submodel. The equations regulating these Dermo submodels are included in Appendix A.

Shell Island Reef population submodel

Shell Island Reef's population submodel (Fig. 55) incorporated the spatial and temporal patterns of an up-estuary population, located within a shorter distance from the Colorado River and influenced by longer duration and volume of freshwater inflows. Shell Island Reef populations were provided a smaller allocation of larvae from their own spawning populations during low-flow conditions in the Colorado River based on the relatively low abundance of "live" market oysters and relatively moderate numbers of "live" submarket oysters on this reef compared to Matagorda and Sammy's Reefs. Larvae were also distributed to the Shell Island Reef oyster population from the Colorado Delta's intertidal oyster population following high-inflow events. Larvae were also transported in an up-estuary direction from the Mad Island and Sammy's Reef population submodels, following the higher tidal amplitude patterns that occur during spring and fall seasons. Shell Island Reef's oyster populations were documented (see Chapter III) as becoming infected by Dermo disease during sustained low inflows of freshwater; and also following (one month lag) larval production by down-estuary infected oyster populations.

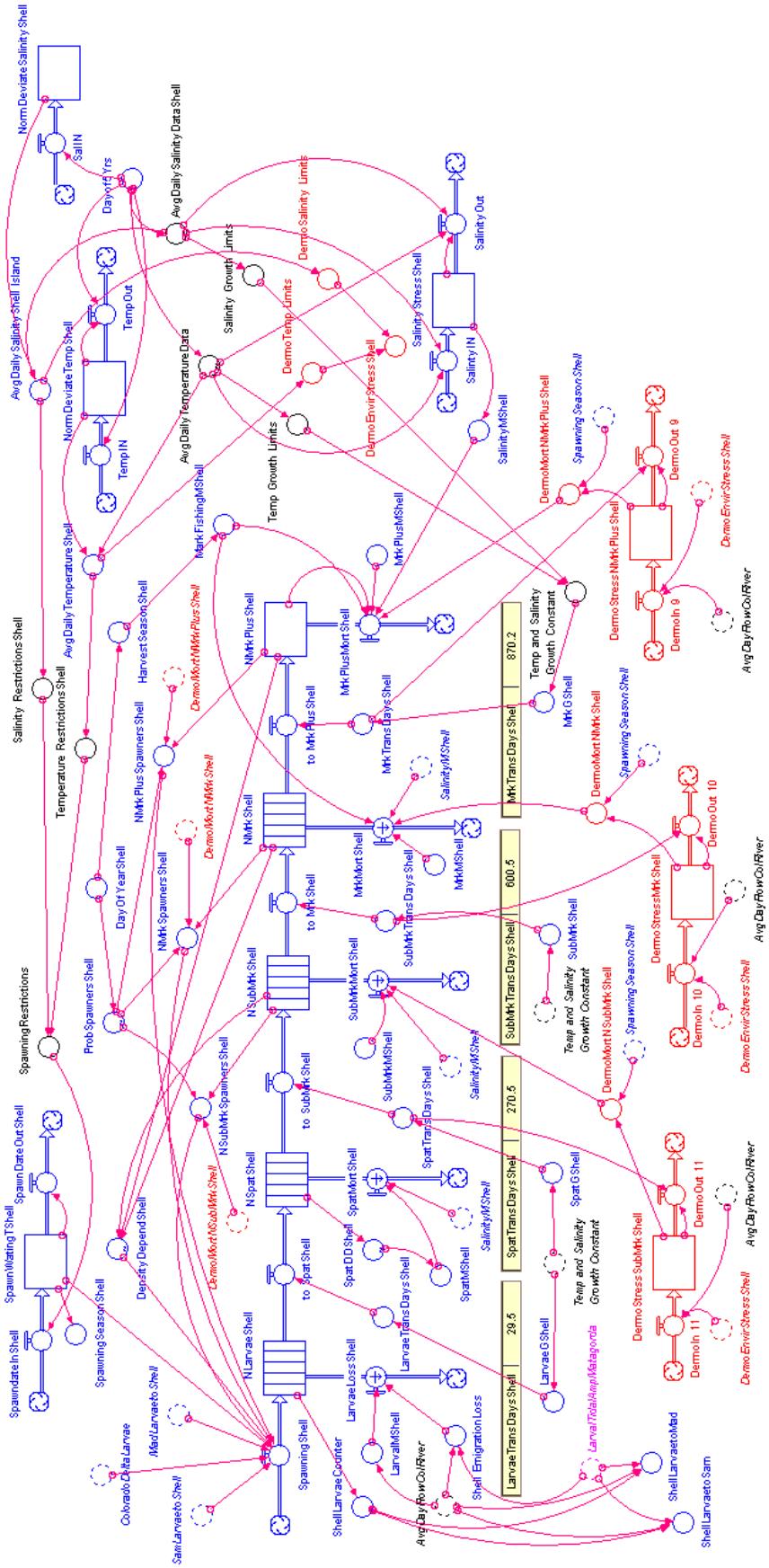

Figure 55. Shell Island Reef oyster population submodel overview of interactions among size classes, environmental variables and Dermo disease.

Mad Island Reef population submodel

Mad Island Reef's oyster population submodel (Fig. 56) incorporated similar growth, spawning and slightly higher ambient salinity and temperature conditions found in up-estuary and down-estuary oyster populations, due to its location between Shell Island and Sammy's Reef, a moderate distance from the Colorado River, (see Chapter II). Larvae in this submodel were contributed by the resident spawners in addition to receiving larvae from down-estuary reef populations such as Sammy's Reef during higher tidal amplitudes that occurred in spring and fall. They also received larvae from up-estuary populations such as Shell Island Reef and the intertidal Colorado Delta during high flow conditions and during seasonal "wind driven" events. Higher levels of Dermo infection within the three size classes (submarket, market, and market-plus oysters) were incorporated in the Mad Island Reef population submodel during high salinity and temperature conditions (see Chapter III) compared to those found on the typical up-estuary populations as represented by the Shell Island population submodel.

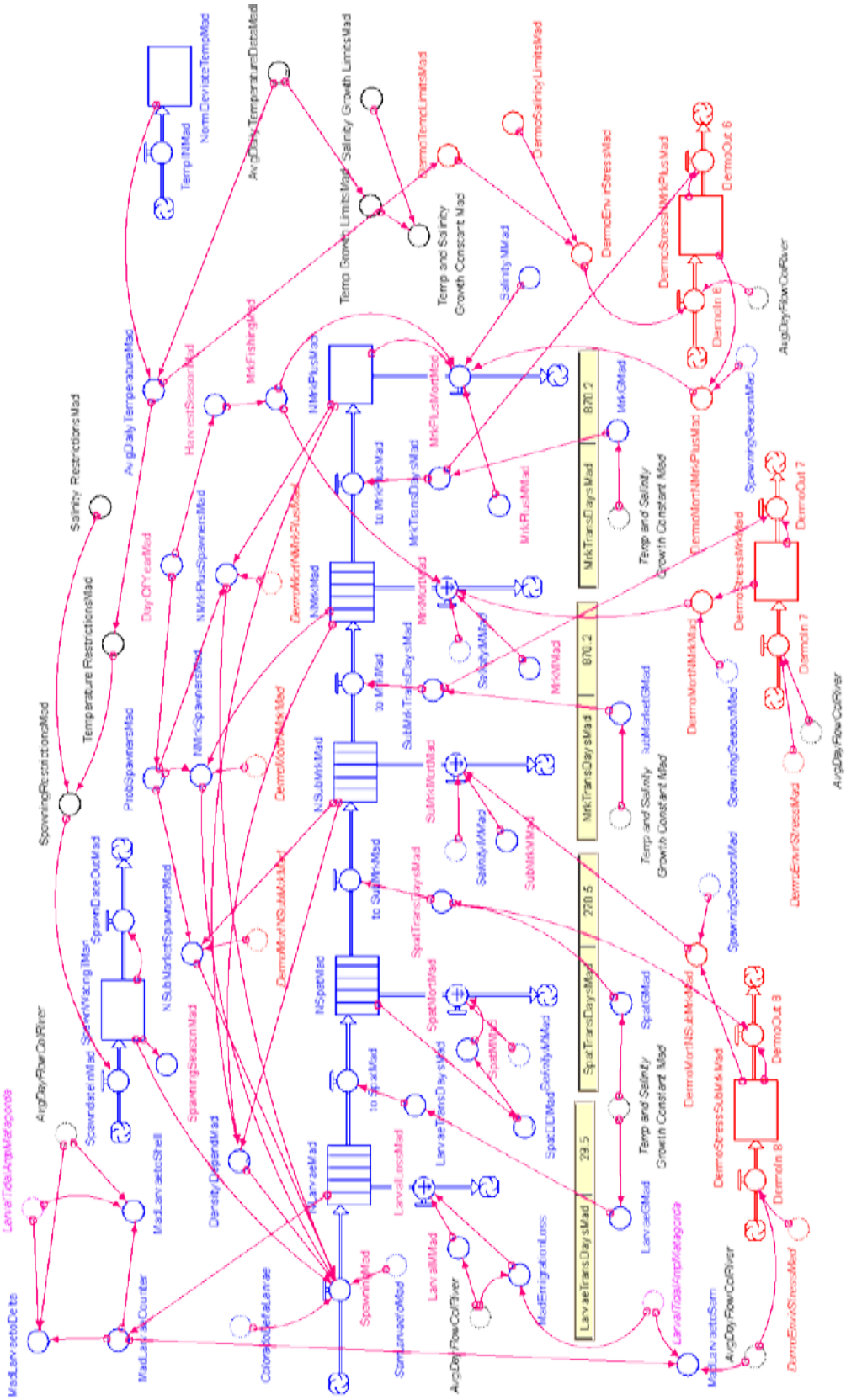

Figure 56. Mad Island Reef oyster population submodel overview of interactions among size classes, environmental variables and Dermo disease.

Sammy's Reef population submodel

Sammy's Reef's oyster population submodel (Fig. 57) incorporated the spatial and temporal environmental patterns, which defined its formation the farthest distance from the Colorado River (see Chapter II). The larvae in this oyster population submodel were recruited primarily from resident spawners due to their relatively greater number of live oysters in all size classes, and their lesser number of larvae contributed from up-estuary populations after high inflows or during down-estuary tidal conditions that prevail in summer and winter seasons. There were no down-estuary or gateway reef populations available to contribute larvae to Sammy's Reef oyster population in this submodel. Spatial and temporal patterns for Dermo infection similar to those for down-estuary oyster populations were incorporated in this submodel (see Chapter III). These patterns showed a greater potential for Dermo disease interactions within each of the three size classes (submarket, market, and market plus oysters) due to their relatively higher abundances of live oysters that can become infected with Dermo, in addition to higher salinity conditions that promote growth of Dermo disease at this reef, the farthest distance from the Colorado River outflow.

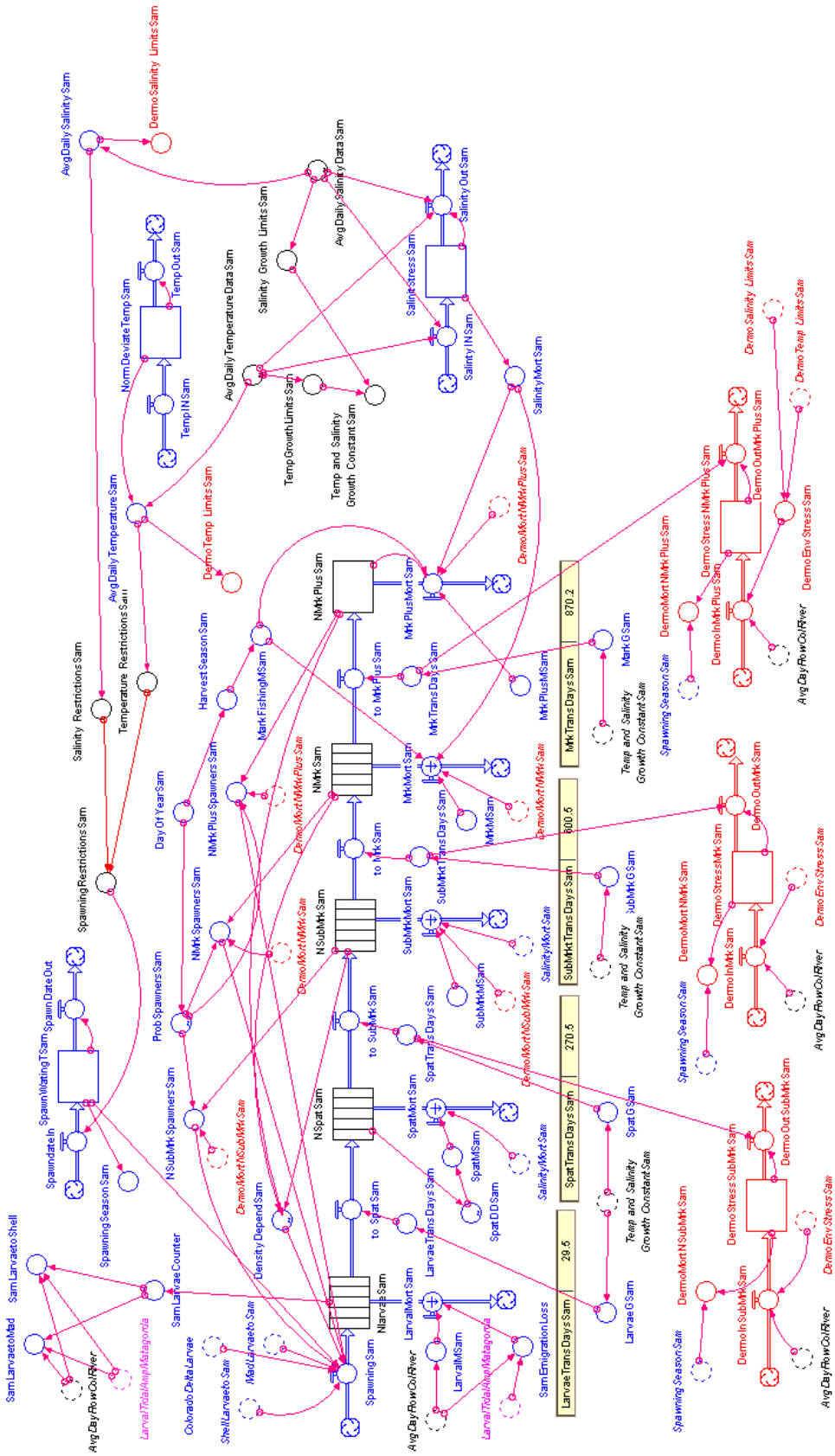

Figure 57. Sammy's Reef oyster population submodel overview of interactions among size classes, environmental variables and Dermo disease.

Larval distribution submodels

Each oyster population submodel included inflows of larvae from submodels for their own resident population of potential spawners, as well as inflows from adjacent up-estuary (Figs. 58, 59) and down-estuary (Fig. 60) potential spawners, and inflows from the Colorado Delta intertidal populations (Fig. 61). Environmental conditions were established in these submodels that regulated the number and direction of larvae transported in up-estuary and down-estuary directions, using environmental variables and patterns discussed in Chapter II for: salinity, temperature, duration and volume of freshwater inflows, tidal amplitude direction and height. These population submodels accounted for emigration of larvae from the reef by removing a proportion of the larvae spawned by the resident reef population (submarket, market and market-plus size classes), which were then distributed to other reefs.

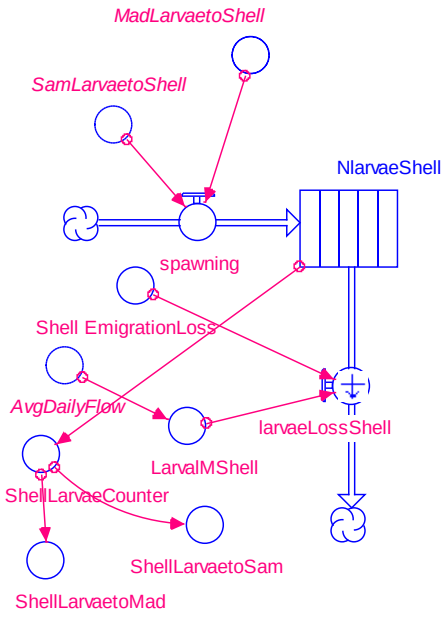

Figure 58. Shell Island Reef larvae population submodel.

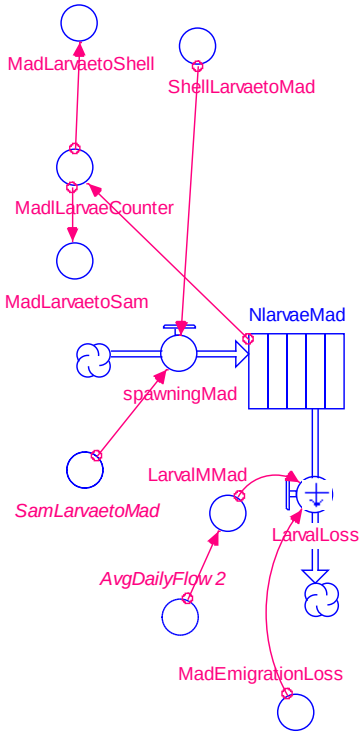

Figure 59. Mad Island Reef larvae population submodel.

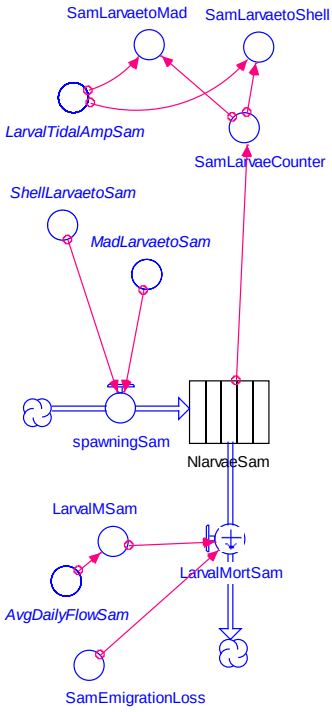

Figure 60. Sammy's Reef larvae population submodel.

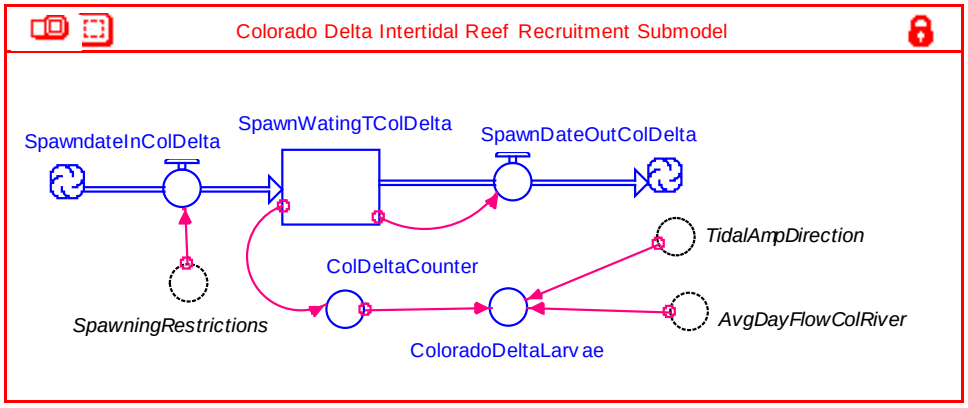

Figure 61. Colorado Delta intertidal larvae population submodel.

Size class submodels

Each population submodel (Shell Island, Mad Island and Sammy's Reefs) was constructed which incorporated four size classes of oysters (spat, submarket, market, and market-plus) using density and numbers established in Table 4 in Chapter II. The first three size classes (spat, submarket, and market oysters) were constructed as "conveyors" (represented by hatched boxes) of multiple groups of similar sized individuals that resulted from different spawning efforts within the same population or from different populations. These three size class conveyors accumulated numbers of individuals that were spawned at different time steps but have the same growth and mortality rates applied, under the same environmental conditions as the other individuals in that same size class before they are transferred to the next size class conveyor with its own growth and mortality rates.

Each group of spat entering this size class conveyor continues to grow and does not interact with the other spat entering this conveyor at different time intervals unless it is through density-dependent growth limitations that result in additional mortality for spat when this size class becomes too densely populated. Each group of spat do not leave

this size class conveyor, moving from one compartment to the next until they have reached the maximum length for spat, when they are transferred to the submarket size class conveyor. These same maximum length restrictions apply to each group of oysters entering the submarket size class conveyor, moving from one conveyor compartment to the next until they are transferred to the market size class conveyor.

When each group of oysters that enters the market size class conveyor reaches a maximum length (140 mm) by the end of their second year (730 days), they are transferred to a final "reservoir" open type of container for market-plus oysters. These oysters continue to grow and reproduce at the same rate as the oysters in the market size class conveyor, but they are not constrained by the time factors used for separating groups of oysters entering (by birth date) or leaving a "conveyor" compartment until they reach a maximum length. These market-plus oysters accumulate in this container until they are removed by harvest, Dermo, or natural mortality.

Results

Comparison of environmental variables among reefs for 2001-2005

The results of the environmental submodels for the five years (2001-2005) of actual monitoring data are graphically depicted using Stella software: salinity (Fig. 62), temperature (Fig 63), Colorado River flow and Matagorda Bay tide (Fig. 64). Average temperature data were similar for all three reefs; and Fig. 60 shows only the third line (green line representing Sammy's Reef) which covers the other two lines. Several high freshwater inflow events (> 10,000 cfs) were recorded from the Colorado River (Fig. 64) during the five year (1825 days) period on specific days (70, 244, 322, 557, 674, 780,

1276, and 1418). These specific inflow events continued for several days to months, where in some cases, tropical storms or hurricanes created major flooding events that had long term effects on the reefs in WMB (see Chapter II).

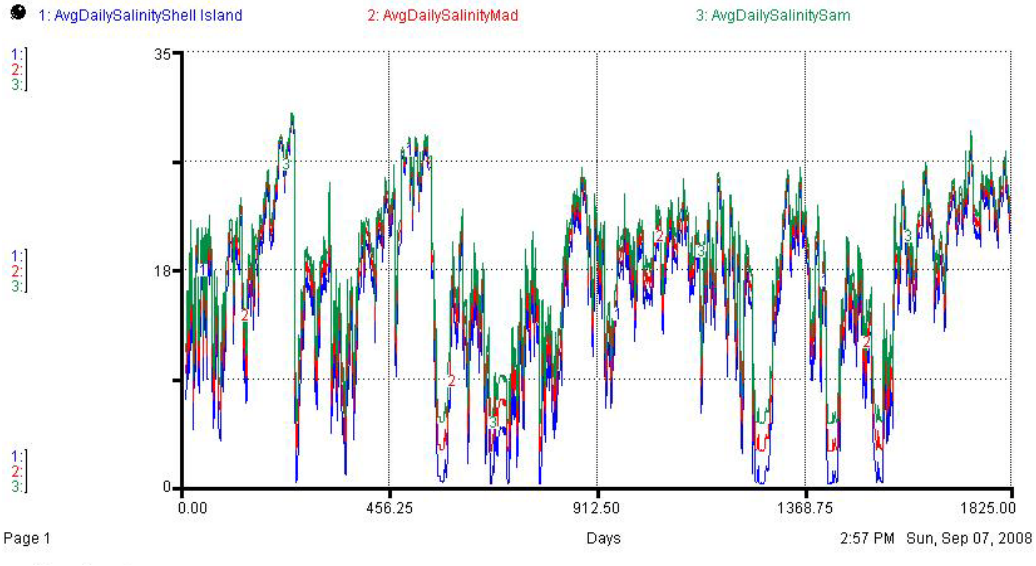

Figure 62. Comparison of average daily salinity among reefs for 2001-2005.

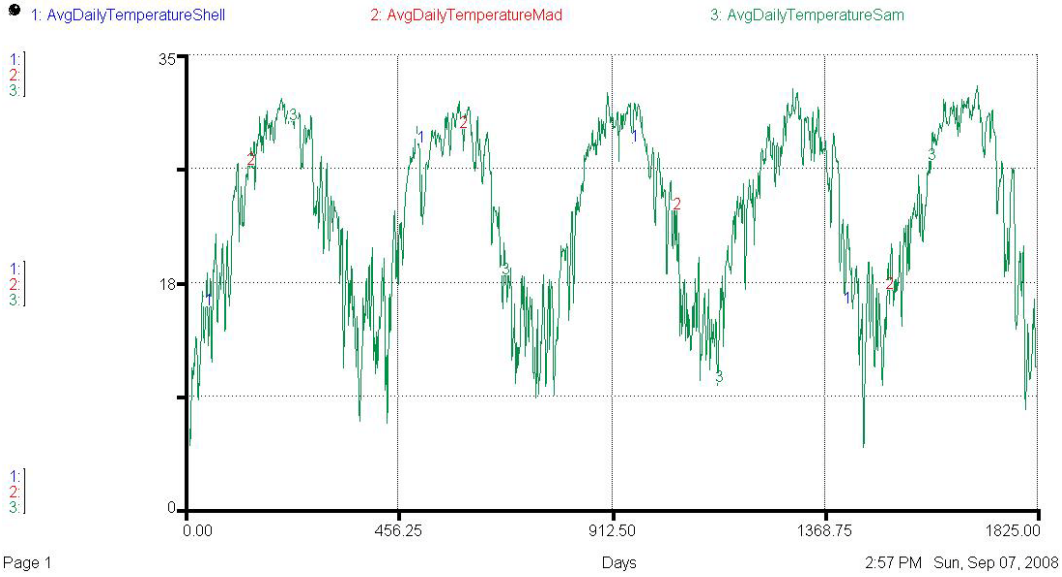

Figure 63. Comparison of average daily temperature among reefs for 2001-2005 were similar; shown are data for Sammy's Reef.

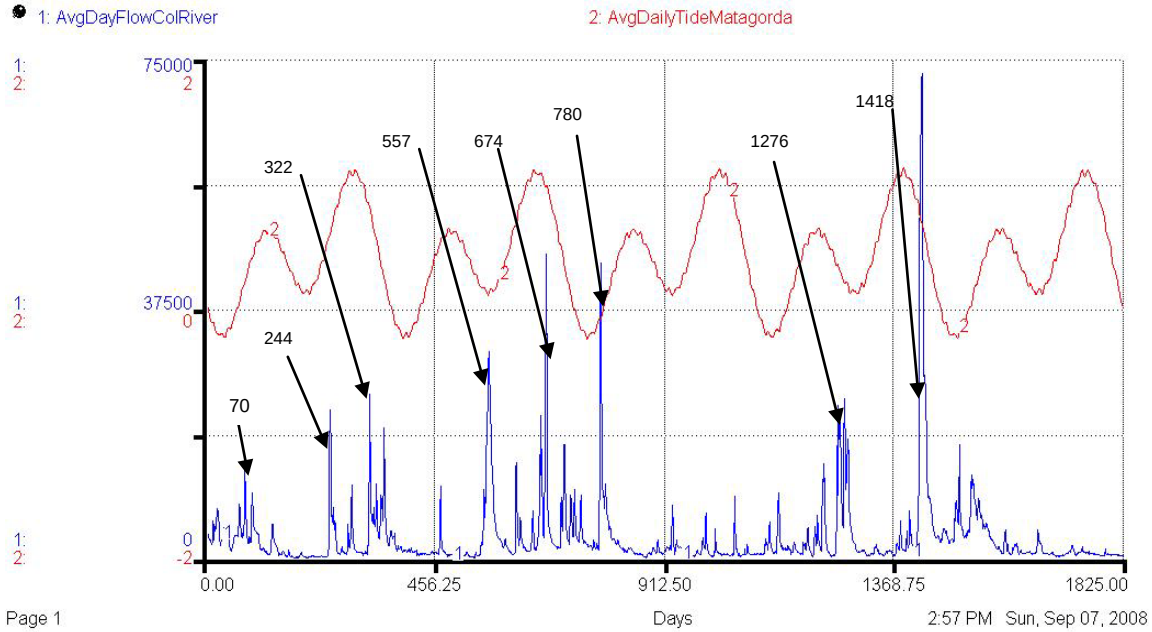

Figure 64. Comparison of Colorado River flow and Matagorda Bay tides among reefs for 2001-2005. Arrows indicate days when freshwater inflows were greater than 10,000 cfs.

Comparison of oyster reef populations among reefs for 2001-2005

Oyster larvae produced by the three oyster reef populations (Fig. 65) and spat set among reefs (Fig. 66) for 2001-2005, were simulated using Stella software (Stella 2007). There are no available data for larvae distributions at the three oyster reef populations during this same time period to compare with the model's simulation output. However, simulated spat numbers, resulting from simulated larvae that set on these reefs (one month prior to their detection in dredge samples) appeared to correspond well with relative abundance of spat described in Chapter II.

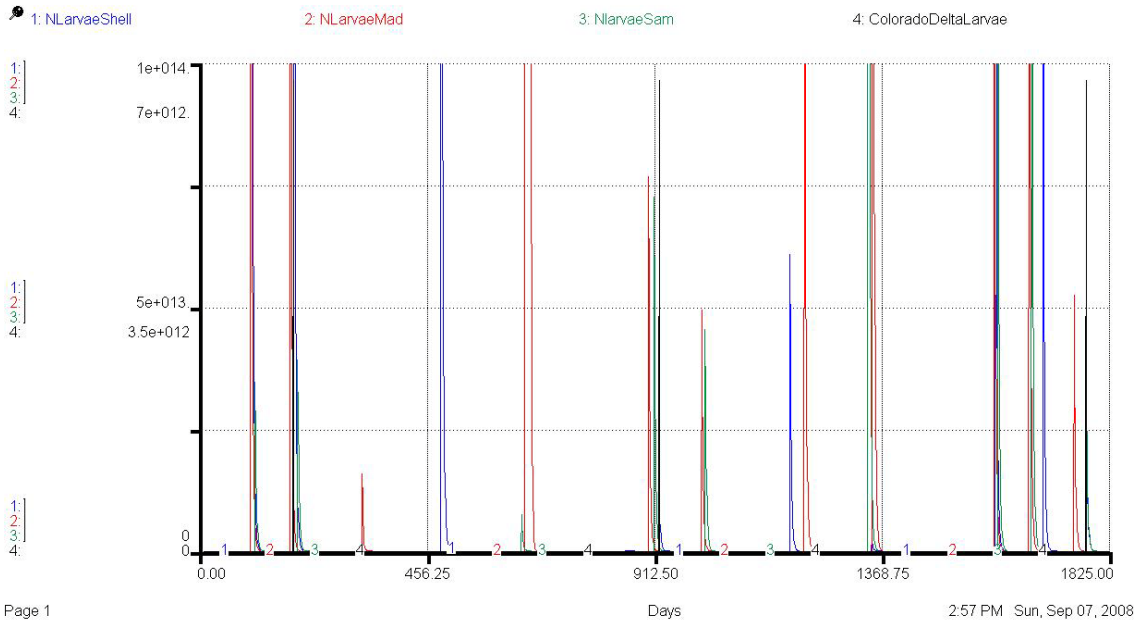

Figure 65. Comparison of larvae among reefs for 2001-2005.

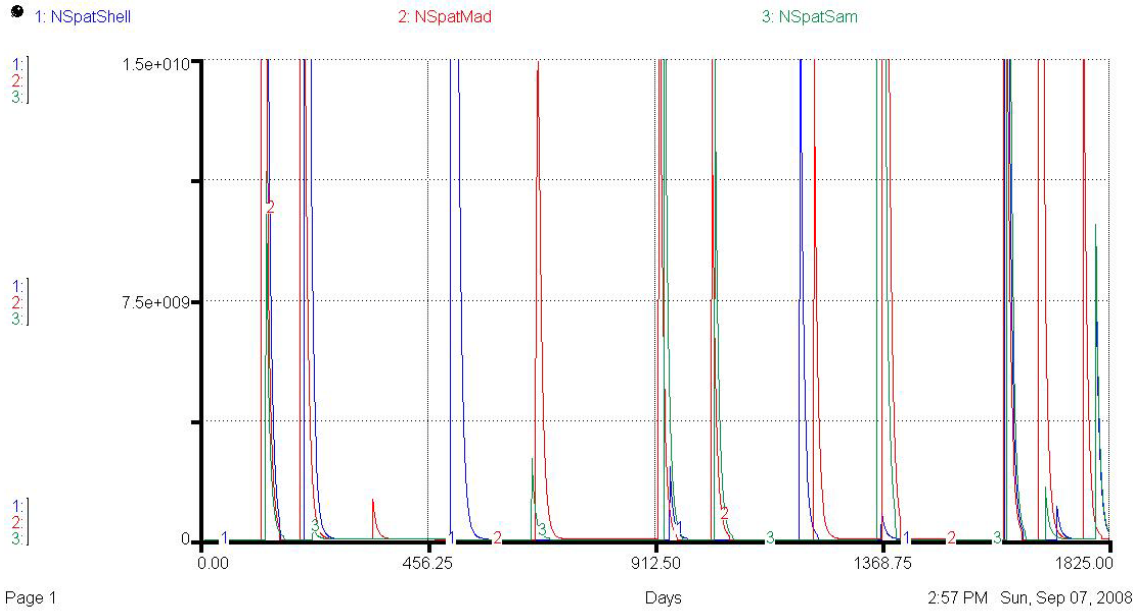

Figure 66. Comparison of spat set among reefs for 2001-2005.

Simulated oyster population numbers in the three size classes (submarket Fig. 67, market Fig. 68, and market-plus Fig. 69) corresponded well with relative abundance of oysters in these size classes in 2001-2005 data (see Chapter II). Market and market-plus

numbers were considered together as comparable to market size class oysters during this time period (see Chapter II); and are only separated here to indicate when market oysters survived longer than two years and continued to provide functional value to the population. Smaller numbers of market oysters were simulated for Shell Island Reef populations, which were typically observed in Chapter II. However, larger numbers of submarket oysters were simulated approximately 280 to 380 days following high inflows events for Shell Island Reef (on days 780 and 1418), and for Mad Island and Sammy's Reef (on days 1276 and 1418), which are indicated by arrows on Fig. 67. Larger numbers of market oysters were also simulated 365 to 730 days after high inflow events for Shell Island Reef (on days 306 and 1800), for Mad Island (on days 1105, 1210, and 1500), and for Sammy's Reef (on days 1105, 1210, 1550, and 1800) which are indicated by arrows on Fig 68.

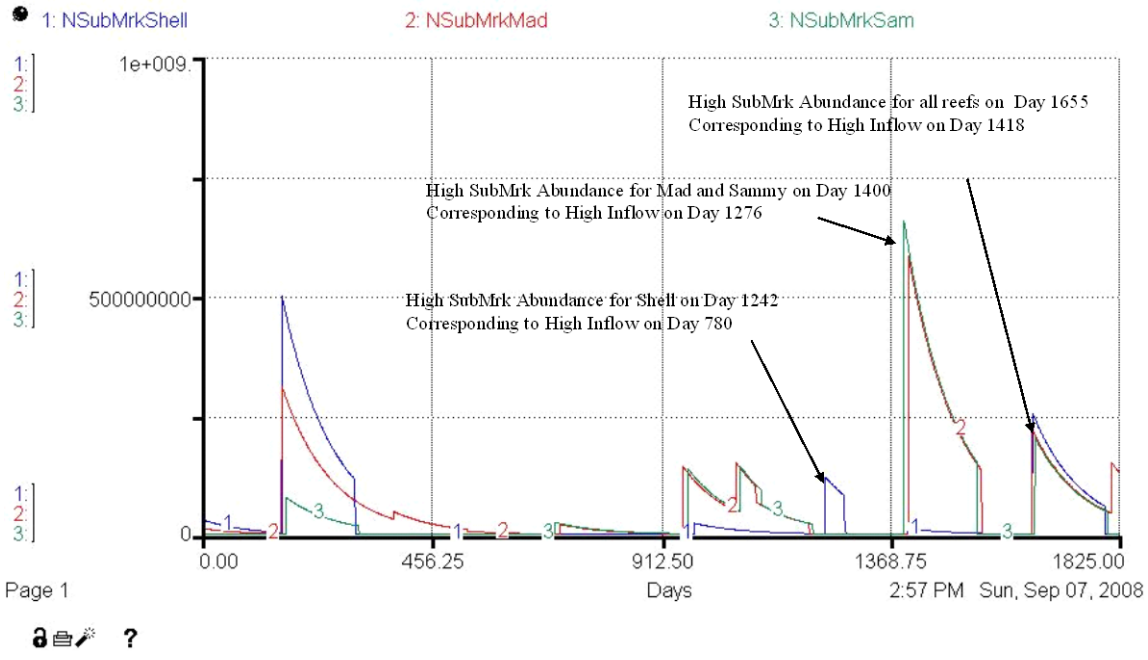

Figure 67. Comparison of submarket oysters among reefs for 2001-2005. Arrows indicate day relative abundance increased 365-730 days following a flood event.

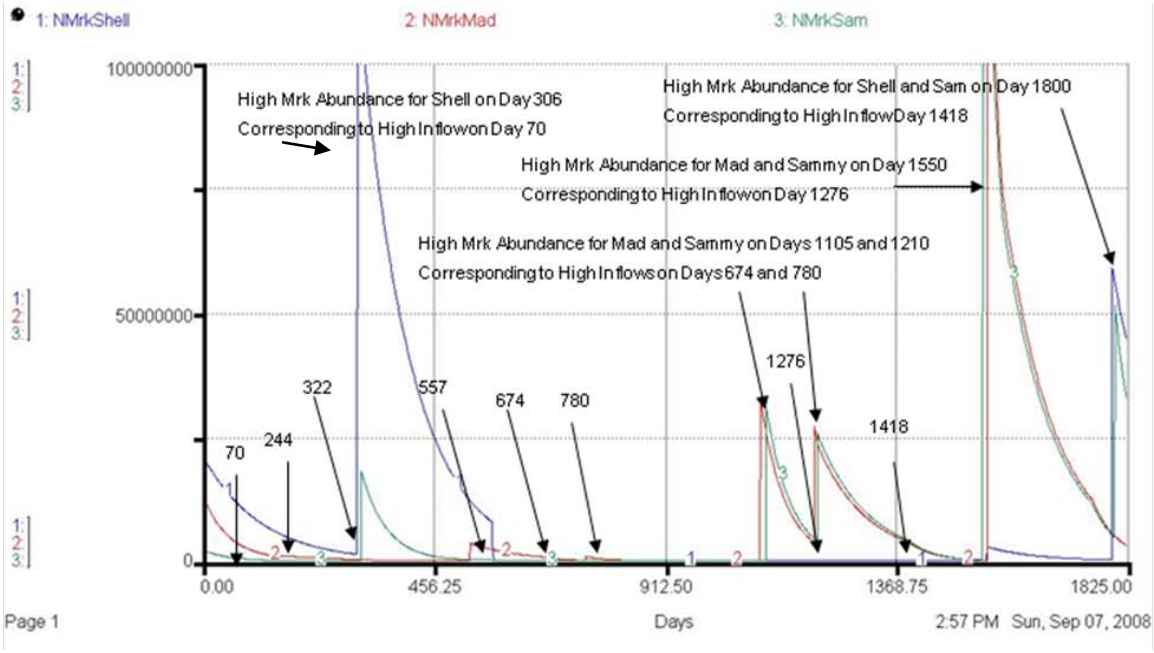

Figure 68. Comparison of market oysters among reefs for 2001-2005. Arrows indicate day relative abundance increased 365-730 days following a flood event.

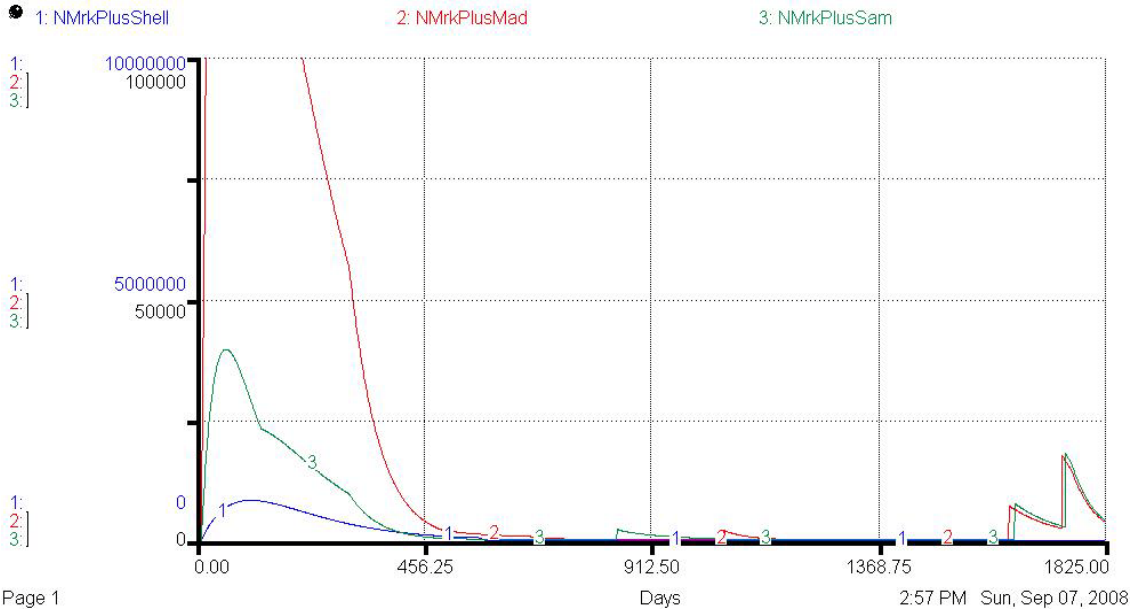

Figure 69. Comparison of market-plus oysters among reefs for 2001-2005.

Comparison of environmental variables among reefs for 50 years (1.0 SD)

The results of the environmental submodels were compared among reefs over the 50 year simulation run, based on 1.0 SD of the actual five year data from 2001-2005 (see Chapter II), and are graphically depicted using Stella software: salinity (Fig. 70), temperature (Fig 71), Colorado River flow and Matagorda Bay tide (Fig. 72). Salinity values at all three reefs appear to follow the same trends and values previously observed in the five year data set. Sammy's Reef had the highest average daily salinity over the 50 year simulation period, with some higher values observed at Mad and Shell Island during higher tidal periods especially in spring and fall. Higher average daily temperatures were observed over several years at Mad Island Reef in the 50 year simulation run compared to trends and values previously observed in the five year data. Colorado River flow and Matagorda Bay tides in the 50 year simulation run were comparable to trends and values previously observed in the five year data.

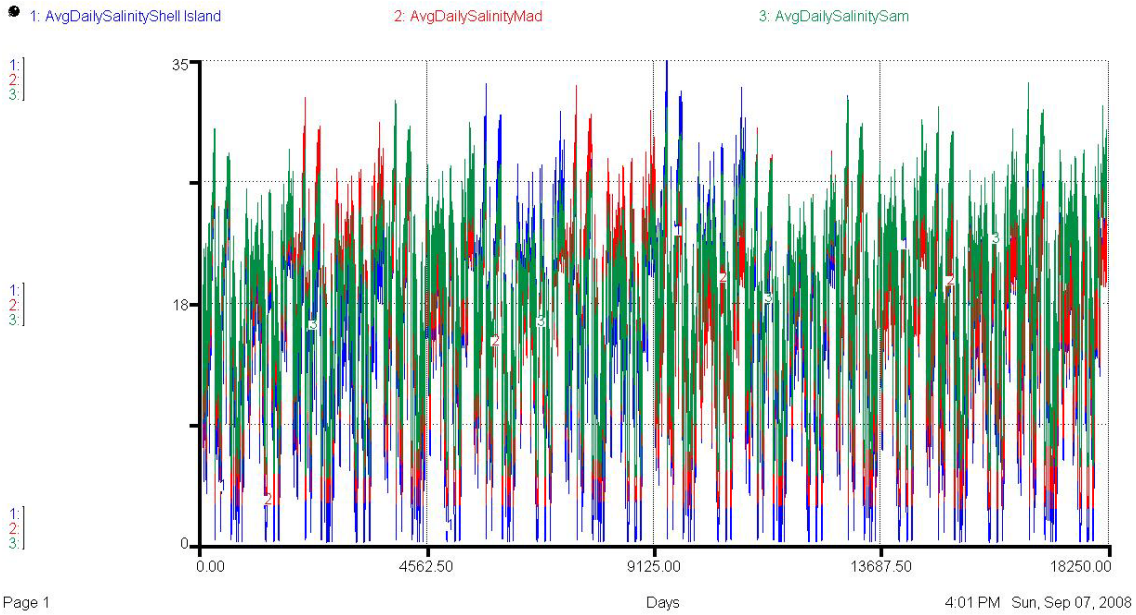

Figure 70. Comparison of average daily salinity among reefs for 50 years (1.0 SD).

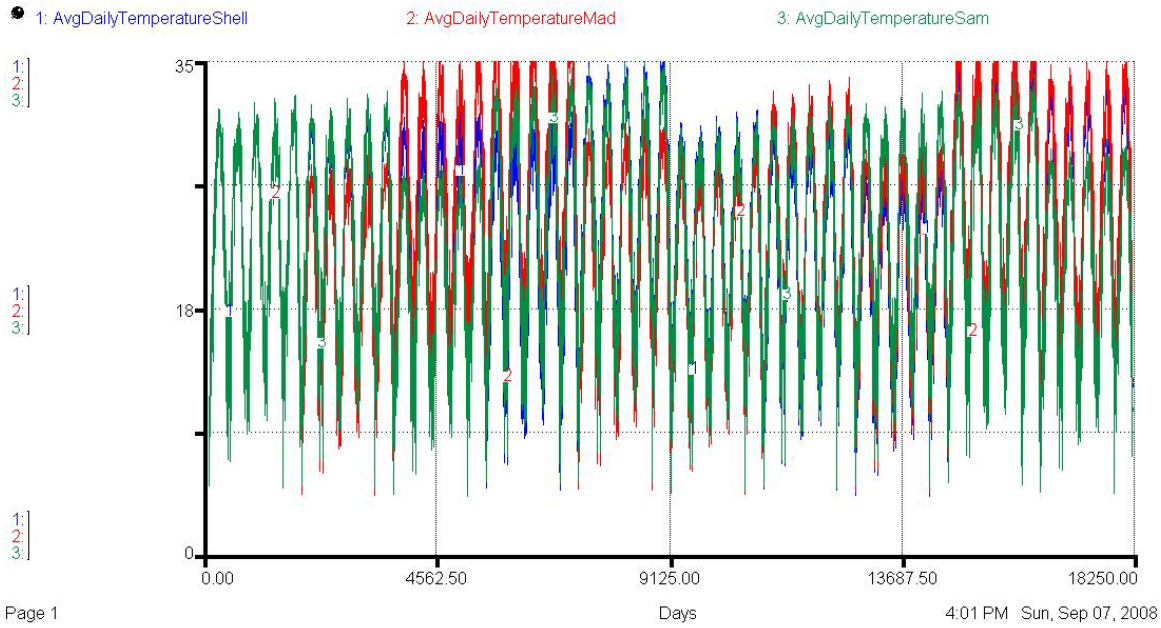

Figure 71. Comparison of average daily temperature among reefs for 50 years (1.0 SD).

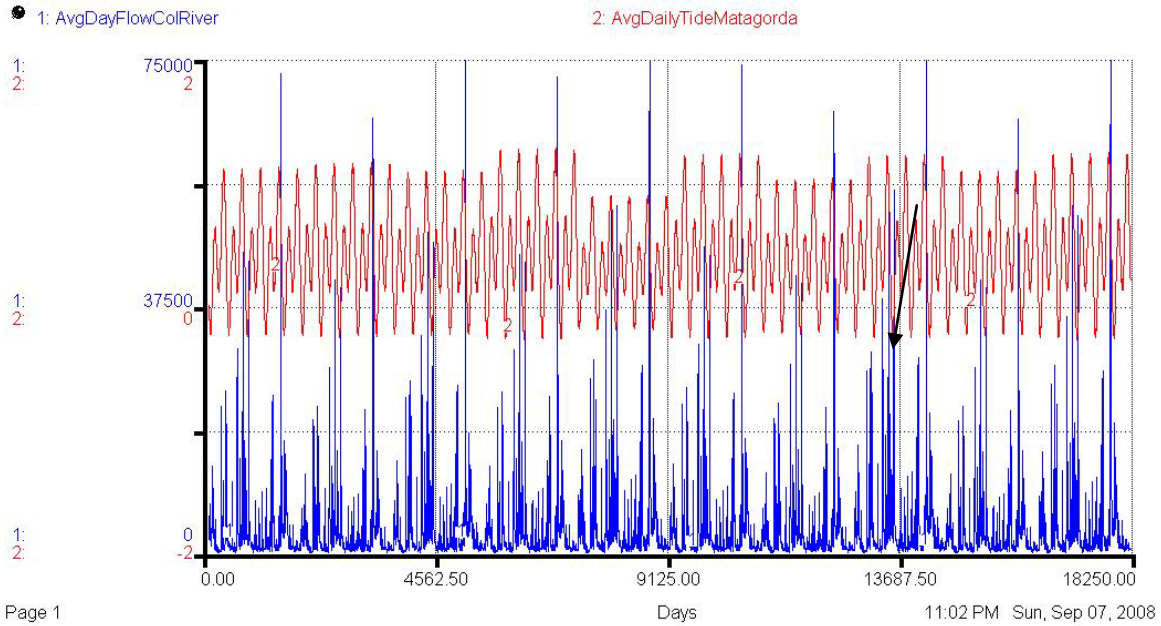

Figure 72. Comparison of Colorado River flow and Matagorda Bay tide among reefs for 50 years (1.0). Arrow indicates a high inflow event lasting longer than 60 days.

Comparison of oyster reef populations among reefs for 50 years (1.0 SD)

Oyster larvae produced by the three oyster reef populations (Fig. 73) and spat set among reefs (Fig. 74), using 50 year simulations that were based on 1.0 SD of the historical data, (see Chapter II), were graphically depicted using Stella software (Stella 2007). There are no available data for larvae distributions of these three oyster reef populations to compare with the model's 50 year simulation output. However, spat numbers, resulting from larvae that set on these reefs (one month prior to their detection in dredge samples) that were simulated for 50 years, appeared to correspond well with relative abundance of spat described in Chapter II. During this 50 year simulation run, high numbers of Colorado Delta larvae (Fig. 73) were produced during a high flow (>10,000) and long duration event (> 10 days) that resulted in higher numbers of spat (Fig. 74) for Sammy's Reef compared to other up-estuary reefs (arrows point to event day). These spat set from Sammy's Reef resulted in higher numbers of submarket oysters (Fig. 75) in the following year and higher numbers of market oysters (Fig 76) two years later (arrows point to event day).

Oyster population numbers in the three size classes (submarket Fig. 75, market Fig. 76, and market-plus Fig. 77), simulated for 50 years using Stella software (Stella 2007), corresponded well with 2001-2005 relative abundance of oysters in these size classes (see Chapter II). Lower numbers of market oysters were simulated for Shell Island Reef, which are typical of Shell Island Reef populations. However, higher numbers of submarket (Fig. 75) and market oysters (Fig. 76) were simulated for 50 years at all three reef populations one to two years (365-730 days) following high inflow years as depicted by arrows.

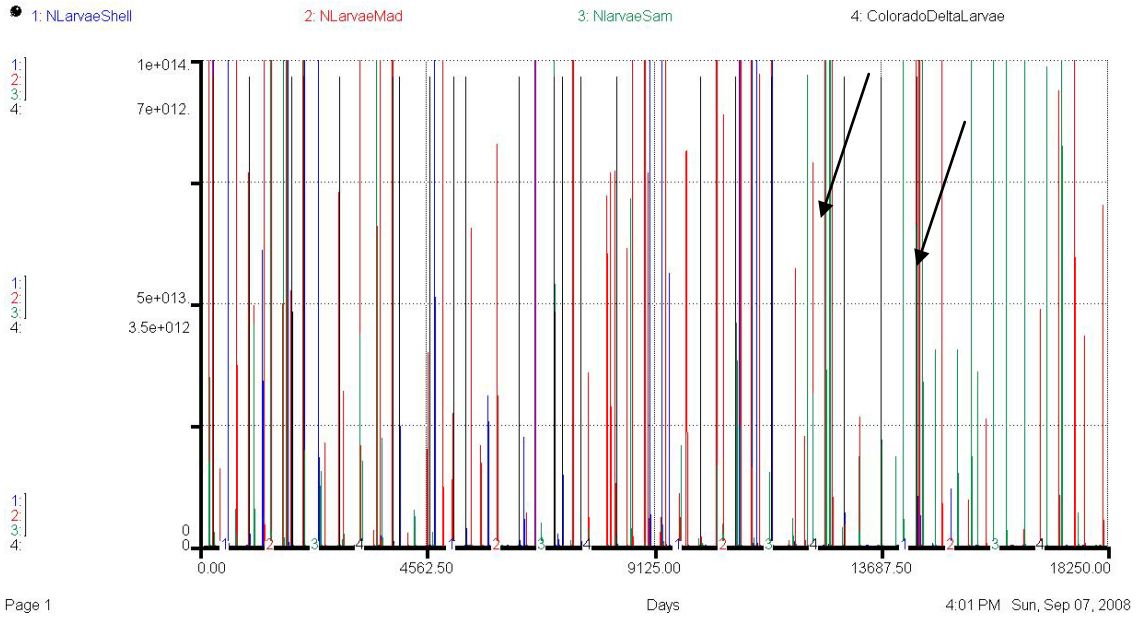

Figure 73. Comparison of larvae among reefs for 50 years (1.0 SD). Arrow indicates larvae spawned by Sammy's Reef populations following a high inflow event lasting longer than 30 days.

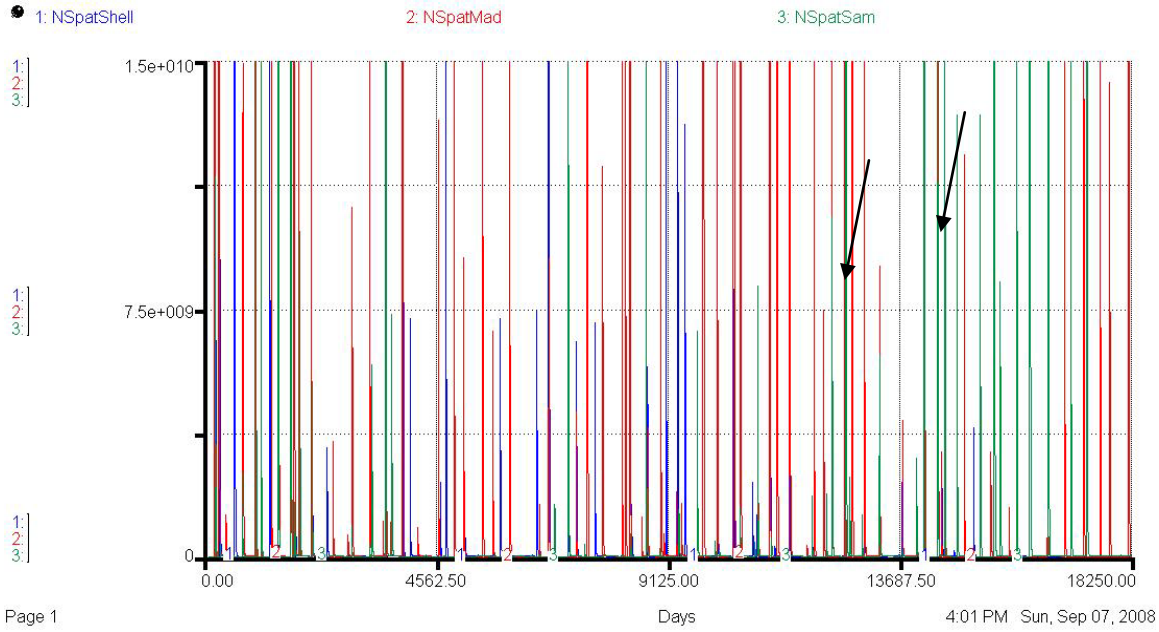

Figure 74. Comparison of spat among reefs for 50 years (1.0 SD). Arrow indicates spat set at Sammy's Reef and Mad Island contributed by larvae that were spawned after a high inflow event lasting longer than 30 days.

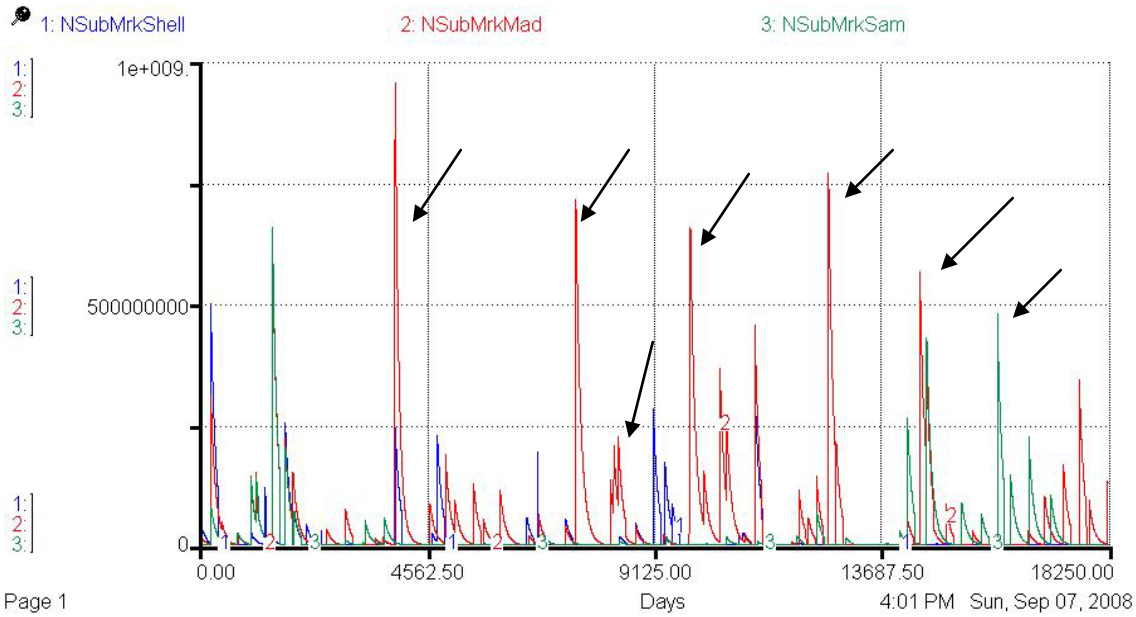

Figure 75. Comparison of submarket oysters among reefs for 50 years (1.0 SD). Submarket oysters associated with high inflow events that occurred 200-380 days earlier.

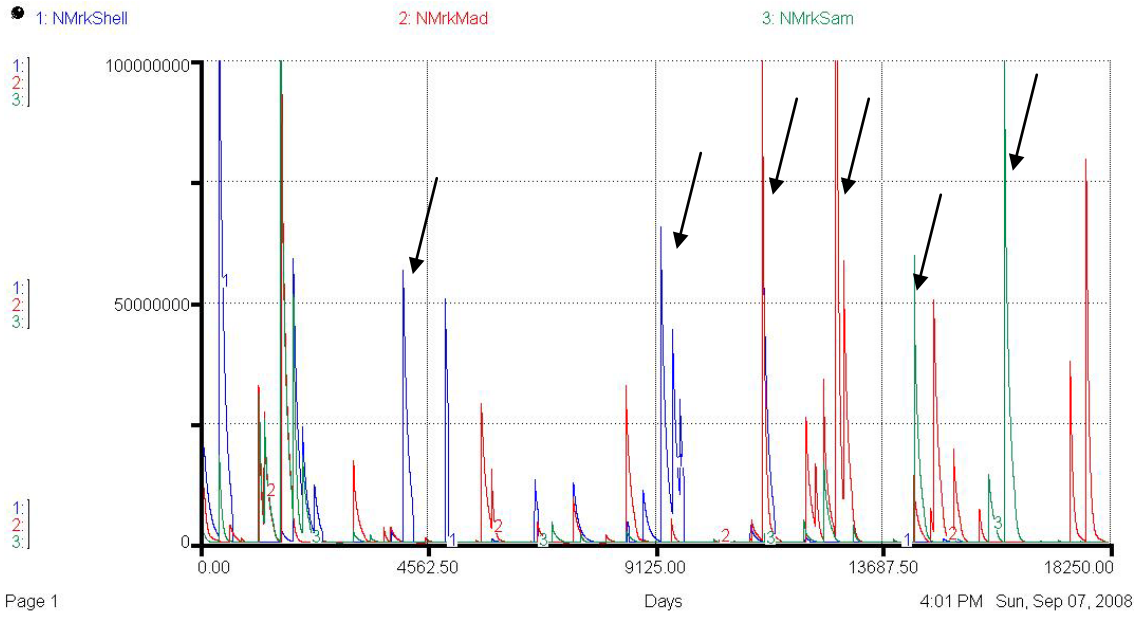

Figure 76. Comparison of market oysters among reefs for 50 years (1.0 SD). Arrows indicates market oysters associated with high inflow events that occurred 365 days earlier.

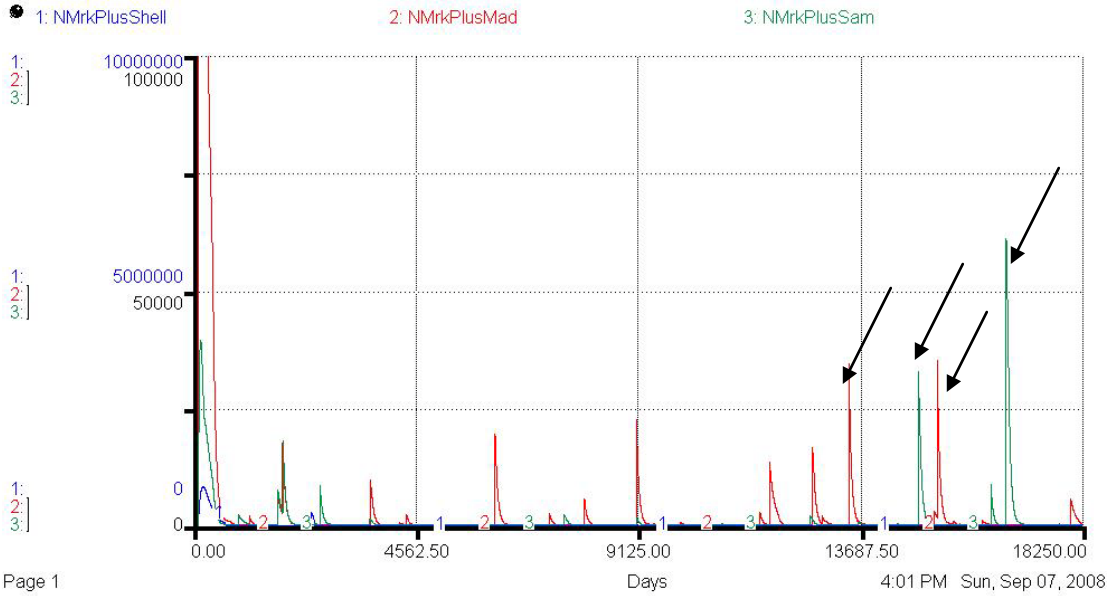

Figure 77. Comparison of market-plus oysters among reefs for 50 years (1.0 SD). Arrows indicate market-plus oysters associated with high inflow events that occurred 365 days earlier.

Comparison of environmental variables among reefs for 50 years (0.5 SD)

Environmental submodel results were compared among reefs using 50 year simulations that were based on 0.5 SD of the actual five year (2001-2005) historical data (see Chapter II), and were graphically depicted using Stella software: salinity (Fig. 78), temperature (Fig 79), Colorado River flow and Matagorda Bay tide (Fig. 80). These results appeared to be similar to those simulated by the 1.0 SD of the historical data with the exception of long duration of higher than normal salinity values occurring at Mad Island Reef from day 5000 until day 6000, while Sammy's Reef had lower salinity values, represented by arrows in Fig 78. Colorado River flow and Matagorda Bay tides in the 50 year simulation run for 0.5 SD (Fig. 80) were comparable to trends and values previously observed in the five year data and 1.0 SD simulation run.

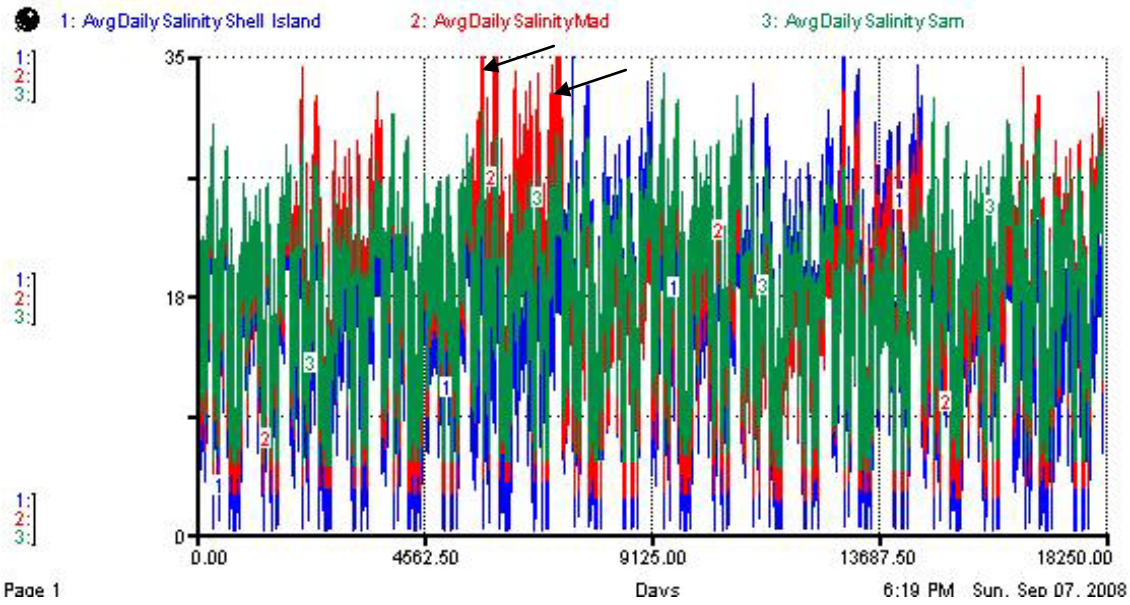

Figure 78. Comparison of average daily salinity among reefs for 50 years (0.5 SD). Arrows indicate when higher than normal salinity was simulated for Mad Island Reef.

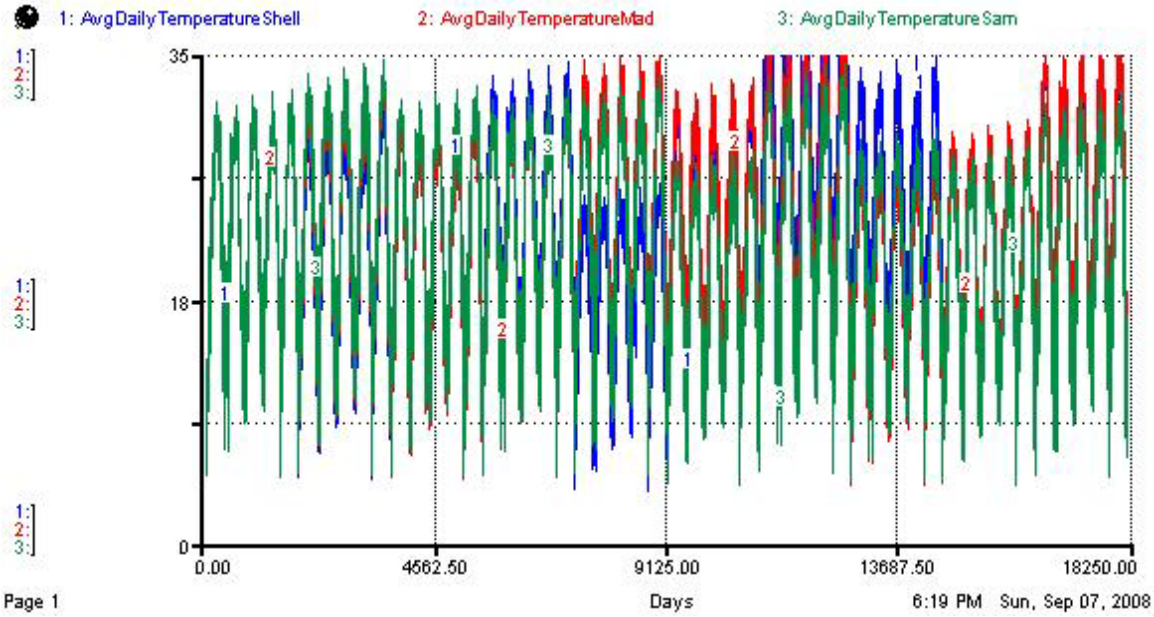

Figure 79. Comparison of average daily temperature among reefs for 50 years (0.5 SD).

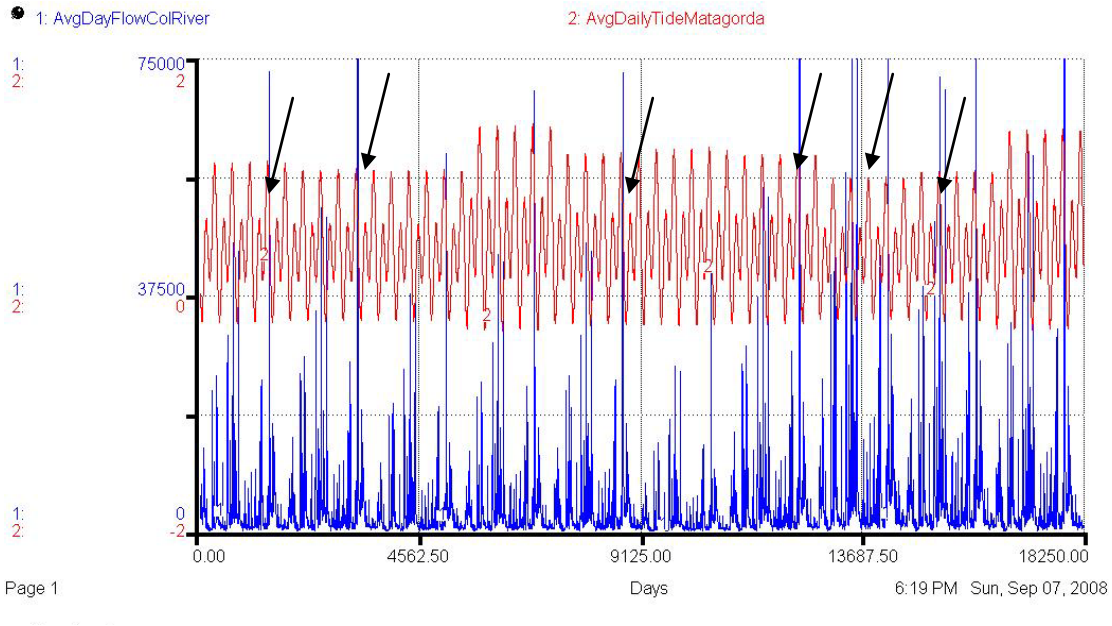

Figure 80. Comparison of Colorado River flow and Matagorda Bay tide among reefs for 50 years (0.5 SD). Arrows indicate high inflow events.

Comparison of oyster reef populations among reefs for 50 years (0.5 SD)

Oyster larvae produced by the three oyster reef populations (Fig. 81) and spat set (Fig. 82) were compared among reefs, using 50 year simulations that were based on 0.5 SD of the historical data, (see Chapter II), and graphically depicted using Stella software (Stella 2007). There were no available data for larvae distributions of these three oyster reef populations to compare with the model's simulation output. Spat numbers, resulting from larvae that set on these reefs (one month prior to their detection in dredge samples) that were simulated for the 50 year simulation run, appeared to correspond well with relative abundance of spat for these three reefs described in Chapter II. High numbers of Sammy's Reef larvae were produced immediately following several high flow and short duration events during this simulation run, which resulted in higher numbers of spat being simulated for Shell Island Reef (Fig 82), as indicated by arrows.

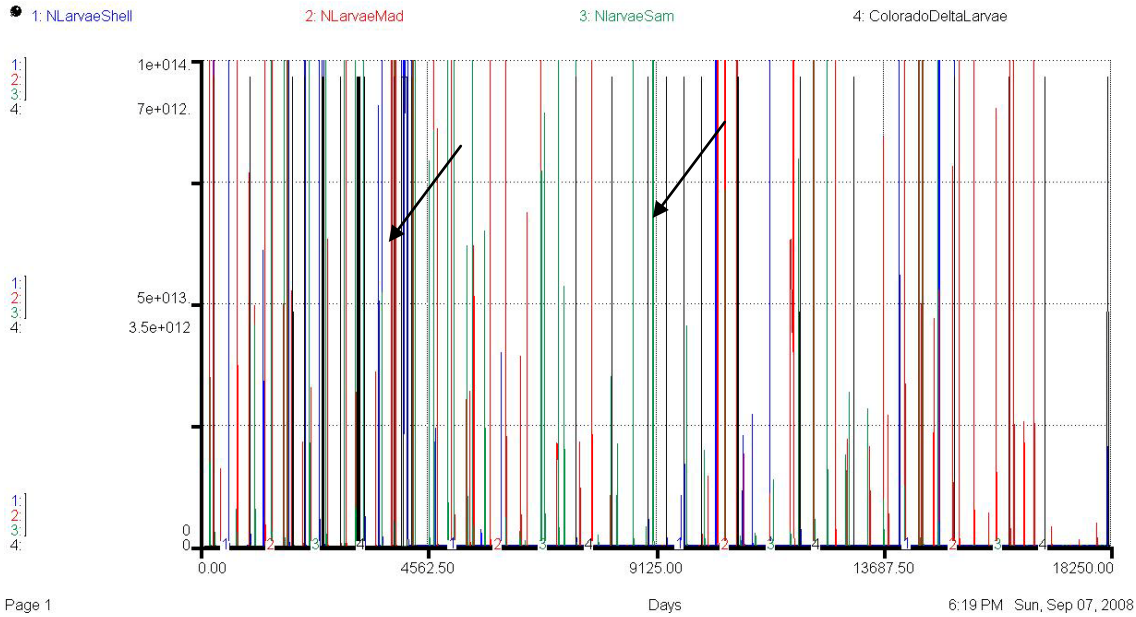

Figure 81. Comparison of larvae among reefs for 50 years (0.5 SD). Arrows indicate larvae spawned by Mad Island and Sammy's Reef populations following high inflow events.

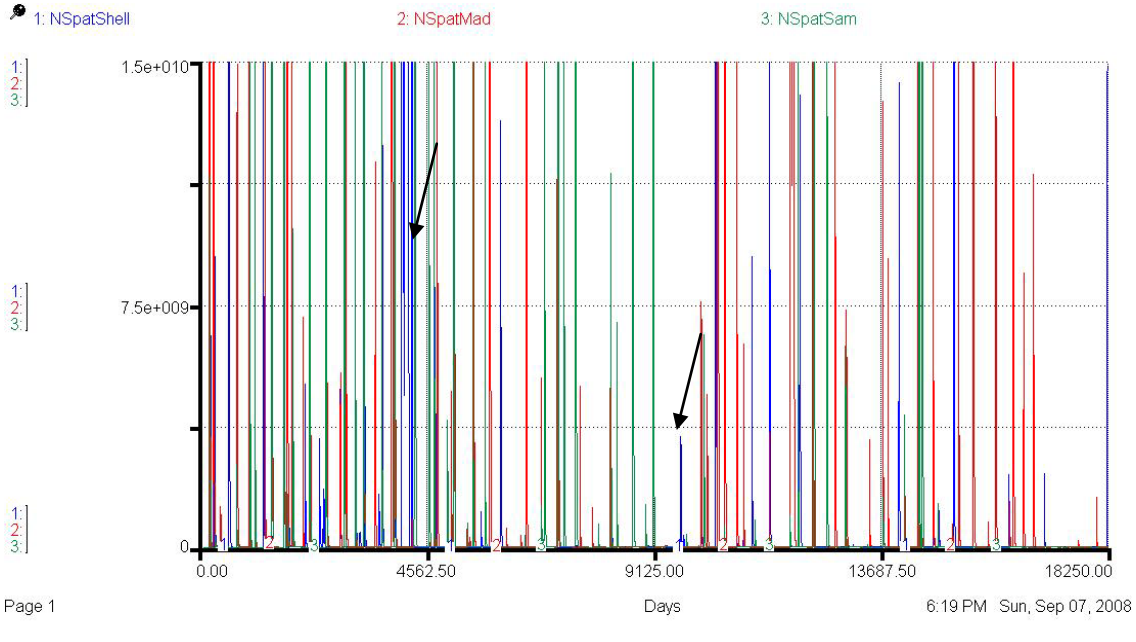

Figure 82. Comparison of spat among reefs for 50 years (0.5 SD). Arrows indicate high abundance of spat at Shell Island Reef contributed by larvae from Mad Island and Sammy's Reef population.

Oyster population numbers in the three size classes (submarket Fig 83, market Fig. 84, and market-plus Fig. 85) simulated for the 50 years using 0.5 SD of the historical data correspond well with 2001-2005 relative abundance of oysters in these size classes (see Chapter II). Although lower numbers of market oysters were generated at Shell Island Reef for the majority of the 50 year simulation run, which are typical of this reef's population trends, there were several days of high spat sets (Fig. 82) that resulted in higher than normal trends for market oyster abundance on Shell Island Reef (Fig. 84) as indicated by arrows. Higher numbers of submarket (Fig. 83) and market (Fig. 84) oysters were also simulated 365 to 730 days following high inflow events at Mad and Sammy's Reef that were comparable to previous trends during 2001-2005 for these two oyster populations (days are indicated by arrows).

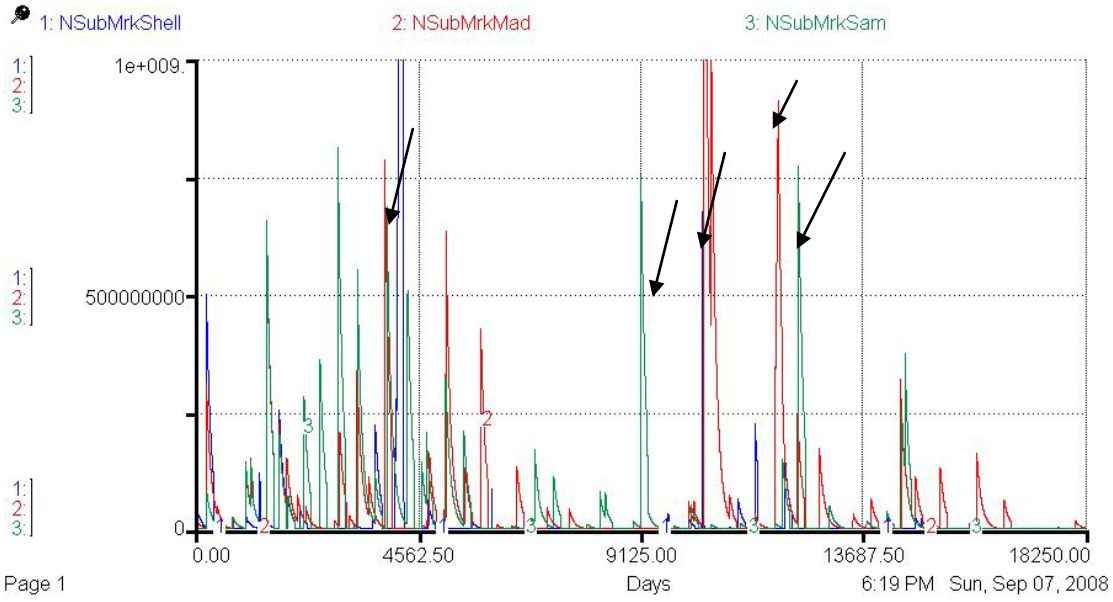

Figure 83. Comparison of submarket oysters among reefs for 50 years (0.5 SD). Arrows indicate submarket oysters that resulted from high inflow event 365-730 days earlier.

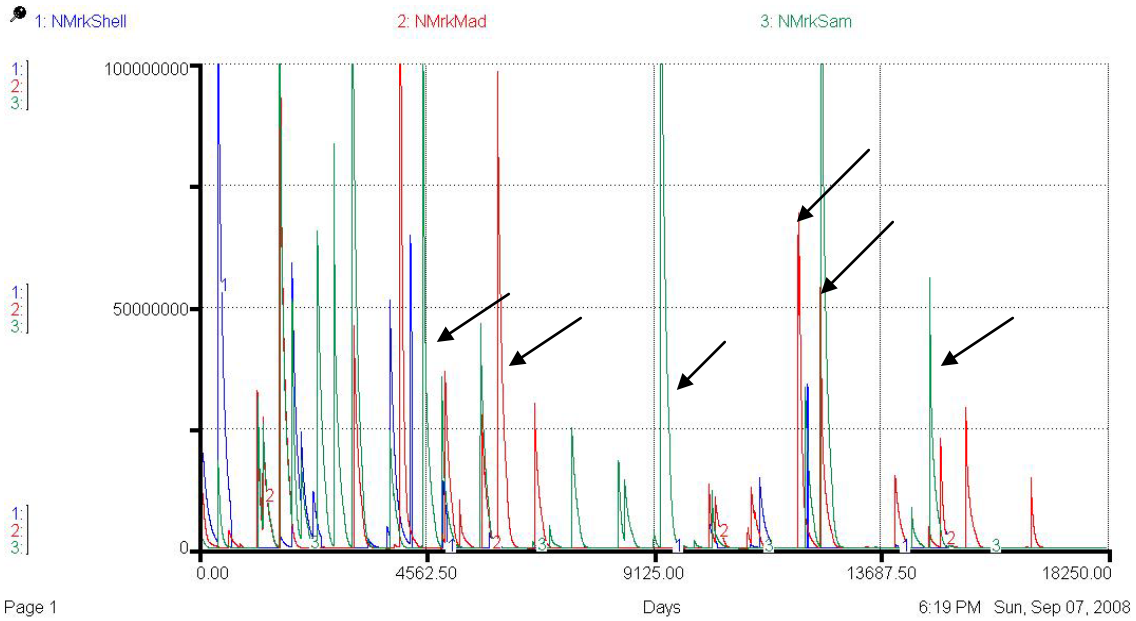

Figure 84. Comparison of market oysters among reefs for 50 years (0.5 SD). Arrows indicate market oysters that resulted from high inflow event 365-730 days earlier.

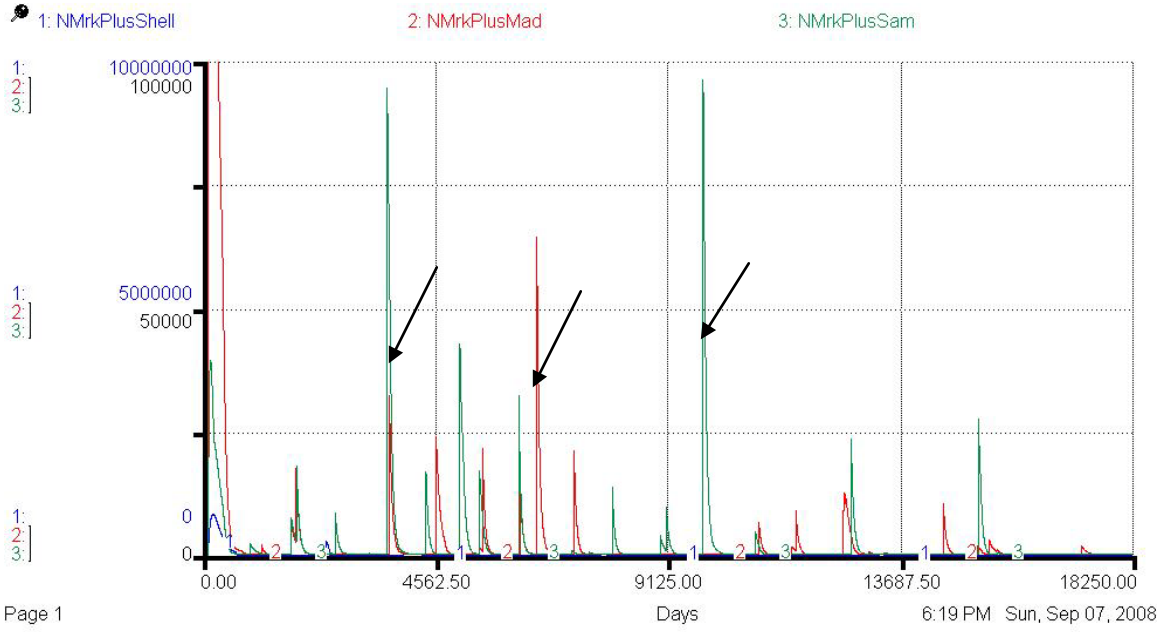

Figure 85. Comparison of market-plus oysters among reefs for 50 years (0.5 SD). Arrows indicate market-plus oysters that resulted from high inflow event 365-730 days earlier.

Comparison of environmental variables among reefs for 50 years (2.0 SD)

Environmental variables were compared among reefs over 50 year simulations that were based on 2.0 SD of the five year 2001-2005 actual continuous monitoring record, (see Chapter II), and graphically depicted using Stella software: salinity (Fig. 86), temperature (Fig 87), Colorado River flow and Matagorda Bay tide (Fig. 88). The salinity submodel, using twice the variation of the five year continuous monitoring record, simulated higher and lower salinities than normal for all three reefs in WMB over the 50 year simulation period (Fig. 86). There were two periods of time extending in this simulation run where the salinity submodel generated high salinity conditions for Mad Island Reef, in contrast to very low to nearly zero salinity conditions at Shell Island or Sammy's Reef during this same time period (arrows indicate these time periods). As the salinity data was generated from the actual five year (2001-2005) continuous monitoring data, this salinity trend had previously occurred in the historical record at these reefs. The temperature submodel also simulated higher and lower temperatures than normal seasonal trends at all three reefs during this 50 year simulation run (Fig 87). Similar high temperature periods occurred twice at Mad Island Reef that corresponds to the higher salinity conditions previously described for this simulation run. The Colorado River flow submodel generated four major floods with one flood extending over several seasons (see arrows on Fig 88). This submodel also generated four major droughts following floods (see arrows on Fig 88). The Matagorda Bay tide model did not simulate extreme tidal amplitudes using twice the variation of the five year continuous monitoring records.

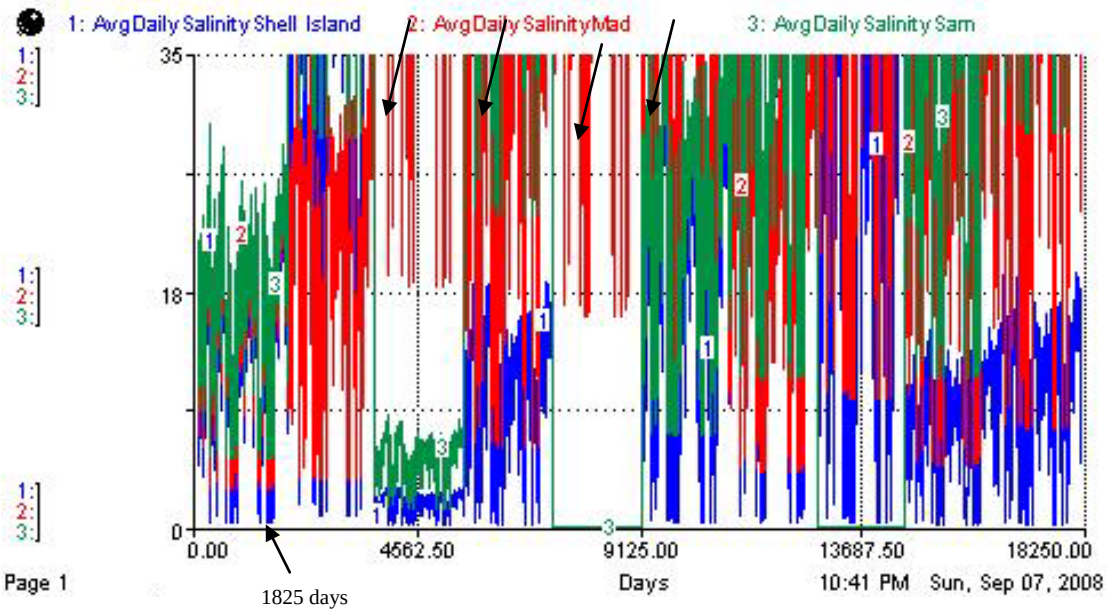

Figure 86. Comparison of average daily salinity among reefs for 50 years (2.0 SD). Simulation run using 2.0 SD begins at 1825 days, as indicated by lower arrow. Arrows at top indicate high salinity data generated for Mad Island Reef submodel.

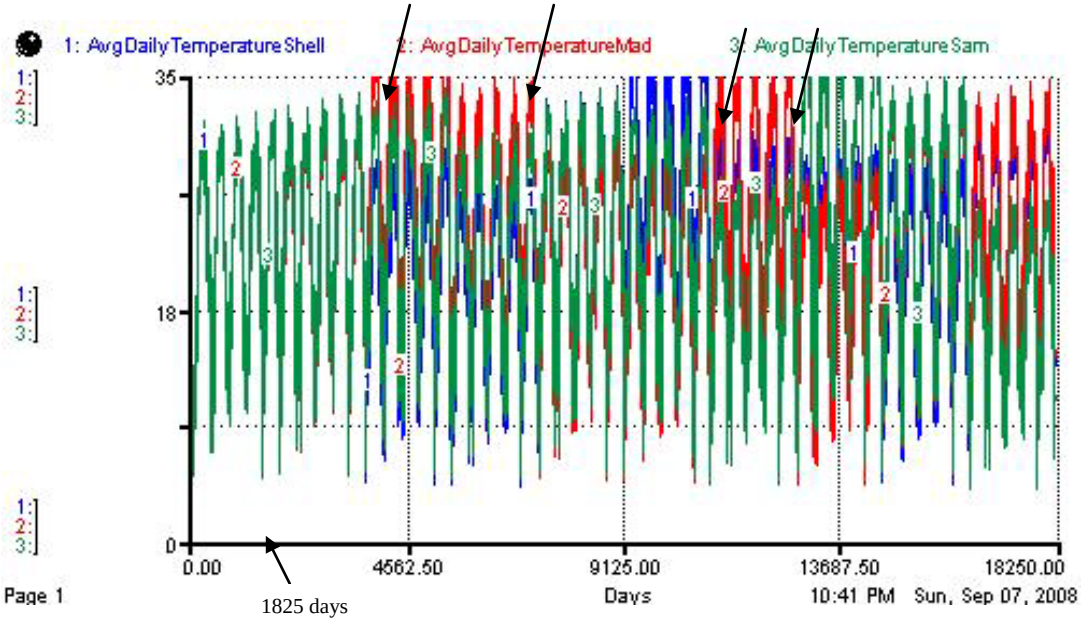

Figure 87. Comparison of average daily temperature among reefs for 50 years (2.0 SD). Simulation run using 2.0 SD begins at 1825 days, as indicated by lower arrow. Arrows at top indicate high temperature data generated for Mad Island Reef submodel.

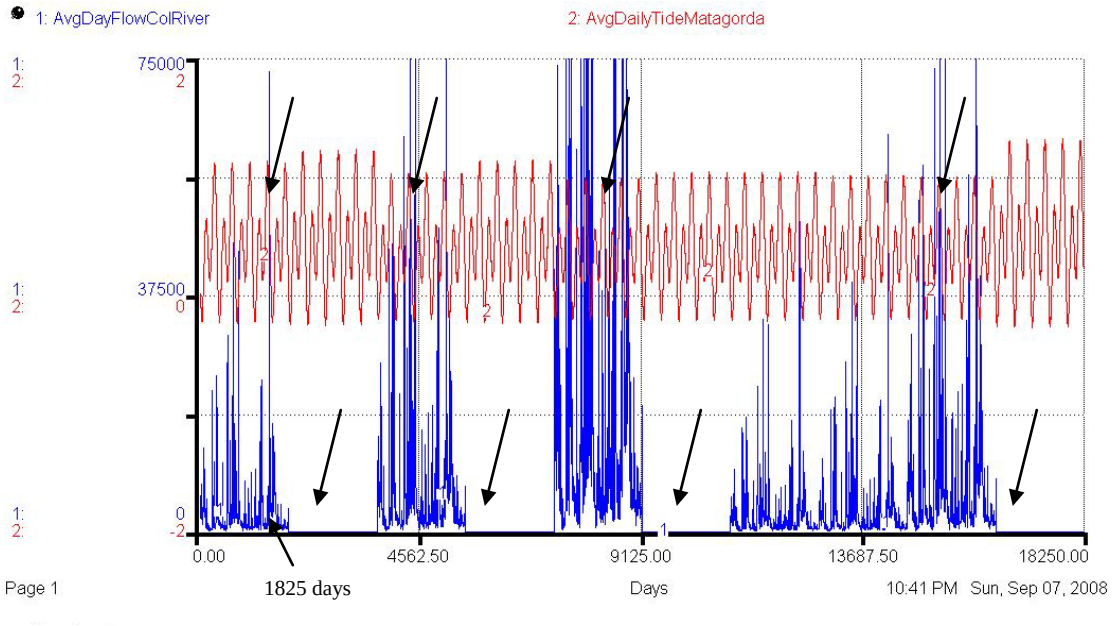

Figure 88. Comparison of Colorado River flow and Matagorda Bay tide among reefs for 50 years (2.0). Simulation run using 2.0 SD begins at 1825 days, as indicated by lower arrows. Four flood days followed by four drought days are referenced by upper arrows. The duration of flood and drought days varied from 10 to > 30 days.

Comparison of oyster reef populations among reefs for 50 years (2.0 SD)

Oyster larvae produced by the three oyster reef populations (Fig. 89) and spat set (Fig. 90) were compared among reefs, for the 50 year simulation run that was based on 2.0 SD of the actual 2001-2005 historical data, (see Chapter II), and graphically depicted using Stella software (Stella 2007). Larvae produced during the first 1825 days followed previous trends that were simulated during the five year simulation run, as well as the 50 year trends for simulation runs using 0.5 and 1.0 SD. Although the Mad Island population submodel continued to simulate larvae for the first 4500 days, only the Colorado Delta submodel simulated larvae from their intertidal reef populations following extended high inflow events (indicated by arrows in Fig. 89) during the remaining 13750 days, when low salinity conditions continued past 60 days for all reefs.

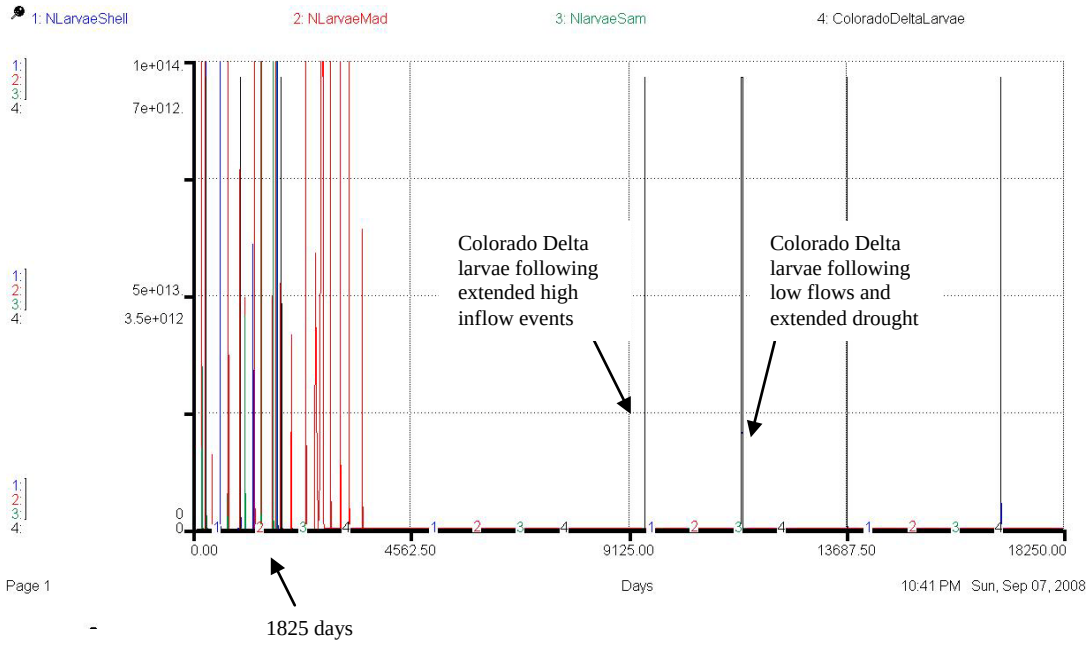

Figure 89. Comparison of larvae among reefs for 50 year simulation (2.0 SD). Simulation run using 2.0 SD begins at 1825 days, as indicated by lower arrow.

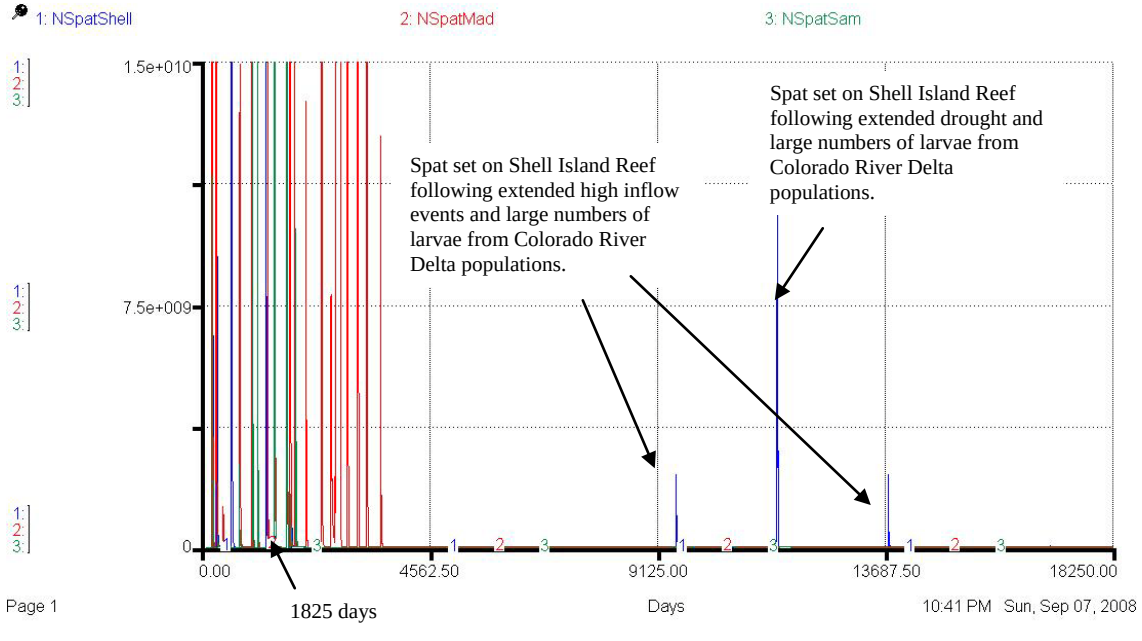

Figure 90. Comparison of spat among reefs for 50 year simulation (2.0 SD). Simulation run begins at 1825 days using 2.0 SD, as indicated by lower arrow. Arrows for moderate spat set related to high inflow events and following extended droughts.

The 50 year simulation run (2.0 SD) using the original five years (2001-2005) of continuous monitoring record resulted in declining numbers of submarket (Fig. 91), market (Fig. 92), and (Fig. 93) market-plus oysters at Shell Island Reef after 1825 days. These trends were somewhat modified for the population submodel at Mad Island Reef, where the 50 year simulation run using 2.0 SD resulted in a period of high abundance of submarket (Fig. 91), market (Fig. 92) and market-plus (Fig. 93) oysters for 4500 days followed by a total loss of these size classes for the remaining simulation run time. However, this same 50 year simulation run resulted in a total loss of submarket (Fig. 91), market (Fig. 92), and market-plus (Fig. 93) oysters from Sammy's Reef after 1825 days. Higher salinity and temperature conditions over a longer time span resulted in declining trends of up-estuary and down-estuary reef populations, which correspond to previous historical records of declining population trends in WMB described by King (1989) after the Colorado River was diverted into the Gulf of Mexico.

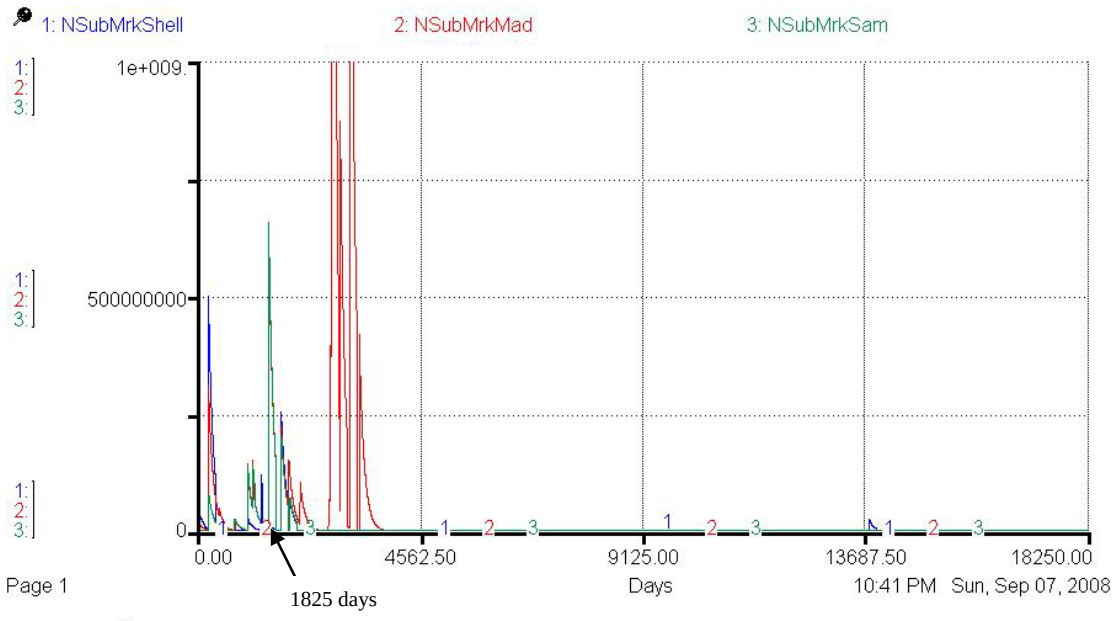

Figure 91. Comparison of submarket oysters among reefs for 50 year simulation (2.0 SD). Simulation run begins at 1825 days using 2.0 SD, as indicated by lower arrow.

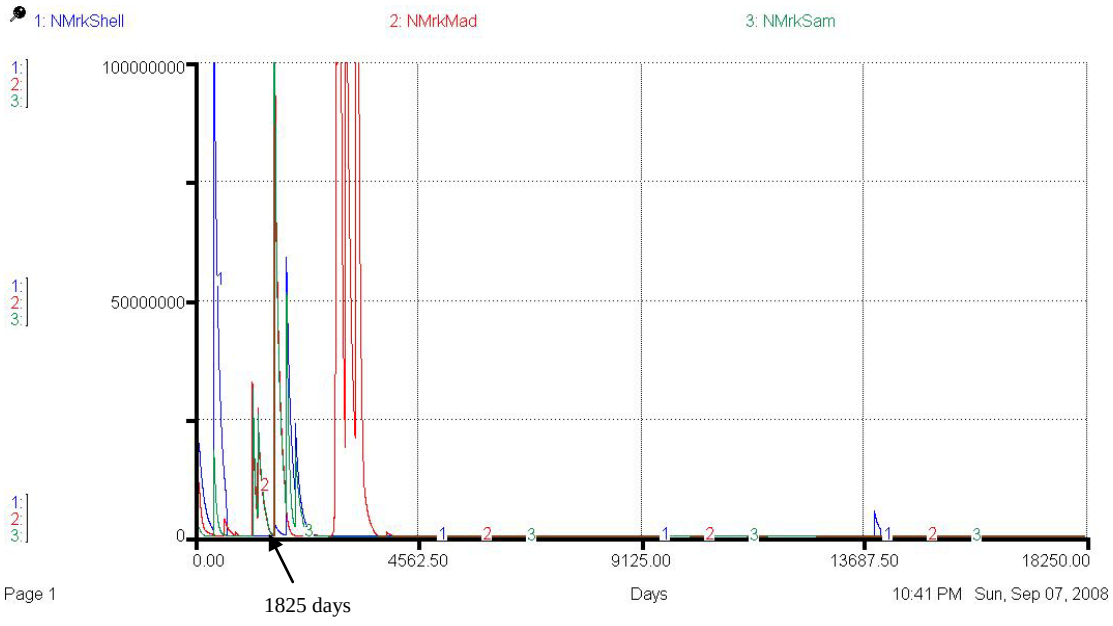

Figure 92. Comparison of market oysters among reefs for 50 year simulation (2.0 SD). Simulation run begins at 1825 days using 2.0 SD, as indicated by lower arrow.

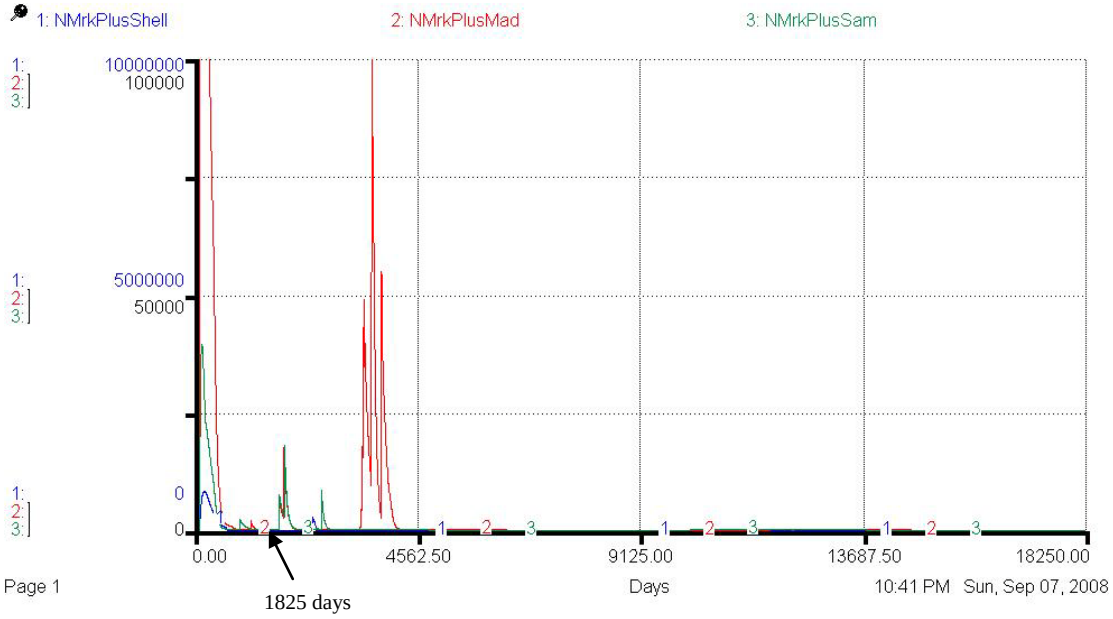

Figure 93. Comparison of market-plus oysters among reefs for 50 year simulation (2.0 SD). Simulation run begins at 1825 days using 2.0 SD, as indicated by lower arrow.

Spatial and temporal trends of Dermo infection among three reef populations

Dermo infection submodels developed in this study for three size classes (submarket, market, and market plus) of each oyster population submodel provided insight into the potential increased mortality that results from the number of days each population tolerates the disease before it effects reproductive success and survival of the population.

The Dermo infection submodel simulated data for 50 years at normal variation (1.0 SD) of the five year monitoring record for each size class (submarket, market, market-plus) were compared among reefs and graphically depicted using Stella software (Stella 2007). The results of this 50 year simulation run for Shell Island Reef oyster populations (Fig. 94) show that Dermo stress (accumulated number of infection-days) can be tolerated for long periods of time by all size classes (> 4000 days for submarket, >2000 days for market and market-plus oysters) under the environmental conditions used for average daily salinity and temperature continuous monitoring data. The results of this same 50 year simulation run for Mad Island Reef oyster populations (Fig. 95) show that Dermo stress can be tolerated for moderate amounts of time (> 200 days for each size class with less days tolerated during high salinity conditions during seasonally high temperature periods. However, Dermo stress is only tolerated for short periods of time resulting in increased mortality of all size classes at Sammy's Reef (Fig. 96) for the same 50 year simulation data (1.0 SD) based on the five year (2001-2005) average daily salinity and temperature continuous monitoring data (see Chapter II).

However, when the Dermo infection submodels were run using simulation data at 2.0 SD of the original five year continuous record, the results for Shell Island Reef's

population (Fig. 94) showed that submarket oysters continued to tolerate Dermo infection for longer periods of time (> 1000 days) unless there were drought-like conditions, and market and market-plus oysters tolerated Dermo infection less than 120 days, which resulted in increased Dermo related mortality for these size classes.

Dermo stress was only tolerated for short periods of time (< 120 days) resulting in increased mortality in all size classes at Mad Island (Fig. 95) for the same 50 year simulation data based on 2.0 SD of the average daily salinity and temperature continuous monitoring data.

The Dermo infection submodels for this same simulation run using 2.0 SD of the average daily salinity and temperature continuous monitoring data at Sammy's Reef (Fig. 96) provided interesting results. Although all size classes only tolerated Dermo infection-days for short periods of time (< 120 days) during higher salinity and temperature conditions that coincided with lower flows from the Colorado River, there were also long periods of time when these same size classes of the population tolerated Dermo infection (> 1000 days) during higher flows. Although twice the variation of normal environmental conditions along with flows was a driving factor for shorter Dermo tolerance time for Mad Island Reef's population, these same conditions appeared to have less effect on Sammy's Reef oyster populations. The accumulation of Dermo "infection days" at Sammy's Reef in this model should be considered in conjunction with declining numbers in all size classes, which indicates increased mortality from factors other than Dermo related mortality, which may in fact be the result of reduced Dermo infection when there are no live oysters to become infected. Dermo "infection-days" continued to remain short for Mad Island Reef populations in this high variance

simulation run; and there were no long periods of tolerance between epizootic events, which may indicate residual levels of Dermo remain in this population for the 50 year simulation run time because there are live oysters remaining in the Mad Island Reef population.

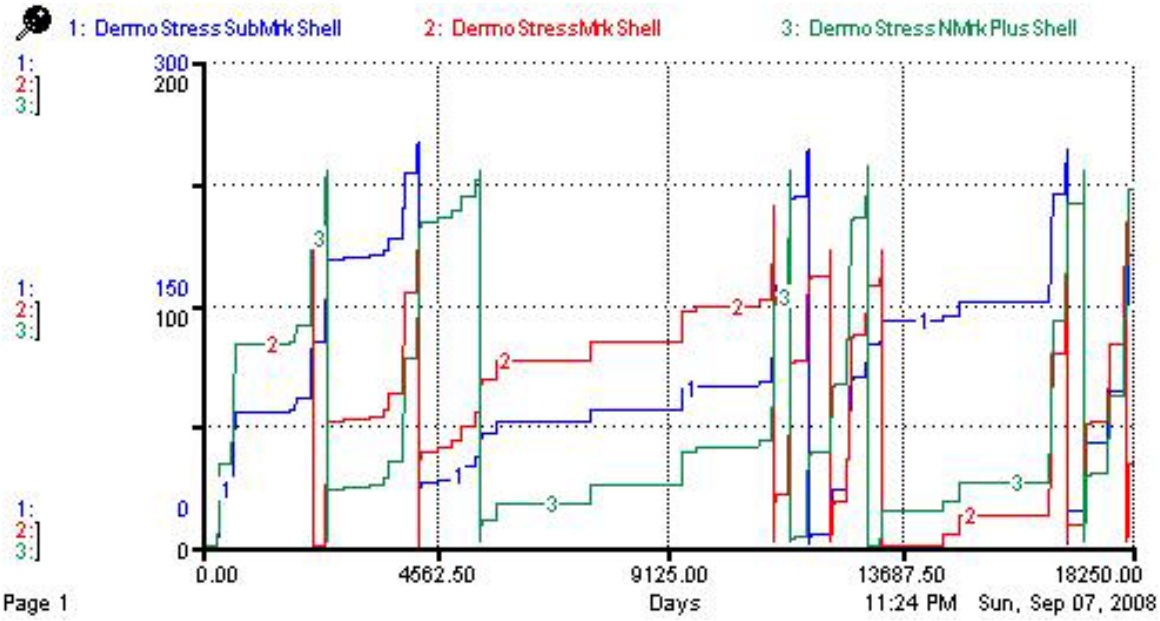

Figure 94. Comparison of Dermo infection in submarket, market, and market-plus classes of Shell Island Reef oyster populations for 50 year simulation (1.0 SD).

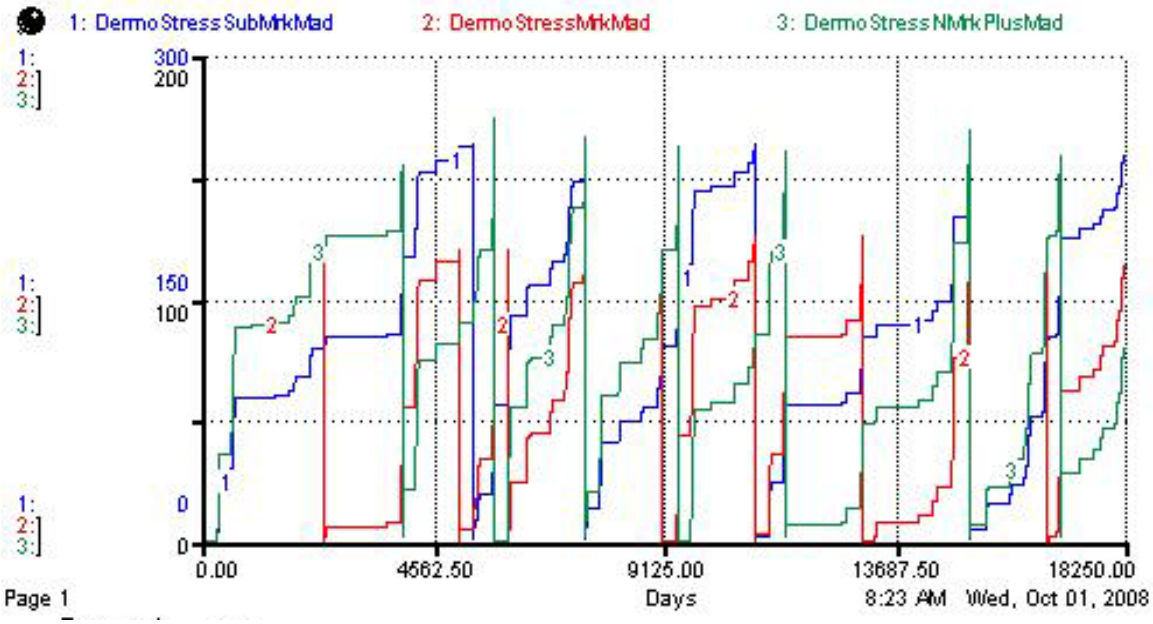

Figure 95. Comparison of Dermo infection in submarket, market, and market-plus size classes of Mad Island Reef oyster populations for 50 year simulation (1.0 SD).

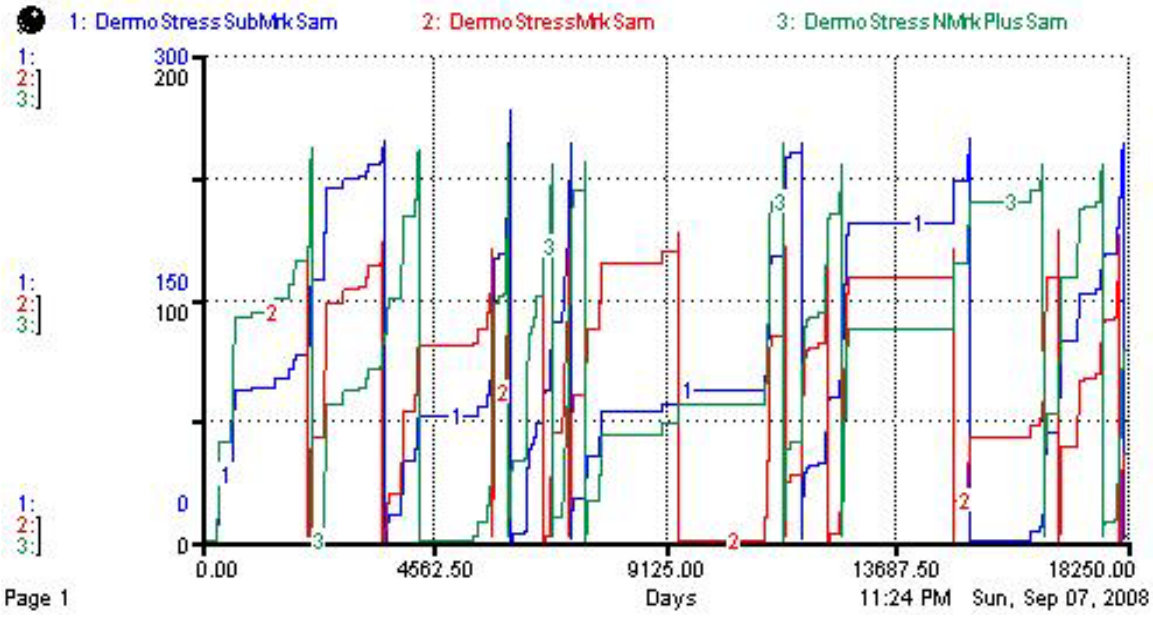

Figure 96. Comparison of Dermo infection in submarket, market, and market-plus size classes of Sammy's Reef oyster populations for 50 year simulation (1.0 SD).

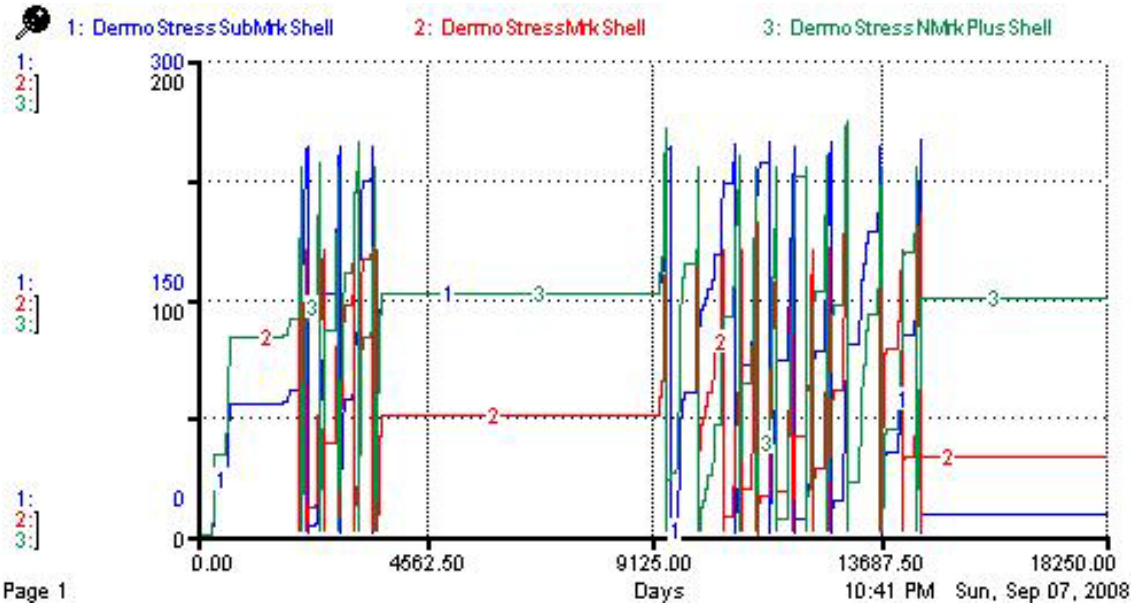

Figure 97. Comparison of Dermo infection in submarket, market, and market-plus classes of Shell Island Reef oyster populations for 50 year simulation (2.0 SD).

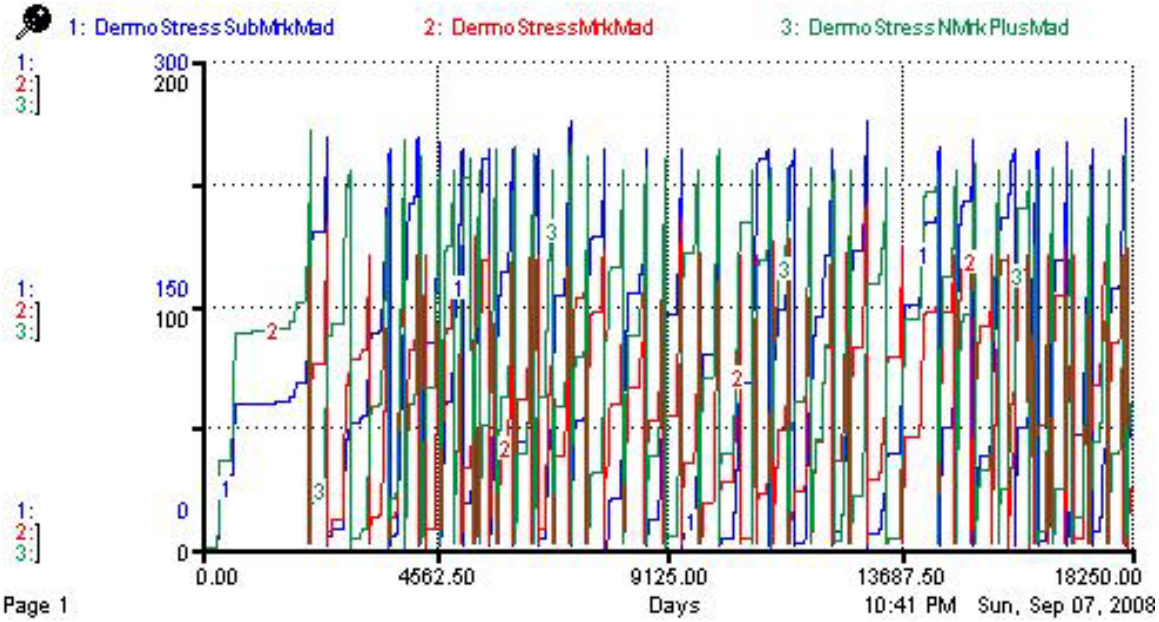

Figure 98. Comparison of Dermo infection in submarket, market, and market-plus size classes of Mad Island Reef oyster populations for 50 year simulation (2.0 SD).

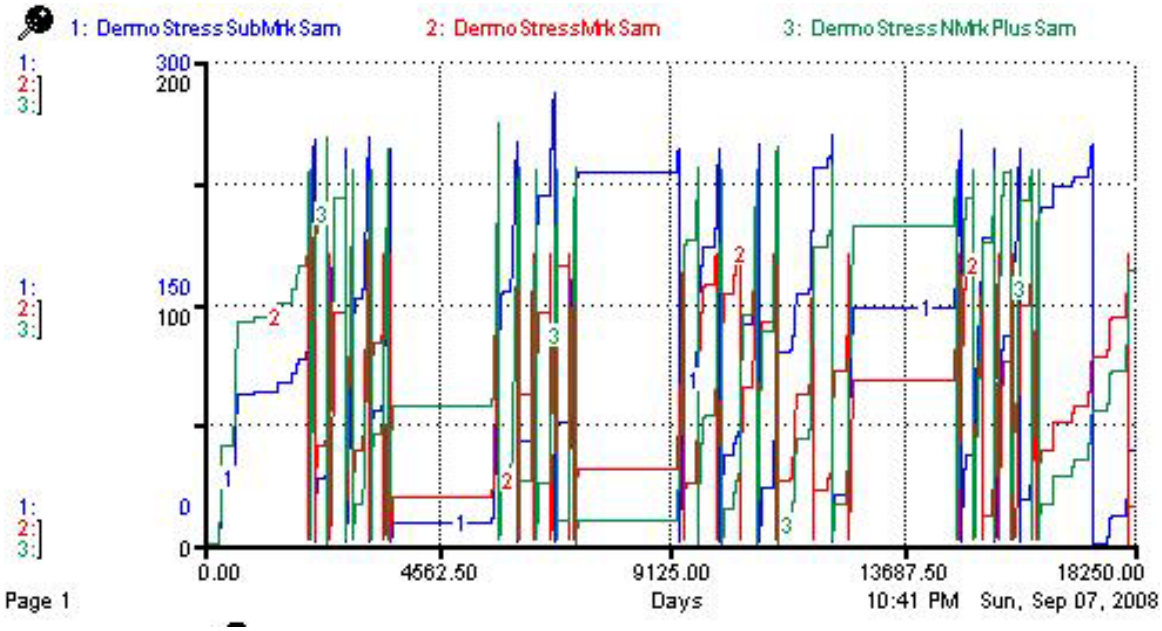

Figure 99. Comparison of Dermo infection in submarket, market, and market-plus size classes of Sammy's Reef oyster populations for 50 year simulation (2.0 SD).

Discussion

The model results showed that WMB oyster populations spawned several times each year according to when optimum environmental conditions occurred during the five year, and 50 year simulation runs using 0.5 and 1.0 SD of the historic data. Spawning declined for all oyster populations when environmental conditions deteriorated during the 50 year simulation run using 2.0 SD resulting in decreased oyster abundance of all size classes.

Model simulation results showed that environmental conditions in WMB promoted high incremental growth rates and were best described by Krauether et al.'s (2007) equations during the five year and 50 year simulation runs using 0.5 and 1.0 SD. However, when environmental conditions declined, slower growth rates previously described by Hofstetter (1977) were observed during the 50 year simulation runs using

2.0 SD. Similar slow growth rates were also observed by King (1964) in Matagorda Bay after nearly 30 years of the Colorado River being diverted to the Gulf of Mexico.

Simulations using higher variation (1.0 SD versus 2.0 SD) of the actual five year salinity continuous monitoring data gradually increased salinity values at all reefs over time (50 years). These simulations also revealed that oyster populations located farthest from the Colorado River (Sammy's Reef) decreased in abundance with increasing salinities (loss of freshwater) over time. These simulations also demonstrated that oyster populations located closest to the Colorado River (Shell Island Reef) survived low flow conditions and droughts for short periods of time, but appeared to be affected by lower larval recruitment following long term declining population abundance at down-estuary reefs (Sammy's Reef).

Oyster populations in these submodels responded to the synergistic affects of changes in salinity, temperature, duration and timing of flows and direction and tidal amplitude over different periods of time (measured in days not months). Low salinity stress related mortality increased for all populations when low salinity and high temperatures prevailed for more than 10 days. Dermo mortality increased for all populations when high salinity and high temperatures prevailed for more than 120 days. Dermo infection levels increased at all reefs in all size classes with increasing salinity variation (1.0 to 2.0 SD) on the 50 year simulation runs.

The sensitivity tests of this model indicate that subtle spatial and temporal trends for these three populations that are based on the historical record can be magnified into long term changes for all reefs within the WMB system. Short term droughts become long term droughts that increased mortality for down-estuary populations, which

ultimately resulted in increased mortality for up-estuary populations. Freshwater inflow conditions that reduce salinity for short periods of time, allow survival of down-estuary populations that provide opportunities to restore up-estuary populations. However, long term low salinity conditions also revealed that Colorado Delta populations have the potential to survive these salinity stress conditions and provide potential larvae recruitment to up-estuary populations.

Conclusions

The interactive Stella oyster community based model quantified and integrated the spatial and temporal patterns influencing reproduction, larval distribution, larval settlement, individual growth of each size class (larvae, spat, submarket, market, market that are older than two years of age) and population growth on these three oyster reefs in WMB. The three population submodels incorporated spatial and temporal trends that were consistent with trends in Chapter II and III. Simulations over a 50 year period using actual five year environmental records showed that reef populations located farthest from Colorado River decreased in abundance as salinity increased with loss of freshwater inflows over time. Simulations also show that reef populations spatially located closest to Colorado River Delta would be impacted by lower larval recruitment following declining numbers in spawning populations due to increased salinity and increased disease levels at reefs located further from the Colorado River.

The three reef population submodels also included a proportion of larvae recruited from the Colorado Delta based on recently mapped areas by the LCRA and average densities of intertidal oyster populations along the Texas Coast. These intertidal

populations formed over buried shell from the former Dog Island Reef, appear to survive flood and drought conditions in the simulation runs. Their ability to adapt to immersion-submersion conditions provide a survival “parachute” by contributing larvae to up-estuary populations during low flow conditions and to down-estuary populations following long term flooding conditions. The down-estuary populations at Sammy’s Reef, which are located furthest from the Colorado River, also appear to survive low salinity conditions following floods and provide a similar survival parachute for contributing larvae to up-estuary populations.

CHAPTER V

SUMMARY AND CONCLUSIONS

Summary

The proceeding chapters explored the spatial and temporal demographic trends in oyster population dynamics and their relationships to freshwater inflows and the pathogen Dermo (*Perkinsus marinus*) on three reefs (Shell, Mad Island, and Sammy's) in West Matagorda Bay, Texas. The objectives were to design and link three population models that simulate oyster population dynamics and integrate the environmental factors that influence growth, reproduction, settlement of larvae and Dermo disease interactions among these three reefs.

The results presented in this research suggest that conceptual "population based" models describing oyster population dynamics for multiple reefs requires the input of daily environmental conditions in order to provide accurate predictions for growth, reproduction, larval recruitment, Dermo disease within and among reefs. Averaging monthly or yearly environmental variables often diminishes the response pattern being investigated and were not used in this model.

The following variables were evaluated for trends to be incorporated in this model: relative abundance of oyster spat, submarket- and market-size oysters, average weighted incidence of Dermo and percent Dermo infection (prevalence) in submarket- and market-size oysters and their relationships to environmental variables of salinity, temperature, flow and distance from freshwater sources. The results of this trend analysis revealed that environmental variables accounted for 36% of the variation in

Dermo-related variables among the three reefs, and were also positively correlated with distance from freshwater sources. The relative abundance of spat and dead oysters was related to peaks in freshwater inflows occurring 30 days prior to larval settlement.

These spatial and temporal relationships among biological and environmental variables and the data from five years of continuous monitoring records for three reefs in WMB were incorporated in an integrated Stella model. This population based model simulated oyster population responses to stochastic environmental changes over a 50 year period using 0.5, 1.0 and 2.0 SD of the historic data.

The model results showed that WMB oyster populations spawned several times each year according to when optimum environmental conditions occurred during the five year, and 50 year simulation runs using 0.5 and 1.0 SD of the historic data. Spawning declined for all oyster populations when environmental conditions deteriorated during the 50 year simulation run using 2.0 SD resulting in decreased oyster abundance of all size classes.

Model simulation results showed that environmental conditions in WMB promoted high incremental growth rates and were best described by Krauether et al.'s (2007) equations during the five year and 50 year simulation runs using 0.5 and 1.0 SD. However, when environmental conditions declined, slower growth rates previously described by Hofstetter (1977) were observed during the 50 year simulation runs using 2.0 SD. Similar slow growth rates were also observed by King (1964) in Matagorda Bay after nearly 30 years of the Colorado River being diverted to the Gulf of Mexico.

Analysis of population trends for WMB revealed that higher distribution of dead oysters at Shell Island Reef following high FWI events the month prior to samples taken

provided valuable substrate for larvae (down-estuary spawned) to set. These trends were incorporated into the model, which resulted in larvae distributed up-estuary to Mad Island and Shell Island Reefs through tidal amplitude and meteorological forced winds between May and June and again in September through October of each year in the in simulation runs. Larvae were distributed down-estuary that spawned from the Colorado Delta's intertidal populations as well as Shell and Mad Island Reefs to Sammy's Reef when spawning occurred up-estuary prior to high inflow events and during minima tidal cycles in simulation runs.

The model simulation results provided evidence that higher Dermo infection levels on down-estuary reefs (Mad and Sammy's Reef have influence on greater mortality rates following spawning cycles for these reefs. The model simulation results also showed that up-estuary populations may contain residual levels of Dermo disease despite long term low salinity conditions, or may become infected by larvae contributed from down-estuary populations infected with Dermo disease.

Although the geological and structural complexity of each reef appeared to be similar, the model showed the relationship of growth, spawning, spat set and Dermo infection were related to distance from freshwater sources and also meteorological wind driven tidal forcing. The model revealed that up-estuary reefs relied on the distribution of larvae from down-estuary reefs following mortality related to freshwater inflow.

The model provided an indication of the spawning connectivity and functional value of oyster populations in West Matagorda Bay as an integrated resource for sustaining all oyster reef populations in this bay system. The model revealed that

Matagorda Bay oyster populations are integral members of a dynamic bay ecosystem that function as an integrated unit and not separate reef populations.

Conclusions

The conceptual "population based" model developed for WMB showed that timing or duration of a flood or a drought resulted in long term population level responses of increased mortality, increased spat settlement, shorter or longer growth rates, delayed or increased reproduction, changes in larval recruitment to other reefs, and increased or decreased mortality from Dermo. Seasonal patterns in tidal amplitude and direction through "meteorological" wind driven forces also had profound influence on oyster population dynamics of these three reefs. These types of "population responses" cannot be determined by "individual oyster" based models as previously developed for Galveston Bay by Hofmann et al. 1992; Powell et al. 1994; Powell et al. 2003).

Oyster population dynamic models previously developed for Galveston Bay have used annual and monthly data to make broad generalizations about the response of all populations within that bay system to changes in hydrodynamics of freshwater inflows and tidal conditions after widening the Houston Ship Channel (Hofmann et al. 1992; Hofmann et al. 1995; Powell et al. 1996; Dekshenieks et al. 2000; Powell et al. 2003). These models attempted to tie in all of the biotic and abiotic factors that influence individual oyster's growth, respiration, assimilation of nutrients, disease interactions, and mortality in contrast to examining specific reef populations and their interactions with other reef populations in Galveston Bay. These "individual oyster" based models include reefs that differ in their structural formation (flat pancake shaped to ridge shaped); their size or footprint on the bottom, their population densities (scattered or

clustered), their flow patterns (along shores or across land masses), their distances from freshwater sources (closest to farthest), and distances from each other (close enough for larvae recruitment or not). These individual based models are often assumed to apply to all Texas bays with different hydrologic regimes despite a lack of empirical evaluation of these models. The predictions for oyster responses in these individual based models may correspond to responses of specific populations within Galveston Bay. However, these responses may not apply to all oyster populations in this bay system or in other bay systems like Matagorda Bay with one main freshwater source.

Hydrologic variation between different reefs and time periods was a consistent factor influencing population dynamics in conceptual population based model of WMB. The model presented in this research provides a basis for understanding the population dynamics of WMB as well as a better understanding of the interaction among the reefs that sustain these populations. The model developed in this investigation provides a basis for developing oyster population models for other bay systems and for future research regarding hydrologic influences on oyster population dynamics and Dermo disease interactions within and among reefs.

LITERATURE CITED

Bahr, L.M. & W. P. Lanier. 1981. The ecology of intertidal oyster reefs of the South Atlantic coast: a community profile. U.S. Fish Wildl. Serv. Office of Biological Services Report FWS/OBS-81/15. 105 pp.

Bartol, I. K., R. Mann & M. Luckenbach. 1999. Growth and mortality of oysters (*Crassostrea virginica*) on constructed intertidal reefs: effects of tidal height and substrate level. *J. Exp. Mar. Biol. Ecol*. 237(2):157-184.

Benefield, R. L. 1976. Shell dredging sedimentations in Galveston and San Antonio Bays 1964-69. Tech. Ser. No. 19. Texas Parks & Wildlife Dept. Austin, TX. 168 pp.

Benefield, R. L. & R. P. Hofstetter. 1976. Mapping of productive oyster reefs in Galveston Bay, Texas. Texas Parks & Wildlife Dept. Austin, TX. Federal Aid Report. PL88-309 2-218R. 34 pp.

Bergquist, D. C., J. A. Hale, P. Baker, & S. M. Baker. 2006. Development of ecosystem indicators for the Suwannee River estuary: oyster reef habitat quality along a salinity gradient. *Estuaries & Coasts*. 29(3): 353-360.

Bernard, H. A. & R. J. LeBlanc. 1965. Résumé of Quaternary Geology of the Northwestern Gulf of Mexico Province. Princeton University Press, Princeton, NJ: Shell Development Company, Exploration and Production Research.

Breuer, J. P. 1962. An ecological survey of the lower Laguna Madre of Texas, 1953-1959. *Publ. Inst. Mar. Sci., Univ. Texas*. 8(15): 3-183.

Britton, J. C. & B. Morton. 1989. Shore ecology of the Gulf of Mexico. Austin, TX: University of Texas Press. Austin, TX.

Bronikowski, J. 2004. Sedimentary environments and processes in a shallow, Gulf Coast Estuary-Lavaca Bay, Texas. Masters Science Thesis. Texas A&M University, College Station.

Butler, P.A. 1949. Gametogenesis in the oyster under conditions of depressed salinity. *Biol. Bull.* 96(3):263-269.

Butler, P. A. 1954. Summary of our knowledge of the oysters in the Gulf of Mexico. In: Gulf of Mexico, its origin, waters, and marine life: U.S. Fish and Wildlife Service, *Fishery Bull*. 89 (55): 479-489.

Buzan, D., W. Lee, J. Culbertson, N. Kuhn, & L. Robinson. 2008. Positive relationship between freshwater inflow and oyster abundance in Galveston Bay, Texas. *Estuaries and Coasts*. Online First™ Technical Communication. DOI 10.1007/s12237-008-9078-z.

Byrne, J. R. 1975. Holocene depositional history of Lavaca Bay, Central Texas Gulf Coast. Doctoral Dissertation. University of Texas, Austin.

Cake, E. W., Jr. 1983. Habitat suitability models: Gulf of Mexico American oysters. U.S. Fish Wildl. Serv. FWS/OBS-82/10.57. 37 pp.

Chatry, M., R. J. Dugas, & K. A. Easley, K. A. 1983. Optimum salinity regime for oyster production in Louisiana's state seed grounds. *Contrib. Mar. Sci. Univ. Texas* 26:81–94.

Choi, K. S., E. A. Wilson, D. H. Lewis, E. N. Powell, & S. M. Ray. 1989. The energetic cost of *Perkinsus marinus* parasitism in oysters: Quantification of the thioglycollate method. *J. Shellfish Res*. 8(1):125-131.

Coen, L. D., M. W. Luckenbach, & D. L. Breitburg, 1999. The role of oyster reefs as essential fish habitat: a review of current knowledge and some new perspectives. In: L.R. Benaka, editor. Fish habitat: Essential fish habitat and rehabilitation. Bethesda, MD: American Fisheries Society. pp. 438-454.

Collier, A. & J. Hedgpeth. 1950. An. Introduction to the hydrography of tidal waters of Texas. *Publ. Inst. Mar. Sci. Univ. Texas* 1(2):120-194.

Craig, A., E. N. Powell, R. R. Fay & J. M. Brooks.1989. Distribution of *Perkinsus marinus* in Gulf Coast oyster populations. *Estuaries* 12(2):82-91

.

Culbertson, J., L. Robinson, P. Campbell, & L. Butler. 2004. Trends in Texas commercial fishery landings, 1981-2001. *Tex. Parks and Wildlife. Dept. Manag. Data Ser.* No. 224, Austin, TX.

Dame, R. F. 1979. The abundance, diversity, and biomass of macrobenthos on North Inlet, South Carolina intertidal oyster reefs. *Proc. Natl. Shellfish. Assoc.* 69:6-10.

Dame, R.F. 1996. Ecology of Marine Bivalves: An Ecosystem Approach. CRC Marine Science Series. Boca Raton FL: CRC Press.

Dame, R. F., R. G. Zingmark, & E. Haskin, 1984. Oyster reefs as processors of estuarine materials. *J. Exper. Mar. Biol. Ecol.* 83:239-247.

Davis, H. C. & P. E. Chanley. 1955. Spawning and egg production of oysters and clams. *Biol. Bull.* (Woods Hole) 110:117-128.

Dekshenieks, M. M. 1996. The effects of environmental variability on the population structure of the Eastern oyster (*Crassostrea virginica*): A modeling study. Ph.D. Dissertation, Old Dominion University, Norfolk.

Dekshenieks, M. M., E. E. Hofmann, & E. N. Powell. 1993. Environmental effects on the growth and development of Eastern oyster, *Crassostrea virginica* (Gmelin, 1791), larvae: A modeling study. *J. Shellfish. Res.* 12:241–254.

Dekshenieks, M. M., E. E. Hofmann, J. M. Klinck, & E. N. Powell. 2000. Quantifying the effects of environmental change on an oyster population: A modeling study. *Estuaries* 23:593–610.

Dittman, D. E., S. E. Ford, & D. K. Padilla. 2001. Effects of *Perkinsus marinus* on reproduction and condition of the Eastern oyster, *Crassostrea virginica*, depend on timing. *J. Shellfish. Res*. 20(3): 1025-1034.

Diener, R. A. 1975. Cooperative Gulf of Mexico Estuarine Inventory and Study-Texas: Area Description. National Technical Information Service, Springfield, VA 22161. NOAA Technical Report NMFS CIRC-393, September 1975. 136 pp.

Eastern Oyster Biological Review Team. 2007. Status review of the eastern oyster (*Crassostrea virginica*). Report to the National Marine Fisheries Service, Northeast Regional Office. February 16, 2007. 105 pp.

Galtsoff, P. S. 1931. Survey of oyster bottoms in Texas. U.S. Dept. of Commerce, Bur. Fisheries Investigation Rept. 6(1):1-30.

Galtsoff, P. S. 1964. The American oyster *Crassostrea virginica* Gmelin. *Fishery Bulletin* 64. U.S. Fish and Wildlife Service, Washington, D. C.

Grave, C. 1901. The oyster reefs of North Carolina. A geological and economic study. Johns Hopkins Univ. Circular No. 151. Baltimore, MD: Johns Hopkins Univ. Press. 9 pp.

Gutierrez, J. L., C. G. Jones, D. L. Strayer, & O. O. Iribarne. 2003. Mollusks as ecosystem engineers: The role of shell production in aquatic habitats. *Oikos* 101:79–90.

Hargis, W. J., Jr., & D. S. Haven. 1999. Chesapeake oyster reefs, their importance, destruction and guidelines for restoring them. In: M. W. Luckenbach, R. Mann, & J. Wesson, (Eds). Oyster reef habitat restoration: A synopsis and synthesis of approaches. Virginia Institute of Marine Science, Gloucester Point, VA. pp. 329-358.

Hayes, M. O. & A. J. Scott. 1964. Environmental complexes South Texas coast. *Gulf Coast Assoc. Geol. Soc. Trans.* 14:237-240.

Hedgpeth, J. W. 1953. An introduction to the zoogeography of the Northwestern Gulf of Mexico with reference to the invertebrate fauna. *Pub. Inst. Mar. Sci., Univ. Texas* 3(1):109-224.

Hedgpeth, J. W. 1954. Bottom communities of the Gulf of Mexico. In: Gulf of Mexico, its origin, waters, and marine life: U.S. Fish Wildlife Service, U.S. Dept. Interior. *Fishery Bull.* 89 (55):203-214.

Heffernan, T. L. 1963. Coast wide survey of the oyster parasite *Dermocystidium marinum*. Texas Game & Fish Comm. Mar. Fish. Div. Project Report. 1961-1962. 4 pp.

Higgins, P. J. 1980. Effects of food availability on the valve movements and feeding behavior juvenile *Crassostrea virginica* (Gmelin). I. Valve movements and periodic activity. *J. Exp. Mar. Biol. Ecol.* 45:229-244.

Hofmann, E. E., E. N. Powell, J. M. Klinck, & E. A. Wilson. 1992. Modeling oyster populations. III. Critical feeding periods, growth and reproduction. *J. Shellfish Res*. 11:399–416.

Hofmann, E. E., E. N. Powell, J. M. Klinck, & G. Saunders. 1995. Modeling diseased oyster populations I. Modeling *Perkinsus marinus* infections in oysters. *J. Shellfish Res.* 14:121–151.

Hofstetter, R. P. 1965. Study of the oyster populations along the Texas Coast. Texas Parks & Wildlife Dept., Coastal Fish. Austin, TX. Project Report. 1965. pp. 97-118.

Hofstetter, R. P. 1966. Oyster mortality studies along the Texas Coast. Texas Parks & Wildlife Dept., Coastal Fish. Austin, TX. Project Report. 1966. pp. 55-64.

Hofstetter, R. P. 1967. Oyster studies along the Texas Coast. Texas Parks & Wildlife Dept., Coastal Fish. Austin, TX. Project Report. 1967. pp. 49-60.

Hofstetter, R. P. 1977. Trends in population levels of the American oyster *Crassostrea virginica* (Gmelin) on public reefs in Galveston Bay, TX. Texas Parks & Wildlife Dept., Austin, TX. Tech. Series 24:1-90.

Hofstetter, R. P. & T. L. Heffernan, 1959. A coastal survey of the oyster parasite, *Dermocystidium marinum*. Texas Game & Fish. Comm., Mar. Fish. Div. Austin, TX. Project Report. 1958-1959. pp 1-8.

Hofstetter, R. P., T. L. Heffernan, & B.D. King 1965. Oyster (*Crassostrea virginica*) mortality studies along the Texas coast. Texas Parks & Wildlife Dept., Coastal Fish. Austin, TX. Project Report: MO-R-7. pp. 119-131.

Hopkins, A. E. 1931. Factors influencing the spawning and setting of oysters in Galveston Bay, Texas. *Bull. U. S. Bur. Fisheries*. 47(3): 57-83.

Hopkins, S. H., J. G. Mackin, & R. W. Menzel. 1954. The annual cycle of reproduction, growth, and fattening in Louisiana oysters. *Proc. Natl. Shellfish. Assoc*. 44: 39-50.

Jackson, J. B. C., M. X. Kirby, W. H. Berger, K. A. Bjorndal & L. W. Botsford. 2001. Historical overfishing and the recent collapse of coastal ecosystems. *Science* 293:629-638.

Jongman, R. H. G., C. J. F. Ter Braak, & O. F. R. Van Tongeren. (Eds.). 1995. Data analysis in community and landscape ecology. Cambridge, MA: Cambridge University Press. 299 pp.

Keck, R., D. Maurer, J. C. Kauer, & W. A. Sheppard. 1971. Chemical stimulants affecting larvae settlement in the American oyster. *Proc. Natl. Shellfish. Assoc*. 61:24-28.

Kennedy, V. S., R. I. E. Newell, & A. F. Ebel (Eds). 1996. The Eastern Oyster *Crassostrea virginica.* University of Maryland, College Park, MD: Maryland Sea Grant Publication. (UM-SG-TS-96-01).

Kim, Y. & E. N. Powell. 1998. Influence of climate change on interannual variation in population attributes of Gulf of Mexico oysters. *J. Shellfish. Res*. 17:265-274.

King, B. D., III. 1964. Study of oyster growth and population structure of the public reefs in Matagorda, Tres Palacios and East Matagorda Bays. Texas Parks & Wildlife Dept., Coastal Fish. Austin, TX. Project Report: MO-R-5, pp. 223-230.

King, B. D., III. 1989. Oyster populations in the eastern arm of Matagorda Bay prior to the diversion of the Colorado River. Houston, TX: U. S. Fish and Wildlife Service Report.

King, T. L., R. Ward, & E. G. Zimmerman. 1994. Population structure of eastern oysters (*Crassostrea virginica*) inhabiting the Laguna Madre, Texas and adjacent bay systems. *Can. J. Fish. Aquat. Sci*. 51:215–222.

Kraueter, J. N., S. Ford, & M. Cummings. 2007. Oyster growth analysis: A comparison of methods. *J. Shellfish Res*. 26(2): 479–491.

Ladd, H. S. 1951. Brackish-water and marine assemblages of the Texas coast, with special reference to mollusks. *Publ. Inst. Mar. Sci. Univ. Texas* 2: 125-164.

Langdon, C. J. & R. I. E. Newell. 1996. Digestion and nutrition of larvae and adults. In: V. S. Kennedy, R. I. E. Newell & A. Eble, editors. The Eastern Oyster, *Crassostrea virginica*. University of Maryland, College Park, MD: Maryland Sea Grant Publication. pp. 231-270.

LeBlanc, R. J. & W. D. Hodgson. 1959. Origin and development of the Texas shoreline: Second Coastal Geography Conf., April 6-9, 1959, Louisiana State Univ. pp. 57-101.

Lenihan, H. S. & C. H. Peterson. 1998. How habitat degradation through fishery disturbance enhances impacts of hypoxia on oyster reefs. *Ecol. Applic*. 8:128-140.

Levine, N.D. 1978. *Perkinsus* gen. n. and other new taxa in the protozoan phylum *Apicomplexa. J. Parasitol*. 64(3):549.

Livingston, R. J., F. G. Lewis, G. C. Woodsum, X. F. Niu, B. Galperin, W. Huange, J. D. Christensen, M. E. Monaco, T. A. Battista, C. J. Klein, R. L. Howell, IV & G. L. Ray. 2000. Modeling oyster population response to variation in freshwater input. *Estuarine, Coastal and Shelf Sci.* 50(5):655-672.

Loosanoff, V. L. & C. A. Nomejko. 1946. Feeding of oysters in relation to tidal stages and to periods of light and darkness. *Biol Bull.* (Woods Hole) 90:244-264.

Mackin, J. G., H. M. Owen, & A. Collier. 1950. Preliminary note on the occurrence of a new protistan parasite *Dermocystidium marinum* n. sp. in *Crassostrea virginica* (Gmelin) *Science* 111:328-329.

Mackin, J. G. 1951. Histopathology of infection of *Crassostrea virginica* (Gmelin) by *Dermocystidium marinum* (Mackin, Owen, and Collier). *Bull. Mar. Sci. Gulf Caribb*. 1:72-87.

Matlock, G. & M. Osburn. 1982. Shallow-water surface areas and shoreline distances on the Texas coast. *Texas Parks & Wildl. Manag. Data Ser.* No. 37. Austin, TX.

McCormick-Ray, M.G. 1998. Oyster reefs in 1878 seascape pattern-Winslow revisited. *Estuaries* 21 (4): 784-800.

Minello, T. J. 1999. Nekton densities in shallow estuarine habitats of Texas and Louisiana and the identification of essential fish habitat. In: Benaka L. R., editor. Fish habitat: Essential fish habitat and rehabilitation. Bethesda, MD: The American Fisheries Society. pp 43–75.

Moffett A. W. & F. A. Murray. 1963. Study of oyster growth and population structure of the public reefs in Matagorda, Tres Palacios and East Matagorda Bays. Texas Game and Fish Comm. Project Report: MO-R-4. pp. 1-13.

Moore, H. T. 1907. Survey of oyster bottoms in Matagorda Bay, Texas. U. S. Bur. Fisheries Doc. 610.

Moore, H. T. & E. Danglade. 1915. Condition and extent of the natural oyster beds and barren bottoms of Lavaca Bay, Texas. U. S. Bur. Fisheries Doc. 809.

Newell, R. I. E. 1988. Ecological changes in Chesapeake Bay: Are they the result of overharvesting the American oyster, *Crassostrea virginica*? In: M. P. Lynch & E. C. Krome, editors. Understanding the Estuary: Advances in Chesapeake Bay Research. Glouchester Point, VA: Chesapeake Bay Research Consortium Publication 129. pp 536-546.

Norris, R. M. 1953. Buried oyster reefs in some Texas Bays. *J. Paleontology*. 27(4):569-576.

O'Beirn, F. X., M. W. Luckenbach, J. A. Nestlerode & G. M. Coates. 2000. Toward design criteria in constructed oyster reefs: Oyster recruitment as a function of substrate type and tidal height. *J. Shellfish Res*.19:387-395.

Officer, C. B., T. J. Smayda & R. Mann. 1982. Benthic filter feeding, a natural eutrophication control. *Mar. Ecol. Prog. Ser*. 9:203-210.

Örnólfsdóttir, E. B. 2002. The ecological role of small phytoplankton in phytoplankton and community composition in Galveston Bay, Texas. Doctoral Dissertation, Texas A&M University, College Station.

Patch, M. C. 2005. Acoustic characteristics of bay bottom sediments in Lavaca Bay, Texas. Masters Science Thesis. Texas A&M University, College Station.

Philander, G. 1989. El Nĩno and La Nĩna. *Am. Sci*. 77: 451-459.

Plunket, J. T. 2003. A Comparison of finfish assemblages on subtidal oyster shell (cultched oyster lease) and mud bottom in Barataria Bay, Louisiana. Master's Thesis. Louisiana State University, Baton Rouge.

Powell, E. N. & J. M. Klinck. 2007. Is oyster shell a sustainable estuarine resource? *J. Shelfish Res.* 26:181-194.

Powell, E. N., E. E. Hofmann, J. M. Klinck & S. M. Ray. 1992. Modeling oyster populations I. A commentary on filtration rate. Is faster always better? *J. Shellfish Res*. 11: 387-398.

Powell, E. N., J. M. Klinck, E. E. Hofmann & S. M. Ray. 1994. Modeling oyster populations IV. Rates of mortality, population crashes, and management. *Fish Bull.* 92: 347-373.

Powell, E. N., J. Song, M. S. Ellis, & E. A. Wilson-Ormond. 1995. The status and long-term trends of oyster reefs in Galveston Bay, Texas. *J. Shellfish Res*. 14:439-457.

Powell, E. N., J. M. Klinck & E. E. Hofmann. 1996. Modeling diseased oyster populations. II. Triggering mechanisms for *Perkinsus marinus* epizootics. *J. Shellfish Res.* 15:141-165.

Powell, E. N., J. M. Klinck, E. E. & S. Ford. 1997. Varying the timing of oyster transplant: Implications for management from simulation studies. *Fisheries Oceanography* 6:213-237.

Powell, E. N., J. M. Klinck, E. E. Hofmann, & M. A. McManus. 2003. Influence of water allocation and freshwater inflow on oyster production: A hydrodynamic oyster population model for Galveston Bay, Texas, USA. *Envir. Management*. 31:100–121. doi:10.1007/s00267-002-2695-6.

Price, W. A. 1954. Oyster reefs of the Gulf of Mexico. In: The Gulf of Mexico, Its origin, waters, and marine life. U.S. Fish & Wildlife Service, *Fishery Bull.* 89(55):491.

Price, W. A. & G. Gunter. 1942. Certain recent geological and biological changes in south Texas, with consideration of probable causes. *Proc. Trans. Tex. Acad. Sci.* 26:138-156.

Quick, J. A., Jr. and J. G. Mackin. 1971. Oyster parasitism by *Labyrinthomyxa marina* in Florida. *Fla. Dep. Nat. Resour. Mar. Fish Lab., Prof. Pap. Ser*. 13: 1-55.

Ray, S. M. 1966. A review of the culture method for detecting *Dermocystidium marinum*, with suggested modification and precautions. *Proc. Natl. Shellfish Assoc*. 54: 55-69.

Ray, S. M. 1987. Salinity requirements of the American oyster, *Crassostrea virginica*. In: A. J. Muller and G.A. Matthews, editors. Freshwater inflow needs of the Matagorda Bay system with focus on the needs of penaeid shrimp. National Oceanic and Atmospheric Administration, Technical Memorandum NMFS-SEFC:189. pp. E1-E28.

Ray, S. M. 1996. Historical perspective in *Perkinsus marinus* disease of oysters in the Gulf of Mexico. *J. Shellfish Res*. 15(1): 9-11.

Ray, S. M. 2008. Current status of dermo disease and oyster harvest in West Bay Galveston, TX. In: *Proc. Natl. Shellfish. Assoc. 100th Annual Meeting*. April 6-10, 2008. Providence, RI. pp. 97.

Roegner, G. C. & R. Mann. 1995. Recruitment and growth of the American oyster *Crassostrea virginica* (Bivalvia: Ostreidae) with respect to tidal zonation and season. *Mar. Ecol. Prog. Ser*. 117:91–101.

Ropelewski, C. F. & M. S. Halpert 1986. North American precipitation and temperature patterns associated with the El Nino/Southern Oscillation (ENSO). *Mon. Weather Rev.* 114: 2352-2362.

Sager, W. W., D. S. Maddox, & T. Dellapenna. 2004. Mapping bottom type and anthropogenic impacts on sediments in Galveston Bay (Phase 2). General Land Office, Final Report, Coastal Management Program Cycle #7 Project Report.

Scott, A. J. 1968. Environmental factors controlling oyster shell deposits, Texas Coast. Proceedings: Fourth Forum on Geology of Industrial Minerals. L. F. Brown, Jr., editor. Austin, TX. pp. 129-150.

Shervette, V. R. & F. Gelwick. 2008. Relative nursery function of oyster, vegetated marsh edge, and nonvegetated bottom habitats for juvenile white shrimp *Litopenaeus setiferus*. *Wetlands Ecol. and Manage*. DOI 10.1007/s11273-007-9077-z .

Shumway, S. E. 1996. Natural environmental factors. In: The Eastern Oyster, *Crassostrea virginica*, editors. V. S. Kennedy, R. I. E. Newell & A. F. Eble. University of Maryland, College Park, MD: Maryland Sea Grant College Publication. pp. 467-513.

Smith, N. P. 1978. Intracoastal tides of the Laguna Madre. *Texas J. Sci*. 30(1): 85-95.

Smyth, W. & J. Anderson. 1988. Seismic facies analysis of entrenched valley-fill; A case study in the Galveston Bay area, Texas. *Trans. Gulf Coast Assoc. Geol. Soc.* 38:385-394.

Solis, R. 1999. Hydrography, mixing characteristics, and residence times of Gulf of Mexico Estuaries. In: Biogeochemistry of Gulf of Mexico Estuaries, editors. T. S. Bianchi, J. R. Pennock, & R. R. Twilley. New York: John Wiley & Sons, Inc. ISBN 0-471-16174-8. pp. 29-61.

Song, J. 1993. Spatial trends in community and health related characteristics of Galveston Bay oyster reefs. Master's Thesis, Texas A&M University, College Station.

Soniat, T. M. & S. M. Ray. 1985. Relationships between possible available food and the composition condition and reproductive state of oysters from Galveston Bay, Texas. *Contrib. Mar. Sci*. 28:109-121.

Soniat, T. M. 1996. Epizootiology of *Perkinsus marinus* disease of eastern oysters in the Gulf of Mexico. *J. Shellfish Res*. 15:35-43.

Soniat, T. M., E. N. Powell, E. E. Hofmann, & J. M. Klinck. 1998. Understanding the success and failure of oyster populations: the importance of sample variables and sample timing. *J. Shellfish Res*. 17:1149-1165.

Soniat, T. M., J. M. Klinck, E. N. Powell, & E. E. Hofmann. 2005. Understanding the success and failure of oyster populations: climatic cycles and *Perkinsus marinus. J. Shellfish Res.* 24(4):83-93.

SPSS 12.0 for Windows Release 12.01. 2003. Copyright @SPSS, Inc. 1989-2003. 233 S. Wacker Drive, 11th floor, Chicago, IL 60606-9653 @ http://www.spss.com/corpinfo/?source=homepage&hpzone=nav_bar.

Stanley, J. G. & M. A. Sellers, 1986. Species profiles: life histories and environmental requirements of coastal fishes and invertebrates (Gulf of Mexico) – American oyster. USFWS Biological Report 82 (11.64). U.S. Army Corps of Engineers, TR EL-82-4. 25 pp.

Stella 9.02 2007. ISEE Systems, Inc. @ www.iseesystems.com. 46 Centerra Parkway, Suite 200, Lebanon, NH 03766.

Stenzel, H. B. 1971. Oysters. pp. N953-N1224. In: K. C. Moore, editor. Treatise on invertebrate paleontology. Part N, Vol 3. Geological Society of America, Boulder, Colorado and University of Kansas, Lawrence.

Stauber, L.A. 1950. The problem of physiological species with special reference to oysters and oyster drills. *Ecology* 31(1):109-118.

Street, M. W., A. S. Deaton, W. S. Chappell, & P. D. Mooreside. 2005. North Carolina coastal habitat protection plan. North Carolina Department of Environment and Natural Resources, Division of Marine Fisheries, Morehead City, NC. 656 pp.

Ter Braak, C. J. F. & P. Smilauer. 2002. CANOCO Reference manual and CanoDraw for Windows User's guide: Software for Canonical Community Ordination (version 4.5). Microcomputer Power. Ithaca, NY, USA. 500 pp.

TPWD. 2002. Marine resource monitoring operations manual. May 2002. Texas Parks & Wildlife Dept. Coastal Fisheries Division. Austin, TX.

TPWD unpublished data. 2007a. Texas commercial fishery landings: 1981-2007. Texas Parks & Wildlife Dept., Coastal Fisheries Division, Austin, TX.

TPWD unpublished data. 2007b. Texas resource monitoring data: 1975-2007. Texas Parks & Wildlife Dept., Coastal Fish. Division. Austin, TX.

Turner, R. E. 2006. Will lowering estuarine salinity increase Gulf of Mexico oyster landings? *Estuaries and Coasts* 29:345-352.

Turner, E. J., R. K. Zimmer-Faust, M. A. Palmer, M. Luckenbach, & N. D. Pentchef. 1994. Settlement of oyster (*Crassostrea virginica*) larvae: Effects of water flow and a water soluble chemical cue. *Limnol. Oceanogr*. 39(7): 1579-1593.

Ward, G. H. Jr., Armstrong, N. E. & Matagorda Bay Project Teams. 1980. Matagorda Bay, Texas: its hydrography, ecology and fishery resources. U.S. Fish & Wildlife Service, Biological Services Program, Washington, D.C. FWS/OBS-81/52.

White, M. E., E. N. Powell, & S. M. Ray. 1988. Effect of parasitism by the pyramidellid gastropod *Boonea impressa* on the net productivity on oysters (*Crassostrea virginica*). *Estuar. Coast. Shelf Sci*. 26:359-377.

Wilber, D. H. 1992. Associations between freshwater inflows and oyster productivity in Apalachicola Bay, Florida. *Estuarine, Coast. Shelf Sci.* 35:179–190. doi:10.1016/S0272-7714(05)80112-X.

Wilber, D. H. & R. Bass. 1998. Effect of the Colorado River diversion on Matagorda Bay epifauna. *Estuar. Coast. Shelf Sci.* 47:309–318.

Wildish, D. J. & D. D. Kristmanson. 1979. Tidal energy and sublittoral macrobenthic animals in estuaries. *J. Fish. Res. Bd. Can*. 36(10): 1197-1206.

Winslow, F. 1889. Report on the sounds and estuaries of North Carolina, with reference to oyster culture. *U.S. Coast and Geodetic Survey, Bull*. 10. 135 pp.

Zajac, R. N., R. B. Whitlatch & R. W. Osman. 1989. Effects of inter-specific density and food supply on survivorship and growth of newly settled benthos. *Mar. Ecol. Progr. Ser*. 56:127-132.

Zuur, A. F., E. N. Leno & G. M. Smith. 2007. Analyzing Ecological Data. New York: Springer Science and Business Media, LLC. 672 pp.

APPENDIX A

Environmental Submodels

Salinity Submodel Equations:

NormDeviateSalinity(t) = NormDeviateSalinity(t - dt) + (SalIN - SalOut) * dtINIT
NormDeviateSalinity = 1
INFLOWS:
SalIN = IF Dayof5Yrs = 1 THEN NORMAL(1,0.1) ELSE 0
OUTFLOWS:
SalOut = IF Dayof5Yrs = 1 THEN NormDeviateSalinity ELSE 0
NormDeviateSalinity_2(t) = NormDeviateSalinity_2(t - dt) + (SalIN_2 - SalOut_2) * dtINIT NormDeviateSalinity_2 = 1
INFLOWS:
SalIN_2 = IF Dayof5Yrs_2 = 1 THEN NORMAL(1,0.1) ELSE 0
OUTFLOWS:
SalOut_2 = IF Dayof5Yrs_2 = 1 THEN NormDeviateSalinity_2 ELSE 0
NormDeviateSalinity_3(t) = NormDeviateSalinity_3(t - dt) + (SalIN_3 - SalOut_3) * dtINIT NormDeviateSalinity_3 = 1
INFLOWS:
SalIN_3 = IF Dayof5Yrs_3 = 1 THEN NORMAL(1,0.1) ELSE 0
OUTFLOWS:
SalOut_3 = IF Dayof5Yrs_3 = 1 THEN NormDeviateSalinity_3 ELSE 0

Temperature Submodel Equations:

NormDeviateTemp(t) = NormDeviateTemp(t - dt) + (TempIN - TempOut) * dtINIT
NormDeviateTemp = 1
INFLOWS:
TempIN = IF Dayof5Yrs = 1 THEN NORMAL(1,0.1) ELSE 0
OUTFLOWS:
TempOut = IF Dayof5Yrs = 1 THEN NormDeviateTemp ELSE 0
NormDeviateTemp_2(t) = NormDeviateTemp_2(t - dt) + (TempIN_2 - TempOut_2) * dtINIT NormDeviateTemp_2 = 1
INFLOWS:
TempIN_2 = IF Dayof5Yrs_2 = 1 THEN NORMAL(1,0.1) ELSE 0
OUTFLOWS:
TempOut_2 = IF Dayof5Yrs_2 = 1 THEN NormDeviateTemp_2 ELSE 0
NormDeviateTemp_3(t) = NormDeviateTemp_3(t - dt) + (TempIN_3 - TempOut_3) * dtINIT NormDeviateTemp_3 = 1
INFLOWS:
TempIN_3 = IF Dayof5Yrs_3 = 1 THEN NORMAL(1,0.1) ELSE 0
OUTFLOWS:
TempOut_3 = IF Dayof5Yrs_3 = 1 THEN NormDeviateTemp_3 ELSE 0

Flow Submodel Equations:

NormDeviateFlow(t) = NormDeviateFlow(t - dt) + (FlowIn - FlowOut) * dtINIT
NormDeviateFlow = 1
INFLOWS:
FlowIn = IF Dayof5Yrs = 1 THEN NORMAL(1,0.1) ELSE 0
OUTFLOWS:
FlowOut = IF Dayof5Yrs = 1 THEN NormDeviateFlow ELSE 0
NormDeviateFlow_2(t) = NormDeviateFlow_2(t - dt) + (FlowIn_2 - FlowOut_2) * dtINIT NormDeviateFlow_2 = 1
INFLOWS:
FlowIn_2 = IF Dayof5Yrs_2 = 1 THEN NORMAL(1,0.1) ELSE 0
OUTFLOWS:
FlowOut_2 = IF Dayof5Yrs_2 = 1 THEN NormDeviateFlow_2 ELSE 0
NormDeviateFlow_3(t) = NormDeviateFlow_3(t - dt) + (FlowIn_3 - FlowOut_3) * dtINIT NormDeviateFlow_3 = 1
INFLOWS:
FlowIn_3 = IF Dayof5Yrs_3 = 1 THEN NORMAL(1,0.1) ELSE 0
OUTFLOWS:
FlowOut_3 = IF Dayof5Yrs_3 = 1 THEN NormDeviateFlow_3 ELSE 0

Tidal Submodel Equations:

NormDeviateTide_2(t) = NormDeviateTide_2(t - dt) + (TideIn_2 - TideOut_2) * dtINIT
NormDeviateTide_2 = 1
INFLOWS:
TideIn_2 = IF Dayof5Yrs_2 = 1 THEN NORMAL(1,0.1) ELSE 0
OUTFLOWS:
TideOut_2 = IF Dayof5Yrs_2 = 1 THEN NormDeviateTide_2 ELSE 0
NormDeviateTide_3(t) = NormDeviateTide_3(t - dt) + (TideIn_3 - TideOut_3) * dtINIT
NormDeviateTide_3 = 1
INFLOWS:
TideIn_3 = IF Dayof5Yrs_3 = 1 THEN NORMAL(1,0.1) ELSE 0
OUTFLOWS:
TideOut_3 = IF Dayof5Yrs_3 = 1 THEN NormDeviateTide_3 ELSE 0
NormDeviateTide_4(t) = NormDeviateTide_4(t - dt) + (TideIn - TideOut_4) * dtINIT
NormDeviateTide_4 = 1
INFLOWS:
TideIn = IF Dayof5Yrs = 1 THEN NORMAL(1,0.1) ELSE 0
OUTFLOWS:
TideOut_4 = IF Dayof5Yrs = 1 THEN NormDeviateTide_4 ELSE 0

Dermo Submodels

Dermo Submodel Equations:

DermoStressMrkMad(t) = DermoStressMrkMad(t - dt) + (DermoIn_7 - DermoOut_7) * dtINIT DermoStressMrkMad = 0
INFLOWS:
DermoIn_7 = If DermoEnvirStressMad=1 AND AvgDayFlowColRiver<10000 THEN 1 ELSE (IF DermoEnvirStressMad=1 AND AvgDayFlowColRiver>10000 THEN 0 ELSE 0)
OUTFLOWS:
DermoOut_7 = If DermoStressMrkMad/SubMrkTransDaysMad<.82 THEN 0 ELSE DermoStressMrkMad
DermoStressMrkSam(t) = DermoStressMrkSam(t - dt) + (DermoInMrkSam - DermoOutMrkSam) * dtINIT DermoStressMrkSam = 0
INFLOWS:
DermoInMrkSam = If DermoEnvStressSam=1 AND AvgDayFlowColRiver<10000 THEN 1 ELSE (IF DermoEnvStressSam=1 AND AvgDayFlowColRiver>10000 THEN 0 ELSE 0)
OUTFLOWS:
DermoOutMrkSam = If DermoStressMrkSam/SubMrktTransDaysSam<.82 THEN 0 ELSE DermoStressMrkSam
DermoStressMrkShell(t) = DermoStressMrkShell(t - dt) + (DermoIn_10 - DermoOut_10) * dtINIT DermoStressMrkShell = 0
INFLOWS:
DermoIn_10 = If DermoEnvirStressShell=1 AND AvgDayFlowColRiver<10000 THEN 1 ELSE (IF DermoEnvirStressShell=1 AND AvgDayFlowColRiver>10000 THEN 0 ELSE 0)
OUTFLOWS:
DermoOut_10 = If DermoStressMrkShell/SubMrkTransDaysShell<.82 THEN 0 ELSE DermoStressMrkShell
DermoStressNMrkPlusMad(t) = DermoStressNMrkPlusMad(t - dt) + (DermoIn_6 - DermoOut_6) * dtINIT DermoStressNMrkPlusMad = 0
INFLOWS:
DermoIn_6 = If DermoEnvirStressMad=1 AND AvgDayFlowColRiver<10000 THEN 1 ELSE (IF DermoEnvirStressMad=1 AND AvgDayFlowColRiver>10000 THEN 0 ELSE 0)
OUTFLOWS:
DermoOut_6 = If DermoStressNMrkPlusMad/MrkTransDaysMad< 0.22 THEN 0 ELSE DermoStressNMrkPlusMad
DermoStressNMrkPlusSam(t) = DermoStressNMrkPlusSam(t - dt) + (DermoInMrkPlusSam - DermoOutMrkPlusSam) * dtINIT DermoStressNMrkPlusSam = 0
INFLOWS:
DermoInMrkPlusSam = If DermoEnvStressSam=1 AND AvgDayFlowColRiver<10000 THEN 1 ELSE (IF DermoEnvStressSam=1 AND AvgDayFlowColRiver>10000 THEN 0 ELSE 0)

OUTFLOWS:
DermoOutMrkPlusSam = If DermoStressNMrkPlusSam/MrkTransDaysSam< 0.22 THEN 0 ELSE DermoStressNMrkPlusSam
DermoStressNMrkPlusShell(t) = DermoStressNMrkPlusShell(t - dt) + (DermoIn_9 - DermoOut_9) * dtINIT DermoStressNMrkPlusShell = 0
INFLOWS:
DermoIn_9 = If DermoEnvirStressShell=1 AND AvgDayFlowColRiver<10000 THEN 1 ELSE (IF DermoEnvirStressShell=1 AND AvgDayFlowColRiver>10000 THEN 0 ELSE 0)
OUTFLOWS:
DermoOut_9 = If DermoStressNMrkPlusShell/MrkTransDaysShell< 0.22 THEN 0 ELSE DermoStressNMrkPlusShell
DermoStressSubMrkMad(t) = DermoStressSubMrkMad(t - dt) + (DermoIn_8 - DermoOut_8) * dtINIT DermoStressSubMrkMad = 0
INFLOWS:
DermoIn_8 = If DermoEnvirStressMad=1 AND AvgDayFlowColRiver<10000 THEN 1 ELSE (IF DermoEnvirStressMad=1 AND AvgDayFlowColRiver>10000 THEN 0 ELSE 0)
OUTFLOWS:
DermoOut_8 = If DermoStressSubMrkMad/SpatTransDaysMad< 6.48 THEN 0 ELSE DermoStressSubMrkMad
DermoStressSubMrkSam(t) = DermoStressSubMrkSam(t - dt) + (DermoInSubMrkSam - DermoOutSubMrkSam) * dtINIT DermoStressSubMrkSam = 0
INFLOWS:
DermoInSubMrkSam = If DermoEnvStressSam=1 AND AvgDayFlowColRiver<10000 THEN 1 ELSE (IF DermoEnvStressSam=1 AND AvgDayFlowColRiver>10000 THEN 0 ELSE 0)
OUTFLOWS:
DermoOutSubMrkSam = If DermoStressSubMrkSam/SpatTransDaysSam< 6.48 THEN 0 ELSE DermoStressSubMrkSam
DermoStressSubMrkShell(t) = DermoStressSubMrkShell(t - dt) + (DermoIn_11 - DermoOut_11) * dtINIT DermoStressSubMrkShell = 0
INFLOWS:
DermoIn_11 = If DermoEnvirStressShell=1 AND AvgDayFlowColRiver<10000 THEN 1 ELSE (IF DermoEnvirStressShell=1 AND AvgDayFlowColRiver>10000 THEN 0 ELSE 0)
OUTFLOWS:
DermoOut_11 = If DermoStressSubMrkShell/SpatTransDaysShell< 6.48 THEN 0 ELSE DermoStressSubMrkShell

Larvae submodel equations:

NLarvaeMad(t) = NLarvaeMad(t - dt) + (SpawningMad - to_SpatMad - LarvalLossMad) * dtINIT NLarvaeMad = 0
TRANSIT TIME = varies
INFLOW LIMIT = INF
CAPACITY = INF
INFLOWS:
SpawningMad = IF SpawnWatingTMad=1 THEN MAX(DensityDependMad*(NMrkPlusSpawnersMad+NMrkSpawnersMad+NSubMarketSpawnersMad) +SamLarvaetoMad+ShellLarvaetoMad+ColoradoDeltaLarvae, 86e+6) ELSE 0
OUTFLOWS:
to_SpatMad = CONVEYOR OUTFLOW
TRANSIT TIME = LarvaeTransDaysMad
LarvalLossMad = LEAKAGE OUTFLOW
LEAKAGE FRACTION = LarvalMMad+MadEmigrationLoss
NO-LEAK ZONE = 0%
NlarvaeSam(t) = NlarvaeSam(t - dt) + (SpawningSam - to_SpatSam - LarvalMortSam) * dtINIT NlarvaeSam = 0
TRANSIT TIME = varies
INFLOW LIMIT = INF
CAPACITY = INF
INFLOWS:
SpawningSam = IF SpawnWatingTSam=1 THEN MAX(DensityDependSam*(NMrkPlusSpawnersSam+NMrkSpawnersSam+NSubMrkSpawnersSam)+MadLarvaetoSam+ShellLarvaetoSam+ColoradoDeltaLarvae, 86e+6) ELSE 0
OUTFLOWS:
to_SpatSam = CONVEYOR OUTFLOW
TRANSIT TIME = LarvaeTransDaysSam
LarvalMortSam = LEAKAGE OUTFLOW
LEAKAGE FRACTION = LarvalMSam+SamEmigrationLoss
NO-LEAK ZONE = 0%
NLarvaeShell(t) = NLarvaeShell(t - dt) + (SpawningShell - to_SpatShell - LarvaeLossShell) * dtINIT NLarvaeShell = 0
TRANSIT TIME = varies
INFLOW LIMIT = INF
CAPACITY = INF
INFLOWS:
SpawningShell = IF SpawnWatingTShell=1 THEN MAX(DensityDependShell*(NMrkPlusSpawnersShell+NMrkSpawnersShell+NSubMrkSpawnersShell) +SamLarvaetoShell+MadLarvaetoShell+ColoradoDeltaLarvae, 86e+6) ELSE 0
OUTFLOWS:
to_SpatShell = CONVEYOR OUTFLOW

TRANSIT TIME = LarvaeTransDaysShell
LarvaeLossShell = LEAKAGE OUTFLOW
LEAKAGE FRACTION = LarvalMShell+Shell_EmigrationLoss
NO-LEAK ZONE = 0%

Spat, submarket, market, and market-plus submodel equations:

NSpatMad(t) = NSpatMad(t - dt) + (to_SpatMad - to_SubMrkMad - SpatMortMad) *
dtINIT NSpatMad = 0
TRANSIT TIME = varies
INFLOW LIMIT = INF
CAPACITY = INF
INFLOWS:
to_SpatMad = CONVEYOR OUTFLOW
TRANSIT TIME = LarvaeTransDaysMad
OUTFLOWS:
to_SubMrkMad = CONVEYOR OUTFLOW
TRANSIT TIME = SpatTransDaysMad
SpatMortMad = LEAKAGE OUTFLOW
LEAKAGE FRACTION = SpatMMad+SalinityMMad
NO-LEAK ZONE = 0%
NSpatSam(t) = NSpatSam(t - dt) + (to_SpatSam - to_SubMrkSam - SpatMortSam) *
dtINIT NSpatSam = 0
TRANSIT TIME = varies
INFLOW LIMIT = INF
CAPACITY = INF
INFLOWS:
to_SpatSam = CONVEYOR OUTFLOW
TRANSIT TIME = LarvaeTransDaysSam
OUTFLOWS:
to_SubMrkSam = CONVEYOR OUTFLOW
TRANSIT TIME = SpatTransDaysSam
SpatMortSam = LEAKAGE OUTFLOW
LEAKAGE FRACTION = SpatMSam+SalinityMortSam
NO-LEAK ZONE = 0%
NSpatShell(t) = NSpatShell(t - dt) + (to_SpatShell - to_SubMrkShell - SpatMortShell) *
dtINIT NSpatShell = 0
TRANSIT TIME = varies
INFLOW LIMIT = INF
CAPACITY = INF
INFLOWS:
to_SpatShell = CONVEYOR OUTFLOW
TRANSIT TIME = LarvaeTransDaysShell
OUTFLOWS:
to_SubMrkShell = CONVEYOR OUTFLOW
TRANSIT TIME = SpatTransDaysShell

SpatMortShell = LEAKAGE OUTFLOW
LEAKAGE FRACTION = SpatMShell+SalinityMShell
NO-LEAK ZONE = 0%
NSubMrkMad(t) = NSubMrkMad(t - dt) + (to_SubMrkMad - to_MrkMad - SuMrkMortMad) * dtINIT NSubMrkMad = 11800000
TRANSIT TIME = varies
INFLOW LIMIT = INF
CAPACITY = INF
INFLOWS:
to_SubMrkMad = CONVEYOR OUTFLOW
TRANSIT TIME = SpatTransDaysMad
OUTFLOWS:
to_MrkMad = CONVEYOR OUTFLOW
TRANSIT TIME = SubMrkTransDaysMad
SuMrkMortMad = LEAKAGE OUTFLOW
LEAKAGE FRACTION = SubMrkMMad+SalinityMMad+DermoMortNSubMrkMad
NO-LEAK ZONE = 0%
NSubMrkSam(t) = NSubMrkSam(t - dt) + (to_SubMrkSam - to_MrkSam - SubMrkMortSam) * dtINIT NSubMrkSam = 1260400
TRANSIT TIME = varies
INFLOW LIMIT = INF
CAPACITY = INF
INFLOWS:
to_SubMrkSam = CONVEYOR OUTFLOW
TRANSIT TIME = SpatTransDaysSam
OUTFLOWS:
to_MrkSam = CONVEYOR OUTFLOW
TRANSIT TIME = SubMrktTransDaysSam
SubMrkMortSam = LEAKAGE OUTFLOW
LEAKAGE FRACTION = SubMrkMSam+SalinityMortSam+DermoMortNSubMrkSam
NO-LEAK ZONE = 0%
NSubMrkShell(t) = NSubMrkShell(t - dt) + (to_SubMrkShell - to_MrkShell - SubMrkMortShell) * dtINIT NSubMrkShell = 29200000
TRANSIT TIME = varies
INFLOW LIMIT = INF
CAPACITY = INF
INFLOWS:
to_SubMrkShell = CONVEYOR OUTFLOW
TRANSIT TIME = SpatTransDaysShell
OUTFLOWS:
to_MrkShell = CONVEYOR OUTFLOW
TRANSIT TIME = SubMrkTransDaysShell
SubMrkMortShell = LEAKAGE OUTFLOW

LEAKAGE FRACTION =
SubMrkMShell+SalinityMShell+DermoMortNSubMrkShell
NO-LEAK ZONE = 0%
NMrkMad(t) = NMrkMad(t - dt) + (to_MrkMad - to_MrkPlusMad - MrkMortMad) *
dtINIT NMrkMad = 11200000
TRANSIT TIME = varies
INFLOW LIMIT = INF
CAPACITY = INF
INFLOWS:
to_MrkMad = CONVEYOR OUTFLOW
TRANSIT TIME = SubMrkTransDaysMad
OUTFLOWS:
to_MrkPlusMad = CONVEYOR OUTFLOW
TRANSIT TIME = MrkTransDaysMad
MrkMortMad = LEAKAGE OUTFLOW
LEAKAGE FRACTION = MrkMMad +
MrkFishingMad+DermoMortNMrkMad+SalinityMMad
NO-LEAK ZONE = 0%
NMrkPlusMad(t) = NMrkPlusMad(t - dt) + (to_MrkPlusMad - MrkPlusMortMad) *
dtINIT NMrkPlusMad = 0
INFLOWS:
to_MrkPlusMad = CONVEYOR OUTFLOW
TRANSIT TIME = MrkTransDaysMad
OUTFLOWS:
MrkPlusMortMad =
NMrkPlusMad*(MrkPlusMMad+MrkFishingMad+DermoMortNMrkPlusMad+Salinity
MMad)
NMrkPlusSam(t) = NMrkPlusSam(t - dt) + (to_MrkPlusSam - MrkPlusMortSam) *
dtINIT NMrkPlusSam = 0
INFLOWS:
to_MrkPlusSam = CONVEYOR OUTFLOW
TRANSIT TIME = MrkTransDaysSam
OUTFLOWS:
MrkPlusMortSam =
NMrkPlusSam*(MrkPlusMSam+MarkFishingMSam+DermoMortNMrkPlusSam+Salini
tyMortSam)
NMrkPlusShell(t) = NMrkPlusShell(t - dt) + (to_MrkPlusShell - MrkPlusMortShell) *
dtINIT NMrkPlusShell = 0
INFLOWS:
to_MrkPlusShell = CONVEYOR OUTFLOW
TRANSIT TIME = MrkTransDaysShell
OUTFLOWS:
MrkPlusMortShell =
NMrkPlusShell*(MrkPlusMShell+MarkFishingMShell+DermoMortNMrkPlusShell+Sal
inityMShell)

NMrkSam(t) = NMrkSam(t - dt) + (to_MrkSam - to_MrkPlusSam - MrkMortSam) *
dtINIT NMrkSam = 1890500
TRANSIT TIME = varies
INFLOW LIMIT = INF
CAPACITY = INF
INFLOWS:
to_MrkSam = CONVEYOR OUTFLOW
TRANSIT TIME = SubMrktTransDaysSam
OUTFLOWS:
to_MrkPlusSam = CONVEYOR OUTFLOW
TRANSIT TIME = MrkTransDaysSam
MrkMortSam = LEAKAGE OUTFLOW
LEAKAGE FRACTION = MrkMSam +
MarkFishingMSam+DermoMortNMrkSam+SalinityMortSam
NO-LEAK ZONE = 0%
NMrkShell(t) = NMrkShell(t - dt) + (to_MrkShell - to_MrkPlusShell - MrkMortShell) *
dtINIT NMrkShell = 19580000
TRANSIT TIME = varies
INFLOW LIMIT = INF
CAPACITY = INF
INFLOWS:
to_MrkShell = CONVEYOR OUTFLOW
TRANSIT TIME = SubMrkTransDaysShell
OUTFLOWS:
to_MrkPlusShell = CONVEYOR OUTFLOW
TRANSIT TIME = MrkTransDaysShell
MrkMortShell = LEAKAGE OUTFLOW
LEAKAGE FRACTION = MrkMShell +
MarkFishingMShell+DermoMortNMrkShell+SalinityMShell
NO-LEAK ZONE = 0%

VITA

Name: Jan Cheryl Culbertson

Address: Texas Parks and Wildlife Department
Coastal Fisheries
1502 FM 517 East,
Dickinson, TX 77539

Email Address: jan.culbertson@tpwd.state.tx.us

Education: B.A., Biology, University of Delaware, Newark, Delaware 1975
M.S., Forest and Natural Resources, University of Georgia, Athens, Georgia 1979
Ph.D., Texas A&M University, College Station 2008